USC UNIVERSIDADE DE SANTIAGO DE COMPOSTELA

CENTRO INTERNACIONAL DE ESTUDOS DE DOUTORAMENTO E AVANZADOS DA USC (CIEDUS)

DOCTORAL THESIS

TECHNOLOGICAL AND BIOLOGICAL ASPECTS OF POLYMERIC NANOCAPSULES FOR THE DESIGN OF NEW NANOVACCINES

José Crecente Campo

INTERNATIONAL DOCTORAL SCHOOL

DOCTORAL PROGRAM IN DRUG RESEARCH AND DEVELOPMENT

SANTIAGO DE COMPOSTELA

2018

USC
UNIVERSIDADE DE SANTIAGO DE COMPOSTELA

CENTRO INTERNACIONAL DE ESTUDOS DE DOUTORAMENTO E AVANZADOS DA USC (CIEDUS)

TESIS DE DOCTORADO

ASPECTOS TECNOLÓGICOS Y BIOLÓGICOS DE LAS NANOCÁPSULAS POLIMÉRICAS PARA EL DISEÑO DE NUEVAS NANOVACUNAS

José Crecente Campo

ESCUELA DE DOCTORADO INTERNACIONAL

PROGRAMA DE DOCTORADO EN I + D DE MEDICAMENTOS

SANTIAGO DE COMPOSTELA

2018

AUTHORIZATION OF THE THESIS SUPERVISORS

Technological and biological aspects of polymeric nanocapsules for the design of new nanovaccines

Prof. María José Alonso Fernández, Full Professor of the Department of Pharmacology, Pharmacy and Pharmaceutical Technology at the University of Santiago de Compostela

REPORT:

That the present thesis, corresponds to the work carried out by Mr. ***José Crecente Campo****, under my supervision, and that I authorize its presentation considering it gathers the necessary requirements of article 34 of the USC Doctoral Studies regulation, and that as supervisor of this thesis, it does not incur in the abstention causes established by the law 40/2015.*

At Santiago de Compostela, on November 9th 2018

Sgd.: **María José Alonso Fernández**

AUTORIZACIÓN DEL DIRECTOR / TUTOR DE LA TESIS

Aspectos tecnológicos y biológicos de las nanocápsulas poliméricas para el diseño de nuevas nanovacunas

Dña. María José Alonso Fernández, Catedrática del Departamento de Farmacología, Farmacia y Tecnología Farmacéutica de la Universidad de Santiago de Compostela

INFORMA:

Que la presente tesis, corresponde con el trabajo realizado por D. ***José Crecente Campo****, bajo mi dirección, y autorizo su presentación, considerando que reúne los requisitos exigidos en el Reglamento de Estudios de Doctorado de la USC, y que como directora de ésta no incurre en las causas de abstención establecidas en Ley 40/2015.*

En Santiago de Compostela, a 9 de Noviembre de 2018

Fdo.: **María José Alonso Fernández**

PhD CANDIDATE STATMENT

Technological and biological aspects of polymeric nanocapsules for the design of new nanovaccines

Mr. José Crecente Campo

I submit my Doctoral thesis, following the procedure according to the Regulation, stating that:

1) *This thesis gathers the results corresponding to my work.*
2) *When applicable, explicit mention is given to the collaborations the work may have had.*
3) *The present document is the final version submitted for its defense and coincides with the document sent in electronic format.*
4) *I confirm that this thesis does not incur in any plagiarism of any other authors or documents submitted by me for obtaining other degrees.*

At Santiago de Compostela, on November 9th 2018

Sgd.: **José Crecente Campo**

DECLARACIÓN DEL AUTOR DE LA TESIS

Aspectos tecnológicos y biológicos de las nanocápsulas poliméricas para el diseño de nuevas nanovacunas

D. José Crecente Campo

Presento mi tesis, siguiendo el procedimiento adecuado al Reglamento, y declaro que:

1) *La tesis abarca los resultados de la elaboración de mi trabajo.*
2) *En su caso, en la tesis se hace referencia a las colaboraciones que tuvo este trabajo.*
3) *La tesis es la versión definitiva presentada para su defensa y coincide con la versión enviada en formato electrónico.*
4) *Confirmo que la tesis no incurre en ningún tipo de plagio de otros autores ni de trabajos presentados por mí para la obtención de otros títulos.*

En Santiago de Compostela, a 9 de Noviembre de 2018

Fdo.: **José Crecente Campo**

Conflict of interests

I declare that there are no competing interests with the subject matter or materials discussed in this thesis.

Sgd.: José Crecente Campo

Á miña xente

Acknowledgements

Non pensaba verme de novo nesta situación, na de escribir e defender unha nova tese de doutoramento, e aquí estou, coa ilusión de quen fai esta andaina por vez primeira. Sen dúbida algunha, de non ser pola xente que aquí nomeo, tal tarefa non sería posible.

En primeiro lugar gustaríame agradecer á miña directora de tese, María José, por toda a confianza depositada en min durante estes últimos anos. Comecei esta etapa dubitativo e algo desorientado e ti axudáchesme a ir gañando confianza e a sentirme parte importante do teu grupo de investigación. A túa paixón polo traballo, dedicación e ímpetu pasan a ser referentes esenciais para o resto da miña traxectoria profesional. Gracias por todo.

Gracias a todos os colaboradores que embeleceron cos seus estudos esta tese. Gracias por deixar patente que a ciencia é sinónimo de colaboración, de sinerxia, de compartir. Gracias en especial ós grupos de África González, Jorge Blanco, Laura Sánchez, Santiago González e Rubén Varela. Gracias a vós aprendín moito máis alá do ámbito da nanociencia.

Gracias ós profesores do Departamento de Farmacoloxía, Farmacia e Tecnoloxía Farmacéutica. En especial gracias a Loli pola túa disposición continua e inmediata a axudar. Gracias Marcos por iniciarme no mundo da tecnoloxía farmacéutica, por todo o que me ensinaches e pola túa cercanía. Gracias Noemi, por compartir a túa experiencia e apoiarme ó longo destes anos.

Gracias Puri, pola túa inestimable axuda durante este tempo. Gracias a Rafa e a Balbi, por facerme o traballo de laboratorio máis doado. Gracias Vanessa por ser compañeira sempre positiva.

Graciñas Belén, porque o laboratorio sen ti sería un Titanic á deriva. Gracias por ensinarme xeografía na nosa lingua e todos os ditos do teu abuelo. Gracias por todas as mostras de cariño que me diches, polas de xenio tamén, polas risadas e saídas de tono, por ser tan especial e auténtica. Eres, sen dúbida, unha das razón polas que cada (algunha) mañá me levanto con ganas de ir traballar. Gracias por ser a miña confidente, o meu apoio, a miña amiga.

Graciñas a todos os nanochachos, sen dúbida fóstedes o mellor que me pasou nestes últimos anos. Gracias por mostrarme que, por enriba de todo, a ciencia une e fai fraternidade; que canto máis xeneroso eres máis che dá a xente a cambio. Gracias por enriquecerme coas vosas diferentes culturas, personalidades e visións da vida; por crear un ambiente de traballo tan sano e estimulante. Gracias polos momentos de festa e polos momentos tristes, que algún tamén houbo. Cada vez que algún de vós deixaba o grupo a pena da marcha recompensábase por saber que teño amigos espallados por todo o mundo. Aínda que non vos nomee un a un tendes reservada unha parte moi importante do meu corazón.

Gracias en especial á aqueles que durante este período tiven a oportunidade de intentar axudar ou guiar na súa aventura científica: Serena, Nacho, Belén Álvarez, Bhanu, Natka, Tamara, Iago, Germán, Carmen. Gracias por mostrarme canto se pode aprender ensinando.

Graciñas Desi, por entenderme e apoiarme tanto. Gracias por ser referente de traballo serio e ben feito, de profesionalidade. Gracias por ser o contrapeso necesario que nos fai manter en pé a moitos.

Gracias Belenciña, porque dende o primeiro momento me ofreciches e me diches confianza. Gracias por todo o que me axudaches, que foi moito, por todo o compartido e por demostrarme que, aínda que ás veces as cousas veñen reviradas, con fortaleza sempre se sae adiante.

Gracias Lena, Leniña, por traer tanta enerxía positiva ó laboratorio. Gracias por ser a miña confidente e amiga, por acabarme a veces coa paciencia, por ensinarme que se pode dar todo polo traballo e aínda así priorizar a amizade cos compañeiros. Gracias por todos os detalles, por todos os sorrisos que irradiaban o despacho, por acoller con tan boa fe as miñas bromas pesadas, por darme a seguridade de saber que estarás aí, pase o que pase.

Gracias a José Vicente, Jorge e Sara por acollerme no grupo nanovac e deixar que me aproveitase da súa veteranía; a Ivana polo seu humor e templanza; a Cadetiña por ensinarme a mellor cara da ambición e pola súa fortaleza; a Ana González pola complicidade e simpatía; a Niu polo seu sentido de humor e proximidade; a Inma por ser xenerosidade e enerxía puras; a Andrea pola súa nobleza e amizade transparente; a Sofía pola súa risa contaxiosa e por todo o seu cariño; a Mati polo seu misterio e á vez cercanía; a Ana Olivera polo ensinado e a súa forza; a Iago polas leccións políticas e por ser tan mandadiño; a Maruthi pola súa positividade e por axudarme a ter a finca limpa.

Un agradecemento especial ás *Astuveivis*, pilar fundamental no que me apoiei estes anos, gracias por aturarme e deixarme formar parte das vosas vidas.

Gracias Sonita, por darme a mellor das acollidas no grupo cando chegaba medio perdido. Gracias por todas as viaxes que fixemos xuntos, polo que discutimos e polo que rimos, por abrirme o teu corazón e por facerme abrir o meu. Gracias porque nunca perdes a alegría e sempre irradias enerxía positiva. Gracias porque sei que sempre estarás aí para min.

Gracias Adri, por todas e cada unha dos centos de veces que me levaches a contraria. Gracias pola túa múltiple personalidade, que tanto podes parecer o ser máis tenro do mundo coma a heroína que salva/destroza o planeta. Gracias por estar sempre ó pé do cañón, por darme ánimos e apoio, por toda a forza que me transmitiches, porque dá gusto discutir contigo tomando unhas cañas, sexa de ciencia ou non.

Gracias a Elena, por ese sentido do humor que fai que me esmendrelle. Por ser tan pasional e a veces temperamental. Gracias por querer manter unida esta pequena familia que montamos, porque sei que podo contar contigo.

Gracias Carmiña, pola túa sensatez, madurez e, cando non hai máis remedio, resignación. Gracias por esas arrincadas de humor e por deixarnos compartir momentos tan bonitos da túa vida.

Gracias a Tamara Macarena, á pequechiña. Gracias por aturarme, a pesar de ter sido contigo a veces algo toxo. Gracias por demostrarme que se pode ser intelixente e humilde á vez, ambiciosa e xenerosa, fráxil e rexa. Gracias por ser excelente no traballo e excelente persoa, por axudarme a non perder a fé na ciencia nin nos científicos. Non perdas nunca ese sonriso de nena boiña nin os chistes malos cos que tanto nos retroalimentamos.

Gracias mamita Irene, porque aínda que o noso non foi un amor a primeira vista acabou por ser un deses matrimonios que dura para toda a vida. Gracias por ser esa persoa que todo o mundo busca nun lugar de traballo, especialmente xenerosa, atenta, buscando a concordia e, como non, algo goberneira. Gracias polos teus berros e manías, por toda a axuda en temas de burocracia e maquetación. Gracias por complementar a miña inseguridade, por ser a voz da conciencia que me dixo en máis dunha ocasión o que había que facer; así é a vida.

Gracias ós meus amigos fóra do labo, porque, á veces, a mellor forma de afrontar un problema é abstraerse del. Gracias a todos os profes do Compostela. Graciñas a Alberto, Rus, Belén Reija, Raquel, Pedro e Manu. Graciñas ós finseros, Fernando, Antonio, María, Lu e Sandriña. Gracias a Diana, pelexiña, por darme acubillo físico e emocional neste longo treito.

Gracias Rober, por todo o apoio que me diches, por entenderme e aguantarme, por ser tan noble. Gracias Rubén, por todas as vivencias destes últimos anos, por obligarme a facerme tantas preguntas, por volverme tolo a veces e por sacarme fóra da zona de confort. A miña vida sería moito máis aburrida de non ser por ti.

Gracias a Suso, por darme tanto ánimo, pola túa complicidade, a risa de neno pequeno, a paciencia infinita e todo o teu cariño.

Gracias á miña familia, sen eles o resto non tería sentido. Gracias por entenderme como perpétuo estudiante, por soportar as miñas neuras e por estar sempre aí para min. Un agradecemento especial tamén para os que non están, porque me siguen guiando e acompañando neste camiño, a veces incerto, que é a vida.

Table of Contents

Table of Contents

Abstract/Resumen

Abstract

Despite the unprecedented contribution of vaccines to the eradication of some infectious diseases and to improve our life expectancy, vaccination still faces some challenges, such as the limited immunogenicity of modern antigens. In this context, nanotechnology has emerged as a useful tool for overcoming this and other limitations. Indeed, nanocarriers have been shown to protect the integrity of their associated antigens once in the body, and to modify their biodistribution, thereby offering the possibility to modulate the immune response towards either a cellular or a humoral arm. Based on the background knowledge in this field, the main objectives of this thesis have been: *i)* to develop new methods to prepare tunable polymeric nanocapsules regarding their particle size, polymeric shell and surface composition; and *ii)* to study the influence of these parameters on the interaction of the nanocapsules with immune cells, their dissemination and lymphatic drainage.

The first chapter describes how novel dextran sulfate – chitosan bilayer nanocapsules can protect and control the release of their associated antigen. More precisely, the IutA antigen from uropathogenic *E. coli* was anchored between the two polymeric layers that surround an immunostimulant oily core. The second layer of dextran sulfate increased the stability and controlled the release of the antigen compared to monolayer chitosan nanocapsules. Interestingly, when used for mice immunization, the bilayer prototype led to higher levels of IgG compared to both the monolayer prototype and Alum, the gold standard for vaccine adjuvants.

In chapter 2, new technological possibilities of the solvent displacement technique are explored. Different modifications in the preparation process allowed the engineering of tailor-made nanocapsules with controllable particle size and with one or multiple polymeric layers. Besides, the described method could be modified to an HTS-adaptable procedure (microliters), and, also, scaled-up (liter) using both a batch mode and microfluidics.

In chapters 3 and 4, and using the technological advances previously achieved in chapter 2, the rational design of novel chitosan and inulin nanocapsules with tunable particle sizes is described. Their toxicity and interaction with both macrophages and dendritic cells were evaluated, exhibiting a size and composition-dependent effect. The dissemination studies in a zebrafish model revealed clear differences in the behavior of small (< 100 nm) and medium (> 100 nm) size nanocapsules, with smaller particles showing a higher and faster dissemination rate after both intramuscular and intravenous injection. Finally, the lymphatic drainage of the nanocapsules after subcutaneous injection and their accumulation in different subsets of lymph node resident immune cells were studied in a murine model. The results indicated that small size inulin nanocapsules had the best capacity to accumulate in the popliteal lymph node and showed the higher interaction with all the subsets of immune cells evaluated.

Overall, this works highlights the technological possibilities of polymeric nanocapsules and the capital importance of the rational design of the nanosystems in order to provide adequate antigen protection and release, showing at the same time proper biodistribution and immune cell-interaction. Besides, these studies will hopefully contribute to a better design of new nanovaccines using particles with lympho-targeting properties.

Resumen

A pesar de la inigualable contribución de las vacunas en la erradicación de ciertas enfermedades infecciosas y en el incremento de nuestra esperanza de vida, la vacunación todavía se enfrenta a numerosos retos, tales como la limitada capacidad inmunogénica de los antígenos modernos. En este contexto, la nanotecnología ha surgido como una herramienta útil para superar esta y otras limitaciones. De hecho, los nanovehículos han demostrado proteger la integridad de los antígenos asociados una vez en el cuerpo y ser capaces de modificar su biodistribución, ofreciendo la posibilidad de modular la respuesta hacia una inmunidad celular o humoral. Teniendo en cuenta los antecedentes en este campo, los principales objetivos en esta tesis han sido: *i)* desarrollar nuevos métodos para preparar nanocápsulas poliméricas con tamaño de partícula, cubierta polimérica y composición superficial controlables; y *ii)* estudiar la influencia de estos parámetros en la interacción de las nanocápsulas con las células del sistema inmunitario, su diseminación y drenaje linfático.

El primer capítulo describe como las nanocápsulas bicapa de quitosano – sulfato de dextrano desarrolladas pueden proteger y controlar la liberación de su antígeno asociado. En concreto, el antígeno IutA de *E. coli* uropatogénica fue atrapado entre dos capas poliméricas que rodean un núcleo inmunoestimulante. La segunda capa de sulfato de dextrano incrementó la estabilidad y controló la liberación del antígeno en comparación con las nanocápsulas monocapa de quitosano. Cuando se emplearon para inmunizar ratones, el prototipo bicapa generó mayores niveles de IgG en comparación con el prototipo monocapa y con Alum, el adyuvante de referencia en vacunas.

En el capítulo 2 se exploran nuevas posibilidades tecnológicas del método de desplazamiento de disolvente. Distintas modificaciones en el proceso de preparación permitieron el diseño de nanocápsulas a medida, con tamaño de partícula controlable y una o varias capas poliméricas. Además, el método de preparación se ajustó a un procedimiento adaptable a HTS (microlitros) y también se escaló (litro) empleando tanto un método discontinuo en lotes como un método continuo por microfluídica.

En los capítulos 3 y 4, y empleando los avances tecnológicos previamente descritos en el capítulo 2, se describe el diseño racional de nanocápsulas de quitosano e inulina con tamaños de partícula controlable. Su toxicidad e interacción con macrófagos y células dendríticas fue evaluado, mostrando un efecto dependiente tanto del tamaño como de la cubierta polimérica. Los estudios de diseminación en peces cebra revelaron diferencias claras en el comportamiento de las nanocápsulas con tamaño pequeño (< 100 nm) y mediano (> 100 nm); mostrando las partículas más pequeñas una mayor y más rápida diseminación tras inyección intramuscular e intravenosa. Finalmente, se estudió el drenaje linfático de las nanocápsulas tras ser administradas por vía subcutánea y su acumulación en distintas subpoblaciones de células inmunitarias residentes en los nódulos linfáticos. Los resultados indican que las

nanocápsulas pequeñas de inulina poseen la mejor capacidad para acumularse en el nódulo linfático poplíteo y mostraron la mayor interacción con los diferentes tipos de células inmunitarias analizados.

En conclusión, este trabajo resalta las posibilidades tecnológicas de las nanocápsulas poliméricas y la importancia transcendental del diseño racional de los nanosistemas para proporcionar una adecuada protección y liberación del antígeno, mostrando al mismo tiempo una adecuada biodistribución e interacción con células inmunitarias. Además, esperamos que estos estudios contribuyan a un mejor diseño de nuevas nanovacunas, empleando partículas con propiedades de direccionamiento a linfa.

Resumen *in extenso*

La nanotecnología es considerada una herramienta adecuada para superar las limitaciones de las vacunas de subunidades, que presentan una capacidad inmunogénica muy reducida [1–3]. De hecho, los nanosistemas han demostrado que protegen la integridad de sus antígenos asociados en el organismo, y que son capaces de modificar su biodistribución, ofreciendo, por tanto, la posibilidad de modular la respuesta inmunitaria hacia un perfil Th1 o Th2 [4–6].

En este trabajo, nos hemos centrado en las nanocápsulas poliméricas (NCs) como vehículos para antígenos proteicos purificados. Las NCs son sistemas nanométricos con un núcleo interior oleoso y una cubierta externa polimérica. Debido a su núcleo lipídico, las NCs fueron, originalmente, concebidas como vehículos especialmente indicados para fármacos lipofílicos. Sin embargo, nuestro grupo ha ampliado esta tecnología para permitir que las NCs transporten macromoléculas hidrosolubles, tales como proteínas [7,8], péptidos [9–11] y polinucleótidos [12], empleándolas en diferentes áreas terapéuticas. En el campo de las vacunas, hemos asociado con éxito a diferentes NCs distintos tipos de antígenos proteicos, tales como el toxoide tetánico [8], el antígeno de la gripe [13] y el antígeno de la hepatitis B [14]. En general, al asociar los antígenos a las NCs, hemos observado un incremento de la respuesta inmunitaria tanto por vía intramuscular como por vía nasal [14,15].

Teniendo en cuenta estos antecedentes, el primer objetivo de este trabajo ha sido el desarrollo de nuevas NCs poliméricas bicapa diseñadas para proteger y controlar la liberación del antígeno IutA de *E. Coli* uropatógena (UPEC). El potencial de este antígeno para el tratamiento de infecciones urinarias recurrentes causadas por UPEC aparece documentado en la bibliografía [16,17].

1. NCs poliméricas bicapa: una estrategia de formulación para el antígeno IutA de *E. coli*

1.1. Desarrollo de NCs bicapa

El comportamiento de las nanovacunas está determinado, en gran medida, por sus propiedades físico-químicas, su composición y la organización estructural del antígeno asociado. Además, la encapsulación eficiente del antígeno en el nanosistema es un pre-requisito en la formulación de nanovacunas [18]. Por esta razón, en un primer momento, nos hemos centrado en la selección de los componentes del nanosistema que favoreciesen la asociación del antígeno. En una etapa posterior, hemos diseñado una organización estructural según la cual el antígeno proteico queda atrapado entre dos capas poliméricas con carga opuesta, creando así un nanosistema bicapa (Fig. 1).

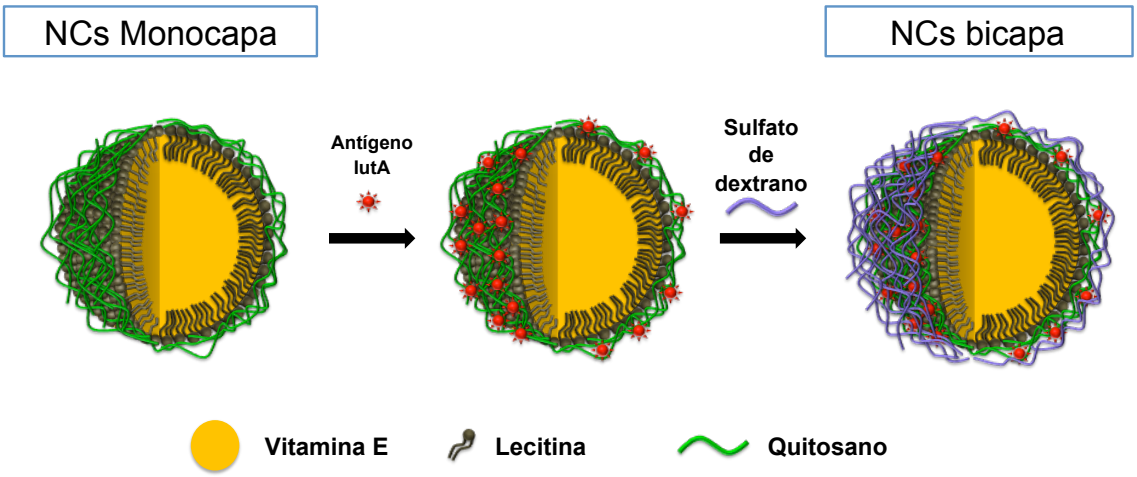

Figura 1. Esquema de preparación de las nanocápsulas (NCs) bicapa. En el nanosistema bicapa el antígeno es atrapado entre dos capas poliméricas: quitosano y sulfato de dextrano.

1.1.1. Selección de los componentes de las NCs

El primer paso en el desarrollo de NCs cargadas con IutA fue probar, de forma sistemática, distintos componentes con interés en el ámbito de las vacunas para preparar nanoemulsiones (NEs) y NCs con una carga de antígeno óptima, manteniendo unas propiedades físico-químicas adecuadas. En este sentido se testaron distintos aceites (escualeno, vitamina E, Miglyol® 812 y ácido oleico), tensoactivos (PEG-estearato, TPGS, Tween® 80, lecitina, poloxámero 407 y colato sódico) y polímeros (CS, protamina y poliarginina). Con estos compuestos se preparó un panel de NCs poliméricas distintas. Tras su caracterización, se asoció el antígeno IutA por simple incubación. La principal conclusión que se extrajo de este estudio fue que, como era de prever, tanto el tensoactivo como el polímero juegan un papel importante en la eficacia de asociación de IutA. Considerando que IutA es una proteína de membrana anfifílica, su asociación a las NCs puede implicar no sólo fuerzas electrostáticas sino también hidrofóbicas. Después de su incubación con las NCs, la proteína interaccionaría con la capa de tensoactivo y con la cubierta polimérica, siendo estos dos los componentes que condicionan los niveles de asociación.

Como resultado del análisis anterior, se seleccionó la composición con un núcleo oleoso de vitamina E, lecitina como tensoactivo y CS en la cubierta polimérica como aquella que proporcionaba unas NCs con las propiedades físico-químicas y eficacia de asociación de IutA más adecuadas (Tabla 1).

1.1.2. Encapsulación del antígeno en las NCs bicapa

Las proteínas asociadas a la cubierta polimérica de las NCs pueden sufrir una exposición prematura al ambiente fisiológico, llevando a su inactivación o liberación

incontrolada. Para prevenir este problema potencial, proponemos en este estudio una estructura tipo sándwich en la cual el antígeno está protegido entre una bicapa que recubre un núcleo inmunoestimulante de vitamina E. Para la formación de la bicapa elegimos sulfato de dextrano (DS), un polímero negativamente cargado que ha sido investigado en la formación de nanocomplejos en asociación con el CS [19–25]. Las condiciones apropiadas para la formación de la capa de DS se determinaron de forma empírica, usando el método de saturación [26,27]. Para tal fin, las NCs CS monocapa fueron incubadas con diferentes ratios de DS (ratios CS:DS desde 10:1 a 1:4, p/p) y la saturación de la superficie de las NCs se determinó monitorizando el potencial-ζ, indicador de la carga superficial del sistema. Tal y como se preveía, los resultados en la Fig. 2 indican la inversión del potencial-ζ tras la adición de DS. Dicha inversión sucede a un ratio CS:DS 4:1 y alcanza un valor mínimo en el ratio 2:1. Un mayor incremento en la cantidad de DS no causó un descenso adicional del potencial-ζ. Benoit *et al.* obtuvieron resultados similares a para el ratio óptimo de CS:DS en un prototipo multicapa [25].

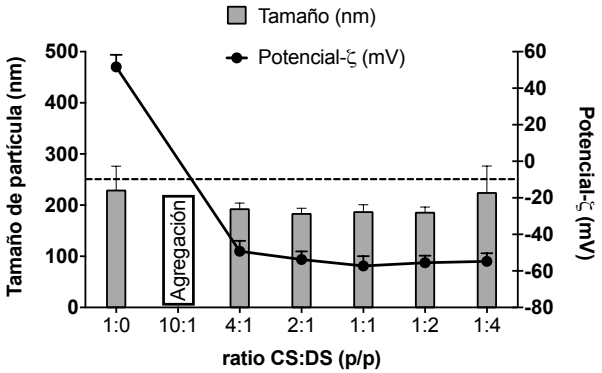

Figura 2. Formación de nanocápsulas bicapa. Evolución del tamaño de partícula y del potencial-ζ de las nanocápsulas de quitosano/lecitina/vitamina E en el proceso de formación de una segunda capa de sulfato de dextrano. Los resultados se muestra como media ± desviación estándar de 4 replicados.

Una vez optimizado el recubrimiento de las NCs blancas, aplicamos las mismas condiciones experimentales a las NCs cargadas con IutA (Tabla 1). La adición de la segunda capa de DS redujo considerablemente el tamaño de las NCs desde los 274 nm, para las NCs monocapa cargadas con IutA, a los 200 nm, para las NCs bicapa. Este cambio se puede atribuir a la compactación de la capa de CS más suelto, debido a las interacciones electrostáticas con el DS. Como era de esperar, la segunda capa polisulfatada invirtió la carga superficial de las nanopartículas desde valores positivos a valores altamente negativos. Finalmente, la eficacia de asociación del antígeno se mantuvo tras la adición de la segunda capa de polímero, confirmando que el DS no desplaza al antígeno sino que lo mantiene protegido en una estructura polimérica tipo sándwich, tal y como supusimos.

Tabla 1. Propiedades físico-químicas y eficacia de asociación del antígeno (AE) de los prototipos seleccionados para los experimentos *in vivo*. Los resultados se muestran como media ± desviación estándar, de, al menos, tres medidas. n/a no se aplica.

Nanosistema	Tamaño de partícula (nm)	PDI	Potencial-ζ (mV)	AE (%)
NCs CS blancas	166 ± 7	0,2	+ 35 ± 4	n/a
NCs CS cargadas	274 ± 19	0,2	+ 44 ± 2	67 ± 5
NCs DS/CS blancas	196 ± 5	0,1	- 52 ± 3	n/a
NCs DS/CS cargadas	200 ± 2	0,1	- 42 ± 4	71 ± 8

1.2. Estabilidad y liberación de antígeno de las NCs bicapa

Para asegurar la estabilidad a largo plazo de los nanosistemas se desarrolló un proceso de liofilización. Se emplearon distintos crioprotectores para mantener las propiedades físico-químicas de las NCs durante el proceso de liofilización (manitol, sacarosa, trehalosa y glucosa). Los mejores resultados, en cuanto a la conservación de las propiedades iniciales, se obtuvieron empleando sacarosa a una concentración del 10% (p/v). Las imágenes de microscopía electrónica de barrido de emisión de campo (FESEM) de las formulaciones liofilizadas mostraron una estructura tipo queso, con hoyos homogéneamente distribuidos sobre la matriz del azúcar (Fig. 3A), estructura parecida a la encontrada para NCs de policaprolactona (PCL) liofilizadas con polivinilalcohol (PVA) [28].

Las NCs bicapa CS/DS mantuvieron su tamaño de partícula (≈ 200 nm) tras su almacenamiento en forma liofilizada durante la duración completa del experimento (12 semanas) (Fig. 3B). Sin embargo, se observó un importante incremento del tamaño de partícula de las NCs CS monocapa cargadas con IutA, desde 270 nm antes de la liofilización, a más de 400 nm tras dicho proceso. Estos resultados respaldan la hipótesis de que la capa adicional de DS tiene un papel protector. De forma destacable, con respecto a la eficacia de asociación, la cantidad de proteína unida permanece constante en las formulaciones liofilizadas durante, al menos, 90 días (Fig. 3C). Estos resultados convertirían a nuestra potencial nanovacuna en una vacuna termoestable [29], evitando la necesidad de mantener la cadena de frío, una característica particularmente deseable cuando se considera su uso en países en desarrollo.

Las NCs en suspensión, liofilizadas previamente o no, fueron incubadas en PBS-Tween® 80 (0.02% p/p) a 37 ºC. Los resultados, mostrados en la Fig. 3D, indican que, cuando el antígeno se atrapa en las NCs bicapa, tiene una liberación más sostenida que cuando se asocia a las NCs monocapa. Esta diferencia es incluso mayor en las formulaciones liofilizadas. En este último caso, las NCs monocapa liberan alrededor del 100% del antígeno durante las 4 primeras horas, mientras que el nanosistema bicapa libera menos del 35% durante el mismo tiempo.

A pesar de la abundante información a cerca de los perfiles de liberación desde micro y nanopartículas pensadas como formulaciones de una única dosis [8,30–33], en el caso de los nanovehículos pensados para dirigir los antígenos hacia las células dendríticas (DCs) y lograr el consiguiente efecto adyuvante, tales como las NEs o las NCs, la información es limitada. Aunque los datos de las liberaciones *in vitro* no se pueden extrapolar a las condiciones *in vivo*, tienen interés en el sentido de que nos permiten excluir la posibilidad de una liberación incontrolada y prematura tras la inyección.

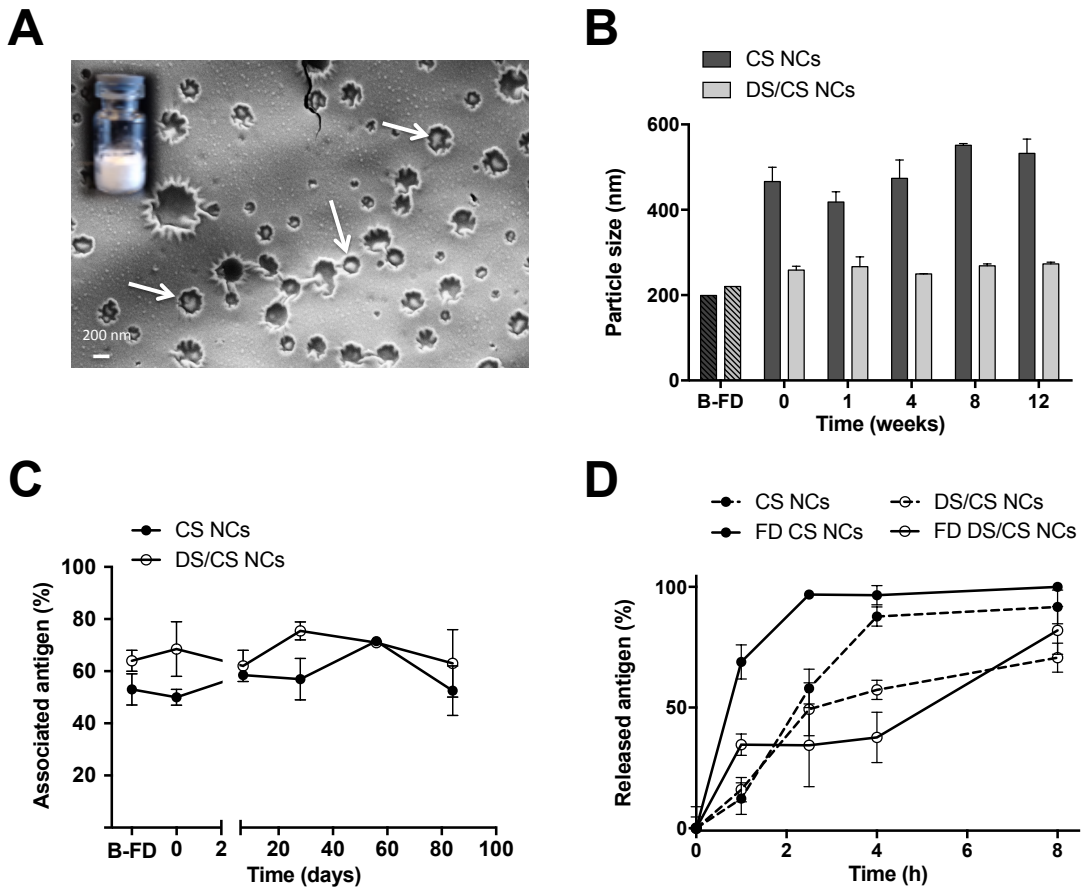

Figura 3. Estructura microscópica, propiedades físico-químicas, eficacia de asociación y liberación del antígeno de las nanocápsulas (NCs) liofilizadas. Imágenes de microscopía electrónica de barrido de emisión de campo (FESEM) de las NCs bicapa liofilizadas con 10% de sacarosa. Las flechas señalan algunas NCs contraídas (A). Estabilidad de las NCs monocapa y bicapa liofilizadas durante, al menos, 3 meses de almacenamiento a temperatura ambiente con respecto al tamaño de partícula (B) y la asociación del antígeno (C) tras su resuspensión. El estudio de la liberación del antígeno IutA desde las NCs monocapa y bicapa, previamente o no liofilizadas (FD), se llevó a cabo en PBS Tween® 80 0.02 % (p/p) a 37 ºC (D). Los resultados se muestran como la media ± desviación estándar de 3 triplicados.

1.3. Estudios *in vitro* en células

Previamente a los estudios *in vivo*, la citotoxicidad de los nanosistemas fue evaluada *in vitro* empleando la línea celular murina de macrófagos (MΦs) RAW 264.7. Se observó

una reducción dosis-dependiente de la viabilidad de las células, tanto para las NCs monocapa como para las bicapa. En el caso de las NCs CS, la viabilidad de los MΦs se redujo paulatinamente a partir de 150 μg/mL. Este valor fue mayor para las NCs DS/CS, con síntomas de toxicidad a partir de 100 μg/mL. Sin embargo, las diferencias entre los valores de toxicidad de ambos prototipos no alcanzaron significación estadística. La dosis letal 50 (DL50) calculada fue de, aproximadamente, 300 μg/mL para las NCs CS y de 200 μg/mL para las NCs DS/CS. Estos valores están dentro del rango de los encontrados para NCs de CS [15] y de protamina [13].

Los estudios de citometría de flujo revelaron que ambos tipos de NCs, con una o dos capas poliméricas, interaccionaron en gran medida con los MΦs, resultado que fue confirmado con imágenes de microscopía confocal.

Posteriormente se determinó la producción de distintas citocinas (IFN-γ, IL-1β, IL-2, IL-4, IL-5, IL-6, IL-8, IL-10, IL-12 p70, TNF-α y TNF-β) en células sanguíneas mononucleares periféricas (PBMCs) de donantes sanos, tras su exposición a un rango de concentraciones de NCs desde 50 a 400 μg/mL durante 24 h. Los resultados de este estudio muestran que las NCs blancas no estimulan la producción de citocinas. Existen publicaciones con resultados similares referentes a las NCs CS, a pesar del hecho de que mostraron un efecto adyuvante *in vivo* significativo y específico frente al antígeno de la hepatitis B que asociaban [15]. Discutiremos esto en más detalle en la sección 3.

1.4. Ensayos *in vivo*

Para evaluar la influencia de la composición y de la disposición estructural (NCs monocapa *vs.* bicapa) de los nanosistemas *in vivo*, se evaluó la respuesta inmunitaria humoral provocada por las distintas formulaciones en ratones. Los ratones fueron inmunizados por vía subcutánea con las NCs cargadas (monocapa y bicapa) recién preparadas, o con sólo la proteína IutA derivada de *E. coli*. Como control positivo, la proteína fue administrada conjuntamente con el adyuvante Alum, estándar de referencia para la vacunación subcutánea. Los grupos control adicionales consistieron en animales no inmunizados (PBS) o inmunizados solamente con Alum. Como era de esperar, la proteína IutA purificada, por sí sola, no pudo generar niveles de IgG significativos, al igual que los grupos tratados solamente con Alum o con PBS. Por otro lado, las NCs monocapa cargadas con IutA provocaron una respuesta inmunitaria similar a la generada cuando la proteína fue administrada con Alum (Fig. 4). Estos resultados concuerdan con datos anteriores referentes a NCs CS, que habían demostrado un efecto adyuvante similar al Alum [7]. Además, el resultado de las NCs bicapa, racionalmente diseñadas, mejoró los valores tanto de las NCs monocapa como del Alum, causando un incremento significativamente mayor de los niveles de IgG.

Por lo tanto, los resultados indican que la protección del antígeno con una segunda capa polimérica, no sólo no reduce la captación por macrófagos, sino que

ofrece ventajas en cuanto a una estabilidad incrementada y unas propiedades físico-químicas adecuadas, permitiendo que el antígeno sea eficazmente procesado y presentado por las células presentadoras de antígenos (APCs).

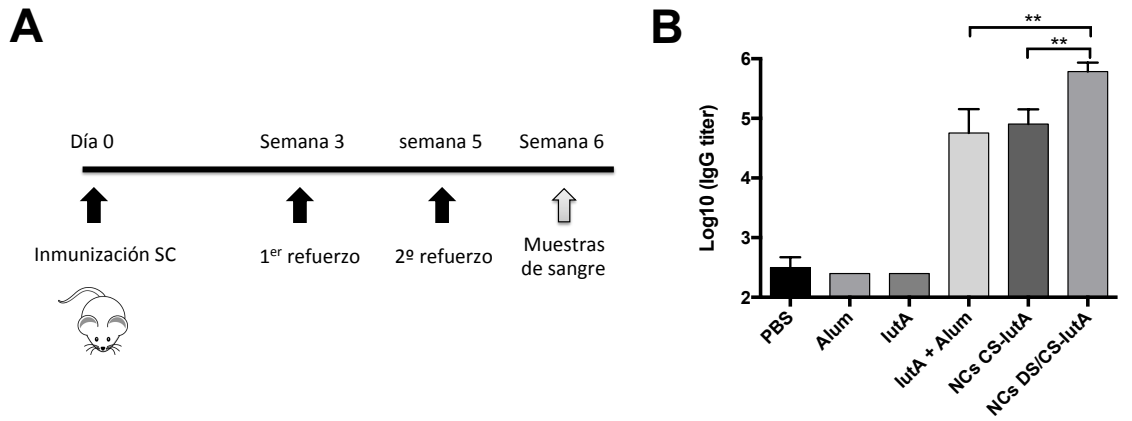

Figura 4. Evaluación *in vivo* de las nanocápsulas (NCs) bicapa cargadas con antígeno. Cronología del protocolo de inmunización para evaluar la respuesta humoral generada por los distintos prototipos desarrollados en ratones (A). Niveles de IgG observados tras la inmunización subcutánea (semanas 0, 3 y 5) de IutA adsorbida sobre Alum o IutA cargada en NCs monocapa de quitosano (CS) o bicapa (DS/CS) (total de 15 µg de IutA por animal). PBS y Alum fueron usados como control (B). Los resultados se muestran como la media ± desviación estándar (n = 10). ** denotan diferencias significativas entre los grupos ($p < 0,01$).

En resumen, el nanosistema de doble-cubierta fue capaz de proteger el antígeno IutA de *E. coli* y controlar su liberación de forma más eficiente que las NCs monocapa. Además, el candidato a nanovacuna demostró tener una buena termoestabilidad en su forma liofilizada. Los resultados positivos observados *in vivo*, en términos de respuesta específica de IgGs dirigidas frente a IutA, resaltan el valor de la tecnología desarrollada. Sin embargo, a pesar de los buenos resultados obtenidos con estas NCs poliméricas, creemos que todavía hay margen de mejora. De hecho, el consenso actual es que, para obtener un progreso significativo en el campo de las vacunas, es necesario hacer un diseño de los nanovehículos de antígenos de una forma más racional. Además de su composición, las propiedades físico-químicas de los nanosistemas, tales como el tamaño de partícula y la carga superficial, han demostrado ser críticos para el resultado final de las nanovacunas [34–36]. Sin embargo, previamente a estudiar la influencia de estos parámetros en el comportamiento biológico de las NCs, se necesitan nuevos métodos capaces de producir nanosistemas con un tamaño y carga superficial controlables y definidos. Por esta razón, el siguiente objetivo de este trabajo ha sido investigar las posibilidades tecnológicas que el método de desplazamiento de disolvente ofrece para preparar NCs hechas a medida.

2. Estudio de las posibilidades tecnológicas de las NCs poliméricas

Desde un punto de vista tecnológico, es fundamental disponer de métodos versátiles que permitan el control del tamaño de partícula de los nanosistemas, ya que esta propiedad influye en su interacción con los sistemas biológicos [37–39].

2.1. Modificación del tamaño de partícula de las NCs

La producción de nanosistemas con tamaños inferiores a 100 nm puede ser de interés en el campo de las vacunas, ya que dichos tamaños favorecen el drenaje linfático [40,41].

Estudios previos en nuestro grupo de investigación demostraron que la dilución de Miglyol® 812 y lecitina en la fase orgánica y la adición gota a gota de esta fase sobre la fase acuosa conllevaba un descenso significativo en el tamaño medio de las NCs obtenidas, de aproximadamente 200 a 100 nm [42]. Basándonos en este resultado, llevamos a cabo un diseño experimental en el cual mantuvimos constante la masa y el ratio de los componentes de las NCs y variamos los siguientes parámetros: i) el volumen de la fase orgánica (etanol), ii) el volumen de la fase acuosa y iii) la forma de adicionar la fase orgánica sobre la acuosa (vertiendo *vs* inyectando). Como composición estándar de las NCs elegimos la indicada en la sección 1, que consistía en una combinación de CS, vitamina E y lecitina. La curva de respuesta, presentada en la Fig. 5, muestra que los tamaños de partícula más pequeños fueron obtenidos con los volúmenes de etanol (5 mL) y de agua (15 mL) más grandes, confirmando que, como era de esperar, la dilución de los componentes lipófilos e hidrófilos en sus respectivas fases favorece la formación de partículas de tamaños menores. Por otro lado, la inyección de la fase orgánica a través de una aguja tuvo un impacto claro en el tamaño de partícula de las NCs cuando se compara con la misma técnica pero vertiendo simplemente una fase sobre la otra. En este punto, quisimos probar si el efecto de reducción de tamaño por inyección era o no dependiente de la composición del sistema. Para ello, ensayamos distintas combinaciones de aceites, tensoactivos y polímeros (Fig. 5B). Se prepararon NEs y NCs tanto positivas como negativas vertiendo la fase orgánica sobre la acuosa o mediante inyección, manteniendo fija la concentración de los componentes. Se observó una reducción considerable del tamaño de partícula para las formulaciones en las que se empleó el método de inyección (entre 50 y 115 nm de diferencia de tamaño) (Fig. 5C), confirmando así que esta modificación puede ser aplicada a distintas composiciones.

Los mecanismos moleculares detrás de la nanodispersión lograda mediante la técnica de desplazamiento de disolvente han sido atribuidos a las turbulencias interfaciales entre la fase disolvente y no-disolvente, conocidas como el efecto Marangoni, que lleva a la separación del sistema en dos fases [43,44]. Otros autores atribuyen la formación de nanoprecipitados al llamado “efecto ouzo” [45,46]. En el

caso de las NCs poliméricas esto significa que la supersaturación local del aceite lleva a una nucleación espontánea en forma de diminutas nanogotas aceitosas. Los núcleos formados crecen por agregación o por difusión de las moléculas de aceite de las proximidades. El crecimiento continúa hasta que la concentración de aceite alcanza la concentración de equilibrio en la saturación [47]. De forma experimental, para obtener tamaños de partícula pequeños deberíamos favorecer una formación de núcleos rápida y un crecimiento de partícula pequeño o nulo. Esto se puede lograr, como se indica en la Fig. 5, disminuyendo la concentración de aceite, para evitar el crecimiento de las partículas, y/o inyectando la fase disolvente sobre la no-disolvente, lo que ocasiona turbulencias y crea múltiples núcleos pequeños de nanogotas de aceite.

A

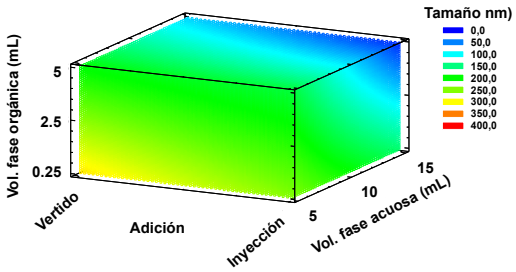

B

Sistema	Polímero	Tensoactivo	Co-tensoactivo	Aceite
NE 1	-	Lecitina	-	Vitamina E
NE 2	-	TPGS	Colato	Vitamina E
NE 3	-	Tween® 80	-	Vitamina E
NE 4	-	Lecitina	-	Escualeno
NE 5	-	Lecitina	-	Miglyol® 812
NE 6	-	Lecitina	CTAB	Vitamina E
NC 1	Alginato	Lecitina	CTAB	Vitamina E
NC 2	Hialuronato	Lecitina	CTAB	Vitamina E
NC 3	Quitosano	Lecitina	-	Vitamina E
NC 4	Poliarginina	Lecitina	-	Vitamina E

C

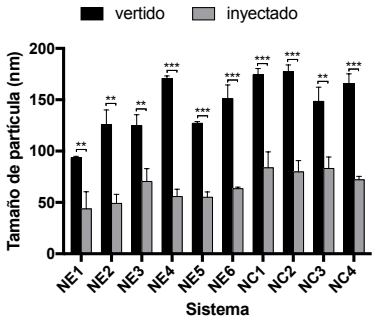

Figura 5. Influencia de distintos parámetros de producción sobre el tamaño de partícula de las nanocápsulas (NCs) poliméricas. Los volúmenes de las fases orgánica y acuosas, la forma de adicionar la primera fase sobre la segunda (vertiendo o inyectando) fueron modificados. Representación del tamaño de partícula de las NCs resultantes frente a estos tres parámetros (A). Se testaron diferentes combinaciones de aceites, tensoactivos y polímeros para producir nanoemulsiones (NEs) y NCs vertiendo o inyectando la fase orgánica sobre la fase acuosa (B). Las diferencias en el tamaño de partícula de las NCs y NEs obtenidas con esta modificación se muestran en C. Para la comparación de tamaños se empleó un test t múltiple. ** y *** denotan diferencias significativas entre las muestras ($p < 0.01$ y $p < 0.001$ respectivamente).

2.2. Modificación de la superficie de las NCs multicapa

A parte del tamaño de partícula, la carga superficial y la composición de los nanosistemas son también parámetros importantes que influyen en su destino final *in vivo* [48,49]. En este sentido, la técnica capa-a-capa (LbL) permite la modificación de la superficie de los nanosistemas y la incorporación de nuevos compuestos en la formulación [50–52]. En la sección 1, hemos visto el interés de combinar la técnica de LbL con el método de desplazamiento de disolvente para producir NCs DS/CS bicapa para la protección y liberación controlada de un antígeno. El objetivo de los siguientes experimentos fue extender el empleo del proceso de autoensamblaje a una variedad de polímeros (NCs bicapa) y determinar el máximo número de capas que se pueden ensamblar sobre un núcleo oleoso (NCs multicapa).

Para la preparación de los nanosistemas bicapa, las NCs monocapa de CS/lecitina/vitamina E fueron incubadas con diferentes ratios de polianiones sulfatados y carboxilados: hialuronato (HA), alginato (Alg) y condroitín sulfato (ChS). El ratio masa/masa al cual se produce la inversión de la carga de las NCs está, en último término, determinado por la carga relativa del segundo polímero. En el caso de los polímeros testados, la carga por monómero a pH 7 es: HA (0,5) < Alg (1) = ChS (1). Estas cargas explican por qué con una pequeña cantidad de ChS y Alg (ratio CS:polímero 1:0,25), se observa ya una importante inversión en el potencial-ζ, significativamente más baja comparada con la cantidad requerida de HA (ratio CS:HA 1:1). Estos resultados están en consonancia con lo encontrado para la formación de la bicapa CS/DS (sección 1) donde un ratio de CS:DS de 1:0,1 invertía el potencial-ζ, gracias a la elevada carga negativa por monómero del DS (2,3).

Basándonos en las NCs bicapa anteriormente descritas, quisimos extender esta metodología para diseñar NCs multicapa. Santos *et. al.* desarrollaron una estrategia similar para el autoensamblaje LbL de polielectrolitos con el fin de encapsular fármacos de baja solubilidad [53]. En su caso, la deposición de los polímeros fue asistida por ultrasonidos. Esto podría ser un problema en el caso de trabajar con biomoléculas lábiles. El grupo del prof. Benoit, experto en NCs lipídicas [54,55], desarrolló NCs CS/DS multicapa (6 capas) empleando el método de inversión de fase, que necesita un paso de purificación por filtración de flujo tangencial entre la deposición de cada capa [25]. Nuestro objetivo fue determinar el máximo número de capas que se podría construir sobre el núcleo oleoso sin pasos de purificación y sin el uso de altas energías que pudiesen desnaturalizar las moléculas lábiles.

De nuevo, en el proceso de diseño de las NCs multicapa, el parámetro crítico a considerar fue el ratio en masa entre los polímeros de carga opuesta (CS y DS). Este ratio debe de ser calculado empíricamente para asegurar un recubrimiento eficaz con la mínima cantidad posible de polímero libre [56], evitando así que dicho polímero pueda contribuir a la formación no deseada de subpoblaciones de nanocomplejos con el polímero añadido para construir la siguiente capa. Empleando esta técnica, se construyeron hasta 5 capas de polímeros sobre la NE, sin la necesidad de pasos de

purificación. El ratio escogido DS:CS fue de 0,5:1 para las dos primeras capas; para las capas 3ª (CS), 4ª (DS) y 5ª (CS) el ratio polímero:CS-1ª-capa fue 1:1, con un ratio final $CS_{5ª}/DS_{4ª}/CS_{3ª}/DS_{2ª}/CS_{1ª}$ 1:1:1:0,5:1. Con cada nueva capa de polímero añadida se observó una inversión en el potencial-ζ: desde un valor altamente positivo, cuando el CS estaba en la capa externa, a altamente negativo, cuando el DS estaba en la capa externa (Fig. 6). Además, la adición de CS incrementó el tamaño de partícula al recubrir la NE o las NCs, tal y como era de esperar. Por el contrario, el DS redujo ligeramente el tamaño de partícula al recubrir las NCs de CS, probablemente, como se discutió en la formación de la bicapa, porque su carga altamente negativa causa una contracción de los polímeros.

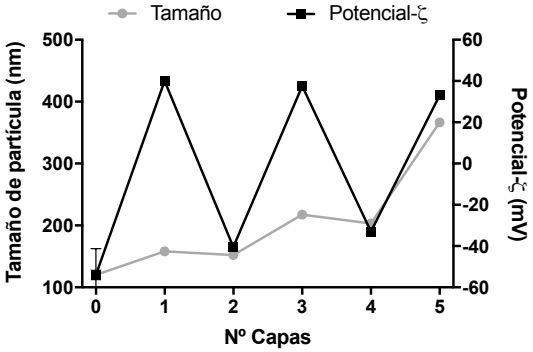

Figura 6. Formación de nanocápsulas (NCs) multicapa. Evolución del tamaño de partícula y del potencial-ζ en función del número de capas de quitosano y sulfato de dextrano.

Hemos demostrado la versatilidad de las NCs poliméricas en términos de composición y propiedades físico-químicas. En particular, las NCs con una o múltiples capas de polímero, pueden ser producidas con un tamaño entre 50 y 500 nm, aproximadamente. Hay que resaltar que estas NCs pueden ser producidas mediante la técnica de desplazamiento de disolvente empleando una cantidad mínima de etanol, evitando así la necesidad de su posterior eliminación.

3. Comportamiento comparativo de las NCs poliméricas con respecto a su interacción con células inmunitarias, biodistribución y direccionamiento a linfa. NCs de Inulina

Aprovechando las nuevas posibilidades tecnológicas que desarrollamos para las NCs poliméricas en la sección anterior, el siguiente objetivo de este trabajo fue tratar de entender la importancia del tamaño de partícula y el polímero de cubierta de las NCs en su interacción con las células inmunitarias, su biodistribución y su direccionamiento al sistema linfático. De forma paralela, quisimos explorar un nuevo polímero, inulina (INU) modificada hidrofóbicamente, como un polímero interesante para la producción

de NCs versátiles, comparándolas con NCs de CS, similares a las descritas en la sección 1.

La INU, formada por cadenas de polifructosa y con una glucosa terminal, ha sido empleada en la industria alimentaria y farmacéutica como agente estabilizante, teniendo estatus GRAS (generalmente reconocido como seguro) [57]. De hecho, el adyuvante Advax^{TM}, constituido por delta-INU en forma microcristalina, ha sido testado en ensayos clínicos de vacunas frente a la hepatitis B, gripe y alergia, entre otros [58,59]. A diferencia de otros adyuvantes, la INU no activa receptores del sistema inmunitario innato tales como TLRs o el inflamasoma. Por su parte, la delta-INU modula directamente la función de las DCs, dando lugar a una presentación de antígenos a las células T y B mejorada a través de un mecanismo no inflamatorio [60,61]. Por lo tanto, teniendo en cuenta esta información y nuestra experiencia dilatada en el diseño de NCs poliméricas [10,62–66], nuestro objetivo fue diseñar y caracterizar nuevas NCs INU y compararlas con NCs CS. Para definir las propiedades físico-químicas de las NCs tuvimos en cuenta estudios previos que señalan que el tamaño y la carga de los nanovehículos son determinantes en su biodistribución y, particularmente, para su acceso al sistema linfático [40,41,67]. Por lo tanto, nuestra estrategia fue producir NCs INU con dos tamaños de partícula diferentes (70 y 250 nm) y comparar su comportamiento *in vitro* e *in vivo* con los de NCs CS de tamaños similares, pero cargadas positivamente. Los estudios *in vitro* se llevaron a cabo en las APCs más importante: MΦs y DCs. Por otro lado, el comportamiento *in vivo* fue evaluado en peces cebra, en términos de toxicidad y diseminación, y en modelo murino, para el drenaje linfático.

3.1. Desarrollo y caracterización de nanosistemas basados en inulina (INU)

La INU modificada con cadenas C12 ha sido empleada en investigación para incrementar la solubilidad de fármacos lipófilos [68–74]. Sin embargo, su potencial para el desarrollo de nanovehículos de liberación e fármacos apenas ha sido estudiado. Empleando vitamina E, un inmunoestimulante potencial, como núcleo oleoso, se ensayaron inicialmente distintos ratios INU:vitamina E para seleccionar la mejor combinación de componentes capaz de producir NCs estables y con baja polidispersidad. Más tarde, y aplicando las modificaciones al método de desplazamiento disolvente que hemos discutido en la sección 2 (inyección de la fase orgánica a la fase acuosa), obtuvimos NCs INU de tamaño de partícula pequeño (S < 100 nm). Empleando un procedimiento similar se desarrollaron NCs CS de tamaños similares y con la misma composición de núcleo (Fig. 7).

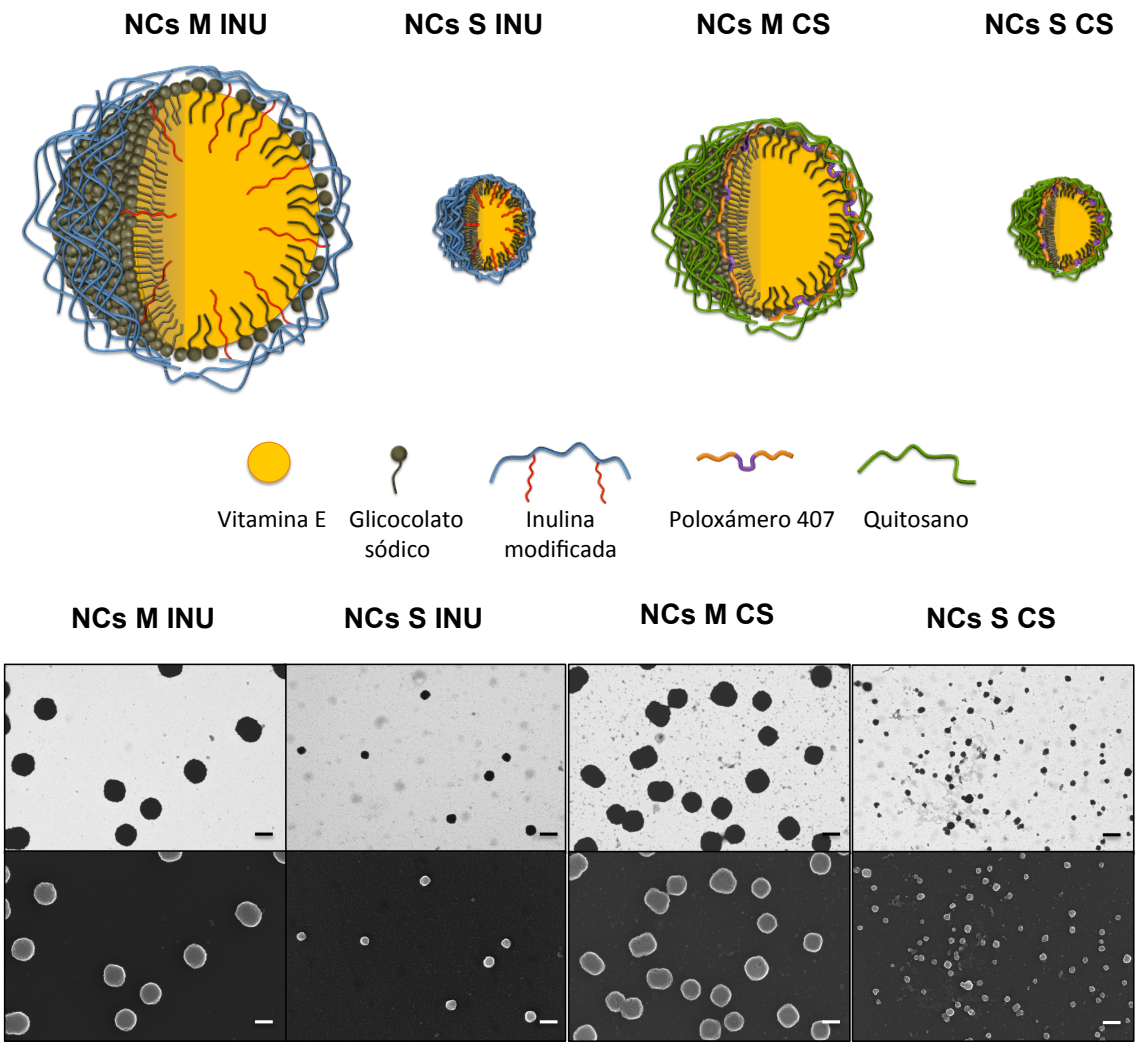

Figura 7. Nanocápsulas (NCs) poliméricas desarrolladas en este estudio. NCs de inulina (NCs INU) y de quitosano (NCs CS) de dos tamaños de partícula distintos, pequeñas (S < 100 nm) y medianas (M > 100 nm). La escala de tamaños entre los prototipos se ha mantenido en la imagen. En la parte inferior, las imágenes de microscopía electrónica de barrido de emisión de campo de los distintos nanosistemas utilizando un detector STEM (primera fila) e InLens (segunda fila). Todas las escalas corresponden a 200 nm.

Se emplearon distintas técnicas para determinar el tamaño de partícula de los nanosistemas (Tabla 2). El análisis de seguimiento de nanopartículas (NTA), que correlaciona el movimiento Browniano de partículas individuales gravadas con un cámara con su tamaño de partícula, complementa las medidas hechas con dispersión dinámica de luz (DLS), donde se relaciona la media de las fluctuaciones en la luz dispersada con ese movimiento. Como consecuencia, el NTA ofrece una mayor resolución, especialmente cuando las muestras no son monodispersas. En este estudio, el tamaño de partícula de las NCs S resultó ser similar empleando ambas técnicas (entre 70 y 80 nm, aproximadamente). Sin embargo, el tamaño de partícula de las NCs M ofreció resultados distintos en función de la técnica, con tamaños de partícula por NTA unos 40 nm más pequeños que por DLS (246 *vs* 197 nm para las NCs

M INU, y 172 *vs* 128 nm para las NCs M CS, respectivamente). En el caso de las NCs M INU, también hemos observado una muestra con polidispersión considerable, con una población de NPs en el rango de 100 – 300 nm. Las imágenes FESEM, empleando detectores STEM e InLens, corroboraron las diferencias en el tamaño de partícula de las NCs S y M. La estructura esférica de las NCs CS e INU fue similar, independientemente de la naturaleza del polisacárido de cubierta (Fig. 7).

Tabla 2. Composición y propiedades físico-químicas de las nanocápsulas (NCs) de quitosano (CS) e inulina (INU) de dos tamaños de partícula diferentes (pequeñas, S < 100 nm y medianas, M > 100 nm).

Nanosistema	**NCs S CS**	**NCs M CS**	**NCs S INU**	**NCs M INU**
Polímero	Quitosano	Quitosano	Inulina modificada	Inulina modificada
Tensoactivo	Poloxámero 407	Poloxámero 407	Inulina modificada	Inulina modificada
Aceite	Vit. E	Vit. E	Vit. E / glicerina	Vit. E / glicerina
Tamaño (nm) DLS	72 ± 5	172 ± 11	69 ± 6	246 ± 16
Tamaño (nm) NTA	76 ± 19	128 ± 30	81 ± 27	197 ± 74
PDI	0,16	0,11	0,18	0,12
Potencial-zeta (mV)	+ 37 ± 4	+ 34 ± 4	- 33 ± 8	- 25 ± 11

* Co-tensoactivo = glicocolato, en todos los casos

3.2. Estudios celulares *in vitro*

Las DCs y MΦs son las principales APCs de nuestro sistema inmunitario. Los MΦs son elementos clave del sistema inmunitario innato. Están especializados en capturar y destruir sustancias extrañas, microbios y deshechos celulares. Los MΦs también ayudan a iniciar la inmunidad adaptativa reclutando otras células inmunitarias y también pueden presentar antígenos a células T. La última función es la principal función de las DCs, que, en su estado inmaduro, patrullan por todo el cuerpo para capturar patógenos y elementos extraños. Una vez activadas, viajan a los nódulos linfáticos (LNs) donde procesan y presentan antígenos a las células T y B, generando una respuesta inmunitaria.

3.2.1 Citotoxicidad

Como se muestra en la Fig. 8, las NCs CS resultaron más tóxicas que las NCs INU de forma significativa en DCs y con la misma tendencia en los MΦs, siendo las NCs INU M

las que mostraron menor toxicidad. Con respecto al tamaño de partícula, aunque las diferencias sólo fueron significativas para NCs INU en MΦs, pudimos observar la misma tendencia para el resto de sistemas en ambas células, siendo las NCs S más tóxicas que las M. En el caso de los MΦs, a bajas concentraciones encontramos un efecto proliferativo de las NCs, razón por la cual los valores de mortalidad se representan como negativos. A concentraciones mayores de 200 μg/mL la mortalidad de las células comienza a incrementarse de una manera dosis-dependiente.

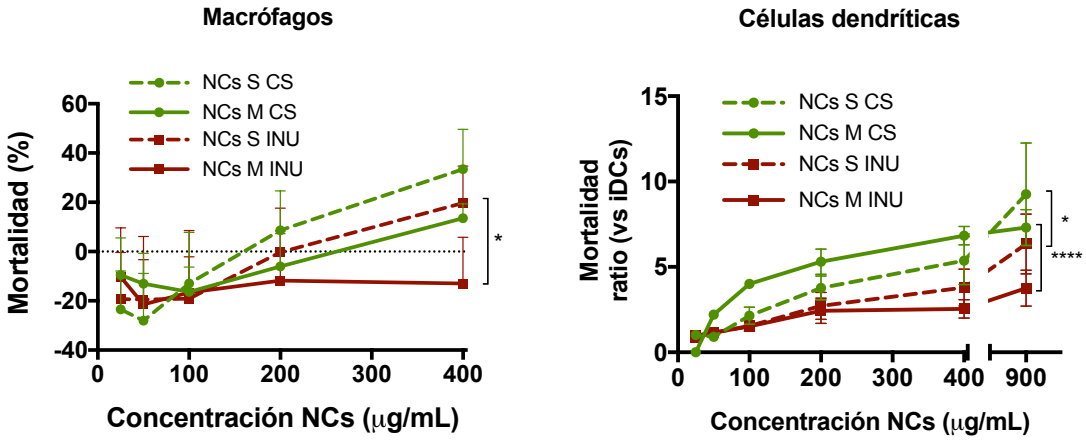

Figura 8. Citotoxicidad *in vitro* de los distintos nanosistemas. Nanocápsulas de inulina (NCs INU) y de quitosano (NCs CS) de dos tamaños distintos: pequeñas (S < 100 nm) y medianas (M > 100 nm). La toxicidad fue evaluada en macrófagos murinos RAW por MTS y en células dendríticas inmaduras (iDCs) por citometría de flujo usando un marcador vital. Los resultados de citometría de flujo están expresados como el ratio entre el porcentaje de iDCs muertas al ser incubadas con NCs *vs* el porcentaje de iDCs muertas al ser incubadas con medio solo. Para el análisis estadístico se calculó el área bajo la curva de cada nanosistema y las diferencias entre el tamaño de partícula (S *vs* M) y el polímero de cubierta (CS *vs* INU) fueron analizadas empleando un ANOVA unidireccional seguido por un test Tukey. Los niveles de significación fueron * $p < 0.05$ y **** $p < 0.0001$.

3.2.2. Interacción de las NCs con las células inmunitarias

Para determinar si la toxicidad está relacionada cuantitativamente con la interacción celular, las células se analizaron por citometría de flujo después de su incubación con los sistemas marcados con DiD, a una dosis no tóxica. Los análisis de citometría de flujo indicaron que casi el 100% de los MΦs y las DCs incubados con los distintas NCs resultaron DiD+, con la excepción de NCs M INU que presentó valores más bajos (Fig. 9). Si consideramos la intensidad media de fluorescencia, los análisis indican distintos comportamientos para las DCs y los MΦs. En concreto, en los MΦs, la toxicidad se correlaciona con el hecho de que los tamaños pequeños y las NCs con carga positiva interaccionan en mayor medida con ellos. Curiosamente, en el caso de las DCs, el comportamiento de todos los sistemas fue similar, siendo las NCs S INU las que mostraron valores de fluorescencia mayores. La tendencia general de estos estudios

fue que tanto los MΦs como las DCs capturaron, de forma preferencial, las partículas de menor tamaño.

El enfoque clásico respecto a la captura de NPs por parte de células inmunitarias, principalmente basado en estudios *in vitro*, sugería que las DCs ingerían preferentemente NPs pequeñas, en el rango viral (20 – 200 nm), mientras que los MΦs preferían tamaños más grandes, de tamaño bacteriano (500 – 2000 nm) [75–77]. Sin embargo, estudios recientes han cuestionado esta afirmación y la tendencia actual es considerar que las NPs pequeñas pueden también ser capturas por MΦs de forma eficaz. Además, la preferencia por partículas más o menos grandes puede ser contrarrestada con otros parámetros, tales como la composición del nanosistema. Por ejemplo, la captura de NPs CS por MΦs murinos demostró ser ligeramente mayor para partículas de 300 nm que para 150 nm [78]. Para NPs de PLGA, se observó una captura tamaño-dependiente en el rango 200 – 1000 nm, siendo las NPs de mayor tamaño las más internalizadas [79]. Sin embargo, esta tendencia no se observó al comparar NCs lipídicas de tamaños muy pequeños (25, 50 y 100 nm), donde la internalización fue similar independientemente de su tamaño. Otros autores publicaron que la captura máxima de NPs de polipirrol [80] y óxido de hierro recubiertas de polivinilpirrolidona [81] estaba en la región entre 10 y 100 nm.

En el caso de las DCs, la mayor parte de la investigación con respecto a la captura de NPs sugiere que los tamaños más pequeños son más fácilmente capturados [82,83], de forma similar a lo encontrado en este estudio.

Con respecto a la carga superficial, podríamos esperar que las partículas positivas interaccionasen en mayor medida debido a la carga negativa superficial de las células inmunitarias [83–85]. Sin embargo, en este estudio, la preferencia por NCs cargadas positivas fue evidente para MΦs, mientras en que en el caso de las DCs este efecto se pudo observar para las NCs de tamaño medio pero no para las más pequeñas. La mayor captura de las NCs S INU comparadas con las NCs S CS resalta el hecho de que la carga superficial no es el único factor – junto con el tamaño de partícula – que influye en la captura, y que la composición puede tener un papel claro en la interacción partícula-célula. En este sentido, se podría especular que la presencia de poloxámero 407, con cadenas de polietilenglicol, en la superficie de las NCs CS podría apantallar la captura celular [86].

En general, se puede concluir que el tamaño de partícula es un parámetro crítico que influye en la captura celular, especialmente en el caso de las DCs, y que el efecto de la carga superficial podría verse compensado, en el caso de NCs muy pequeñas, dependiendo de su composición.

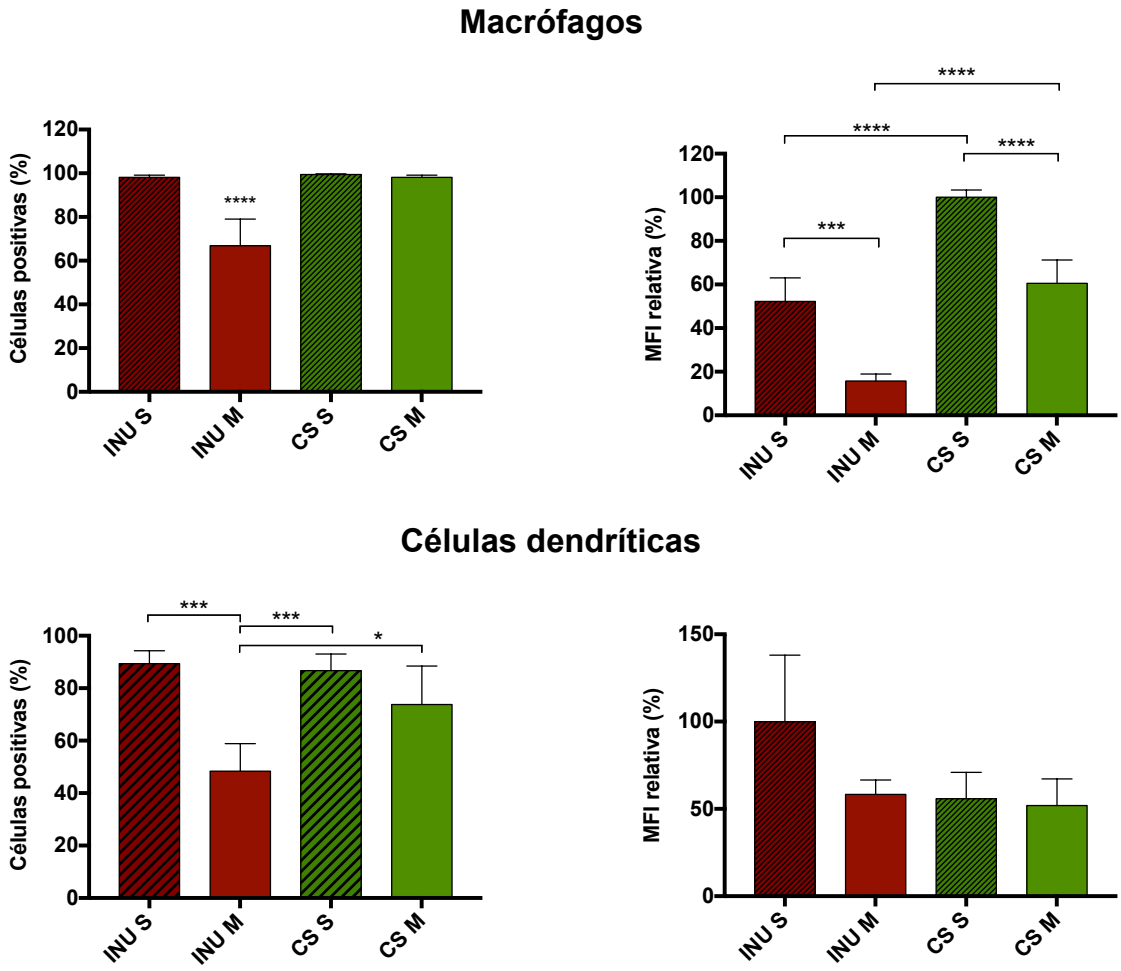

Figura 9. Interacción de los distintos nanosistemas con macrófagos y células dendríticas. La interacción con las células inmunitarias se ha expresado en términos de células positivas (DiD+) e intensidad media de fluorescencia normalizada (MFI) relativa al mayor valor obtenido. Se analizaron nanocápsulas de inulina (NCs INU) y quitosano (NCs CS) de dos tamaños diferentes, pequeño (S < 100 nm) y mediano (M > 100 nm). El análisis estadístico fue hecho empleando un test ANOVA unidireccional seguido de un test Tukey. Los niveles de significación corresponden a * $p < 0.05$, *** $p < 0.001$ and **** $p < 0.0001$.

3.2.3. Cambio en el fenotipo de las DCs

Sabiendo el papel crítico de las DCs en la generación de una respuesta inmunitaria adaptativa, investigamos el tipo de respuesta que las NCs producen en estas células. Se analizaron, por citometría de flujo, distintos biomarcadores de activación tras incubar las DCs con cada uno de los cuatro nanosistemas. Después de 2 h de incubación, ambas NCs CS, S y M mostraron una mayor capacidad de activación de las DCs comparadas con las NCs INU (Fig. 10A y 10B), causando un mayor incremento en la expresión de los marcadores de activación CD80 y CD83. Estudios previos ya habían encontrado la activación de estos dos marcadores en DCs por diferentes NPs CS [87,88]. En el caso de las NCs INU, sólo las partículas pequeñas mostraron un incremento leve en la sobreexpresión de CD83. Estos datos apuntan a la idea de que

las NCs CS son más tóxicas comparadas con las NCs INU, y que la inducción de una mayor muerte celular podría contribuir a la liberación de señales inflamatorias que explicarían una mayor capacidad de activación de las DCs [89].

A continuación, decidimos evaluar si las DCs pre-incubadas con cada uno de los nanosistemas eran capaces de activar linfocitos T CD8+ en un ensayo *in vitro* alogénico (Fig. 10C). La pre-incubación de las iDCs con los distintos nanosistemas incrementó de forma significativa el porcentaje de linfocitos CD8+ activados (cuantificado como células CD28+). De entre todos los nanosistemas evaluados, las NCs S CS presentaron el nivel más alto de respuesta de linfocitos T CD8+. En general, se considera que las NPs de tamaño pequeño (< 200 nm), debido a su semejanza con el tamaño de los virus, se procesan como ellos, siguiendo rutas de endocitosis similares, llevando a una fuerte respuesta de células T CD8+ [90]. Este fue el caso de NPs de poliestireno conjugadas con OVA de 40 – 49 nm, que causaron una mayor producción de IFN-γ inducido por células T CD8+ que partículas iguales de 100 – 120 nm [91]. De forma similar, Tochigi *et al.* publicaron que NPs de sílice amorfas cargadas con OVA, con tamaños 70 – 100 nm provocaron mayores niveles de IL-2 que partículas mayores (> 100 nm), estando los niveles de esta citocina relacionados con la frecuencia de presentación de OVA en MHC-I y, por tanto, de activación de células T CD8+ [92].

Para analizar en mayor medida el tipo de activación que los distintos nanosistemas producen en las DCs, cuantificamos las citocinas que secretaron al medio de cultivo cuando se incubaron con las distintas NCs durante 24 h (Fig. 10D). De nuevo, las NCs CS indujeron en las DCs una mayor secreción de citocinas comparadas con las NCs INU, un resultado que está en consonancia con trabajos previos [88,93,94].

Los resultados *in vitro* sugieren diferencias claras entre las NCs de CS e INU en cuanto a activación de DCs. En comparación con las NCs INU, las NCs CS provocaron una mayor sobreexpresión de distintos marcadores de activación, estimularon mayores niveles de citocinas y activaron una mayor proliferación de células T CD8+ que puede ser explicado, al menos parcialmente, debido a su mayor toxicidad. Sin embargo, estos resultados no implican, necesariamente, que las NCs INU no puedan tener un papel adyuvante *in vivo*. De hecho, Advax® no muestra activación de DCs *in vitro* pero sí lo hace *in vivo*, modulando la función de la DC y aumentando la presentación de antígeno a las células T y B [60,95]. Es de resaltar, que la delta INU ha mostrado ser segura en mujeres embarazadas y en animales jóvenes [96,97], una característica que puede ser atribuida a su mecanismo de acción no inflamatorio.

Con respecto al tamaño de partícula, aunque se encontraron diferencias en términos de interacción, con las NCs S causando un mayor número de células positivas que las M, estas diferencias no se tradujeron en una mayor sobreexpresión de biomarcadores de activación o producción de citocinas. Sin embargo, en el caso de CS, las partículas pequeñas produjeron una mayor proliferación de células T CD8+. Probablemente, la activación no depende de manera lineal con el número de

partículas que puedan entrar en las células (células DiD+), sino que se desata tras alcanzar un umbral de interacción NCs-célula.

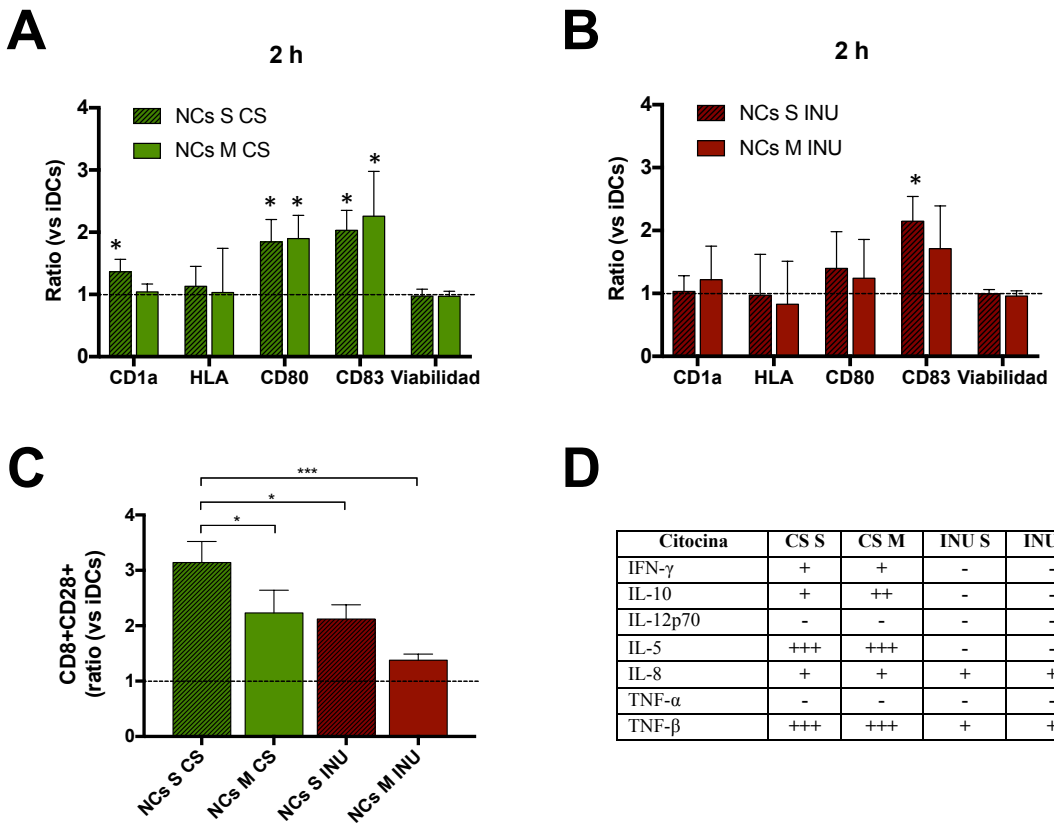

Citocina	CS S	CS M	INU S	INU M
IFN-γ	+	+	-	-
IL-10	+	++	-	-
IL-12p70	-	-	-	-
IL-5	+++	+++	-	-
IL-8	+	+	+	+
TNF-α	-	-	-	-
TNF-β	+++	+++	+	+

Figura 10. Activación de las células dendríticas (DCs) por los distintos tipos de nanocápsulas (NCs). (A, B) Cambio en el fenotipo de las DCs inducido por la incubación con NCs de quitosano (CS) e inulina (INU). Se testaron tamaños de NC pequeño (S < 100 nm) y mediano (M > 100 nm). Los resultados se muestran como el ratio de las iDCs incubadas con NCs vs iDCs incubadas con medio solo. *: ratio significativamente mayor a 1 ($p<0.05$; test T de Student). n.d. No determinado. (C) Se determinó la capacidad de las iDCs pretratadas con NCs para activar linfocitos CD8+ alogénicos mediante citometría de flujo cuantificando la sobreexpresión de CD28. Excepto las NCs M INU ($p=1,0$, ANOVA unidireccional, Bonferroni post hoc) todas las NCs muestran incrementos significativos del porcentaje de linfocitos T CD8+ activados con respecto a las iDCs no tratadas (NCs S CS, $p=0,0001$; NCs M CS, $p=0,006$; NCs S INU, $p=0,012$; ANOVA unidireccional, Bonferroni post hoc)(resultados no mostrados en la gráfica). De las cuatro NCs evaluadas, las NCs S CS mostraron una mayor capacidad de estimulación de linfocitos T CD8+ (ANOVA unidireccional, Bonferroni post hoc). Las diferencias fueron consideradas significativas para * $p < 0,05$, ** $p < 0,01$ and *** $p < 0,001$ and **** $p < 0,0001$. (D) Producción de citocinas secretadas por iDCs después de su incubación con NCs. Los valores se expresaron como el ratio de las citocinas secretadas por las iDCs después de ser incubadas con las NCs entre las citocinas secretadas por las iDCs incubadas en medio sólo. Símbolos: -: ratio ≤ 1; +: ratio 1-2; ++: ratio 2-3; +++: ratio > 3.

3.3. Biodistribución de NCs de inulina y quitosano en peces cebra y su acceso a macrófagos

Durante las 4 primeras semanas de su vida, los peces cebra no han desarrollado una inmunidad adaptativa, permitiendo estudiar la importancia del sistema inmunitario innato. Además, los MΦs de los peces cebra tiene una morfología y funciones similares a sus homólogos mamíferos [98]. Por este motivo, el uso de peces cebra con MΦs marcados ofrece un potente sistema para monitorizar *in vivo* la interacción NPs-células inmunitarias.

Para analizar la influencia del tamaño de partícula y de la cubierta polimérica de los nanosistemas en su biodistribución, se inyectaron las NCs marcadas fluorescentemente por vía intramuscular en embriones de peces cebra con 48 horas post-fertilización (hpf) (Fig. 11A). Se encontraron diferencias claras en cuanto al comportamiento de las NCs con distinto tamaño de partícula. Las NCs S se distribuyeron más y más rápido que las NCs M, extendiéndose por todo el miómero y claramente delimitadas por el miosepto, permaneciendo con elevada intensidad de fluorescencia en los tejidos hasta las 24 horas post-inyección (h) (Fig 11B). Por otro lado, las NCs M apenas se mueven del sitio de inyección a las 4 h pero presentan un mayor aclaramiento después de 24 h, principalmente mediado por MΦs.

Con respecto a la influencia de la composición de las NCs, las NCs CS, especialmente de tamaño medio, mostraron gran capacidad para reclutar MΦs en el sitio de inyección. Por el contrario, las NCs INU no mostraron tal capacidad.

Es de resaltar que las micropartículas de INU, comercializadas como Advax®, tienden a formar un depósito al ser inyectadas y son capturas por los MΦs, que las conducen a los órganos linfoides secundarios [99]. La mayor capacidad de diseminar observada para las NCs S INU y, posiblemente, su capacidad de llegar al sistema linfático de forma más eficaz debido a su tamaño pequeño [100], podrían ser ventajas para provocar una mejor respuesta inmunitaria [36]. Por este motivo, en la siguiente sección analizamos el drenaje linfático de las distintas NCs en un modelo murino.

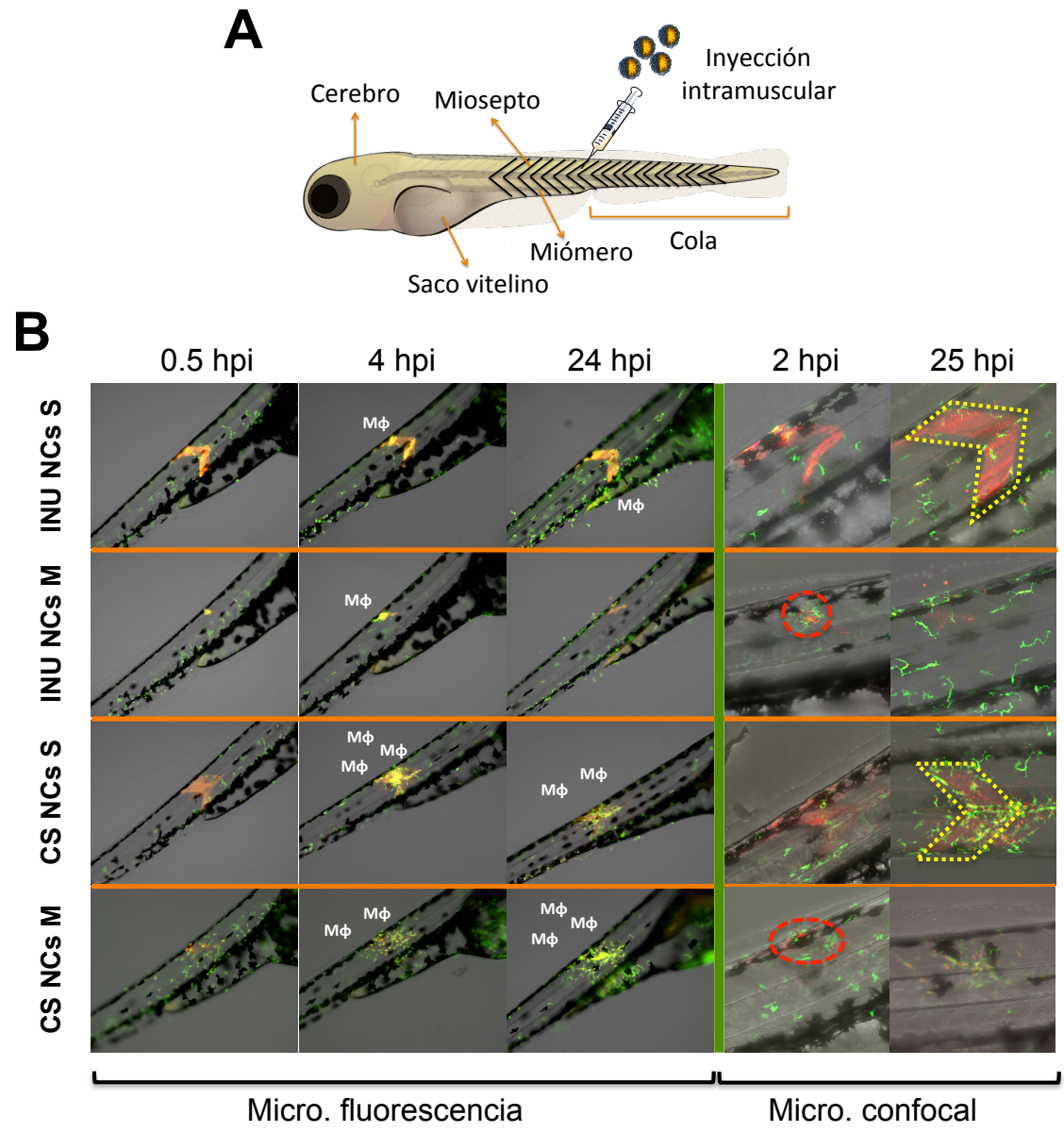

Figura 11. Biodistribución de las nanocápsulas (NCs) en peces cebra. Esquema representativo de los estudios de biodistribución de NCs en embriones de peces cebra (A). Las NCs de quitosano (CS) e inulina (INU) de dos tamaños diferentes (S <100 nm y M >100 nm) fueron administradas de forma intramuscular en embriones de peces cebra con 48 horas post-fertilización (hpf). Las imágenes fueron sacadas a las 0,5, 4 y 24 horas post-inyección (h) con un microscopio de fluorescencia y a las 2 y 25 h con un microscopio confocal (B). Canal rojo: NCs, canal verde: macrófagos, círculo rojo a trazos: baja diseminación desde el lugar de inyección, área amarilla punteada: diseminación a lo largo del miómero, MΦ: reclutamiento de macrófagos. El esquema del embrión de pez cebra fue adaptado de Lizzy Griffiths http://zebrafishart.blogspot.com/.

3.4. Drenaje linfático de NCs de inulina y quitosano en ratones

Como se acaba de señalar, los estudios actuales apoyan la hipótesis de que el libre drenaje de los nanosistemas a los LNs puede mejorar la eficacia de las vacunas [36].

Estas nanoestructuras, normalmente con tamaños de partícula inferiores a 100 nm, han demostrado favorecer la presentación-cruzada cuando interaccionan con las DCs residentes en los LNs, desatando una respuesta celular importante [40,101]. Además, la interacción directa con células B puede mejorar también la parte humoral de la respuesta inmunitaria [102]. Teniendo en mente el panel de NCs que hemos desarrollado en este trabajo, nuestro objetivo ha sido llevar a cabo un estudio sistemático de la influencia del tamaño de partícula (70 *vs* 170-250 nm) y del polímero de cubierta (INU *vs* CS) de las NCs en su drenaje y acumulación en los distintos subtipos de células inmunitarias de los LNs.

Cada uno de los nanosistemas, marcados con DiD, fueron inyectados en las patas de ratones y su llegada al nódulo linfático poplíteo (PLN) evaluada empleando dos técnicas diferentes, la citometría de flujo (Fig. 12A), tras la digestión del LN y su posterior tinción, y mediante microscopía de 2-fotones (Fig. 12B). Esta última es una técnica potente para evaluar las propiedades de las NCs en cuanto a su direccionamiento a linfa, con gran interés en el ámbito de la nanomedicina [15,65,103,104].

Como resultado de estos experimentos (Fig. 12), tras 12 h desde la inyección de las NCs en la pata de los ratones, se observó que los cuatro nanosistemas fueron capaces de llegar al PLN, independientemente de su carga o tamaño. Sin embargo, empleando tanto la citometría de flujo como la 2PM, pudimos observar que las NCs S INU llegaron al PLN de una manera mucho más notable que el resto de prototipos. El menor tamaño de partícula, comparado con las NCs M INU (70 *vs* 250 nm) explica las diferencias en este drenaje. Por otro lado, la mayor acumulación con respeto a las NCs S CS podría estar relacionada con la carga positiva de éstas últimas. En cambio, al analizar ambos tamaños de las NCs CS, su acumulación es similar. Nuestra hipótesis es que la menor diferencia en cuanto al tamaño de las NCs S CS y las NCs M CS (sólo 50 nm por NTA), comparadas con las NCs S INU y NCs M INU (120 nm de diferencia) no es suficientemente grande como para observar una diferencia en el drenaje de las partículas. Finalmente, las NCs M INU son las que presentan una menor acumulación en el PLN. En general, podemos concluir que tanto el pequeño tamaño como la carga negativa fueron factores determinantes para mejorar el drenaje linfático de las NCs S INU.

Si analizamos la biodistribución dentro del LN, la acumulación de las NCs ocurre principalmente en la región medular, probablemente asociada con la presencia de distintas poblaciones de células altamente fagocíticas, tales como los macrófagos medulares (MM) y distintos subtipos de DCs residentes en los LNs. Las imágenes de los PLNs extirpados también mostraron esta misma distribución (Fig. 12C): las NCs marcadas con DiD aparecen en blanco, los folículos se pueden distinguir por la presencia de los macrófagos del seno subcapsular (SSM) (puntos rojos) que cubren esas áreas. En el canal verde, se visualizaron las células de origen mieloide que expresan el receptor CX3CR1. Estos resultados están en consonancia con experimentos

previos [105], que demuestran la acumulación de los nanosistemas en la médula de los LNs.

De forma similar a lo encontrado en este estudio, otros autores observaron el drenaje libre de partículas dentro del intervalo de 10 – 200 nm [106–108], aunque de forma preferente se señalan los 100 nm como límite superior para este drenaje [40,101]. Dentro de este rango, distintos autores han encontrado que el tamaño óptimo para una mayor acumulación en los nódulos linfáticos estaría en el intervalo 20 – 50 nm [82,105,109]. Estos estudios, estarían en consonancia con lo encontrado para las NCs INU, si bien como se ha señalado, los límites de tamaño establecidos no han de ser considerados de modo general ya que la composición superficial de las partículas dicta en gran medida su biodistribución.

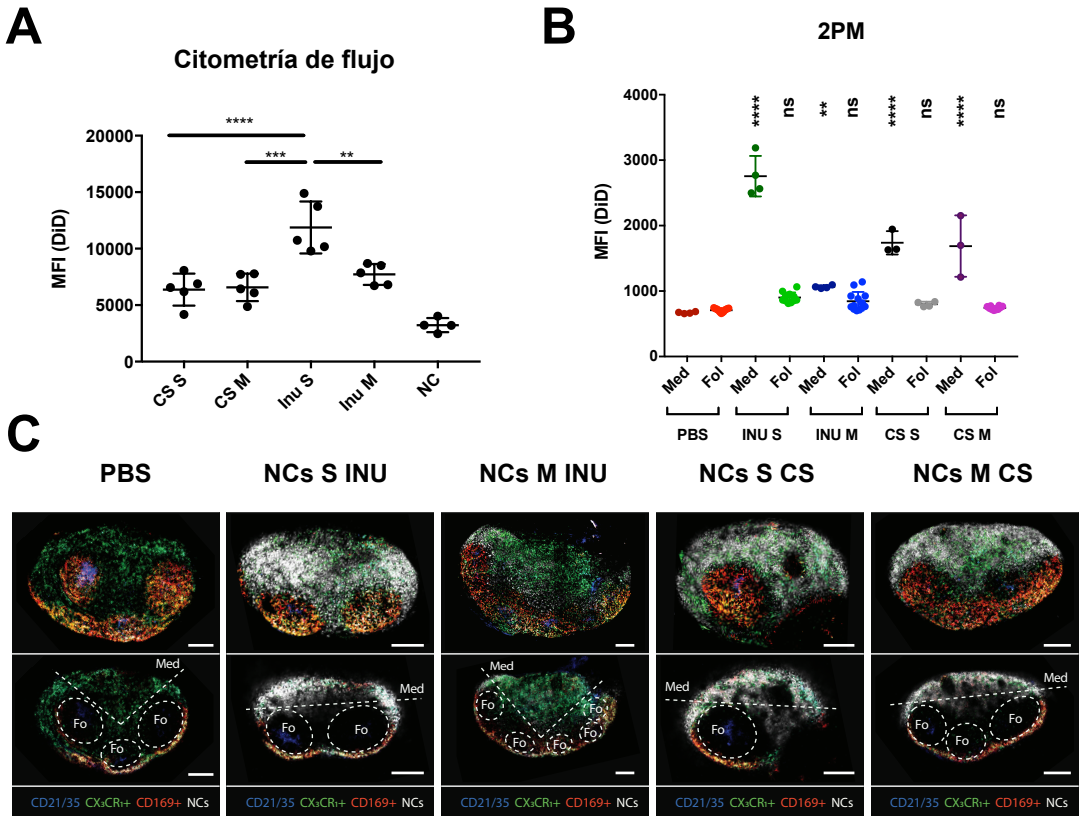

Figura 12: Acumulación de los distintos nanosistemas en el nódulo linfático poplíteo (PLN). Las nanocápsulas (NCs) de quitosano (CS) e inulina (INU) de dos tamaños distintos (S < 100 nm y M > 100 nm), marcadas con DiD, fueron inyectadas en la pata de ratones $CX_3CR_1^{+/gfp}$ y C57BL/6JRj (5 animales por grupo). Después de 12 horas los PLNs de los ratones C57BL/6JRj fueron digeridos y la intensidad media de fluorescencia (MFI) evaluada (A). Los PLNs de los ratones $CX_3CR_1^{+/gfp}$ fueron evaluados usando la microscopía de 2-fotones (2PM). Con esta técnica se evaluó la MFI de cada sistema en la región medular (med) y folicular (fol) (B). En C se muestran imágenes representativas de los PLNs extirpados. El panel superior muestra la proyección máxima y la superposición en z del nódulo linfático, mientras que la parte inferior muestra una capa con las distintas zonas señaladas. Los macrófagos del seno subcapsulares (CD169+) se muestran en rojo, las nanocápsulas (NCs) en blanco, las células dendríticas foliculares (CD21/35+) en azul y en verde las células de origen mieloide que expresan el receptor CX_3CR_1. ANOVA unidireccional con test Brown-Forsythe. Las diferencias se consideraron significativas para * $p < 0,05$, ** $p < 0,01$, *** $p < 0,001$ y **** $p < 0,0001$.

En esta sección, hemos desarrollado nuevas NCs poliméricas basadas en INU modificada. Particularmente, se han desarrollado y caracterizado dos NCs poliméricas de tamaños distintos. Al ser comparadas con NCs CS de tamaño similar, presentaron una menor interacción con MΦs y con DCs pero una considerable menor toxicidad. Las NCs CS activaron las DCs en una mayor proporción comparadas con las NCs INU, probablemente, en parte, debido a su mayor toxicidad. Sin embargo, los adyuvantes basados en INU han demostrado funcionar a través de un mecanismo no-inflamatorio, explicando su baja reactogenicidad. En peces cebra, los tamaños de partícula menores de 100 nm permitieron que las NCs se diseminaran más rápido y a mayor profundidad en los tejidos en comparación con las NCs de 170 – 250 nm. Además, el CS parece tener un papel crítico en el reclutamiento de MΦs.

Finalmente, el drenaje linfático después de la administración subcutánea, demostró que las NCs S INU se acumularon en mayor medida en el PLN comparadas con el resto de prototipos.

Como conclusión, debido a su mecanismo adyuvante no-inflamatorio, probada seguridad, buena capacidad para diseminar y acumularse en los LNs, creemos que las NCs S INU deberían ser exploradas como nuevas nanovacunas con propiedades de direccionamiento a linfa.

Referencias

[1] I. Toth, M. Skwarczynski, The immune system likes nanotechnology, Nanomedicine. 9 (2014) 2607–2609. doi:10.2217/nnm.14.199.
[2] J.V. Gonzalez-Aramundiz, A.S. Cordeiro, N. Csaba, M. de la Fuente, M.J. Alonso, Nanovaccines : nanocarriers for antigen delivery, Biol. Aujourdhui. 206 (2012) 249–261. doi:10.1051/jbio/2012027.
[3] Y. Liu, Y. Xu, Y. Tian, C. Chen, C. Wang, X. Jiang, Functional Nanomaterials Can Optimize the Efficacy of Vaccines, Small. 10 (2014) 4505–4520. doi:10.1002/smll.201401707.
[4] H. Yue, G. Ma, Polymeric micro / nanoparticles : Particle design and potential vaccine delivery applications, Vaccine. 33 (2015) 5927–5936. doi:10.1016/j.vaccine.2015.07.100.
[5] M.-L. De Temmerman, J. Rejman, J. Demeester, D.J. Irvine, B. Gander, S.C. De Smedt, Particulate vaccines: on the quest for optimal delivery and immune response., Drug Discov. Today. 16 (2011) 569–82. doi:10.1016/j.drudis.2011.04.006.
[6] A.C. Rice-ficht, A.M. Arenas-gamboa, M.M. Kahl-mcdonagh, T.A. Ficht, Polymeric particles in vaccine delivery, Curr. Opin. Microbiol. 13 (2010) 106–112. doi:10.1016/j.mib.2009.12.001.
[7] S. Vicente, B. Diaz-Freitas, M. Peleteiro, A. Sanchez, D.W. Pascual, A. Gonzalez-Fernandez, et al., A Polymer/Oil Based Nanovaccine as a Single-Dose Immunization Approach, PLoS One. 8 (2013) e62500. doi:10.1371/journal.pone.0062500.
[8] M. Tobio, S.P. Schwendeman, Y. Guo, J. McIver, R. Langer, M.J. Alonso, Improved immunogenicity of a core-coated tetanus toxoid delivery system, Vaccine. 18 (1999) 618–622. doi:10.1016/S0264-410X(99)00313-8.
[9] C. Prego, D. Torres, M.J. Alonso, Chitosan nanocapsules: a new carrier for nasal peptide delivery, J. Drug Deliv. Sci. Technol. 16 (2006) 331–337. doi:10.1016/S1773-2247(06)50061-9.
[10] C. Prego, D. Torres, M.J. Alonso, Chitosan Nanocapsules as Carriers for Oral Peptide Delivery: Effect of Chitosan Molecular Weight and Type of Salt on the In Vitro Behaviour and In Vivo Effectiveness, J. Nanosci. Nanotechnol. 6 (2006) 2921–2928. doi:10.1166/jnn.2006.429.
[11] Z. Niu, E. Tedesco, F. Benetti, A. Mabondzo, I.M. Montagner, I. Marigo, et al., Rational design of polyarginine nanocapsules intended to help peptides overcoming intestinal barriers, J. Control. Release. 263 (2017) 4–17. doi:10.1016/j.jconrel.2017.02.024.
[12] M. V. Lozano, G. Lollo, M. Alonso-Nocelo, J. Brea, A. Vidal, D. Torres, et al., Polyarginine nanocapsules: A new platform for intracellular drug delivery, J. Nanoparticle Res. 15 (2013). doi:10.1007/s11051-013-1515-7.
[13] J.V. González-Aramundiz, E. Presas, I. Dalmau-Mena, S. Martínez-Pulgarín, C. Alonso, J.M. Escribano, et al., Rational design of protamine nanocapsules as antigen delivery carriers, J. Control. Release. 245 (2017) 62–69. doi:10.1016/j.jconrel.2016.11.012.
[14] S. Vicente, M. Peleteiro, J.V. González-Aramundiz, B. Díaz-Freitas, S. Martínez-Pulgarín, J.I. Neissa, et al., Highly versatile immunostimulating nanocapsules for specific immune potentiation., Nanomedicine (London). 9 (2014) 2273–2289. doi:10.2217/nnm.14.10.
[15] S. Vicente, M. Peleteiro, B. Díaz-Freitas, A. Sanchez, Á. González-Fernández, M.J. Alonso, Co-delivery of viral proteins and a TLR7 agonist from polysaccharide nanocapsules: A needle-free vaccination strategy, J. Control. Release. 172 (2013) 773–781. doi:10.1016/j.jconrel.2013.09.012.
[16] H. Mobley, C. Alteri, Development of a Vaccine against Escherichia coli Urinary Tract Infections, Pathogens. 5 (2015) 1. doi:10.3390/pathogens5010001.
[17] L.A. Mike, S.N. Smith, C.A. Sumner, K.A. Eaton, H.L.T. Mobley, Siderophore vaccine conjugates protect against uropathogenic Escherichia coli urinary tract infection, Proc. Natl. Acad. Sci. 113 (2016) 13468–13473. doi:10.1073/pnas.1606324113.
[18] B. Slütter, P.C. Soema, Z. Ding, R. Verheul, W. Hennink, W. Jiskoot, Conjugation of ovalbumin to trimethyl chitosan improves immunogenicity of the antigen, J. Control. Release. 143 (2010) 207–214. doi:10.1016/j.jconrel.2010.01.007.
[19] S. Sharma, T.K.S. Mukkur, H.A.E. Benson, Y. Chen, Enhanced Immune Response Against Pertussis Toxoid by IgA-Loaded Chitosan–Dextran Sulfate Nanoparticles, J. Pharm. Sci. 101 (2012) 233–244. doi:10.1002/jps.22763.
[20] S. Sharma, H. a E. Benson, T.K.S. Mukkur, P. Rigby, Y. Chen, Preliminary studies on the development of IgA-loaded chitosan-dextran sulphate nanoparticles as a potential nasal delivery system for protein antigens., J. Microencapsul. 30 (2013) 283–94. doi:10.3109/02652048.2012.726279.
[21] D.P. Gnanadhas, M. Ben Thomas, M. Elango, A.M. Raichur, D. Chakravortty, Chitosan-dextran

sulphate nanocapsule drug delivery system as an effective therapeutic against intraphagosomal pathogen Salmonella, J. Antimicrob. Chemother. 68 (2013) 2576–2586. doi:10.1093/jac/dkt252.
[22] T. Delair, Colloidal polyelectrolyte complexes of chitosan and dextran sulfate towards versatile nanocarriers of bioactive molecules., Eur. J. Pharm. Biopharm. 78 (2011) 10–8. doi:10.1016/j.ejpb.2010.12.001.
[23] P. Zaman, J. Wang, A. Blau, W. Wang, T. Li, D.S. Kohane, et al., Incorporation of heparin-binding proteins into preformed dextran sulfate-chitosan nanoparticles, Int. J. Nanomedicine. 11 (2016) 6149–6159. doi:10.2147/IJN.S119174.
[24] W. Chaiyasan, S.P. Srinivas, W. Tiyaboonchai, Mucoadhesive Chitosan–Dextran Sulfate Nanoparticles for Sustained Drug Delivery to the Ocular Surface, J. Ocul. Pharmacol. Ther. 29 (2013) 200–207. doi:10.1089/jop.2012.0193.
[25] S. Hirsjärvi, Y. Qiao, A. Royere, J. Bibette, J. Benoit, Layer-by-layer surface modification of lipid nanocapsules, Eur. J. Pharm. Biopharm. 76 (2010) 200–207. doi:10.1016/j.ejpb.2010.07.010.
[26] K. Szczepanowicz, D. Dronka-Góra, G. Para, P. Warszyński, Encapsulation of liquid cores by layer-by-layer adsorption of polyelectrolytes, J. Microencapsul. 27 (2010) 198–204. doi:10.3109/02652040903052069.
[27] K. Szczepanowicz, U. Bazylińska, J. Pietkiewicz, L. Szyk-Warszyńska, K.A. Wilk, P. Warszyński, Biocompatible long-sustained release oil-core polyelectrolyte nanocarriers: From controlling physical state and stability to biological impact, Adv. Colloid Interface Sci. 222 (2015) 678–691. doi:10.1016/j.cis.2014.10.005.
[28] W. Abdelwahed, G. Degobert, S. Stainmesse, H. Fessi, Freeze-drying of nanoparticles: Formulation, process and storage considerations, Adv. Drug Deliv. Rev. 58 (2006) 1688–1713. doi:10.1016/j.addr.2006.09.017.
[29] D. Chen, D. Kristensen, Opportunities and challenges of developing thermostable vaccines, Expert Rev. Vaccines. 8 (2009) 547–557. doi:10.1586/erv.09.20.
[30] M.M. Tobío, J. Nolley, Y. Guo, J. McIver, M.J. Alonso, A Novel System Based on a Poloxamer/PLGA Blend as a Tetanus Toxoid Delivery Vehicle, Pharm. Res. 16 (1999) 682–688. doi:10.1023/a:1018820507379.
[31] A. Vila, A. Sánchez, C. Évora, I. Soriano, O. McCallion, M.J. Alonso, PLA-PEG particles as nasal protein carriers: The influence of the particle size, Int. J. Pharm. 292 (2005) 43–52. doi:10.1016/j.ijpharm.2004.09.002.
[32] A. Vila, A. Sánchez, K. Janes, I. Behrens, T. Kissel, J.L. V Jato, et al., Low molecular weight chitosan nanoparticles as new carriers for nasal vaccine delivery in mice, Eur. J. Pharm. Biopharm. 57 (2004) 123–131. doi:10.1016/j.ejpb.2003.09.006.
[33] C. Prego, P. Paolicelli, B. Díaz, S. Vicente, A. Sánchez, Á. González-Fernández, et al., Chitosan-based nanoparticles for improving immunization against hepatitis B infection, Vaccine. 28 (2010) 2607–2614. doi:10.1016/j.vaccine.2010.01.011.
[34] T.G. Dacoba, A. Olivera, D. Torres, J. Crecente-Campo, M.J. Alonso, Modulating the immune system through nanotechnology., Semin. Immunol. 34 (2017) 78–102. doi:10.1016/j.smim.2017.09.007.
[35] Y. Liu, B. Workalemahu, X. Jiang, The Effects of Physicochemical Properties of Nanomaterials on Their Cellular Uptake In Vitro and In Vivo, Small. 13 (2017) 1–13. doi:10.1002/smll.201701815.
[36] H. Jiang, Q. Wang, X. Sun, Lymph node targeting strategies to improve vaccination efficacy, J. Control. Release. 267 (2017) 47–56. doi:10.1016/j.jconrel.2017.08.009.
[37] U. Bilati, E. Allémann, E. Doelker, Development of a nanoprecipitation method intended for the entrapment of hydrophilic drugs into nanoparticles, Eur. J. Pharm. Sci. 24 (2005) 67–75. doi:10.1016/j.ejps.2004.09.011.
[38] D. Moinard-Chécot, Y. Chevalier, S. Briançon, L. Beney, H. Fessi, Mechanism of nanocapsules formation by the emulsion-diffusion process., J. Colloid Interface Sci. 317 (2008) 458–68. doi:10.1016/j.jcis.2007.09.081.
[39] J.W. Hickey, J.L. Santos, J.M. Williford, H.Q. Mao, Control of polymeric nanoparticle size to improve therapeutic delivery, J. Control. Release. 219 (2015) 535–547. doi:10.1016/j.jconrel.2015.10.006.
[40] K.T. Gause, A.K. Wheatley, J. Cui, Y. Yan, S.J. Kent, F. Caruso, Immunological Principles Guiding the Rational Design of Particles for Vaccine Delivery, ACS Nano. 11 (2017) 54–68. doi:10.1021/acsnano.6b07343.
[41] D.J. Irvine, M.A. Swartz, G.L. Szeto, Engineering synthetic vaccines using cues from natural immunity, Nat. Mater. 12 (2013) 978–990. doi:10.1038/nmat3775.

[42] R. Abellan-Pose, C. Teijeiro-Valiño, M.J. Santander-Ortega, E. Borrajo, A. Vidal, M. Garcia-Fuentes, et al., Polyaminoacid nanocapsules for drug delivery to the lymphatic system: Effect of the particle size, Int. J. Pharm. 509 (2016) 107–117. doi:10.1016/j.ijpharm.2016.05.034.
[43] D. Quintanar-Guerrero, E. Allémann, H. Fessi, E. Doelker, Preparation techniques and mechanism of formation of biodegradable nanoparticles from preformed polymers, Drug Dev. Ind. Pharm. 24 (1998) 1113–1128. doi:10.3109/03639049809108571.
[44] S. Galindo-rodriguez, E. Alle, H. Fessi, E. Doelker, Physicochemical Parameters Associated with Nanoparticle Formation in the Salting-out , Nanoprecipitation Methods, Pharm. Res. 21 (2004) 1428–1439. doi:10.1023/B:PHAM.0000036917.75634.be.
[45] F. Ganachaud, J.L. Katz, Nanoparticles and nanocapsules created using the ouzo effect: Spontaneous emulsification as an alternative to ultrasonic and high-shear devices, ChemPhysChem. 6 (2005) 209–216. doi:10.1002/cphc.200400527.
[46] M. Beck-Broichsitter, E. Rytting, T. Lebhardt, X. Wang, T. Kissel, Preparation of nanoparticles by solvent displacement for drug delivery: A shift in the " ouzo region" upon drug loading, Eur. J. Pharm. Sci. 41 (2010) 244–253. doi:10.1016/j.ejps.2010.06.007.
[47] W.S. Saad, R.K. Prud'Homme, Principles of nanoparticle formation by flash nanoprecipitation, Nano Today. 11 (2016) 212–227. doi:10.1016/j.nantod.2016.04.006.
[48] S. Hirsjärvi, S. Dufort, G. Bastiat, P. Saulnier, C. Passirani, J.L. Coll, et al., Surface modification of lipid nanocapsules with polysaccharides: From physicochemical characteristics to in vivo aspects, Acta Biomater. 9 (2013) 6686–6693. doi:10.1016/j.actbio.2013.01.038.
[49] H.X. Wang, Z.Q. Zuo, J.Z. Du, Y.C. Wang, R. Sun, Z.T. Cao, et al., Surface charge critically affects tumor penetration and therapeutic efficacy of cancer nanomedicines, Nano Today. 11 (2016) 133–144. doi:10.1016/j.nantod.2016.04.008.
[50] J. Cui, M.P. Van Koeverden, M. Müllner, K. Kempe, F. Caruso, Emerging methods for the fabrication of polymer capsules, Adv. Colloid Interface Sci. 207 (2014) 14–31. doi:10.1016/j.cis.2013.10.012.
[51] E. Guzmán, A. Mateos-Maroto, M. Ruano, F. Ortega, R.G. Rubio, Layer-by-Layer polyelectrolyte assemblies for encapsulation and release of active compounds, Adv. Colloid Interface Sci. 249 (2017) 290–307. doi:10.1016/j.cis.2017.04.009.
[52] S. Correa, E.C. Dreaden, L. Gu, P.T. Hammond, Engineering nanolayered particles for modular drug delivery, J. Control. Release. 240 (2016) 364–386. doi:10.1016/j.jconrel.2016.01.040.
[53] A.P. Pandey, S.S. Singh, G.B. Patil, P.O. Patil, C.J. Bhavsar, P.K. Deshmukh, Sonication-assisted drug encapsulation in layer-by-layer self-assembled gelatin-poly (styrenesulfonate) polyelectrolyte nanocapsules : process optimization, 405 (2014) 1–12. doi:10.3109/21691401.2014.898646.
[54] B. Heurtault, P. Saulnier, B. Pech, J. Proust, J. Benoit, A Novel Phase Inversion-Based Process for the Preparation of Lipid Nanocarriers, Pharm. Res. 19 (2002) 875–880. doi:10.1023/A:1016121319668.
[55] N.T. Huynh, C. Passirani, P. Saulnier, J.P. Benoit, Lipid nanocapsules: A new platform for nanomedicine, Int. J. Pharm. 379 (2009) 201–209. doi:10.1016/j.ijpharm.2009.04.026.
[56] J. Crecente-Campo, S. Lorenzo-Abalde, A. Mora, J. Marzoa, N. Csaba, J. Blanco, et al., Bilayer polymer nanocapsules: a formulation approach for a thermostable and adjuvanted E. coli antigen vaccine, J. Control. Release. Submitted (2018).
[57] M.A. Mensink, H.W. Frijlink, K. Van Der Voort Maarschalk, W.L.J. Hinrichs, Inulin, a flexible oligosaccharide. II: Review of its pharmaceutical applications, Carbohydr. Polym. 134 (2015) 418–428. doi:10.1016/j.carbpol.2015.08.022.
[58] D.G. Silva, P.D. Cooper, N. Petrovsky, Inulin-derived adjuvants efficiently promote both Th1 and Th2 immune responses, Immunol. Cell Biol. 82 (2004) 611–616. doi:10.1111/j.1440-1711.2004.01290.x.
[59] N. Petrovsky, P.D. Cooper, Advax™, a novel microcrystalline polysaccharide particle engineered from delta inulin, provides robust adjuvant potency together with tolerability and safety, Vaccine. 33 (2015) 5920–5926. doi:10.1016/j.vaccine.2015.09.030.
[60] L. Li, Y. Honda-Okubo, C. Li, D. Sajkov, N. Petrovsky, Delta inulin adjuvant enhances plasmablast generation, expression of activation-induced cytidine deaminase and B-cell affinity maturation in human subjects receiving seasonal influenza vaccine, PLoS One. 10 (2015) 1–18. doi:10.1371/journal.pone.0132003.
[61] M. Hayashi, T. Aoshi, Y. Haseda, K. Kobiyama, E. Wijaya, N. Nakatsu, et al., Advax, a delta inulin microparticle, potentiates in-built adjuvant property of co-administered vaccines, EBioMedicine. 15 (2017) 127–136. doi:10.1016/j.ebiom.2016.11.015.
[62] C. Losa, L. Marchal-Heussler, F. Orallo, J.L. Vila Jato, M.J. Alonso, Design of new formulations for

topical ocular administration: polymeric nanocapsules containing metipranolol., Pharm. Res. 10 (1993) 80–7. doi:10.1023/A:1018977130559.
[63] F.A. Oyarzun-Ampuero, G.R. Rivera-Rodríguez, M.J. Alonso, D. Torres, G.R. Rivera-Rodriguez, M.J. Alonso, et al., Hyaluronan nanocapsules as a new vehicle for intracellular drug delivery, Eur. J. Pharm. Sci. 49 (2013) 483–490. doi:10.1016/j.ejps.2013.05.008.
[64] G. Lollo, P. Hervella, P. Calvo, P. Aviles, M.J. Guillen, M. Garcia-Fuentes, et al., Enhanced in vivo therapeutic efficacy of plitidepsin-loaded nanocapsules decorated with a new poly-aminoacid-PEG derivative, Int. J. Pharm. 483 (2015) 212–219. doi:10.1016/j.ijpharm.2015.02.028.
[65] L.N. Thwala, A. Beloqui, N.S. Csaba, D. González-Touceda, S. Tovar, C. Dieguez, et al., The interaction of protamine nanocapsules with the intestinal epithelium: A mechanistic approach, J. Control. Release. 243 (2016) 109–120. doi:10.1016/j.jconrel.2016.10.002.
[66] G. Lollo, A. Gonzalez-Paredes, M. Garcia-Fuentes, P. Calvo, D. Torres, M.J. Alonso, Polyarginine Nanocapsules as a Potential Oral Peptide Delivery Carrier, J. Pharm. Sci. 106 (2017) 611–618. doi:10.1016/j.xphs.2016.09.029.
[67] K. Siram, G. Marslin, C.V. Raghavan, K. Balakumar, H. Rahman, G. Franklin, A brief perspective on the diverging theories of lymphatic targeting with colloids, Int. J. Nanomedicine. 11 (2016) 2867–2872. doi:10.2147/IJN.S105852.
[68] C. V. Stevens, A. Meriggi, K. Booten, Chemical modification of inulin, a valuable renewable resource, and its industrial applications, Biomacromolecules. 2 (2001) 1–16. doi:10.1021/bm005642t.
[69] C. V. Stevens, A. Meriggi, M. Peristeropoulou, P.P. Christov, K. Booten, B. Levecke, et al., Polymeric surfactants based on inulin, a polysaccharide extracted from chicory. 1. Synthesis and interfacial properties, Biomacromolecules. 2 (2001) 1256–1259. doi:10.1021/bm015570l.
[70] G. Van den Mooter, I. Weuts, T. De Ridder, N. Blaton, Evaluation of Inutec SP1 as a new carrier in the formulation of solid dispersions for poorly soluble drugs, Int. J. Pharm. 316 (2006) 1–6. doi:10.1016/j.ijpharm.2006.02.025.
[71] P. Srinarong, S. Hämäläinen, M.R. Visser, W.L.J. Hinrichs, J. Ketolainen, H.W. Frijlink, Surface-Active Derivative of Inulin (Inutec® SP1) Is a Superior Carrier for Solid Dispersions with a High Drug Load, J. Pharm. Sci. 100 (2011) 2333–2342. doi:10.1002/jps.22471.
[72] P.R. Mishra, L. Al Shaal, R.H. Müller, C.M. Keck, Production and characterization of Hesperetin nanosuspensions for dermal delivery, Int. J. Pharm. 371 (2009) 182–189. doi:10.1016/j.ijpharm.2008.12.030.
[73] P. Muley, S. Kumar, F. El Kourati, S.S. Kesharwani, H. Tummala, Hydrophobically modified inulin as an amphiphilic carbohydrate polymer for micellar delivery of paclitaxel for intravenous route, Int. J. Pharm. 500 (2016) 32–41. doi:10.1016/j.ijpharm.2016.01.005.
[74] T.F. Tadros, A. Vandamme, K. Booten, B. Levecke, C. V. Stevens, Stabilisation of emulsions using hydrophobically modified inulin (polyfructose), Colloids Surfaces A Physicochem. Eng. Asp. 250 (2004) 133–140. doi:10.1016/j.colsurfa.2004.03.041.
[75] A. Gamvrellis, D. Leong, J.C. Hanley, S.D. Xiang, P. Mottram, M. Plebanski, Vaccines that facilitate antigen entry into dendritic cells, Immunol. Cell Biol. 82 (2004) 506–516. doi:10.1111/j.0818-9641.2004.01271.x.
[76] N. Doshi, S. Mitragotri, Macrophages recognize size and shape of their targets, PLoS One. 5 (2010) 1–6. doi:10.1371/journal.pone.0010051.
[77] T. Fifis, A. Gamvrellis, B. Crimeen-Irwin, G.A. Pietersz, J. Li, P.L. Mottram, et al., Size-Dependent Immunogenicity: Therapeutic and Protective Properties of Nano-Vaccines against Tumors, J. Immunol. 173 (2004) 3148–3154. doi:10.4049/jimmunol.173.5.3148.
[78] C. He, Y. Hu, L. Yin, C. Tang, C. Yin, Effects of particle size and surface charge on cellular uptake and biodistribution of polymeric nanoparticles, Biomaterials. 31 (2010) 3657–3666. doi:10.1016/j.biomaterials.2010.01.065.
[79] J.S. Choi, J. Cao, M. Naeem, J. Noh, N. Hasan, H.K. Choi, et al., Size-controlled biodegradable nanoparticles: Preparation and size-dependent cellular uptake and tumor cell growth inhibition, Colloids Surfaces B Biointerfaces. 122 (2014) 545–551. doi:10.1016/j.colsurfb.2014.07.030.
[80] S. Kim, W.K. Oh, Y.S. Jeong, J.Y. Hong, B.R. Cho, J.S. Hahn, et al., Cytotoxicity of, and innate immune response to, size-controlled polypyrrole nanoparticles in mammalian cells, Biomaterials. 32 (2011) 2342–2350. doi:10.1016/j.biomaterials.2010.11.080.
[81] J. Huang, L. Bu, J. Xie, K. Chen, Z. Cheng, X. Li, et al., Effects of nanoparticle size on cellular uptake and liver MRI with polyvinylpyrrolidone-coated iron oxide nanoparticles, ACS Nano. (2010). doi:10.1021/nn101643u.

[82] T. Fifis, A. Gamvrellis, B. Crimeen-Irwin, G.A. Pietersz, J. Li, P.L. Mottram, et al., Size-dependent immunogenicity: therapeutic and protective properties of nano-vaccines against tumors, J. Immunol. 173 (2004) 3148–3154. doi:10.4049/jimmunol.173.5.3148.
[83] C. Foged, B. Brodin, S. Frokjaer, A. Sundblad, Particle size and surface charge affect particle uptake by human dendritic cells in an in vitro model, Int. J. Pharm. 298 (2005) 315–322. doi:10.1016/j.ijpharm.2005.03.035.
[84] C.A. Fromen, T.B. Rahhal, G.R. Robbins, M.P. Kai, T.W. Shen, J.C. Luft, et al., Nanoparticle surface charge impacts distribution, uptake and lymph node trafficking by pulmonary antigen-presenting cells, Nanomedicine Nanotechnology, Biol. Med. 12 (2016) 677–687. doi:10.1016/j.nano.2015.11.002.
[85] L. Thiele, B. Rothen-Rutishauser, S. Jilek, H. Wunderli-Allenspach, H.P. Merkle, E. Walter, Evaluation of particle uptake in human blood monocyte-derived cells in vitro. Does phagocytosis activity of dendritic cells measure up with macrophages?, J. Control. Release. 76 (2001) 59–71.
[86] L.J. Cruz, P.J. Tacken, R. Fokkink, C.G. Figdor, The influence of PEG chain length and targeting moiety on antibody-mediated delivery of nanoparticle vaccines to human dendritic cells, Biomaterials. 32 (2011) 6791–6803. doi:10.1016/j.biomaterials.2011.04.082.
[87] C. Villiers, M. Chevallet, H. Diemer, R. Couderc, H. Freitas, A. Van Dorsselaer, et al., From Secretome Analysis to Immunology, Mol. Cell. Proteomics. 8 (2009) 1252–1264. doi:10.1074/mcp.M800589-MCP200.
[88] B. Koppolu, D.A. Zaharoff, The effect of antigen encapsulation in chitosan particles on uptake, activation and presentation by antigen presenting cells, Biomaterials. 34 (2013) 2359–2369. doi:10.1016/j.biomaterials.2012.11.066.
[89] K.L. Rock, H. Kono, The Inflammatory Response to Cell Death, Annu. Rev. Pathol. Mech. Dis. 3 (2008) 99–126. doi:10.1146/annurev.pathmechdis.3.121806.151456.
[90] B. Slütter, W. Jiskoot, Sizing the optimal dimensions of a vaccine delivery system: a particulate matter, Expert Opin. Drug Deliv. 13 (2016) 167–170. doi:10.1517/17425247.2016.1121989.
[91] P.L. Mottram, D. Leong, B. Crimeen-Irwin, S. Gloster, S.D. Xiang, J. Meanger, et al., Type 1 and 2 Immunity Following Vaccination Is Influenced by Nanoparticle Size: Formulation of a Model Vaccine for Respiratory Syncytial Virus, Mol. Pharm. 4 (2007) 73–84. doi:10.1021/mp060096p.
[92] T. Hirai, Y. Yoshioka, H. Takahashi, K. Ichihashi, T. Yoshida, S. Tochigi, et al., Amorphous silica nanoparticles enhance cross-presentation in murine dendritic cells, Biochem. Biophys. Res. Commun. 427 (2012) 553–556. doi:10.1016/j.bbrc.2012.09.095.
[93] L. Jia, X. Gao, Y. Wang, N. Yao, X. Zhang, Structural, phenotypic and functional maturation of bone marrow dendritic cells (BMDCs) induced by Chitosan (CTS), Biologicals. 42 (2014) 334–338. doi:10.1016/j.biologicals.2014.07.004.
[94] M. Oliveira, S. Santos, M. Oliveira, A. Torres, M. Barbosa, Chitosan drives anti-inflammatory macrophage polarisation and pro-inflammatory dendritic cell stimulation, Eur. Cells Mater. 24 (2012) 136–153. doi:10.22203/eCM.v024a10.
[95] J. Tomar, H.P. Patil, G. Bracho, W.F. Tonnis, H.W. Frijlink, N. Petrovsky, et al., Advax augments B and T cell responses upon influenza vaccination via the respiratory tract and enables complete protection of mice against lethal influenza virus challenge, J. Control. Release. 288 (2018) 199–211. doi:10.1016/j.jconrel.2018.09.006.
[96] Y. Honda-Okubo, A. Kolpe, L. Li, N. Petrovsky, A single immunization with inactivated H1N1 influenza vaccine formulated with delta inulin adjuvant (Advax^{TM}) overcomes pregnancy-associated immune suppression and enhances passive neonatal protection, Vaccine. 32 (2014) 4651–4659. doi:10.1016/j.vaccine.2014.06.057.
[97] Y. Honda-Okubo, C.H. Ong, N. Petrovsky, Advax delta inulin adjuvant overcomes immune immaturity in neonatal mice thereby allowing single-dose influenza vaccine protection, Vaccine. 33 (2015) 4892–4900. doi:10.1016/j.vaccine.2015.07.051.
[98] N.D. Meeker, N.S. Trede, Immunology and zebrafish: Spawning new models of human disease, Dev. Comp. Immunol. 32 (2008) 745–757. doi:10.1016/j.dci.2007.11.011.
[99] L. Wang, T. Barclay, Y. Song, P. Joyce, I.G. Sakala, N. Petrovsky, et al., Investigation of the biodistribution, breakdown and excretion of delta inulin adjuvant, Vaccine. 35 (2017) 4382–4388. doi:10.1016/j.vaccine.2017.06.045.
[100] E. Blanco, H. Shen, M. Ferrari, Principles of nanoparticle design for overcoming biological barriers to drug delivery, Nat. Biotechnol. 33 (2015) 941–951. doi:10.1038/nbt.3330.
[101] D.J. Irvine, M.C. Hanson, K. Rakhra, T. Tokatlian, Synthetic Nanoparticles for Vaccines and

Immunotherapy, Chem. Rev. 115 (2015) 11109–11146. doi:10.1021/acs.chemrev.5b00109.
[102] S.N. Mueller, S. Tian, J.M. DeSimone, Rapid and Persistent Delivery of Antigen by Lymph Node Targeting PRINT Nanoparticle Vaccine Carrier To Promote Humoral Immunity, Mol. Pharm. 12 (2015) 1356–1365. doi:10.1021/mp500589c.
[103] S. Reimondez-troitiño, I. Alcalde, N. Csaba, A. Íñigo-portugués, M. De Fuente, F. Bech, Polymeric nanocapsules : a potential new therapy for corneal wound healing, Drug Deliv. Transl. Res. (2016) 708–721. doi:10.1007/s13346-016-0312-0.
[104] E. Borrajo, R. Abellan-Pose, A. Soto, M. Garcia-Fuentes, N. Csaba, M.J. Alonso, et al., Docetaxel-loaded polyglutamic acid-PEG nanocapsules for the treatment of metastatic cancer, J. Control. Release. 238 (2016) 263–271. doi:10.1016/j.jconrel.2016.07.048.
[105] V. Manolova, A. Flace, M. Bauer, K. Schwarz, P. Saudan, M.F. Bachmann, Nanoparticles target distinct dendritic cell populations according to their size., Eur. J. Immunol. 38 (2008) 1404–13. doi:10.1002/eji.200737984.
[106] M.F. Bachmann, G.T. Jennings, Vaccine delivery: a matter of size, geometry, kinetics and molecular patterns, Nat. Rev. Immunol. 10 (2010) 787–796. doi:10.1038/nri2868.
[107] M. Pitorre, G. Bastiat, E.M. dit Chatel, J.-P. Benoit, Passive and specific targeting of lymph nodes: the influence of the administration route, Eur. J. Nanomedicine. 7 (2015) 121–128. doi:10.1515/ejnm-2015-0003.
[108] R. Abellán-pose, N. Csaba, M.J. Alonso, Lymphatic Targeting of Nanosystems for Anticancer Drug Therapy, (2016) 1194–1209.
[109] F. Shima, T. Uto, T. Akagi, M. Baba, M. Akashi, Size effect of amphiphilic poly(γ-glutamic acid) nanoparticles on cellular uptake and maturation of dendritic cells in vivo., Acta Biomater. 9 (2013) 8894–901. doi:10.1016/j.actbio.2013.06.010.

Introduction

Nanotechnology and the immune system

This introduction has been adapted/extracted from a published review: Crecente-Campo et al. "Modulating the immune system through nanotechnology". Seminars in Immunology 34 (2017) 78-102.

The immune system is a complex network of cells and organs that constitutes the main guard of our health. Any alteration or malfunction in its proper activity can lead or contribute to important maladies, such as autoimmune diseases and cancer. Besides, the immune system protects us from the daily external threats (pollutants, microorganisms, mechanical damage, etc.). Considering the essential role of the immune system in some of the most worrying diseases of our time (cancer, HIV, diabetes), the possibility to influence or modulate it is the basis for new and encouraging therapies. In this scenario, the nanotechnology may facilitate the communication with the immune system [1–3]. In this crosstalk between the immune cells and the nanoparticles (NPs), the composition, the surface and the physicochemical features of the nanocarriers dictate the type and degree of interaction with the immune cells. In that regard, and mainly based on the knowledge about the molecular principles that govern the interaction between pathogens and immune cells, micro and nanocarriers have been designed to mimic the size of microorganisms (bacteria and viruses) and their danger signals. Besides, the use of nanocarriers decorated with targeting ligands can influence their preferential access to specific subset of immune cells [2,4–10]. Depending on the combination of these factors, the immunomodulation may lead to the activation of the immune system to generate and, hence, favor a response against a specific antigen, with application in cancer and vaccines, or the induction of tolerance against self or external antigens, of interest for autoimmunity and allergies respectively. The first option improves the chances of controlling infectious diseases that do not respond well to traditional vaccines, such as HIV or tuberculosis, among others [11–13].

In this introduction, we first make a brief summary of the most relevant milestones in the timeline of vaccine history and the emergence of nanotechnology as a tool to increase the immunogenicity of modern antigens. Then, considering the need of a rational design of new nanovaccines we analyze how the nanocarriers can access to the tissues where the immune cells are present. Later, we evaluated the influence of the physicochemical properties and composition of the nanocarriers in their interaction with the different subsets of immune cells. Finally, we study how to modify the balance between the humoral and cellular arms when generating an immune response.

1. A brief historical perspective of classical and nano- vaccines

1.1. About the antigens

Although Edward Jenner is considered the father of vaccination, centuries before, the Chinese had already used pathogens to prevent infectious diseases. As early as in the tenth century, they used pustules from individuals who suffered from a mild version of smallpox to make a dry powder. Then, the powder was insufflated into the nose of healthy individuals or directly in an open wound to intentionally infect them with a less

severe form of the disease. In that way, the individuals acquired a protection from future exposure to the disease.

Nevertheless, the recognition to Edward Jenner is well deserved, as he was the one spreading the practice of vaccination all over the world. In 1796, using material of cowpox, he infected a child that lately was challenged with smallpox without apparently developing the disease. It was the first documented effective case of a heterologous vaccination [14].

A century later, Robert Koch and Louis Pasteur discovered that infectious diseases were caused by microorganisms, leading to the foundation of the microbiology. Once the causal agents were discovered the evolution of vaccines accelerated quickly. First, in 1885 was the rabies vaccine and then antitoxins and vaccines against diphtheria, anthrax, typhoid, tetanus, cholera, plague, tuberculosis, and others were developed through the 1930s.

Despite their effectiveness, these first vaccines were extremely reactogenic, showing in most of the cases adverse effects, such as swelling at the injection site, fever and pain.

The middle of the last century was a very productive time for vaccine development. Technological advances allowed researchers to grow viruses in the laboratory that would lead to the creation first of the polio vaccine and later against rubella, measles and mumps. These discoveries remarkably contributed to the increase in the life expectancy and were crucial for the eradication of these diseases [15,16].

In the 1970s, new vaccines emerged based on the development of purified polysaccharides from the capsule of different germs such us meningoccocus, pnseumococcus and influenza. However, these vaccines failed to be effective in infants. The synthesis of glycoconjugate vaccines, where the antigen was conjugated to a polysaccharide, solved this problem [17] and represents the first milestone in the vaccine engineering era.

Thanks to the recombinant DNA technology, purified proteins and peptides could be produced as totally safe antigens, without the use of the pathogens they derived from. More recently, based on the advances in gene therapy, the use of antigens encoded by DNA and RNA became available. Nevertheless, due to their low immunogenicity, these modern antigens are unable to produce long-lasting protective immune responses, making necessary the uses of adjuvants [18].

1.2. About antigen nanocarriers

The potential of nanotechnology for vaccination was firstly reported 40 years ago. At that time, Birrenbanch and Speiser showed that polyacrylamide NPs could work as adjuvants, increasing the immune response against human IgG and tetanus toxoid after subcutaneous administration to guinea pigs [19]. Years later, Preis and Langer

proposed the idea of “single-dose vaccines” based on the possibility to control the release of proteins from polymeric beads [20]. These results were the foundation for the development of controlled antigen delivery systems and nanovaccines.

The development of nanotechnology-based vaccines with a more translational perspective started in the early 90s when the World Health Organization (WHO) proposed the initiative of developing a single-dose vaccine for tetanus toxoid. From this point on, many studies with polyester-based microsystems, particularly poly(lactic-co-glycolic acid) (PLGA), were conducted [21]. Unfortunately, despite their good antigen release profiles, a certain protein denaturation was observed due to the pH acidification caused by the degradation of the polymer. To solve this problem different approaches were considered, among them, the use of a protective oil-core surrounded by a PLGA shell or the inclusion of poloxamer 188 to prevent interaction between polymer and antigen [22,23]. At the same time, the potential of nano-sized systems started to gain importance. Almeida *et al*. developed 500 and 800 nm polylactic acid (PLA) microspheres for nasal administration of tetanus toxoid with promising results [24]. Later on, our group found that the PEGylation of PLA was essential in order to enhance the stability of NPs and the penetration of the associated antigens across mucosal surfaces [25]. Indeed, the results from experiments using PEG-PLA NPs, did show an increase in the access of the associated antigen to the blood circulation and LNs [26]. Moreover, high and long-lasting anti-tetanus Ig titers were reported with these nanosystems, due to their ability to cross the nasal epithelium [27,28].

Subsequently, more hydrophilic polymers were explored with regard to their ability to transport antigens across mucosal surfaces. In particular, our group pioneered the development of chitosan NPs as alternative candidates for the development of nanovaccines, especially for those administered through mucosal routes [29]. Our studies concluded that the intranasal administration of chitosan NPs loaded with tetanus toxoid resulted in an increase in the humoral and mucosal responses, in comparison to the results obtained with the administration of the free antigen or even with those obtained when the antigen administered was associated to alum [25,30]. Our group has also been involved in the development of nanoformulations of the recombinant hepatitis B surface antigen (rHBsAg). In particular, rHBsAg was associated to chitosan NPs and administered by the intramuscular route. The results showed an IgG immunogenic response that was higher than the one observed for the control alum formulation [31]. The same antigen was also adsorbed on chitosan-based nanocapsules [32], a system that was also pioneered by our group [33]. These nanosystems are composed of an oily core surrounded by a chitosan shell, where the protein is adsorbed. After intramuscular administration of rHBsAg attached to chitosan-based nanocapsules, an important antibody responses as well as a more balanced Th1/Th2 profile were obtained [32].

Along the 40 years of the history of nanovaccines, many different nanostructures has been proposed as efficient vehicles for modern antigens. Briefly,

nanosystems used for vaccination could be classified in three main categories: i) polymeric nanosystems (polyester NPs, polysaccharide-based NPs, polyaminoacid-based NPs, etc), ii) lipid-based nanosystems (liposomes, solid lipid nanoparticles, nanocapsules, nanoemulsions, etc) and iii) pathogen-mimicking particles (bacteria-derived particles, virosomes, virus-like particles, etc.) [4]. Despite these advances in the nanotechnology field, some infectious diseases are still elusive to be prevented or treated with classical or nano-vaccines (malaria, tuberculosis and HIV, among others). This makes a more rational design of the nanosystems necessary. In the next sections, we analyze stepwise the necessary stages to trigger an immune response (access of the NPs to the immune cells, interaction NP-cell and developing the response) and how the NPs properties can be modulated to interfere in each of these stages.

2. Access of nanostructures to target cells

The first consideration to design a new nanosystem intended to interact with the immune cells is the pathway it must follow to access the tissues where the target cells are present. Depending on the administration route, different physiological barriers must be overcome to reach these cells.

The immune cells are patrolling all over the body as peripheral cells but they are mostly concentrated in their operation center, the lymphoid tissues. Hence, targeting these tissues facilitates the access to immune cells and, consequently, increases the efficacy of the nano-immunotherapies. Lymphoid tissues can be reached through the mucosal surfaces (airways, the intestinal tract, and vagina, among others) and also by parenteral injection (Fig. 1).

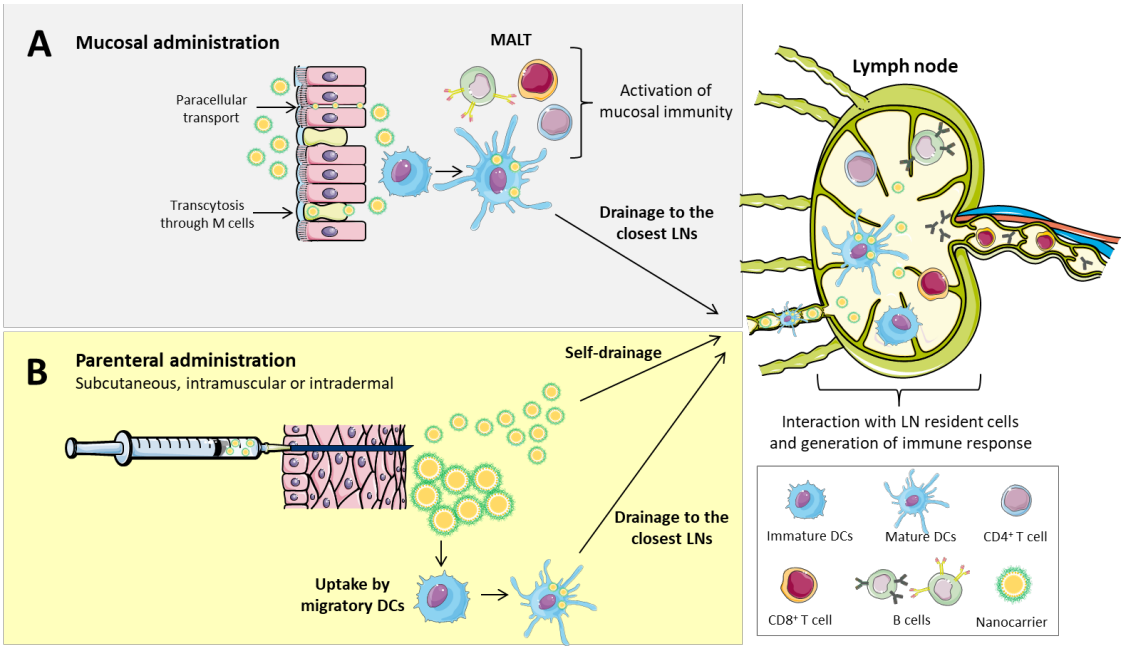

Figure 1. Vaccine administration routes. Vaccines can be administered following different routes. (A) In the mucosal administration, mainly through the nasal, oral or vaginal routes, nanocarriers need to reach the mucosal-associated lymphoid tissues (MALT). This can be principally achieved either by a paracellular or transcellular transport across the microfold (M) cells. Then, nanocarriers will encounter and activate the resident dendritic cells, generating a mucosal immunity. At the same time, some dendritic cells will drain to the closest lymph node and trigger a systemic immune response. (B) In the parenteral administration (subcutaneous, intramuscular or intradermal) the nanocarriers are injected in the interstitium, then they can freely drain to the closest lymph node or be taken up by migratory dendritic cells, which then will migrate to the closest lymph node.

2.1. Mucosal administration

The mucosal administration, apart from being a needle-free, patient-friendly route for vaccines, allows the induction of both, mucosal and systemic, immune responses [34]. In order to elicit an adequate response, NPs need, first, to overcome the mucus layer that covers the mucosal surfaces. Then, once in contact with the epithelium, nanocarriers are transported mainly by M cells and epithelial cells [35–37], paracellular transport [38] or, in same cases, captured by the dendrites of dendritic cells [39,40].

Nowadays, a precise balance between mucoadhesive and mucodiffusive properties is believed to be critical for the effectiveness of nanocarriers delivered through mucosal routes. For good mucodiffusion properties, it has been reported that particle size should be smaller than the mucus mesh size [41]. Despite some studies showing that microparticles (MPs) had a better performance than NPs through oral administration [42,43], in general, the current and most widespread opinion is that nanoparticles offer better results than microparticles [28,44–48]. For instance, our research group reported that the transport of PEGylated polylactic acid (PEG-PLA) NPs

across the nasal mucosa was higher than that of MPs. In the micrometric range, the smaller sizes (1 and 5 μm) also crossed the epithelium more efficiently than larger (10 μm) particles, being the differences between 1 and 5 μm no significant [49]. Interestingly, based on recent *in vivo* data, very small nanometric sizes (30 nm) might not be better than larger ones (200 nm) [50].

Apart from the size, the nanocarrier's surface characteristics also have an influence in its mucopermeation. Our group described, for the first time, the importance of PEGylation in NPs made of PLA to increase their transport rate through the nasal [26] and intestinal epithelia [51]. Later, other authors suggested that particles with sizes "*a priori"* not favorable for mucopermeation (200 – 500 nm) could penetrate across the mucus if they were engineered with adequate PEG coating [52,53].

2.2. Parenteral administration

The vast majority of vaccines are administered through the parenteral route (intramuscular, subcutaneous, and intradermal administrations). Following this modality of administration, NPs can drain directly to the closest lymph node and interact with the resident immune cells, or stay in the injection site and attract migratory dendritic cells or macrophages. Considering that the lymph nodes contain a larger number of phagocytically active DCs compared with the peripheral tissues, we could presume that the targeting and retention of nanoparticles to the lymph nodes might evoke a stronger immune response. Besides, the presence in the lymphatics of resident CD8+ DCs, which can cross-present antigens, could lead to an enhanced cellular response [54].

Different studies showed the free drainage of particles in the range of 10 – 200 nm [55–57] towards the lymphatic system, although generally an upper limit of 100 nm is normally established, specially in the case of rigid particles [58,59]. However, very small particles (< 10 nm) can directly drain to blood capillaries [60] and those that reach the lymph nodes have shown limited retention [61]. Within this range (10 – 100 nm), different groups has pointed out that between 20 - 50 nm could be the optimum particle size for the efficient distribution from the subcutaneous region to the lymph nodes. For example, 40 nm polyglutamic acid-based NPs migrated more rapidly to the lymph nodes and were captured more efficiently by resident DCs compared with 100 and 200 nm NPs after subcutaneous injection [62]. Similarly, Manolova *et al.* showed that 20 nm polystyrene drained more rapidly towards the lymphatics compared with 500 and 1000 nm particles after being administered subcutaneously [63]. Finally, following intradermal injection of polystyrene particles in the 20 – 2000 nm range, Fifis et al. found that, the 40 nm ones were those exhibiting the highest lymphatic drainage [64].

Regarding the surface charge, some authors have indicated that the drainage of negatively charged NPs to the LN is favored by their repulsion with the negatively charged extracellular matrix. This repulsion acts as a driving force moving NPs to the lymphatic system [65–67]. On the other hand, cationic nanosystems tend to form a depot after parenteral administration, which attracts peripheral and migratory APCs, while reducing their draining to LNs [68]. Nevertheless, this charge effect may be counterbalanced by the appropriate adjustment of the particle size. For example, Zeng *et al.* showed that 30 nm cationic micelles were able to self-drain to the closest lymph nodes [69]. Similarly, Kim *et al.* have reported that both small cationic and anionic poly(γ-glutamic acid)-based nanosystems (30–60 nm) were able to self-drain to the closest lymph node [70]. Finally, the presence of PEG on the surface of the nanocarriers, that usually renders their surface charge close to neutrality, has a positive effect in the drainage to the LN [71–74]. This does not necessarily translate into a higher interaction with immune cells [66,71,75], as the degree of PEGylation and the PEG molecular weight may have an impact on the NP opsonization [8,76].

Overall, the conclusion from the reported studies is that the final outcome of the nanocarriers is determined by the simultaneous influence of their properties including particle size, surface charge, shape, hydrophobicity and stiffness, among others (Fig. 2).

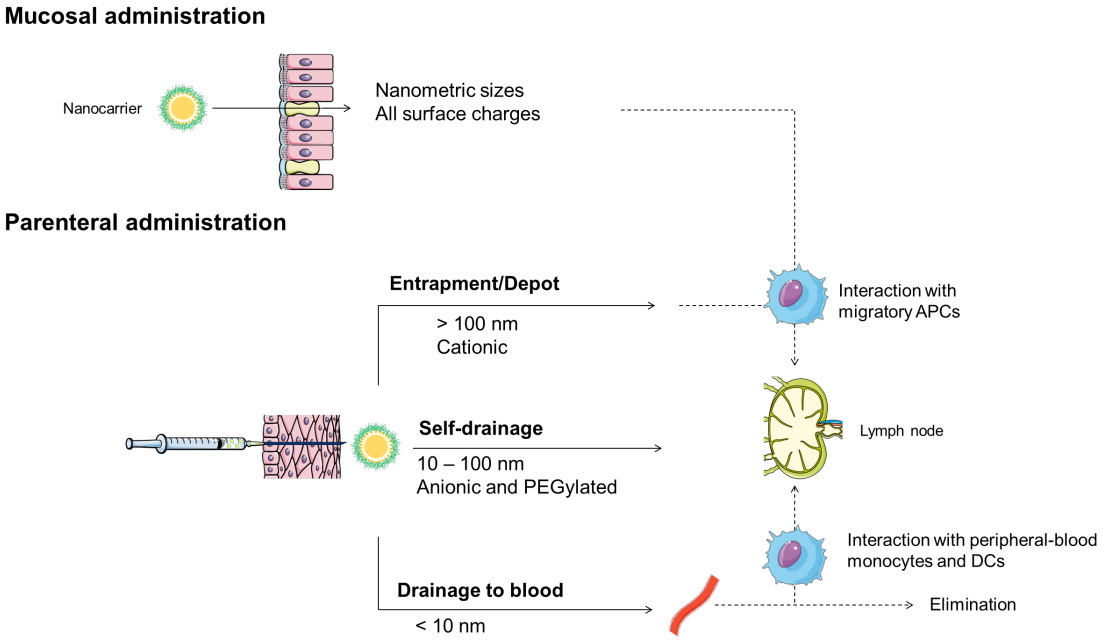

Figure 2. Summary of the influence of the particle size and the surface charge in the fate of the nanosystems once administered in the body. The physicochemical characteristics of the nanocarriers, particularly the particle size and the surface charge, play an important role in their biodistribution towards the lymphatic system once administered, either by mucosal or parenteral routes.

3. Interaction of particulated systems with specific subsets of immune cells

When a nanostructure enters the human body it normally interacts with the innate immune cells, such as monocytes, macrophages and dendritic cells, and initiates an immune response, in a similar way to a pathogen infection.

Monocytes and macrophages are one of the most abundant phagocytic cells in the body and represent the first innate defense line. They can be either circulating or resident in tissues, clearing pathogens and apoptotic cells. These cells are able to drain to the injury site, attracted by chemokines, and, hence, they have an important role in presenting antigens and releasing cytokines that modulate the immune response. In addition, they mediate inflammatory processes, which are relevant in a large variety of inflammatory diseases as well as in tumor growth and metastasis [77].

Several *in vitro* studies have been conducted in order to elucidate the key characteristics of NPs and MPs for the passive targeting to macrophages. All these studies have shown that both, particle size and shape influence the internalization efficiency by macrophages (Table 1). In this sense, in the past and mainly based on *in vitro* studies, it was assumed that particles in the micrometric range were well recognized by macrophages [78–84]. Nevertheless, recent studies have questioned this assertion and the current tendency is to believe that NPs can be very efficiently taken up by macrophages [85,86]. On the other hand, regarding the influence of the surface charge on the uptake of NPs by macrophages, several *in vitro* and *in vivo* studies have shown different results. Indeed, while in most of the cases cationic nanosystems were taken up by macrophages at a greater extent than the neutral and negative ones [85,87–90], in others, the negative charge was preferable for an efficient uptake [91–96]. For example, Nakanishi *et al.* reported that positive multilamellar vesicles elicited stronger cellular and humoral immune responses both *in vitro* and *in vivo* than neutral or negative systems [90]. On the contrary, Fromen *et al.* observed that after a pulmonary instillation of anionic and cationic PRINT hydrogels, negative nanosystems were engulfed in a greater manner by pulmonary macrophages [91]. More examples of these somehow contradictory results are summarized in Table 1.

Table 1. Summary of the different strategies considered for a passive targeting to monocytes and/or macrophages

Studied feature	Composition	Particle size	Surface charge	Key results	Ref.
Particle size	Non-functionalized polystyrene	0.9, 1.9, 2.3, 3, 4.3, 5.7, 9 µm	n.d.	≈ 2 - 3 µm more readily phagocytosed *in vitro* than smaller (≈ 1 µm) and larger particles (≈ 6 µm)	[80]
	Polystyrene and PLGA	1, 2, 3.2, 6.4, 10.1 µm	- 87.6 mV / - 9.7 mV	≈ 6 µm polystyrene particles and ≈ 3 µm PLGA particles were the most efficiently phagocytosed particles *in vitro*	[82]
	PLGA	1.5, 3.3, 6.1, 10 µm	n.d.	More efficient *in vitro* delivery of the cargo achieved with ≈ 3 µm particles than with larger (≈ 6 - 10 µm) and smaller ones (≈ 1 µm)	[83]
	Carboxylated polystyrene	0.02, 0.04 and 1 µm	Anionic	48 h after *in vivo* administration, more 1 µm particles were co-localized with macrophages in the draining LNs than the smaller particles (0.02 - 0.04 µm)	[84]
	Carboxymethyl chitosan grafted and chitosan hydrochloride grafted	149.2 – 157.3, 300.7 and 456.5 nm	- 38.4 to - 13.2 mV; + 14.8 to + 34.6 mV	Larger NPs were more efficiently taken up *in vitro*	[85]
	Carboxylated polystyrene	0.5 – 4.5 µm	Anionic	Small-particles group (0.5, 1 and 2 µm) was internalized *in vitro* at a higher rate than the group of larger particles (3 and 4.5 µm)	[86]
Shape	Non-functionalized polystyrene	Axis from 1 to 12.5 µm	n.d.	Better phagocytosis *in vitro* in alveolar macrophages for MPs that allow a lower contact angle (ellipsoids and disks)	[78]
Particle size and shape	Non-functionalized polystyrene	0.5 – 3 µm	n.d.	Particles with the longest dimension of 2 - 3 µm showed the maximum attachment to macrophages *in vitro*	[81]
Surface charge	Carboxylated polystyrene covalently coated with BSA or PLL	1 – 4.5 µm	- 58.3 to -18.4 mV; + 39.6 to + 49.7 mV	Cationic particles were better taken up than anionic particles by macrophages *in vitro*	[87]
	Carboxylated polystyrene covalently coated with BSA, PLL, IgG or PEI	1 µm	- 21.1 to -0.8 mV; + 38.2 to + 45.7 mV	Cationic MPs were better taken up by macrophages than negative particles *in vitro*	[88]
	Carboxymethyl chitosan grafted and chitosan hydrochloride grafted	149.2 – 157.3; 300.7 and 456.5 nm	- 38.4 to +34.6 mV	Positively charged NPs were more efficiently taken up than negatively charged ones *in vitro*	[85]

Surface charge	DOPC/DODAP and DOPC/DOPS liposomes	120 nm	Cationic, neutral and anionic	Positively charged liposomes were better taken up than negative and neutral liposomes by rat macrophages *in vitro*	[89]
	PC/Chol/SA, PC/Chol/PA, PC/Chol multilamelar vesicles	n.d.	- 18.6 to + 8.9 mV	Positively charged liposomes showed a higher uptake rate by macrophages *in vitro* and better immune responses *in vivo* than neutral and negative liposomes	[90]
	PRINT hydrogel, derived from HP_4A	80 nm × 80 nm × 320 nm	Cationic and anionic	After pulmonary instillation, anionic NPs were more efficiently taken up by macrophages than cationic NPs	[91]
	Cyanoacrylate NPs coated with dextran or diethylaminoethyl-dextran	200 nm	+ 30 mV / - 20 mV	Anionic NPs showed a higher internalization by macrophages *in vitro*, and also higher anti-inflammatory properties than the cationic ones	[92]
	DSPC/DODAB/Chol or DSPC/DSPG/Chol liposomes	180- 190 nm	- 29, 0.1 and + 25 mV	Anionic liposomes were more effective than neutral ones *in vivo* and *in vitro*. Cationic liposomes were more potent, but this was associated with a higher cytotoxicity of the forming polymers	[93]
	Neutral, carboxylated and aminated polystyrene	500 nm	- 50, - 0.5 and + 40 mV	Anionic particles decreased the infiltration of inflammatory monocyte-derived macrophages *in vivo* to a larger extent than cationic or neutral NPs of the same size	[95]

BSA: bovine serum albumin; Chol: cholesterol; DODAB: dimethyl dioctadecyl ammonium bromide; DODAP: 1,2-dioleoyl-3-dimethylammonium propanediol; DOPC: 1,2-dioleolyl-sn-glycero-3-phosphatidylcholine; DOPS: 1,2-dioleolyl-sn-glycero-3-phosphatidylserine; DSPC: 1,2-distearoyl-sn-glycero- 3-phosphocholine; DSPG: distearoyl-phosphatidylglycerol; HP_4A: tetra(ethylene glycol) monoacrylate; IgG: immunoglobulin G; LN: lymph node; MP: microparticle; n.d.: not determined; NP: nanoparticle; PA: L-a-dimyristoyl phosphatidic acid; PEI: polyethylenimine; PC: egg phosphatidylcholine; PLGA: poly(lactic-co-glycolic) acid; PLL: poly-L-lysine; PRINT: particle replication in non-wetting templates; SA: stearylamine

Dendritic cells (DCs) are the most important antigen-presenting cells (APCs) and have a key role in the modulation of the immune system [102]. Significant attempts have been made to passively (Table 2) target DCs using nanocarriers. DCs have a high phagocytic capacity similar to that of macrophages, however, unlike them, DCs preferentially ingest small virus-size particles [84,103,104]. Therefore, a way to passively target DCs is through the reduction of the nanocarriers' size. On the other hand, it is also known that providing nanocarriers with a positive surface charge enhances the chances for them to interact with DCs [87,91,104–106]. Nevertheless, irrespective of the influence of size and surface charge in the specific uptake of particles by dendritic cells, it seems clear that the most effective approach to precisely target DCs would be providing the nanocarriers with specific targeting ligands [107], for instance antibodies targeting CD40 (TNF-α family receptor), CD11c (integrin receptor) or DEC-205 (C-type lectin receptor) receptors. [108]. The targeting of the mannose receptor has also been reported as a strategy to increase the activation of DCs *in vitro* and *in vivo* [109,110].

Table 2. Summary of the different strategies followed for a passive targeting to dendritic cells

Studied feature	Composition	Particle size	Surface charge	Key results	Ref.
Particle size	Carboxylated polystyrene	0.02, 0.04 and 1 µm	n.d.	48 h after *in vivo* administration, smaller sizes (0.02 - 0.04 µm) were found in a higher amount in DCs, in comparison to 1 µm particles	[84]
	Carboxylated polystyrene plain or coated with PLL, PA, PrS, TT or WGA	0.1, 0.5, 0.9 and 4.5 µm	- 66.9 to + 41.4 mV	Particles smaller than 0.5 µm had better *in vitro* uptake by DCs	[104]
Surface charge	PC/PG/Chol, PC/PS/Chol, PC/TAP/Chol liposomes	180 to 279 nm	- 54.2 to + 44.2 mV	Positively charged liposomes had a greater interaction with DCs *in vitro* than anionic ones	[105]
	Carboxylated polystyrene covalently coated with BSA or PLL	1 – 4.5 µm	- 58.3 to -18.4 mV; + 39.6 to + 49.7 mV	Cationic particles uptake by DCs *in vitro* was higher than for anionic particles	[87]
	PRINT hydrogel derived from HP_4A	248 to 285 nm	- 38 to + 45 mV	Pulmonary administration of cationic NPs elicited stronger antibody responses than negative NPs administration, which correlates with a higher uptake *in vitro* of the former by DCs	[106]
	PRINT hydrogel derived from HP_4A	80 nm × 80 nm × 320 nm	Cationic and anionic	After pulmonary administration cationic NPs, rather than negative ones, preferentially associated to lung DCs	[91]
	Carboxylated polystyrene plain or coated with PLL, PA, PrS, TT or WGA	0.1, 0.5, 0.9 and 4.5 µm	- 66.9 to + 41.4 mV	Positively charged particles were better internalized by DCS *in vitro* than negative ones, especially when they were of micrometric sizes	[104]

Chol: cholesterol; DC: dendritic cell; HP_4A: tetra(ethylene glycol) monoacrylate; n.d.: not determined; NP: nanoparticle; PC: dimyristoyl phosphatidylcholine; PG: dimyristoyl phosphatidylglycerol; PA: L-a-dimyristoyl phosphatidic acid; PLL: poly-L-lysine; PRINT: particle replication in non-wetting templates; PrS: protamine sulphate; TAP: dimyristoyl trimethylammoniumpropane; TT: tetanus toxoid; WGA: wheat germ agglutinin

4. Humoral versus cellular responses

As illustrated in Fig. 3, DCs internalize antigens from their surroundings, process them in endosomes/lysosomes and present the resulting peptides through the class II major histocompatibility complex (MHC II), leading to a specific $CD4^+$ T cell activation and proliferation [111]. On the other hand, if the antigens are found in the cytosol of DCs, as in the case of intracellular infections, the peptides will be presented by class I MHC (MHC I) to naïve $CD8^+$ T cells, activating cellular responses. In some cases, external antigens can be translocated from endosomes to the cytosol and, thus, be presented via MHC I, process known as cross-presentation [3,112]. This phenomenon is of great importance in antitumor and infectious disease vaccination where a potent cellular response is required [113]. In both cases, besides antigen presentation, a co-stimulation of T cells through cytokines or co-stimulatory signals is normally needed [114].

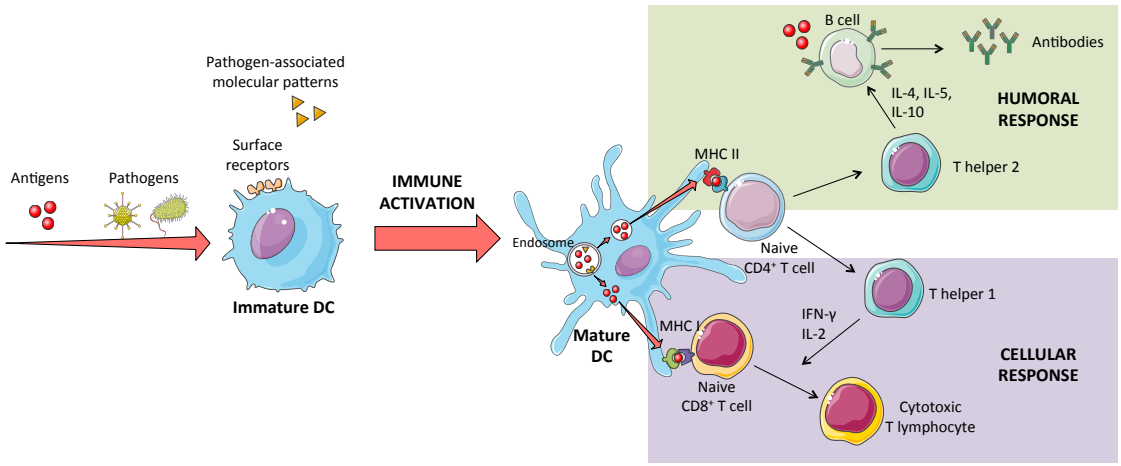

Figure 3. Cell network in the generation of an immune response

Schematic overview of the generation of an immune response by dendritic cells. Antigens, pathogens and other molecules are taken up by immature dendritic cells. In the case of pathogens or systems expressing pathogen-associated molecular patterns (PAMPs), their internalization by dendritic cells leads to their presentation by class II major histocompatibility complexes (MHC II) to naïve $CD4^+$ T cells, which activate T helper cells (Th). Th2 cells produce IL-4, IL-5 and IL-10, which stimulate B cells to produce antibodies against the antigen. At the same time, antigens themselves can interact directly with B cells and activate them. Antigens can also be found in the cytosol of dendritic cells, which allows them to be presented by class I major histocompatibility complexes (MHC I), directly activating cytotoxic T lymphocytes. In this case, Th1 cells produce IFN-γ and IL-2, which favor cellular activation and hence, cytotoxic T cell responses.

4.1. Cellular responses

In order to fight some infectious diseases (i.e., HIV, malaria) or other diseases, i.e. cancer, the stimulation of a powerful cellular response is believed to be necessary. In this context, a correlation between NP size and its ability to favor cross-presentation has been reported [3,9]. In general, studies have shown that smaller sizes enhance cross-presentation and CD8+ T cell responses [115–117]. It has been hypothesized that this effect might be related to the capacity of the these NPs to self-drain to the lymph nodes and thus, directly interact with resident $CD8^+$ DCs [118], and also to the specific uptake pathway they follow for internalization. Regarding their uptake, it has been described that particles with sizes similar to virus are endocytosed by DCs through an internalization route that facilitates endosomal escape and drives cellular responses [119–121]. Also, as mentioned above, active targeting to DC205, CD40 or CD11c has shown higher $CD8^+$ T cell activation [108].

As previously discussed, to drive cellular immunity, DCs need to present antigens on MHC I. To achieve this cross-presentation, the antigen has to be present in the cytosol of DCs, thus favoring endosomal escape of the antigen is a requirement for achieving a cellular response (Fig. 4D, Table 3). This endosomal escape can be promoted by the disruption of the endosome membrane, as discussed by several authors [122,123]. Keller *et al.* showed how pH-responsive micelles significantly enhance cytotoxic T lymphocyte responses, in comparison to micelles without these properties [124]. This effect was achieved because the forming polymers are protonated at endosomal pH which allows them to interact with the membrane and disrupt the endosome [124,125]. The same tendency was reported in the case of pH-sensitive liposomes, cationic liposomes and bioreducible linkages [126–129]. Other example of cross-presentation and increased cytotoxic T lymphocyte activity has been shown by the ISCOMATRIX adjuvant in both, preclinical and clinical studies, due to a rapid antigen translocation from the endosome [130,131].

With regard to the use of adjuvants, toll-like receptors (TLRs) are extensively used for immunomodulation (Fig. 4A, Table 3). More specifically, for Th1 biased responses, endosomal TLRs (TLR3, 7, 8 and 9) are an interesting target. These receptors recognize bacterial and viral genetic material, thus their activation will trigger a cellular response, as would a viral or intracellular-bacterial infection. In addition, the combination of nanotechnology and adjuvants has shown a great $CD8^+$ T cell activation with a decrease in the toxicity associated with these molecules [132–134]. Furthermore, since it is known that pathogens normally express several PAMPs at the same time, the combination of several immunomodulatory molecules can further enhance the elicited immune response [7,9,135].

Table 3. Strategies to facilitate the endosomal escape of antigens in dendritic cells

Mechanism	Critical feature	Nanosystem	Key results	Ref.
Membrane disruption	pH-responsive diblock copolymers	Polyacrylic micelles	pH-responsive micelles caused a higher increase of $CD8^+$ T cell responses *in vitro* and *in vivo* than non-pH-responsive controls	[124]
Fusion with the membrane	pH-sensitive poly(glycidol) polymers	EPC/DOPE/polymer liposomes	Modified liposomes elicit stronger cellular responses than unmodified systems *in vivo*	[126]
Unknown	Positive lipids (DOTAP or DC-Chol)	DOTAP/Chol/DSPE-mPEG, DC-Chol/DOPE/DSPE-mPEG, EPC/Chol/DSPE-mPEG liposomes	Liposomes with cationic lipids, but not with anionic ones, increased cross-presentation and $CD8^+$ T cell activation *in vitro*	[127]
Membrane disruption (?)	Disulfide crosslinking of the gel	Bioreducible alginate/PEI nanogels	Humoral and cellular responses where enhanced *in vitro* by the bioreducible nanogel in comparison to the non-reducible one	[128]
Unknown	Disulfide bond to nanocarrier	Propylene sulfide NPs	More efficient cross-presentation of the antigen when attached by a reducible link rather than by a non-reducible one	[129]
Unknown	ISCOMATRIX adjuvant	ISCOMATRIX + antigen (OVA or *E. coli* protein)	ISCOMATRIX adjuvant allowed a rapid translocation of the antigen from lysosomes to the cytosol and a greater cross-presentation *in vitro*, in comparison to immune complexes	[130]
Activation of endosomal TLR3 or TLR9	Poly(I:C), CpG or plasmid DNA	Liposome-Ag-nucleic acid complexes	Complexation of TLR agonists showed an increased $CD8^+$ T cell activation independent of $CD4^+$ T cell help, in comparison to liposomes without TLRs. Also, both prophylactic and therapeutic effects were achieved in two different mice models	[132]
Activation of endosomal TLR3	Poly(I:C)	Cationic adjuvant system (CAF01), composed of DDA and TDB	Immunization with OVA + DDA/TDB/poly(I:C) elicited stronger and longer $CD8^+$ T cell responses in mice than CAF01 alone. In addition, less inflammatory side effects were observed than when administering poly(I:C) alone	[133]

Activation of endosomal TLR7/8	Resiquimod	Temperature-responsive self-assembling particles, based on resiquimod anchored to HPMA or NIPAM scaffolds	Particle formation was key to diminish systemic toxicity and to generate Th1 bias responses, high antibody titers and $CD8^+$ T cell activation *in vivo*	[134]

Ag: antigen; CSF21: cationic adjuvant system; Chol: cholesterol; DC-Chol: 3β-[N-(N',N'-dimethylaminoethane)-carbamoyl] cholesterol; DDA: dimethyldioctadecylammonium; DOPE: 1,2-dioleoyl-sn-glycero-3-phosphoethanolamine; DOTAP: ,2-dioleoyl-3-trimethylammonium-propane; DSPE-mPEG: 1,2-distearoyl-sn-glycero-3-phosphoethanolamine-N-[methoxy(polyethyleneglycol)-2000]; EPC: egg phosphatylcholine; HPMA: hydrophilic N-(2-hydroxypropyl) methacrylamide; NIPAM: N-isopropylacrylamide; NP: nanoparticle; OVA: ovalbumin; PEI: polyethylenimine; poly(I:C): polyinosinic–polycytidylic acid; TDB: trehalose 6,6'-dibehenate; Th1: T helper 1; TLR: toll-like receptor

An alternative procedure to generate cellular responses is a direct targeting to $CD8^+$ T cells (Fig. 4E). For this, some authors have employed the so-called artificial antigen presenting cells (aAPCs), which present in their surface major histocompatibility complex molecules and also specific cell markers for T cell recognition and activation [136]. Using this strategy with paramagnetic particles and quantum dots, an increase in $CD8^+$ T cell activation and a decrease in tumor growth were observed [137]. Similarly, ellipsoidal PLGA nano-aAPCs were shown to be more efficient than the spherical ones in driving $CD8^+$ T cell activation [138].

4.2. Humoral responses

Since B cells are in charge of antibody production, a sustained activation of these cells is crucial to guarantee humoral responses. This is the mechanism of action by which most vaccines on the market lead to long-lasting antibody responses. Normally, B cell activation is driven by both, the direct interaction of the antigen with the B cell receptor (BCR) and the co-stimulation by $CD4^+$ T cells [139,140].

Some authors have suggested that the location of the antigen on the NP's structure may influence the resulting humoral response. For example, Temchura *et al.* observed that calcium-phosphate NPs with the antigen covalently attached to their surface, led to a substantial increase in B cell activation *in vitro*, in comparison to the soluble antigen [141]. Similarly, Moon *et al.* showed that the display of the antigen onto the surface of multilamellar vesicles provided an enhanced humoral response as compared to the antigen encapsulated [142]. In agreement with these data, several reports showed that the covalent conjugation of the antigen to liposomes could generate stronger antibody responses as compared to those obtained for other types of antigen association (Table 3) [143–153]. Nevertheless, the number of studies on the importance of the linking process of the antigen to the nanocarrier is very limited and it requires further exploration.

With regard to the influence of the size on the humoral responses of antigens associated to NPs, it has been reported that for some specific compositions micrometric sizes have a tendency to preferentially generate Th2 responses, in comparison to smaller sizes [119–121]. The mechanism behind this behavior could be related to the uptake pathway. It has been described that for sizes bigger than 500 nm the internalization and processing route of the antigen lead to a more efficient presentation by MHC II, generating stronger humoral responses [120,121].

Another possibility to favor humoral responses could be the administration of TLR2 agonists, since these are able to generate Th2-biased responses [154,155]. Similarly, the activation of surface TLRs (TLR2 and TLR4) showed that they can efficiently inhibit $CD8^+$ T cell activation [156].

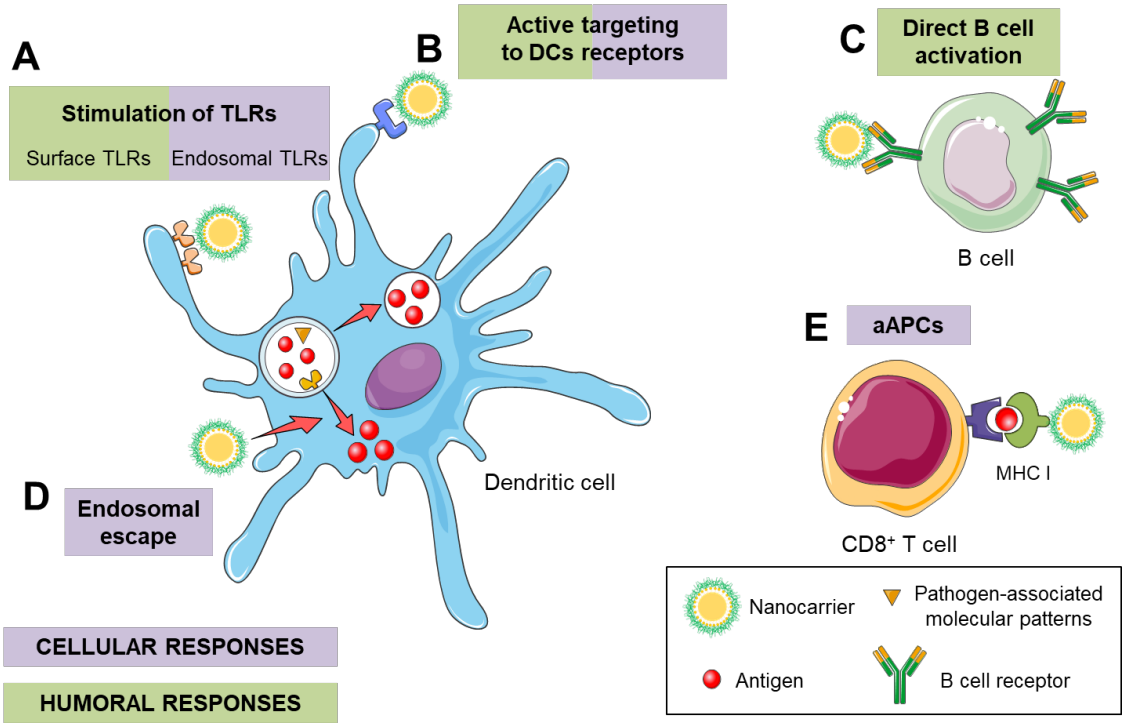

Figure 4. Nanotechnology-based approaches to modify the immune response to enhance humoral or cellular responses. Nanocarriers can drive both humoral and cellular responses, depending on their features and composition. (A) Nanocarriers can deliver toll-like receptor (TLR) agonists that can activate surface or endosomal receptors, driving humoral or cellular responses, respectively. (B) Decorating nanocarriers with antibodies against specific receptors of dendritic cells (DCs) (e.g., CD40, CD11c, DEC-205, mannose, etc.) can activate these cells. (C) The direct targeting to B cells can stimulate them and, thus, favor antibody production and humoral responses. (D) Nanocarriers with properties that promote endosomal escape of the antigens, favor cellular responses. (E) A direct activation of $CD8^+$ T cells through artificial antigen presenting cells (aAPCs) stimulates cytotoxic T lymphocytes.

5. Approved adjuvants and nanovaccines in clinical trials

As a consequence of all the efforts in the nanotechnology field, some NP-based adjuvants have already reached the market (table 3). This is the case of MF59, AS03, and AS01. MF59 is a 160 nm nanoemulsion of squalene, Tween®80 and Span®85 that is part of an Influenza vaccine, commercialized mostly in Europe since 1997 by Novartis under the name of Fluad™ [157]. AS03 is also a nanoemulsion-based adjuvant, composed of squalene, tocopherol and Tween®80, property of GSK. Currently, this adjuvant can be found in the pandemic influenza vaccine Prepandrix™, approved in 2008 [158]. Also, Epaxal® and Inflexal® V are two virosome-based vaccines for hepatitis A and influenza, respectively, that are commercialized in some European countries [159].

Table 3. Summary of adjuvants present on marketed vaccines for human use. Those of nanometric size are highlighted [12,160–162]

Adjuvant name (year licensed)	Composition	Disease	Commercial name
Alum (1924)	Aluminium salts	D.T. pertussis, IPV, hepatitis A & B, meningococcal and pneumococcal	Various
MF59 (1997)	**O/W nanoemulsion** (squalene, polysorbate 80, sorbitan trioleate)	Seasonal Influenza, pandemic influenza	Fluad™, Focetria®, Celtura®
Virosomes (2000)	**Liposomes**	Seasonal influenza, hepatitis A	Epaxal®, Inflexal®
AS04 (2005)	MPL (TLR4 agonist) adsorbed into alum	Hepatitis B, human papilloma virus	Fendrix®, Cervarix®
AS03 (2009)	**O/W nanoemulsion** (squalene, Tween® 80, α-tocopherol)	Prepandemic and pandemic flu	Prepandrix®, Pandemrix®, Arepanrix®
AS01 (2017)	MPL, QS-21, **liposome**	Herpes zoster	Shingrix®
Montanide ISA 51 (2017)	W/O **nanoemulsion**	Lung cancer	Cimavax®

In addition to these adjuvants and vaccines, a great number of nanoformulations for vaccine delivery are currently in clinical trials and they are illustrated in Table 4.

Table 4. Summary of some relevant nanovaccine-delivery systems that are being evaluated in clinical trials

Name / Company	Nanocarrier	Disease	Vaccination route	Clinical Phase	Ref.
SELA-070 / Selecta Biosciences	Synthetic Vaccine Particles (SVP™) (PLGA-based)	Smoking cessation and relapse prevention	Parenteral (SC)	Phase I	[163,164]
MAS-1 / Nova Immunothera-peutics Limited	Nanoparticular emulsion-based adjuvant	Seasonal Influenza	Parenteral	Phase I	[165,166]
FluGem® / Mucosis BV	Bacterium-like particles	Influenza	Intranasal	Phase I	[167,168]
SynGem® / Mucosis BV		RSV	Intranasal	Phase I	[167,169]
VCL-HB01 / Vical Inc	Vaxfectin® adjuvant: cationic lipid-based liposomes	HSV-2	Parenteral (IM)	Phase II	[170,171]
ASP0113 / Vical Inc	Poloxamer CRL1005+ DNA	CMV in hematopoietic cell transplant patients	Parenteral (IM)	Phase III	[172,173]
		CMV		Phase II	[172,174]
HBV003 / Vaxine Pty Ltd	Advax®: D-inulin microparticles	Hepatitis B	Parenteral (IM)	Phase I/II	[175,176]
FLU003 / Vaxine Pty Ltd		H5N1 Avian Influenza	Parenteral (IM)	Phase I	[175,177]
R21 + Matrix M1 / University of Oxford & Novavax	Antigen + Matrix M™: saponin-based nanoparticles (saponins, synthetic Chol and phospholipids)	Malaria	Parenteral (IM)	Phase I/II	[178,179]
RSV F Vaccine / Novavax	RSV F Vaccine: rF-protein nanoparticles from RSV	RSV	Parenteral (IM)	Phase III	[180,181]
RSV F Vaccine + Matrix M / Novavax	RSV F Vaccine + Matrix M™	RSV	Parenteral (IM)	Phase II and III	[178,181,182]
LV305 / Immune Design	LVR305: Antigen-specific ZVex® viral vector	Non-small cell lung cancer, Melanoma and Sarcoma	Parenteral (ID)	Phase I	[183–185]
CMB305 / Immune Design	LV305 + G305 (GLA adjuvant system)	Sarcoma, Melanoma, Non-small cell lung cancer and Ovarian cancer	Parenteral (ID and IM)	Phase I	[183,184,186]
JVRS-100 / Juvaris Biotherapeutics Inc	JVRS-100: cationic lipids/non-coding DNA plasmid complexes	Leukaemia	Parenteral (IV)	Phase I	[187,188]

1790GAHB / GlaxoSmithKline	GMMA: outer membrane particles from bacteria	Dysentery	Parenteral (IM)	Phase I	[189,190]
CTH522-CAF01 / Statens Serum Institut	CAF01: cationic adjuvant system composed of DDA and TDB	Chlamydia trachomatis	Parenteral (IM)	Phase I	[133,191]

Chol: cholesterol; CMV: cytomegalovirus; DDA: dimethyldioctadecylammonium; GLA: glucopyranosyl lipid A; GMMA: generalized modules of membrane antigen; HSV-2: Herpes Simplex Virus - 2; ID: intradermal; IM: intramuscular; RSV: Respiratory Syncital Virus; SC: subcutaneous; TDB: trehalose 6,6′-dibehenate

6. Conclusions

In the last decades, nanotechnology has shown an important potential in the immunotherapeutic field. Now it is known that the modulation of a broad variety of immune processes can be achieved with nanotechnology, with promising results not only *in vitro* but also *in vivo*. The nanocarriers size and composition may influence their biodistribution and subsequent interaction with the immunocompetent cells. Ultimately, this results in the modulation of the immune response. In particular, a very small size has been found to favor lymphatic drainage and promote cellular responses. However, the size threshold for this behavior is highly dependent on the nanocarriers composition. In addition, the incorporation of immunomodulators into the nanocarriers could substantially improve the immune response. Consequently, the analysis of the factors that influence the performance of nanocarriers should be done in a case-by-case basis.

The variety of nanotechnology-based approaches for immune modulation have resulted in a significant number of nanoformulations for vaccine delivery, which are currently being tested in clinical trials, and a few of them which have already reached the market. Without any doubt, a deeper knowledge of the nanosystem behavior in the biological system, in terms of dissemination through the body and interaction with the immune cells, will contribute to a more rational design of the future nanovaccines.

References

[1] M.F. Bachmann, G.T. Jennings, Vaccine delivery: a matter of size, geometry, kinetics and molecular patterns., Nat. Rev. Immunol. 10 (2010) 787–96. doi:10.1038/nri2868.

[2] D.M. Smith, J.K. Simon, J.R. Baker Jr, Applications of nanotechnology for immunology, Nat. Rev. Immunol. 13 (2013) 592–605. doi:10.1038/nri3517.

[3] D.J. Irvine, M.C. Hanson, K. Rakhra, T. Tokatlian, Synthetic nanoparticles for vaccines and immunotherapy, Chem. Rev. 115 (2015) 11109–11146. doi:10.1021/acs.chemrev.5b00109.

[4] A.S. Cordeiro, M.J. Alonso, Recent advances in vaccine delivery, Pharm. Pat. Anal. 5 (2015) 49–73. doi:10.4155/ppa.15.38.

[5] A.S. Cordeiro, M.J. Alonso, M. de la Fuente, Nanoengineering of vaccines using natural polysaccharides, Biotechnol. Adv. 33 (2015) 1279–1293. doi:10.1016/j.biotechadv.2015.05.010.

[6] D. Van Duin, R. Medzhitov, A.C. Shaw, Triggering TLR signaling in vaccination, Trends Immunol. 27 (2006) 49–55. doi:10.1016/j.it.2005.11.005.

[7] A. Gutjahr, G. Tiraby, E. Perouzel, B. Verrier, S. Paul, Triggering intracellular receptors for vaccine adjuvantation, Trends Immunol. 37 (2016) 573–587. doi:10.1016/j.it.2016.07.001.

[8] D.R. Getts, L.D. Shea, S.D. Miller, N.J.C. King, Harnessing nanoparticles for immune modulation, Trends Immunol. 36 (2015) 419–427. doi:10.1016/j.it.2015.05.007.

[9] K.T. Gause, A.K. Wheatley, J. Cui, Y. Yan, S.J. Kent, F. Caruso, Immunological Principles Guiding the Rational Design of Particles for Vaccine Delivery, ACS Nano. 11 (2017) 54–68. doi:10.1021/acsnano.6b07343.

[10] J. Du, Y.S. Zhang, D. Hobson, P. Hydbring, Nanoparticles for immune system targeting, Drug Discov. Today. 22 (2017) 1295–1301. doi:10.1016/j.drudis.2017.03.013.

[11] B.D. Walker, D.R. Burton, Toward an AIDS vaccine, Science (80-.). 320 (2008) 760–764. doi:10.1126/science.1152622.

[12] S.G. Reed, M.T. Orr, C.B. Fox, Key roles of adjuvants in modern vaccines, Nat. Med. 19 (2013) 1597–1608. doi:10.1038/nm.3409.

[13] I. Delany, R. Rappuoli, E. De Gregorio, Vaccines for the 21st century, EMBO Mol. Med. 6 (2014) 708–720. doi:10.1002/emmm.201403876.

[14] S. Plotkin, History of vaccination, Proc. Natl. Acad. Sci. 111 (2014) 12283–12287. doi:10.1073/pnas.1400472111.

[15] E. De Gregorio, R. Rappuoli, From empiricism to rational design: a personal perspective of the evolution of vaccine development, Nat Rev Immunol. 14 (2014) 505–514. doi:10.1038/nri3694.

[16] S.H.E. Kaufmann, The contribution of immunology to the rational design of novel antibacterial vaccines., Nat. Rev. Microbiol. 5 (2007) 491–504. doi:10.1038/nrmicro1688.

[17] F. Micoli, R. Adamo, P. Costantino, Protein Carriers for Glycoconjugate Vaccines: History, Selection Criteria, Characterization and New Trends, Molecules. 23 (2018) 1451. doi:10.3390/molecules23061451.

[18] M.M. Levine, M.B. Sztein, Vaccine development strategies for improving immunization: the role of modern immunology, Nat. Immunol. 5 (2004) 460–464. doi:10.1038/ni0504-460.

[19] G. Birrenbach, P.P. Speiser, Polymerized micelles and their use as adjuvants in immunology, J. Pharm. Sci. 65 (1976) 1763–1766. doi:10.1002/jps.2600651217.

[20] I. Preis, R.S. Langer, A single-step immunization by sustained antigen release, J. Immunol. Methods. 28 (1979) 193–197. doi:10.1016/0022-1759(79)90341-7.

[21] M.T. Aguado, P.H. Lambert, Controlled-release vaccines - Biodegradable polylactide/polyglycolide (PL/PG) microspheres as antigen vehicles, Immunobiology. 184 (1992) 113–125. doi:10.1016/S0171-2985(11)80470-5.

[22] A. Sánchez, R.K. Gupta, M.J. Alonso, G.R. Siber, R. Langer, Pulsed controlled-released system for potential use in vaccine delivery, J Pharm Sci. 85 (1996) 547–52. doi:10.1021/js960069y.

[23] M. Tobío, J. Nolley, Y. Guo, J. McIver, M.J. Alonso, A novel system based on a poloxamer/PLGA blend as a tetanus toxoid delivery vehicle, Pharm. Res. 16 (1999) 682–688. doi:10.1023/a:1018820507379.

[24] A.J. Almeida, H.O. Alpar, M.R.W. Brown, Immune Response to Nasal Delivery of Antigenically Intact Tetanus Toxoid Associated with Poly(L-lactic acid) Microspheres in Rats, Rabbits and Guinea-pigs, J. Pharm. Pharmacol. 45 (1993) 198–203. doi:10.1111/j.2042-7158.1993.tb05532.x.

[25] A. Vila, A. Sánchez, M. Tobío, P. Calvo, M.J. Alonso, Design of biodegradable particles for protein

delivery, J. Control. Release. 78 (2002) 15–24. doi:10.1016/S0168-3659(01)00486-2.

[26] M. Tobío, R. Gref, A. Sánchez, R. Langer, M.J. Alonso, Stealth PLA-PEG nanoparticles as protein carriers for nasal administration, Pharm. Res. 15 (1998) 270–275. doi:10.1023/A:1011922819926.

[27] A. Vila, A. Sánchez, C. Évora, I. Soriano, J.L. Vila Jato, M.J. Alonso, PEG-PLA nanoparticles as carriers for nasal vaccine delivery, J. Aerosol Med. 17 (2004) 174–185. doi:10.1089/0894268041457183.

[28] A. Vila, H. Gill, O. McCallion, M.J. Alonso, Transport of PLA-PEG particles across the nasal mucosa: Effect of particle size and PEG coating density, J. Control. Release. 98 (2004) 231–244. doi:10.1016/j.jconrel.2004.04.026.

[29] P. Calvo, C. Remuñán-López, J.L. Vila-Jato, M.J. Alonso, Novel hydrophilic chitosan-polyethylene oxide nanoparticles as protein carriers, J. Appl. Polym. Sci. 63 (1997) 125–132. doi:10.1002/(SICI)1097-4628(19970103)63:1<125::AID-APP13>3.0.CO;2-4.

[30] A. Vila, A. Sánchez, K. Janes, I. Behrens, T. Kissel, J.L. V Jato, et al., Low molecular weight chitosan nanoparticles as new carriers for nasal vaccine delivery in mice, Eur. J. Pharm. Biopharm. 57 (2004) 123–131. doi:10.1016/j.ejpb.2003.09.006.

[31] C. Prego, P. Paolicelli, B. Díaz, S. Vicente, A. Sánchez, Á. González-Fernández, et al., Chitosan-based nanoparticles for improving immunization against hepatitis B infection, Vaccine. 28 (2010) 2607–2614. doi:10.1016/j.vaccine.2010.01.011.

[32] S. Vicente, B. Díaz-Freitas, M. Peleteiro, A. Sánchez, D.W. Pascual, Á. González-Fernández, et al., A polymer/oil based nanovaccine as a single-dose immunization approach, PLoS One. 8 (2013) 2–9. doi:10.1371/journal.pone.0062500.

[33] C. Prego, D. Torres, M.J. Alonso, Chitosan nanocapsules: a new carrier for nasal peptide delivery, J. Drug Deliv. Sci. Technol. 16 (2006) 331–337. doi:10.1016/S1773-2247(06)50061-9.

[34] N. Csaba, M. Garcia-Fuentes, M.J. Alonso, Nanoparticles for nasal vaccination, Adv. Drug Deliv. Rev. 61 (2009) 140–157. doi:10.1016/j.addr.2008.09.005.

[35] Y. Huang, M.D. Donovan, Microsphere transport pathways in the rabbit nasal mucosa, Int. J. Pharm. Adv. 1 (1996) 298–309.

[36] R. Ghirardelli, F. Bonasoro, C. Porta, D. Cremaschi, Identification of particular epithelial areas and cells that transport polypeptide-coated nanoparticles in the nasal respiratory mucosa of the rabbit, Biochim. Biophys. Acta - Biomembr. 1416 (1999) 39–47. doi:10.1016/S0005-2736(98)00209-0.

[37] M. Amidi, S.G. Romeijn, G. Borchard, H.E. Junginger, W.E. Hennink, W. Jiskoot, Preparation and characterization of protein-loaded N-trimethyl chitosan nanoparticles as nasal delivery system, J. Control. Release. 111 (2006) 107–116. doi:10.1016/j.jconrel.2005.11.014.

[38] M. Li, M. Zhao, Y. Fu, Y. Li, T. Gong, Z. Zhang, et al., Enhanced intranasal delivery of mRNA vaccine by overcoming the nasal epithelial barrier via intra- and paracellular pathways, J. Control. Release. 228 (2016) 9–19. doi:10.1016/j.jconrel.2016.02.043.

[39] M. Rescigno, M. Urbano, B. Valzasina, M. Francolini, G. Rotta, R. Bonasio, et al., Dendritic cells express tight junction proteins and penetrate gut epithelial monolayers to sample bacteria, Nat. Immunol. 2 (2001) 361–367. doi:10.1038/86373.

[40] J.H. Niess, CX3CR1-mediated dendritic cell access to the intestinal lumen and bacterial clearance, Science (80-.). 307 (2005) 254–258. doi:10.1126/science.1102901.

[41] S.S. Olmsted, J.L. Padgett, A.I. Yudin, K.J. Whaley, T.R. Moench, R.A. Cone, Diffusion of Macromolecules and Virus-Like Particles in Human Cervical Mucus, Biophys. J. 81 (2001) 1930–1937. doi:10.1016/S0006-3495(01)75844-4.

[42] I. Gutierro, R.M. Hernández, M. Igartua, A.R. Gascón, J.L. Pedraz, Size dependent immune response after subcutaneous, oral and intranasal administration of BSA loaded nanospheres, Vaccine. 21 (2002) 67–77. doi:10.1016/S0264-410X(02)00435-8.

[43] J.F.S. Mann, E. Shakir, K.C. Carter, A.B. Mullen, J. Alexander, V.A. Ferro, Lipid vesicle size of an oral influenza vaccine delivery vehicle influences the Th1/Th2 bias in the immune response and protection against infection, Vaccine. 27 (2009) 3643–3649. doi:10.1016/j.vaccine.2009.03.040.

[44] M.P. Desai, V. Labhasetwar, G.L. Amidon, R.J. Levy, Gastrointestinal uptake of biodegradable microparticles: Effect of particle size, Pharm. Res. 13 (1996) 1838–1845. doi:10.1023/A:1016085108889.

[45] M. Shakweh, G. Ponchel, E. Fattal, Particle uptake by Peyer's patches: a pathway for drug and vaccine delivery, Expert Opin. Drug Deliv. 1 (2004) 141–163. doi:10.1517/17425247.1.1.141.

[46] M.O. Oyewumi, A. Kumar, Z. Cui, Nano-microparticles as immune adjuvants: correlating particle sizes and the resultant immune responses., Expert Rev. Vaccines. 9 (2010) 1095–107. doi:10.1586/erv.10.89.

[47] J.F. Correia-Pinto, N. Csaba, M.J. Alonso, Vaccine delivery carriers: insights and future perspectives, Int. J. Pharm. 440 (2013) 27–38. doi:10.1016/j.ijpharm.2012.04.047.

[48] V. Bernasconi, K. Norling, M. Bally, F. Höök, N.Y. Lycke, Mucosal Vaccine Development Based on Liposome Technology, J. Immunol. Res. 2016 (2016). doi:10.1155/2016/5482087.

[49] A. Vila, A. Sánchez, C. Évora, I. Soriano, O. McCallion, M.J. Alonso, et al., PLA-PEG particles as nasal protein carriers: the influence of the particle size, Int. J. Pharm. 292 (2005) 43–52. doi:10.1016/j.ijpharm.2004.09.002.

[50] A. Stano, C. Nembrini, M.A. Swartz, J.A. Hubbell, E. Simeoni, Nanoparticle size influences the magnitude and quality of immune response after intransal immunization, Vaccine. 30 (2012) 7541–6.

[51] M. Tobío, A. Sánchez, A. Vila, I. Soriano, C. Evora, J.L. Vila-Jato, et al., The role of PEG on the stability in digestive fluids and in vivo fate of PEG-PLA nanoparticles following oral administration, Colloids Surfaces B Biointerfaces. 18 (2000) 315–323. doi:10.1016/S0927-7765(99)00157-5.

[52] S.K. Lai, D.E. O'Hanlon, S. Harrold, S.T. Man, Y.-Y. Wang, R. Cone, et al., Rapid transport of large polymeric nanoparticles in fresh undiluted human mucus, Proc. Natl. Acad. Sci. 104 (2007) 1482–1487. doi:10.1073/pnas.0608611104.

[53] S.K. Lai, Y.Y. Wang, J. Hanes, Mucus-penetrating nanoparticles for drug and gene delivery to mucosal tissues, Adv. Drug Deliv. Rev. 61 (2009) 158–171. doi:10.1016/j.addr.2008.11.002.

[54] H. Jiang, Q. Wang, X. Sun, Lymph node targeting strategies to improve vaccination efficacy, J. Control. Release. 267 (2017) 47–56. doi:10.1016/j.jconrel.2017.08.009.

[55] M.F. Bachmann, G.T. Jennings, Vaccine delivery: a matter of size, geometry, kinetics and molecular patterns, Nat. Rev. Immunol. 10 (2010) 787–796. doi:10.1038/nri2868.

[56] M. Pitorre, G. Bastiat, E.M. dit Chatel, J.-P. Benoit, Passive and specific targeting of lymph nodes: the influence of the administration route, Eur. J. Nanomedicine. 7 (2015) 121–128. doi:10.1515/ejnm-2015-0003.

[57] R. Abellán-pose, N. Csaba, M.J. Alonso, Lymphatic Targeting of Nanosystems for Anticancer Drug Therapy, (2016) 1194–1209.

[58] K.T. Gause, A.K. Wheatley, J. Cui, Y. Yan, S.J. Kent, F. Caruso, Immunological Principles Guiding the Rational Design of Particles for Vaccine Delivery, ACS Nano. 11 (2017) 54–68. doi:10.1021/acsnano.6b07343.

[59] D.J. Irvine, M.C. Hanson, K. Rakhra, T. Tokatlian, Synthetic Nanoparticles for Vaccines and Immunotherapy, Chem. Rev. 115 (2015) 11109–11146. doi:10.1021/acs.chemrev.5b00109.

[60] L.M. Kaminskas, J. Kota, V.M. McLeod, B.D. Kelly, P. Karellas, C.J. Porter, PEGylation of polylysine dendrimers improves absorption and lymphatic targeting following sc administration in rats, J. Control. Release. 140 (2009) 108–116. doi:10.1016/j.jconrel.2009.08.005.

[61] I.C. Kourtis, S. Hirosue, A. de Titta, S. Kontos, T. Stegmann, J.A. Hubbell, et al., Peripherally Administered Nanoparticles Target Monocytic Myeloid Cells, Secondary Lymphoid Organs and Tumors in Mice, PLoS One. 8 (2013) 1–11. doi:10.1371/journal.pone.0061646.

[62] F. Shima, T. Uto, T. Akagi, M. Baba, M. Akashi, Size effect of amphiphilic poly(γ-glutamic acid) nanoparticles on cellular uptake and maturation of dendritic cells in vivo., Acta Biomater. 9 (2013) 8894–901. doi:10.1016/j.actbio.2013.06.010.

[63] V. Manolova, A. Flace, M. Bauer, K. Schwarz, P. Saudan, M.F. Bachmann, Nanoparticles target distinct dendritic cell populations according to their size., Eur. J. Immunol. 38 (2008) 1404–13. doi:10.1002/eji.200737984.

[64] T. Fifis, A. Gamvrellis, B. Crimeen-Irwin, G.A. Pietersz, J. Li, P.L. Mottram, et al., Size-dependent immunogenicity: therapeutic and protective properties of nano-vaccines against tumors, J. Immunol. 173 (2004) 3148–3154. doi:10.4049/jimmunol.173.5.3148.

[65] S.T. Reddy, D.A. Berk, R.K. Jain, M.A. Swartz, A sensitive in vivo model for quantifying interstitial convective transport of injected macromolecules and nanoparticles, J. Appl. Physiol. 101 (2006) 1162–1169. doi:10.1152/japplphysiol.00389.2006.

[66] S.N. Mueller, S. Tian, J.M. DeSimone, Rapid and Persistent Delivery of Antigen by Lymph Node Targeting PRINT Nanoparticle Vaccine Carrier To Promote Humoral Immunity, Mol. Pharm. 12 (2015) 1356–1365. doi:10.1021/mp500589c.

[67] D.A. Rao, M.L. Forrest, A.W.G. Alani, G.S. Kwon, J.R. Robinson, Biodegradable PLGA Based Nanoparticles for Sustained Regional Lymphatic Drug Delivery, J. Pharm. Sci. 99 (2010) 2018–2031. doi:10.1002/jps.21970.

[68] S. Vicente, B.A. Goins, A. Sanchez, M.J. Alonso, W.T. Phillips, Biodistribution and lymph node retention of polysaccharide-based immunostimulating nanocapsules, Vaccine. 32 (2014) 1685–1692. doi:10.1016/j.vaccine.2014.01.059.

[69] Q. Zeng, H. Jiang, T. Wang, Z. Zhang, T. Gong, X. Sun, Cationic micelle delivery of Trp2 peptide for efficient lymphatic draining and enhanced cytotoxic T-lymphocyte responses, J. Control. Release. 200 (2015) 1–12. doi:10.1016/j.jconrel.2014.12.024.

[70] S.Y. Kim, Y.W. Noh, T.H. Kang, J.E. Kim, S. Kim, S.H. Um, et al., Synthetic vaccine nanoparticles target to lymph node triggering enhanced innate and adaptive antitumor immunity, Biomaterials. 130 (2017) 56–66. doi:10.1016/j.biomaterials.2017.03.034.

[71] M.G. Carstens, M.G.M. Camps, M. Henriksen-Lacey, K. Franken, T.H.M. Ottenhoff, Y. Perrie, et al., Effect of vesicle size on tissue localization and immunogenicity of liposomal DNA vaccines, Vaccine. 29 (2011) 4761–4770. doi:10.1016/j.vaccine.2011.04.081.

[72] R. Kaur, V.W. Bramwell, D.J. Kirby, Y. Perrie, Pegylation of DDA:TDB liposomal adjuvants reduces the vaccine depot effect and alters the Th1/Th2 immune responses, J. Control. Release. 158 (2012) 72–77. doi:10.1016/j.jconrel.2011.10.012.

[73] R. Kaur, V.W. Bramwell, D.J. Kirby, Y. Perrie, Manipulation of the surface pegylation in combination with reduced vesicle size of cationic liposomal adjuvants modifies their clearance kinetics from the injection site, and the rate and type of T cell response, J. Control. Release. 164 (2012) 331–337. doi:10.1016/j.jconrel.2012.07.012.

[74] S. De Koker, J. Cui, N. Vanparijs, L. Albertazzi, J. Grooten, F. Caruso, et al., Engineering Polymer Hydrogel Nanoparticles for Lymph Node-Targeted Delivery, Angew. Chemie - Int. Ed. 55 (2016) 1334–1339. doi:10.1002/anie.201508626.

[75] S. Takano, Y. Aramaki, S. Tsuchiya, Physicochemical properties of liposomes affecting apoptosis induced by cationic liposomes in macrophages, Pharm. Res. 20 (2003) 962–968. doi:10.1023/A:1024441702398.

[76] D.E. Owens, N.A. Peppas, Opsonization, biodistribution, and pharmacokinetics of polymeric nanoparticles, Int. J. Pharm. 307 (2006) 93–102. doi:10.1016/j.ijpharm.2005.10.010.

[77] Y.R. Na, S. Je, S.H. Seok, Metabolic features of macrophages in inflammatory diseases and cancer, Cancer Lett. 413 (2018) 46–58. doi:10.1016/j.canlet.2017.10.044.

[78] J.A. Champion, S. Mitragotri, Role of target geometry in phagocytosis., Proc. Natl. Acad. Sci. U. S. A. 103 (2006) 4930–4. doi:10.1073/pnas.0600997103.

[79] J.A. Champion, Y.K. Katare, S. Mitragotri, Particle shape: A new design parameter for micro- and nanoscale drug delivery carriers, J. Control. Release. 121 (2007) 3–9. doi:10.1016/j.jconrel.2007.03.022.

[80] J.A. Champion, A. Walker, S. Mitragotri, Role of particle size in phagocytosis of polymeric microspheres, Pharm. Res. 25 (2008) 1815–1821. doi:10.1007/s11095-008-9562-y.

[81] N. Doshi, S. Mitragotri, Macrophages recognize size and shape of their targets, PLoS One. 5 (2010) 1–6. doi:10.1371/journal.pone.0010051.

[82] T. Hasegawa, K. Hirota, K. Tomoda, F. Ito, H. Inagawa, C. Kochi, et al., Phagocytic activity of alveolar macrophages toward polystyrene latex microspheres and PLGA microspheres loaded with anti-tuberculosis agent, Colloids Surfaces B Biointerfaces. 60 (2007) 221–228. doi:10.1016/j.colsurfb.2007.06.017.

[83] K. Hirota, T. Hasegawa, H. Hinata, F. Ito, H. Inagawa, C. Kochi, et al., Optimum conditions for efficient phagocytosis of rifampicin-loaded PLGA microspheres by alveolar macrophages, J. Control. Release. 119 (2007) 69–76. doi:10.1016/j.jconrel.2007.01.013.

[84] T. Fifis, A. Gamvrellis, B. Crimeen-Irwin, G.A. Pietersz, J. Li, P.L. Mottram, et al., Size-Dependent Immunogenicity: Therapeutic and Protective Properties of Nano-Vaccines against Tumors, J. Immunol. 173 (2004) 3148–3154. doi:10.4049/jimmunol.173.5.3148.

[85] C. He, Y. Hu, L. Yin, C. Tang, C. Yin, Effects of particle size and surface charge on cellular uptake and biodistribution of polymeric nanoparticles, Biomaterials. 31 (2010) 3657–3666. doi:10.1016/j.biomaterials.2010.01.065.

[86] P. Pacheco, D. White, T. Sulchek, Effects of Microparticle Size and Fc Density on Macrophage Phagocytosis, PLoS One. 8 (2013) 1–9. doi:10.1371/journal.pone.0060989.

[87] L. Thiele, B. Rothen-Rutishauser, S. Jilek, H. Wunderli-Allenspach, H.P. Merkle, E. Walter,

Evaluation of particle uptake in human blood monocyte-derived cells in vitro. Does phagocytosis activity of dendritic cells measure up with macrophages?, J. Control. Release. 76 (2001) 59–71. doi:10.1016/S0168-3659(01)00412-6.

[88] L. Thiele, H.P. Merkle, E. Walter, Phagocytosis and phagosomal fate of surface-modified microparticles in dendritic cells and macrophages, Pharm. Res. 20 (2003) 221–228. doi:10.1023/A:1022271020390.

[89] C.R. Miller, B. Bondurant, S.D. McLean, K.A. McGovern, D.F. O'Brien, Liposome-cell interactions in vitro: Effect of liposome surface charge on the binding and endocytosis of conventional and sterically stabilized liposomes, Biochemistry. 37 (1998) 12875–12883. doi:10.1021/bi980096y.

[90] T. Nakanishi, J. Kunisawa, A. Hayashi, Y. Tsutsumi, K. Kubo, S. Nakagawa, et al., Positively charged liposome functions as an efficient immunoadjuvant in inducing cell-mediated immune response to soluble proteins, Biochem. Biophys. Res. Commun. 240 (1997) 793–797. doi:10.1006/bbrc.1997.7749.

[91] C.A. Fromen, T.B. Rahhal, G.R. Robbins, M.P. Kai, T.W. Shen, J.C. Luft, et al., Nanoparticle surface charge impacts distribution, uptake and lymph node trafficking by pulmonary antigen-presenting cells, Nanomedicine Nanotechnology, Biol. Med. 12 (2016) 677–687. doi:10.1016/j.nano.2015.11.002.

[92] Y. Tomita, A. Rikimaru-Kaneko, K. Hashiguchi, S. Shirotake, Effect of anionic and cationic n-butylcyanoacrylate nanoparticles on NO and cytokine production in Raw264.7 cells, Immunopharmacol. Immunotoxicol. 33 (2011) 730–7. doi:10.3109/08923973.2011.565345.

[93] H. Epstein-Barash, D. Gutman, E. Markovsky, G. Mishan-Eisenberg, N. Koroukhov, J. Szebeni, et al., Physicochemical parameters affecting liposomal bisphosphonates bioactivity for restenosis therapy: Internalization, cell inhibition, activation of cytokines and complement, and mechanism of cell death, J. Control. Release. 146 (2010) 182–195. doi:10.1016/j.jconrel.2010.03.011.

[94] D. Gutman, H. Epstein-Barash, M. Tsuriel, G. Golomb, Alendronate Liposomes for Antitumor Therapy: Activation of γδ T Cells and Inhibition of Tumor Growth, in: Nano-Biotechnology Biomed. Diagnostinc Res., Springer Netherlands, 2012: pp. 165–179.

[95] D.R. Getts, R.L. Terry, M.T. Getts, C. Deffrasnes, M. Müller, C. Van Vreden, et al., Therapeutic Inflammatory Monocyte Modulation Using, Sci. Transl. Med. 6 (2014) 1–14. doi:10.1126/scitranslmed.3007563.

[96] T. Harel-Adar, T. Ben Mordechai, Y. Amsalem, M.S. Feinberg, J. Leor, S. Cohen, Modulation of cardiac macrophages by phosphatidylserine-presenting liposomes improves infarct repair, Proc. Natl. Acad. Sci. 108 (2011) 1827–1832. doi:10.1073/pnas.1015623108.

[97] A. Beduneau, Z. Ma, C.B. Grotepas, A. Kabanov, B.E. Rabinow, N. Gong, et al., Facilitated monocyte-macrophage uptake and tissue distribution of superparmagnetic iron-oxide nanoparticles, PLoS One. 4 (2009) 1–12. doi:10.1371/journal.pone.0004343.

[98] L.W. Locke, M.W. Mayo, A.D. Yoo, M.B. Williams, S.S. Berr, PET imaging of tumor associated macrophages using mannose coated 64Cu liposomes, Biomaterials. 33 (2012) 7785–7793. doi:10.1016/j.biomaterials.2012.07.022.

[99] L. Ma, T.W. Liu, M.A. Wallig, I.T. Dobrucki, L.W. Dobrucki, E.R. Nelson, et al., Efficient targeting of adipose tissue macrophages in obesity with polysaccharide nanocarriers, ACS Nano. 10 (2016) 6952–6962. doi:10.1021/acsnano.6b02878.

[100] J. Lesley, R. Hyman, P.W. Kincade, CD44 and its interaction with extracellular matrix, Adv. Immunol. 54 (1993) 271–335. doi:10.1016/S0065-2776(08)60537-4.

[101] R.A. Clark, R. Alon, T.A. Springer, CD44 and hyaluronan-dependent rolling interactions of lymphocytes on tonsillar stroma, J. Cell Biol. 134 (1996) 1075–1087. doi:10.1083/jcb.134.4.1075.

[102] P. Guermonprez, J. Valladeau, L. Zitvogel, C. Théry, S. Amigorena, Antigen presentation and T cell stimulation by dendritic cells, Annu. Rev. Immunol. 20 (2002) 621–667. doi:10.1146/annurev.immunol.20.100301.064828.

[103] A. Gamvrellis, D. Leong, J.C. Hanley, S.D. Xiang, P. Mottram, M. Plebanski, Vaccines that facilitate antigen entry into dendritic cells, Immunol. Cell Biol. 82 (2004) 506–516. doi:10.1111/j.0818-9641.2004.01271.x.

[104] C. Foged, B. Brodin, S. Frokjaer, A. Sundblad, Particle size and surface charge affect particle uptake by human dendritic cells in an in vitro model, Int. J. Pharm. 298 (2005) 315–322. doi:10.1016/j.ijpharm.2005.03.035.

[105] C. Foged, C. Arigita, A. Sundblad, W. Jiskoot, G. Storm, S. Frokjaer, Interaction of dendritic cells with antigen-containing liposomes: Effect of bilayer composition, Vaccine. 22 (2004) 1903–1913.

doi:10.1016/j.vaccine.2003.11.008.

[106] C.A. Fromen, G.R. Robbins, T.W. Shen, M.P. Kai, J.P.Y. Ting, J.M. DeSimone, Controlled analysis of nanoparticle charge on mucosal and systemic antibody responses following pulmonary immunization, Proc. Natl. Acad. Sci. 112 (2015) 488–493. doi:10.1073/pnas.1422923112.

[107] C. Macri, C. Dumont, A.P. Johnston, J.D. Mintern, Targeting dendritic cells: a promising strategy to improve vaccine effectiveness, Clin. Transl. Immunol. 5 (2016) e66. doi:10.1038/cti.2016.6.

[108] L.J. Cruz, R.A. Rosalia, J.W. Kleinovink, F. Rueda, C.W.G.M. Löwik, F. Ossendorp, Targeting nanoparticles to CD40, DEC-205 or CD11c molecules on dendritic cells for efficient CD8+ T cell response: A comparative study, J. Control. Release. 192 (2014) 209–218. doi:10.1016/j.jconrel.2014.07.040.

[109] Z. Ghotbi, A. Haddadi, S. Hamdy, R.W. Hung, J. Samuel, A. Lavasanifar, Active targeting of dendritic cells with mannan-decorated PLGA nanoparticles, J. Drug Target. 19 (2011) 281–292. doi:10.3109/1061186X.2010.499463.

[110] J.M. Silva, E. Zupancic, G. Vandermeulen, V.G. Oliveira, A. Salgado, M. Videira, et al., In vivo delivery of peptides and Toll-like receptor ligands by mannose-functionalized polymeric nanoparticles induces prophylactic and therapeutic anti-tumor immune responses in a melanoma model, J. Control. Release. 198 (2015) 91–103. doi:10.1016/j.jconrel.2014.11.033.

[111] P.A. Roche, K. Furuta, The ins and outs of MHC class II - mediated antigen processing and presentation, Nat. Rev. Immunol. 15 (2015) 203–216. doi:10.1038/nri3818.

[112] O.P. Joffre, E. Segura, A. Savina, S. Amigorena, Cross-presentation by dendritic cells, Nat. Rev. Immunol. 12 (2012) 557–569. doi:10.1038/nri3254.

[113] M.A. Williams, M.J. Bevan, Effector and Memory CTL Differentiation, Annu. Rev. Immunol. 25 (2007) 171–192. doi:10.1146/annurev.immunol.25.022106.141548.

[114] D.J. Irvine, M. a Swartz, G.L. Szeto, Engineering synthetic vaccines using cues from natural immunity., Nat. Mater. 12 (2013) 978–90. doi:10.1038/nmat3775.

[115] T. Hirai, Y. Yoshioka, H. Takahashi, K. Ichihashi, T. Yoshida, S. Tochigi, et al., Amorphous silica nanoparticles enhance cross-presentation in murine dendritic cells, Biochem. Biophys. Res. Commun. 427 (2012) 553–556. doi:10.1016/j.bbrc.2012.09.095.

[116] A. Mant, F. Chinnery, T. Elliott, A.P. Williams, The pathway of cross-presentation is influenced by the particle size of phagocytosed antigen, Immunology. 136 (2012) 163–175. doi:10.1111/j.1365-2567.2012.03558.x.

[117] S. Ahn, I.H. Lee, S. Kang, D. Kim, M. Choi, P.E. Saw, et al., Gold nanoparticles displaying tumor-associated self-antigens as a potential vaccine for cancer immunotherapy, Adv. Healthc. Mater. 3 (2014) 1194–1199. doi:10.1002/adhm.201300597.

[118] S.T. Schmidt, S. Khadke, K.S. Korsholm, Y. Perrie, T. Rades, P. Andersen, et al., The administration route is decisive for the ability of the vaccine adjuvant CAF09 to induce antigen-specific CD8+ T-cell responses: The immunological consequences of the biodistribution profile, J. Control. Release. 239 (2016) 107–117. doi:10.1016/j.jconrel.2016.08.034.

[119] S. Kumar, A.C. Anselmo, A. Banerjee, M. Zakrewsky, S. Mitragotri, Shape and size-dependent immune response to antigen-carrying nanoparticles, J. Control. Release. 220 (2015) 141–148. doi:10.1016/j.jconrel.2015.09.069.

[120] F. Lebre, C.H. Hearnden, E.C. Lavelle, Modulation of Immune Responses by Particulate Materials, Adv. Mater. 28 (2016) 5525–5541. doi:10.1002/adma.201505395.

[121] N. Benne, J. van Duijn, J. Kuiper, W. Jiskoot, B. Slütter, Orchestrating immune responses: How size, shape and rigidity affect the immunogenicity of particulate vaccines, J. Control. Release. 234 (2016) 124–134. doi:10.1016/j.jconrel.2016.05.033.

[122] A.K. Varkouhi, M. Scholte, G. Storm, H.J. Haisma, Endosomal escape pathways for delivery of biologicals, J. Control. Release. 151 (2011) 220–228. doi:10.1016/j.jconrel.2010.11.004.

[123] L.I. Selby, C.M. Cortez-Jugo, G.K. Such, A.P.R. Johnston, Nanoescapology: Progress toward understanding the endosomal escape of polymeric nanoparticles, Wiley Interdiscip. Rev. Nanomedicine Nanobiotechnology. (2017) e1452. doi:10.1002/wnan.1452.

[124] S. Keller, J. T.wilson, G.I. Patilea, H.B. Kern, A.J. Convertine, P.S. Stayton, Neutral polymer micelle carriers with pH-responsive, endosome-releasing activity modulate antigen trafficking to enhance CD8+ T cell responses, J. Control. Release. 191 (2014) 24–33. doi:10.1016/j.jconrel.2014.03.041.

[125] A.J. Convertine, C. Diab, M. Prieve, A. Paschal, A.S. Hoffman, P.H. Johnson, et al., pH-responsive polymeric micelle carriers for siRNA drugs, Biomacromolecules. 11 (2010) 2904–2911.

doi:10.1021/bm100652w.

[126] E. Yuba, A. Harada, Y. Sakanishi, S. Watarai, K. Kono, A liposome-based antigen delivery system using pH-sensitive fusogenic polymers for cancer immunotherapy, Biomaterials. 34 (2013) 3042–3052. doi:10.1016/j.biomaterials.2012.12.031.

[127] J. Gao, L.J. Ochyl, E. Yang, J.J. Moon, Cationic liposomes promote antigen cross-presentation in dendritic cells by alkalizing the lysosomal pH and limiting the degradation of antigens, Int. J. Nanomedicine. 12 (2017) 1251–1264. doi:10.2147/IJN.S125866.

[128] P. Li, Z. Luo, P. Liu, N. Gao, Y. Zhang, H. Pan, et al., Bioreducible alginate-poly(ethylenimine) nanogels as an antigen-delivery system robustly enhance vaccine-elicited humoral and cellular immune responses, J. Control. Release. 168 (2013) 271–279. doi:10.1016/j.jconrel.2013.03.025.

[129] S. Hirosue, I.C. Kourtis, A.J. van der Vlies, J.A. Hubbell, M.A. Swartz, Antigen delivery to dendritic cells by poly(propylene sulfide) nanoparticles with disulfide conjugated peptides: Cross-presentation and T cell activation, Vaccine. 28 (2010) 7897–7906. doi:10.1016/j.vaccine.2010.09.077.

[130] M. Schnurr, M. Orban, N.C. Robson, A. Shin, H. Braley, D. Airey, et al., ISCOMATRIX Adjuvant Induces Efficient Cross-Presentation of Tumor Antigen by Dendritic Cells via Rapid Cytosolic Antigen Delivery and Processing via Tripeptidyl Peptidase II, J. Immunol. 182 (2009) 1253–1259. doi:10.4049/jimmunol.182.3.1253.

[131] T. Nicholaou, W. Chen, I.D. Davis, H.M. Jackson, N. Dimopoulos, C. Barrow, et al., Immunoediting and persistence of antigen-specific immunity in patients who have previously been vaccinated with NY-ESO-1 protein formulated in ISCOMATRIX, Cancer Immunol. Immunother. 60 (2011) 1625–1637. doi:10.1007/s00262-011-1041-3.

[132] K. Zaks, M. Jordan, A. Guth, K. Sellins, R. Kedl, A. Izzo, et al., Efficient Immunization and Cross-Priming by Vaccine Adjuvants Containing TLR3 or TLR9 Agonists Complexed to Cationic Liposomes, J. Immunol. 176 (2006) 7335–7345. doi:10.4049/jimmunol.176.12.7335.

[133] P. Nordly, F. Rose, D. Christensen, H.M. Nielsen, P. Andersen, E.M. Agger, et al., Immunity by formulation design: Induction of high CD8+ T-cell responses by poly(I:C) incorporated into the CAF01 adjuvant via a double emulsion method, J. Control. Release. 150 (2011) 307–317. doi:10.1016/j.jconrel.2010.11.021.

[134] G.M. Lynn, R. Laga, P.A. Darrah, A.S. Ishizuka, A.J. Balaci, A.E. Dulcey, et al., In vivo characterization of the physicochemical properties of polymer-linked TLR agonists that enhance vaccine immunogenicity., Nat. Biotechnol. 33 (2015) 1201–10. doi:10.1038/nbt.3371.

[135] S.P. Kasturi, I. Skountzou, R.A. Albrecht, D. Koutsonanos, T. Hua, H.I. Nakaya, et al., Programming the magnitude and persistence of antibody responses with innate immunity., Nature. 470 (2011) 543–7. doi:10.1038/nature09737.

[136] J.C. Sunshine, J.J. Green, Nanoengineering approaches to the design of artificial antigen-presenting cells, Nanomedicine. 8 (2013) 1173–89. doi:10.2217/nnm.13.98.

[137] K. Perica, A. De León Medero, M. Durai, Y.L. Chiu, J.G. Bieler, L. Sibener, et al., Nanoscale artificial antigen presenting cells for T cell immunotherapy, Nanomedicine Nanotechnology, Biol. Med. 10 (2014) 119–129. doi:10.1016/j.nano.2013.06.015.

[138] R.A. Meyer, J.C. Sunshine, K. Perica, A.K. Kosmides, K. Aje, J.P. Schneck, et al., Biodegradable Nanoellipsoidal Artificial Antigen Presenting Cells for Antigen Specific T-Cell Activation, Small. 11 (2015) 1519–1525. doi:10.1002/smll.201402369.

[139] F.D. Batista, N.E. Harwood, The who, how and where of antigen presentation to B cells., Nat. Rev. Immunol. 9 (2008) 15–27. doi:10.1038/nri2454.

[140] T.J. Moyer, A.C. Zmolek, D.J. Irvine, Beyond antigens and adjuvants: formulating future vaccines, J. Clin. Invest. 126 (2016) 799–808. doi:10.1172/JCI81083.

[141] V. V. Temchura, D. Kozlova, V. Sokolova, K. Überla, M. Epple, Targeting and activation of antigen-specific B-cells by calcium phosphate nanoparticles loaded with protein antigen, Biomaterials. 35 (2014) 6098–6105. doi:10.1016/j.biomaterials.2014.04.010.

[142] J.J. Moon, H. Suh, a. V. Li, C.F. Ockenhouse, A. Yadava, D.J. Irvine, Enhancing humoral responses to a malaria antigen with nanoparticle vaccines that expand Tfh cells and promote germinal center induction, Proc. Natl. Acad. Sci. 109 (2012) 1080–1085. doi:10.1073/pnas.1112648109.

[143] D. Davis, G. Gregoriadis, Liposomes as adjuvants with immunopurified tetanus toxoid: influence of liposomal characteristics, Immunol. Lett. 61 (1987) 229–234.

[144] E. Shahum, H.M. Thérien, Immunopotentiation of the humoral response by liposomes: encapsulation versus covalent linkage, Immunology. 65 (1988) 315–317.

[145] H.H. Guan, W. Budzynski, R.R. Koganty, M.J. Krantz, M.A. Reddish, J.A. Rogers, et al., Liposomal formulations of synthetic MUC1 peptides: Effects of encapsulation versus surface display of peptides on immune responses, Bioconjug. Chem. 9 (1998) 451–458. doi:10.1021/bc970183n.

[146] W.E. Vannier, S.L. Snyder, Antibody responses to liposome-associated antigen, Immunol. Lett. 19 (1988) 59–64. doi:10.1016/0165-2478(88)90120-4.

[147] H.M. Thérien, D. Lair, E. Shahum, Liposomal vaccine: influence of antigen association on the kinetics of the humoral response, Vaccine. 8 (1990) 558–562. doi:10.1016/0264-410X(90)90008-A.

[148] K. Brynestad, B. Babbit, L. Huang, B.T. Rouse, Influence of peptide acylation, liposome incorporation, and synthetic immunomodulators on the immunogenicity of a 1-23 peptide of glycoprotein D of herpes simplex virus: implications for subunit vaccines, J. Virol. 64 (1990) 680–685.

[149] B. Frisch, S. Muller, J.P. Briand, M.H. V Van Regenmortel, F. Shuber, Parameters affecting the immunogenicity of a liposome-associated synthetic hexapeptide antigen, Eur. J. Immunol. 21 (1991) 185–193.

[150] L. Tan, V. Weissig, G. Gregoriadis, Comparison of the immune response against polio peptides covalently-surface-linked to and internally-entrapped in liposomes, Asian Pacific J. Allergy Immunol. 9 (1991) 25–30.

[151] E. Shahum, H.M. Thérien, Correlation between in vitro and in vivo behaviour of liposomal antigens, Vaccine. 12 (1994) 1125–1131. doi:10.1016/0264-410X(94)90183-X.

[152] E. Shahum, H.M. Thérien, Liposomal adjuvanticity: Effect of encapsulation and surface-linkage on antibody production and proliferative response, Int. J. Immunopharmacol. 17 (1995) 9–20. doi:10.1016/0192-0561(94)00082-Y.

[153] W.I. White, D.R. Cassatt, J. Madsen, S.J. Burke, R.M. Woods, N.M. Wassef, et al., Antibody and cytotoxic T-lymphocyte responses to a single liposome-associated peptide antigen, Vaccine. 13 (1995) 1111–1122. doi:10.1016/0264-410X(94)00058-U.

[154] S. Dillon, A. Agrawal, T. Van Dyke, L. Mccauley, A. Koh, C. Maliszewski, et al., A Toll-Like Receptor 2 Ligand Stimulates Th2 Responses In Vivo, via Induction of Extracellular Signal-Regulated Kinase Mitogen-Activated Protein Kinase and c-Fos in Dendritic Cells, J. Immunol. 172 (2004) 4733–4743. doi:10.4049/jimmunol.172.8.4733.

[155] V. Redecke, H. Hacker, S.K. Datta, A. Fermin, P.M. Pitha, D.H. Broide, et al., Cutting Edge: Activation of Toll-Like Receptor 2 Induces a Th2 Immune Response and Promotes Experimental Asthma, J. Immunol. 172 (2004) 2739–2743. doi:10.4049/jimmunol.172.5.2739.

[156] R. Mandraju, S. Murray, J. Forman, C. Pasare, Differential Ability of Surface and Endosomal TLRs To Induce CD8 T Cell Responses In Vivo, J. Immunol. 192 (2014) 4303–4315. doi:10.4049/jimmunol.1302244.

[157] D.T. O'Hagan, G.S. Ott, E. De Gregorio, A. Seubert, The mechanism of action of MF59 – An innately attractive adjuvant formulation, Vaccine. 30 (2012) 4341–4348. doi:10.1016/j.vaccine.2011.09.061.

[158] G. Ledet, L.A. Bostanian, T.K. Mandal, Nanoemulsions as a Vaccine Adjuvant, in: A. Tiwari, A. Tiwari (Eds.), Bioeng. Nanomater., CRC press, 2013: pp. 125–148.

[159] A.C. Anselmo, S. Mitragotri, Nanoparticles in the clinic, Bioeng. Transl. Med. 1 (2016) 10–29. doi:10.1002/btm2.10003.

[160] A.S. McKee, P. Marrack, Old and new adjuvants, Curr. Opin. Immunol. 47 (2017) 44–51. doi:10.1016/j.coi.2017.06.005.

[161] S.R. Bonam, C.D. Partidos, S.K.M. Halmuthur, S. Muller, An Overview of Novel Adjuvants Designed for Improving Vaccine Efficacy, Trends Pharmacol. Sci. 38 (2017) 771–793. doi:10.1016/j.tips.2017.06.002.

[162] N. Garçon, A. Di Pasquale, From discovery to licensure, the Adjuvant System story, Hum. Vaccines Immunother. 13 (2017) 19–33. doi:10.1080/21645515.2016.1225635.

[163] Safety and pharmacodynamcis of SELA-070 nicotine vaccine in smokers, (2017). https://clinicaltrials.gov/ct2/show/NCT03148925?term=NCT03148925&rank=1 (accessed July 4, 2017).

[164] SVP™ Platform, (2017). http://selectabio.com/platform/svp-platform/ (accessed July 4, 2017).

[165] L. Zhang, P. Londono, S. Grimes, P. Blackburn, P. Gottlieb, G.S. Eisenbarth, MAS-1 adjuvant immunotherapy generates robust Th2 type and regulatory immune responses providing long-term protection from diabetes in late-stage pre-diabetic NOD mice, Autoimmunity. 47 (2014)

341–350. doi:10.3109/08916934.2014.910768.
[166] The safety, tolerance, and immunogenicity of MAS-1-adjuvanted seasonal inactivated influenza vaccine (MER4101), (2015). https://clinicaltrials.gov/ct2/show/NCT02500680?term=NCT02500680&rank=1 (accessed July 4, 2017).
[167] Mimopath®, (2017). http://www.mucosis.com/mimopath.php (accessed July 4, 2017).
[168] FluGEM®, (2017). http://www.mucosis.com/flugem.php (accessed July 4, 2017).
[169] Mucosis initiates first-in-human study of SynGEM®, a needle-free nasal spray RSV vaccine, (2016). http://www.mucosis.com/press_releases_07-11-16.php (accessed July 4, 2017).
[170] Vaxfectin® adjuvant, (2017). http://www.vical.com/technology/vaxfectin/default.aspx (accessed July 4, 2017).
[171] Safety and efficacy study of herpes simplex virus type 2 (HSV-2) therapeutic DNA vaccine (HSV-2), (2016). https://clinicaltrials.gov/ct2/show/NCT02837575 (accessed July 4, 2017).
[172] Poloxamer delivery system, (2017). http://www.vical.com/technology/dna-technology/poloxamer/default.aspx (accessed July 4, 2017).
[173] A study to evaluate a therapeutic vaccine, ASP0113, in cytomegalovirus (CMV)-seropositive recipients undergoing allogeneic, hematopoietic cell transplant (HCT) (HELIOS), (2013). https://clinicaltrials.gov/ct2/show/NCT01877655 (accessed July 4, 2017).
[174] A study to evaluate the efficacy and safety of a vaccine, ASP0113, in cytomegalovirus (CMV)-seronegative kidney transplant recipients receiving an organ from a CMV-seropositive donor, (2013). https://clinicaltrials.gov/ct2/show/NCT01974206 (accessed July 4, 2017).
[175] M. Hayashi, T. Aoshi, Y. Haseda, K. Kobiyama, E. Wijaya, N. Nakatsu, et al., Advax, a delta inulin microparticle, potentiates in-built adjuvant property of co-administered vaccines, EBioMedicine. 15 (2017) 127–136. doi:10.1016/j.ebiom.2016.11.015.
[176] A randomised controlled phase 1 study of vaccine therapy for control or cure of chronic hepatitis B virus infection (HBV003), (2017). https://clinicaltrials.gov/ct2/show/NCT03038802 (accessed July 4, 2017).
[177] A phase 1 study to evaluate the immunogenicity and safety of a pandemic avian influenza vaccine in adults (FLU003), (2015). https://clinicaltrials.gov/ct2/show/NCT02335164 (accessed July 4, 2017).
[178] Matrix-M™ technology, (n.d.). http://novavax.com/page/10/matrix-m-adjuvant-technology (accessed July 4, 2017).
[179] A study to assess the safety and immunogenicity of the malaria vaccine, R21, with Matrix-M1 adjuvant, (2016). https://clinicaltrials.gov/ct2/show/NCT02925403 (accessed July 4, 2017).
[180] Vaccine technology, (n.d.). http://novavax.com/page/8/vaccine-technology (accessed July 4, 2017).
[181] A study to determine the safety and efficacy of the RSV F vaccine to protect infants via maternal immunization, (2015). https://clinicaltrials.gov/ct2/show/NCT02624947 (accessed July 4, 2017).
[182] Safety and immunogenicity study to evaluate single- or two-dose regimens of RSV F vaccine with and without aluminum phosphate or Matrix-M1™ adjuvants in clinically-stable older adults, (2017). https://clinicaltrials.gov/ct2/show/NCT03026348 (accessed July 4, 2017).
[183] Discovery platforms, (2017). http://www.immunedesign.com/platforms/ (accessed July 4, 2017).
[184] Pipeline, (2017). http://www.immunedesign.com/pipeline/ (accessed July 4, 2017).
[185] Phase 1 study of intradermal LV305 in patients with locally advanced, relapsed or metastatic cancer expressing NY-ESO-1, (2014).
[186] A phase 1b safety study of CMB305 (sequentially administered LV305 and G305) in patients with locally advanced, relapsed, or metastatic Cancer expressing NY-ESO-1, (2015). https://clinicaltrials.gov/ct2/show/NCT02387125?term=NCT02387125&rank=1 (accessed July 4, 2017).
[187] Overview of Juvaris' technology platform, (2014). http://www.juvaris.com/technology/overview.html (accessed July 4, 2017).
[188] JVRS-100 for the treatment of patients with relapsed or refractory leukemia, (2009). https://clinicaltrials.gov/ct2/show/NCT00860522?term=NCT00860522&rank=1 (accessed July 4, 2017).
[189] C. Gerke, A.M. Colucci, C. Giannelli, S. Sanzone, C.G. Vitali, L. Sollai, et al., Production of a Shigella sonnei vaccine based on generalized modules for membrane antigens (GMMA), 1790GAHB, PLoS One. 10 (2015) 1–22. doi:10.1371/journal.pone.0134478.

[190] A study to evaluate safety and immunogenicity of 1 booster dose of 1790GAHB vaccine in healthy adults primed with 3 doses of 1790GAHB vaccine in study H03_01TP compared to 1 vaccination of 1790GAHB in either subjects who received placebo in the same study, (2017). https://clinicaltrials.gov/ct2/show/NCT03089879?term=NCT03089879&rank=1 (accessed July 4, 2017).

[191] Safety of Chlamydia vaccine CTH522 in healthy women aged 18 to 45 years, (2016). https://clinicaltrials.gov/ct2/show/NCT02787109?term=NCT02787109&rank=1 (accessed July 4, 2017).

Background, Hypothesis and Objectives

Background

Despite the unprecedented contribution of vaccines to eradicate some infectious diseases and to improve our life expectancy in the last two centuries, vaccination still faces some challenges, and the research in the field is still very active [1,2]. In this sense, one limitation has been the development of modern antigens, such as proteins, peptides or polynucleotides, which have a better safety profile than inactivated or attenuated microorganisms but they are much less immunogenic [3]. On the other hand, some of the most threatening infectious diseases of our time, such as HIV, malaria or tuberculosis [4–6], are still elusive to be controlled with vaccines. In some of these cases, a powerful cellular response, something hardly achievable with classical adjuvant alum, is considered a critical aspect for the vaccine to be effective [6]. In this context, nanotechnology has emerged as a useful tool for overcoming these and other limitations [7–9]. Indeed, nanocarriers have been shown to protect the integrity of their associated antigens once in the body, and to modify their biodistribution, thereby offering the possibility to modulate the immune response towards either a Th1 or a Th2 profile [10–12].

Polymeric nanocapsules (NCs), consisting of an oily core and a polymeric shell, have shown the capacity to load and deliver drugs, antigens and immunomodulatory compounds. Our group has made contributions to this field by developing a variety of NCs with different polymer shells, i.e. chitosan [13–15], hyaluronic acid [16], poly-L-asparagine [17,18], polyarginine [19] and poly-glutamic acid [20–22]. In the vaccinology field, we have associated to the NCs different types of protein antigens, such as tetanus toxoid [23], influenza antigen [24] and recombinant hepatitis B surface antigen [25–27]. We have also shown the possibility of co-encapsulating adjuvants, such as imiquimod, with an increased immunogenic response following either, intramuscular o nasal immunization [25,27].

The current understanding is that, in order to make significant progress in the vaccine formulation field, it is necessary to design the antigen nanocarriers in a more rational manner. In this sense, a deeper knowledge is needed to understand the influence of the composition and the physicochemical properties of a particular nanosystem in its biological behavior [28–30]. More precisely, researchers aim at knowing how to modulate of the nanoparticles properties to achieve an adequate biodistribution, interaction with the immune cells and desired immune response.

Hypothesis

1. Polymeric NCs may be useful carriers for the encapsulation of IutA antigen and for the development of a new nanovaccine against uropathogenic *E. coli*.

2. The versatility of the solvent displacement technique may allow the preparation of polymeric NCs with controlled particle size and with one or multiple layers.

3. Hydrophobized inulin can be an adequate biomaterial to prepare polymeric NCs. Due to their biocompatibility and adjuvant properties the resulting NCs will show a good safety profile and potential adjuvant capacity.

4. The polymeric shell and the physicochemical properties of the NCs may influence on their biodistribution and cell interaction. By modifying the particle size it maybe possible to favor the cell uptake, the drainage and accumulation in the lymph nodes of the NCs, what may lead to an enhanced immune response.

Objectives

Based on the background knowledge in the field and the hypothesis above outlined, the main objectives of this thesis were, first to develop new methods to prepare tunable polymeric NCs regarding their particle size, polymeric shell and surface composition; and second, to study the influence of these parameters in the interaction of the NCs with immune cells, their dissemination and lymphatic drainage and their capacity to protect and release antigens to generate an adequate immune response. More precisely, to achieve these objectives the following experimental activities were undertaken:

A) Development of polymeric NCs to protect and control the release of IutA antigen.
   a. Study of the influence of the NC's components (oil, surfactants, polymer) in the capacity to associate antigen IutA while maintaining adequate physicochemical properties.
   b. Engineering of NCs with a double layer of chitosan and dextran sulfate and evaluation of its influence over the stability and release of the antigen.
   c. Evaluation of the capacity of the IutA-loaded NCs to produce adequate levels of IgG when injected subcutaneously to mice.

   The results corresponding to this objective are presented in Chapter 1: "Bilayer polymeric nanocapsules: A formulation approach for a thermostable and adjuvanted *E. coli* antigen vaccine" and have already been published [31].

B) Design of formulation and technological approaches in order to produce tailor-made polymeric NCs.
   a. Development an experimental design to study the influence of the dilution of the components in the organic and the aqueous phases and the way of addition (pouring *vs* injection) of the first one over the second one in the particle size of NCs prepared by solvent displacement technique.
   b. Evaluation of the layer-by-layer approach to modify the surface and composition of polymeric NCs.
   c. Development of a miniaturized high-throughput screening-adaptable procedure of NCs preparation.
   d. Scale-up of the preparation procedure using a batch production and a continuous microfluidics method.

   The results corresponding to this objective are presented in Chapter 2: "Engineering, on-demand manufacturing, and scaling-up of polymeric nanocapsules" and have already been published [32].

C) Development and characterization of C12 modified-inulin NCs.
   a. Rational development, physicochemical and morphological characterization of inulin NCs with controllable charge and particle size.
   b. Study of the interaction with macrophages *in vitro* and comparison with chitosan NCs of similar size.
   c. Evaluation of the dissemination in transgenic zebrafish model, with GFP-expressing macrophages, after intramuscular and intravenous injection.

   The results corresponding to this objective are presented in Chapter 3: "New inulin nanocapsules: size-dependent interaction with macrophages and biodistribution in zebrafish"

D) Study the influence of the particle size and shell composition in the cell interaction and lymphatic drainage of inulin and chitosan NCs
    a. Study of the particle size of inulin and chitosan NCs using different techniques complementary to dynamic light scattering.
    b. *In vitro* evaluation of the interaction and activation capacity of inulin and chitosan NCs of different sizes with human derived dendritic cells.
    c. Analysis of the drainage capacity of the NCs to the lymph nodes after intradermal administration to mice and the influence of the particle size and the composition in this process.

The results corresponding to this objective are presented in Chapter 4: "Polysaccharidic nanocapsules with lympho-targeting properties: simultaneous effect of size and composition".

References

[1] E. De Gregorio, R. Rappuoli, From empiricism to rational design: a personal perspective of the evolution of vaccine development, Nat Rev Immunol. 14 (2014) 505–514. doi:10.1038/nri3694.

[2] S. a. Plotkin, S.L. Plotkin, The development of vaccines: how the past led to the future, Nat. Rev. Microbiol. 9 (2011) 889–893. doi:10.1038/nrmicro2668.

[3] S.R. Bonam, C.D. Partidos, S.K.M. Halmuthur, S. Muller, An Overview of Novel Adjuvants Designed for Improving Vaccine Efficacy, Trends Pharmacol. Sci. 38 (2017) 771–793. doi:10.1016/j.tips.2017.06.002.

[4] B.D. Walker, D.R. Burton, Toward an AIDS vaccine, Science. 320 (2008) 760–764. doi:10.1126/science.1152622.

[5] S.G. Reed, M.T. Orr, C.B. Fox, Key roles of adjuvants in modern vaccines., Nat. Med. 19 (2013) 1597–608. doi:10.1038/nm.3409.

[6] I. Delany, R. Rappuoli, E. De Gregorio, Vaccines for the 21st century, EMBO Mol. Med. 6 (2014) 708–720. doi:10.1002/emmm.201403876.

[7] I. Toth, M. Skwarczynski, The immune system likes nanotechnology, Nanomedicine. 9 (2014) 2607–2609. doi:10.2217/nnm.14.199.

[8] J.V. Gonzalez-Aramundiz, A.S. Cordeiro, N. Csaba, M. de la Fuente, M.J. Alonso, Nanovaccines : nanocarriers for antigen delivery, Biol. Aujourdhui. 206 (2012) 249–261. doi:10.1051/jbio/2012027.

[9] Y. Liu, Y. Xu, Y. Tian, C. Chen, C. Wang, X. Jiang, Functional Nanomaterials Can Optimize the Efficacy of Vaccines, Small. 10 (2014) 4505–4520. doi:10.1002/smll.201401707.

[10] H. Yue, G. Ma, Polymeric micro / nanoparticles : Particle design and potential vaccine delivery applications, Vaccine. 33 (2015) 5927–5936. doi:10.1016/j.vaccine.2015.07.100.

[11] M.-L. De Temmerman, J. Rejman, J. Demeester, D.J. Irvine, B. Gander, S.C. De Smedt, Particulate vaccines: on the quest for optimal delivery and immune response., Drug Discov. Today. 16 (2011) 569–82. doi:10.1016/j.drudis.2011.04.006.

[12] A.C. Rice-ficht, A.M. Arenas-gamboa, M.M. Kahl-mcdonagh, T.A. Ficht, Polymeric particles in vaccine delivery, Curr. Opin. Microbiol. 13 (2010) 106–112. doi:10.1016/j.mib.2009.12.001.

[13] M. V. Lozano, D. Torrecilla, D. Torres, A. Vidal, F. Domínguez, M.J. Alonso, Highly Efficient System To Deliver Taxanes into Tumor Cells: Docetaxel-Loaded Chitosan Oligomer Colloidal Carriers, Biomacromolecules. 9 (2008) 2186–2193. doi:10.1021/bm800298u.

[14] D. Torrecilla, M. V. Lozano, E. Lallana, J.I. Neissa, R. Novoa-Carballal, A. Vidal, et al., Anti-tumor efficacy of chitosan-g-poly(ethylene glycol) nanocapsules containing docetaxel: Anti-TMEFF-2 functionalized nanocapsules vs. non-functionalized nanocapsules, Eur. J. Pharm. Biopharm. 83 (2013) 330–337. doi:10.1016/j.ejpb.2012.10.017.

[15] M. V Lozano, H. Esteban, J. Brea, M.I. Loza, D. Torres, M.J. Alonso, Intracellular delivery of docetaxel using freeze-dried polysaccharide nanocapsules., J. Microencapsul. 30 (2013) 181–8. doi:10.3109/02652048.2012.714411.

[16] F.A. Oyarzun-Ampuero, G.R. Rivera-Rodríguez, M.J. Alonso, D. Torres, G.R. Rivera-Rodriguez, M.J. Alonso, et al., Hyaluronan nanocapsules as a new vehicle for intracellular drug delivery, Eur. J. Pharm. Sci. 49 (2013) 483–490. doi:10.1016/j.ejps.2013.05.008.

[17] G.R. Rivera-Rodríguez, M.J. Alonso, D. Torres, Poly-l-asparagine nanocapsules as anticancer drug delivery vehicles, Eur. J. Pharm. Biopharm. 85 (2013) 481–487. doi:10.1016/j.ejpb.2013.08.001.

[18] G.R. Rivera-Rodriguez, G. Lollo, T. Montier, J.P. Benoit, C. Passirani, M.J. Alonso, et al., In vivo evaluation of poly-l-asparagine nanocapsules as carriers for anti-cancer drug delivery, Int. J. Pharm. 458 (2013) 83–89. doi:10.1016/j.ijpharm.2013.09.038.

[19] M. V. Lozano, G. Lollo, M. Alonso-Nocelo, J. Brea, A. Vidal, D. Torres, et al., Polyarginine nanocapsules: A new platform for intracellular drug delivery, J. Nanoparticle Res. 15 (2013).

doi:10.1007/s11051-013-1515-7.

[20] G. Lollo, G.R. Rivera-Rodriguez, J. Bejaud, T. Montier, C. Passirani, J.P. Benoit, et al., Polyglutamic acid-PEG nanocapsules as long circulating carriers for the delivery of docetaxel, Eur. J. Pharm. Biopharm. 87 (2014) 47–54. doi:10.1016/j.ejpb.2014.02.004.

[21] T. Gonzalo, G. Lollo, M. Garcia-Fuentes, D. Torres, J. Correa, R. Riguera, et al., A new potential nano-oncological therapy based on polyamino acid nanocapsules, J. Control. Release. 169 (2013) 10–16. doi:10.1016/j.jconrel.2013.03.037.

[22] G. Lollo, P. Hervella, P. Calvo, P. Aviles, M.J. Guillen, M. Garcia-Fuentes, et al., Enhanced in vivo therapeutic efficacy of plitidepsin-loaded nanocapsules decorated with a new poly-aminoacid-PEG derivative, Int. J. Pharm. 483 (2015) 212–219. doi:10.1016/j.ijpharm.2015.02.028.

[23] M. Tobio, S.P. Schwendeman, Y. Guo, J. McIver, R. Langer, M.J. Alonso, Improved immunogenicity of a core-coated tetanus toxoid delivery system, Vaccine. 18 (1999) 618–622. doi:10.1016/S0264-410X(99)00313-8.

[24] J.V. González-Aramundiz, E. Presas, I. Dalmau-Mena, S. Martínez-Pulgarín, C. Alonso, J.M. Escribano, et al., Rational design of protamine nanocapsules as antigen delivery carriers, J. Control. Release. 245 (2017) 62–69. doi:10.1016/j.jconrel.2016.11.012.

[25] S. Vicente, B. Diaz-Freitas, M. Peleteiro, A. Sanchez, D.W. Pascual, A. Gonzalez-Fernandez, et al., A Polymer/Oil Based Nanovaccine as a Single-Dose Immunization Approach, PLoS One. 8 (2013) e62500. doi:10.1371/journal.pone.0062500.

[26] S. Vicente, M. Peleteiro, J.V. González-Aramundiz, B. Díaz-Freitas, S. Martínez-Pulgarín, J.I. Neissa, et al., Highly versatile immunostimulating nanocapsules for specific immune potentiation., Nanomedicine (London). 9 (2014) 2273–2289. doi:10.2217/nnm.14.10.

[27] S. Vicente, M. Peleteiro, B. Díaz-Freitas, A. Sanchez, Á. González-Fernández, M.J. Alonso, Co-delivery of viral proteins and a TLR7 agonist from polysaccharide nanocapsules: A needle-free vaccination strategy, J. Control. Release. 172 (2013) 773–781. doi:10.1016/j.jconrel.2013.09.012.

[28] T.G. Dacoba, A. Olivera, D. Torres, J. Crecente-Campo, M.J. Alonso, Modulating the immune system through nanotechnology., Semin. Immunol. 34 (2017) 78–102. doi:10.1016/j.smim.2017.09.007.

[29] Y. Liu, B. Workalemahu, X. Jiang, The Effects of Physicochemical Properties of Nanomaterials on Their Cellular Uptake In Vitro and In Vivo, Small. 13 (2017) 1–13. doi:10.1002/smll.201701815.

[30] H. Jiang, Q. Wang, X. Sun, Lymph node targeting strategies to improve vaccination efficacy, J. Control. Release. 267 (2017) 47–56. doi:10.1016/j.jconrel.2017.08.009.

[31] J. Crecente-Campo, S. Lorenzo-Abalde, A. Mora, J. Marzoa, N. Csaba, J. Blanco, et al., Bilayer polymeric nanocapsules: A formulation approach for a thermostable and adjuvanted E. coli antigen vaccine., J. Control. Release. 286 (2018) 20–32. doi:10.1016/j.jconrel.2018.07.018.

[32] J. Crecente-Campo, M.J. Alonso, Engineering, on-demand manufacturing, and scaling-up of polymeric nanocapsules, Bioeng. Transl. Med. (2018). doi:10.1002/btm2.10118.

Chapter 1

Bilayer polymeric nanocapsules: a formulation approach for a thermostable and adjuvanted *E. coli* antigen vaccine

Chapter 1

Bilayer polymeric nanocapsules: a formulation approach for a thermostable and adjuvanted *E. coli* antigen vaccine

The results from this chapter have already been published in [1].

Abstract

One of the strategies used to improve the immunogenicity of purified protein antigens has relied on their association with synthetic nanocarriers, which, in general, have functioned as simple antigen containers. Here, we present a more advanced strategy based on the design of an antigen nanocarrier at the molecular level. The nanocarrier is composed of a vitamin E oily core, surrounded by two layers: a first layer of chitosan and a second of dextran sulfate. The selected antigen, IutA protein from *Escherichia coli*, was harbored between the two polymeric layers. The final bilayer nanocapsules had a nanometric size (≈ 200 nm), a negative zeta potential (< -40 mV) and good antigen association efficiency (≈ 70%). The bilayer architecture led to an improvement on the formulation stability and the controlled release of the associated antigen. Remarkably, after being administered to mice, bilayer nanocapsules elicited higher IgG levels than those obtained with antigen precipitated with Alum. Moreover, freeze-dried nanocapsules were stable at room temperature for, at least, 3 months. These promising data, in addition to their contribution to the development of an uropathogenic *E. coli* vaccine, has allowed us to validate these novel bilayer nanocapsules as adequate platforms for the delivery of protein antigens.

Graphical abstract

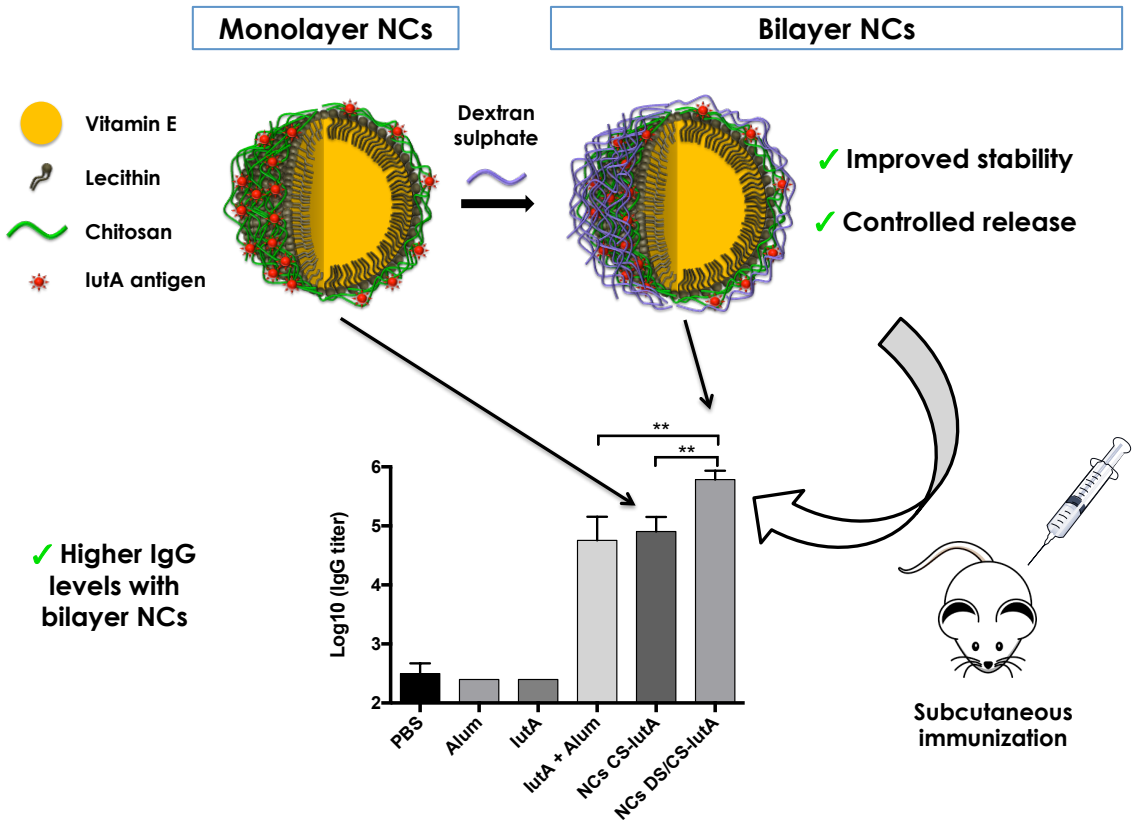

1. Introduction

Nowadays, nanotechnology is considered a useful tool for overcoming the limitations of newly developed and poorly immunogenic subunit vaccines [2–4]. Indeed, nanocarriers have been shown to protect the integrity of their associated antigens once in the body, and to modify their biodistribution, thereby offering the possibility to modulate the immune response towards either a Th1 or a Th2 profile [5–7]. The classical nanotechnology approach simply relied on the entrapment/association of the antigen with the nanocarrier (emulsions, liposomes and nanoparticles, among others) [8,9]. However, the current understanding is that, in order to make significant progress in the vaccine formulation field, it is necessary to design the antigen nanocarriers in a rational manner. This advanced formulation strategy involves the use of multiple functional components, all of them contributing to the fate of the antigen upon *in vivo* administration, and to the subsequent immunological response. Besides the composition, the physicochemical properties of the nanosystem have been shown to be critical for the nanovaccine final outcome [10–12]. Hence, a technique that would allow for the assembly of the different components, as well as for the modulation of the particle size and surface properties would be of great interest in the rational design of the nanovaccines. In this regard, the so-called layer-by-layer (LbL) technique, used for the development of drug delivery carriers [13–19], represents an interesting approach in the modernization of vaccine formulation strategies [20–25].

In this study, we have combined the LbL technique with the solvent displacement technique, previously disclosed by our group for the formation of polymeric nanocapsules (NCs) [26–31] and their association to antigens [27,29,32,33]. These NCs are composed of an oily core capable of harboring hydrophobic molecules, i.e., immunostimulants, and a hydrophilic polymeric surface where polar molecules, such as proteins, can be efficiently anchored. This architectural organization and composition makes this carrier a very attractive choice for the delivery of antigens [34,35]. In fact, we have previously reported that NCs with a chitosan shell were efficient vehicles for the delivery of a recombinant hepatitis B vaccine [33]. Furthermore, we additionally disclosed that the incorporation of the immunostimulant imiquimod to the oily core could further contribute to achieve a significant and long-lasting IgG response, following either nasal or intramuscular administration [27,32].

Taking this background experience and information into consideration, our goal was to design and develop a new antigen delivery carrier consisting of a bilayer sandwich-like polymeric NC capable of associating and delivering, in a controlled manner, antigenic proteins. As the oily core, we selected vitamin E because of its immunostimulating properties [36–39]. For the formation of the bilayer shell, we chose, in addition to chitosan, dextran sulfate. A freeze-dry process was optimized to convert the nanosystem to a powder form and achieve a thermostable formulation.

The capacity of these nanostructures to stimulate macrophages *in vitro* and to

induce an immune response *in vivo* was validated using IutA as a model antigen, a specific outer membrane receptor protein for ferric aerobactin from uropathogenic *E. coli* (UPEC), which could benefit from the proposed polymeric NCs. Pathogen-associated outer membrane iron receptors have already been discussed as putative vaccine targets for UPEC [40,41], the most common cause of urinary tract infections. Nowadays, the only two vaccines approved in Europe to prevent recurrent episodes of this pathology (Uro-Vaxom® and SolcoUrovac®, based on extracts of different uropathogenic strains) have shown limited protection [42,43]. Consequently, advances in the development of new adjuvants and delivery systems could potentially contribute to the design of new vaccines that might prevent this pathology.

2. Materials and Methods

2.1. Materials

DL-α-tocopherol (vitamin E) (Calbiochem®) and squalene (density: 0.855 g/mL) were obtained from Merck Millipore (Billerica, MA, USA). Miglyol® 812 was kindly gifted by Cremer Oleo GmbH & Co. KG (Hamburg, Germany).

Deoiled phosphatidylcholine-enriched L-α-lecithin (Epikuron™ 145V) was a gift from Cargill (Barcelona, Spain). Pluronic® 127 was obtained from BASF (Ludwigshafen, Germany). Oleic acid, D-α-Tocopherol polyethylene glycol 1000 succinate (TPGS), polyoxyethylene (40) stearate (PEG-stearate), polyethylene glycol sorbitan monooleate (Tween® 80), sodium cholate hydrate, D-(+)Glucose, Sucrose, D-(+)-Trehalose dehydrate, D-Mannitol, and fluorescent marker Nile Red were purchased from Sigma-Aldrich (St. Louis, MO, USA).

Ultrapure chitosan (CS) hydrochloride salt (Protasan™ UP CL 113, Mw 125 kDa, deacetylation degree of 86%) was purchased from Novamatrix (Sandvika, Norway). Dextran sulfate sodium salt Mw 6000-8000 Da was bought from MP Biomedicals (Illkirch, France). Protamine sulfate (5 kDa) was purchased from Yuki Gosei Kogyo, Ltd. (Japan). Polyarginine Mw 29000 Da was obtained from PTS (Valencia, Spain). Phosphate buffered saline (PBS) was obtained from Medicago (Uppsala, Sweden).

All other chemicals were of reagent grade or higher purity. For *in vitro* and *in vivo* experiments endotoxin free water and sterile/autoclaved material were used.

2.2. Purification of recombinant IutA

The gene encoding the IutA protein was amplified by PCR from *E. coli* CFT073 genomic DNA and cloned into pBAD-*myc*-HisA (Invitrogen, San Diego, CA, USA). 20 ng of genomic DNA were used for PCR amplification using *Pfu* polymerase (Thermo Scientific, Waltham, MA, USA), r_iutA_PF1 (CATGCCATGGCGCAGCGGCAGCCGG), and

r_iutA_PR2 (CCCAAGCTTGAACAGCACTGAGTAGTTCAGACCAAAGGTTCGG) as primers, to add a NcoI and a HindIII restriction site, respectively, to the reading frame encoding *iutA* gene. The PCR amplified product was extracted from agarose gel after electrophoresis, and digested with NcoI and HindIII before ligation into the pBAD plasmid. The resulting construct was verified by sequencing. Recombinant protein expression from pBAD plasmid was induced in *E. coli* TOP10 cultured to OD_{600} = 0.6 by addition of L-arabinose to 0.02% p/v for 2 h. Induced cultures were harvested by centrifugation at 10,000 *g* for 15 min at 4 °C, and the pellets thus obtained were lysed with lysis buffer (20 mM sodium phosphate buffer, 0.5 M NaCl, 0.1% Triton X-100, pH 7.6) containing EDTA free protease inhibitors and 1 mg/mL hen egg white lysozyme (both from Sigma-Aldrich, St. Louis, MO, USA) by incubation on ice for 1 h. Lysed samples were sonicated on ice for 30 s. The insoluble fraction was collected by centrifugation at 10,000 *g* for 30 min at 4 °C, separated from the soluble fraction, washed with washing buffer (20 mM sodium phosphate, 0.5 M NaCl, 0.1% Triton X-100, pH 7.6) and solubilized with solubilization buffer (50 mM sodium phosphate buffer, 0.5 M NaCl, 8 M urea, 10% glycerol, and 20 mM imidazole, pH 7.6). The remaining insoluble material was removed by centrifugation. His_6-tagged protein was bound to a HisTrap FF 5 mL nickel column (GE Healthcare Life Sciences, Barcelona, Spain), washed with solubilization buffer, and eluted with elution buffer (20 mM sodium phosphate monobasic, 0.5 M NaCl, 8 M urea, pH 4.5). After adjusting the pH of the eluate to 7.5, it was concentrated using 30 kDa molecular weight cut-off spin concentrators (MerckMillipore, Billerica, MA, USA) according to the manufacturer's instructions to a final concentration of 10 mg/mL. The concentrated protein was either stored at -20 °C, or used directly in folding studies.

2.2.1. Refolding of IutA

For refolding experiments, samples containing IutA at 10 mg/mL were diluted 1:10 in 20 mM sodium phosphate buffer, pH 7.5 containing 10 mg/mL amidosulfobetaine-14 (ASB-14). Diluted samples were incubated at 37 °C for 15 h. Refolded samples were washed after binding to a HisTrap FF column with washing buffer II (20 mM sodium phosphate buffer, 0.5 mg/mL SB3-14 pH 7.6), eluted with washing buffer II complemented with 250 mM imidazole and extensively dialyzed at 4 °C for 3 days in washing buffer II. In order to assess folding, samples were resolved on a 10% precast polyacrilamide gel (Bio-Rad Laboratories, CA, USA) and stained with Coomassie Brilliant Blue G-250. Refolded samples were not subjected to heating at 95 °C before SDS-PAGE unless otherwise indicated.

As shown in Fig. S1, a sample of refolded IutA heated at 95 ºC for 10 min ran at the position of 77 kDa, which is consistent with a denatured state (lane 1). Folded IutA without heat treatment migrated more rapidly, at to a position corresponding to a

molecular weight of approximately 52 kDa (Fig. S1, lane 2), which is consistent with the more compact conformation of the folded state [44].

2.3. Preparation of the nanosystems

2.3.1. Screening of materials for nanocapsule preparation

Nanoemulsions and nanocapsules were prepared by the solvent displacement technique [45]. Briefly, 30 mg of the oil (DL-α-tocopherol, squalene, oleic acid or Miglyol® 812) were co-dissolved in 2.5 mL of ethanol with 6 mg of surfactant (lecithin, Pluronic® 127, TPGS, PEG-stearate or Tween® 80). In the case of TPGS and PEG-stearate, sodium cholate hydrate (2.5 mg dissolved in 25 µL of water) was used as co-surfactant in the organic phase. Pluronic® 127 was dissolved in acetone (60 µL). Immediately, the organic phase was poured into 5 mL of water for nanoemulsions, or 5 mL of 1 mg/mL aqueous solution of the polymer (chitosan, polyarginine or protamine) for nanocapsules. Organic solvents were removed under vacuum (Büchi Labortechnik AG, Flawil, Switzerland), and the volume was adjusted to 5 mL with ultrapure water. Then, the formulations were ultracentrifuged (Universal 32R, Hettich Zentrifugen, Germany) at 82,435 g for 1 h at 15 ºC, and resuspended in water to a final polymer concentration of 1 mg/mL.

For antigen association, 735 µL of nanoemulsions or nanocapsules were incubated with 15 µL of antigen (1 mg/mL) for 20 min, at room temperature and under magnetic stirring.

2.3.2. Monolayer NCs

The monolayer CS prototype was prepared as described above, using an organic phase composed of 30 mg of DL-α-tocopherol and 10 mg of lecithin dissolved in 2.5 mL of ethanol. The aqueous phase was prepared with 5 mg of chitosan dissolved in 5 mL of ultrapure water. After rotaevaporation and centrifugation in the same conditions described above, the nanocapsules were resuspended to a final concentration of chitosan of 3.33 mg/mL.

For antigen association, 975 µL of the isolated nanocapsules were incubated with 25 µL of antigen (1 mg/mL) for 20 min, under magnetic stirring at room temperature. The final concentration of the antigen was 25 µg/mL.

2.3.3. Bilayer NCs

775 µL of isolated monolayer CS nanocapsules were incubated with 25 µL of antigen (IutA 1 mg/mL) for 20 min, under magnetic stirring at room temperature. Afterwards, 200 µL of a solution of dextran sulfate 6.67 mg/mL were added and the suspension was maintained under magnetic stirring at room temperature for another 30 minutes. Again, the final concentration of the antigen was 25 µg/mL.

2.4. Physicochemical characterization

Particle size, polydispersity index, and zeta-potential were measured by photon correlation spectroscopy using a Zetasizer Nano-S (Malvern Instruments; Malvern, UK). Unless otherwise indicated, analyses were performed at 25 ºC with a detection angle of 173 º in distilled water.

The morphology of the nanocapsules was examined by transmission electron microscopy (TEM) and field emission scanning electron microscopy (FESEM). For TEM analysis (CM 12 Philips, Eindhoven, The Netherlands), the nanocapsules were placed on copper grids with Formvar films and stained with 2% (w/v) phosphotungstic acid solution. The grids were left to dry overnight in a desiccator under vacuum, and then observed by TEM. For FESEM studies (ZEISS FESEM ULTRA Plus, Germany) a diluted suspension of the nanocapsules (1:50) was placed in silicon wafers and the water was evaporated overnight in the open air. In the case of solid freeze-dried nanocapsules, samples of the powder were covered with a thin layer of gold prior to the analysis. The working distance was 2.4–2.5 mm and the extra high tension (EHT) 3.00 kV.

Elemental microanalysis was performed with an energy dispersive X-ray detector. The voltage was 20 kV and the working distance 8.5 mm.

The pH of the solutions and formulations was determined with a Sartorius Docu-pH Benchtop Meter (Thermo Fisher Scientific, Waltham, MA, USA).

2.5. Preparation yield

Nanocapsules were isolated by ultracentrifugation (Universal 32R, Hettich Zentrifugen, Tuttlingen, Germany) at 82,435 g for 60 min at 15 ºC, and the undernatants were discarded. The nanocapsules were then freeze-dried to eliminate all water and weighed. The preparation yield was calculated as follows (Eq. 1):

$$Preparation\ yield\ (\%) = \frac{Nanocapsules\ weight}{Theoretical\ weight\ of\ all\ components} \cdot 100$$

2.6. Freeze-drying studies

Nanocapsules were freeze-dried in the presence of different sugar cryoprotectants (mannitol, glucose, sucrose, and trehalose) at concentrations of 2.5, 5, and 10% (w/v). Chitosan nanocapsules and sugar solution were mixed 1:1 (v/v) to 1 mL in 5 mL freeze-drying glass vials. Vials were quickly frozen at -80 ºC and then transferred to the freeze-drier Genesis 25 ES, VirTis Model-Wizard 2.0 (SP Industries, USA). The primary drying lasted for 35 h with temperatures increasing from -40 to -20 ºC. In the secondary drying step, the temperature of the samples was raised gradually up to +20 ºC.

2.7. Antigen association efficiency

Nanocapsules were loaded with the antigen IutA as described in section 2.3. Nanocapsules were isolated by ultracentrifugation for 1 h, at 82,435 g and 15 ºC. After removing the undernatant, the nanocapsules were resuspended in ultrapure water to their original volume. The amount of associated antigen was quantified after disrupting the nanocapsules. Different methods to extract and isolate the protein attached to the nanosystems were tested. Among them: disruption with organic solvents (EtOH and DMSO), and using a detergent such as Triton-X100® 1% or SDS 20%. Finally, a solution of SDS 20% at a 1:1 volume ratio was used to destroy the nanostructures, and the attached antigenic protein was quantified using a fluorescence-based western blot analysis (Fig. S2). In all cases, blank nanocapsules were processed in parallel with the samples and used as control for accurate quantification. After running a conventional polyacrylamide gel, protein bands were transferred to a PVDF-FL membrane (Millipore, Billerica, MA, USA), optimal for fluorescent immunodetection. The membrane was, first, incubated with a mouse monoclonal anti-6X His-tag® (Abcam, Cambridge, UK) and then, with a goat anti-mouse IgG labeled with DyLight 680 (Thermo Fisher Scientific, Waltham, MA, USA). The amount of antigen was quantified by quantitative infrared fluorescent western blot (Li-Cor Bioscience, Odissey v.3.0, Lincoln, NE, US).

2.8. Antigen release study

The release studies were preformed by mixing 100 µL of fresh nanocapsules (section 2.3.2 and 2.3.3) or resuspended freeze-dried nanocapsules (sucrose 10%, section 2.6) in 400 µL PBS - Tween® 80 (0.02%). Samples were maintained at 37 ºC under horizontal shaking. At defined time points (0, 1, 2.5, 4, and 8 hours) samples were centrifuged (21,250 g, 1 h, 15 ºC), and the isolated nanocapsules were separated and

taken to 0.5 mL with a solution of SDS 20%. Finally, the antigen content was evaluated as described in section 2.7.

2.9. Colloidal stability

2.9.1. Storage conditions

Suspensions of monolayer and bilayer nanocapsules with an antigen concentration of 25 µg/mL were stored at 4 ºC for 3 months. Freeze-dried nanocapsules were stored perfectly sealed at room temperature. At fixed time points (up to 12 weeks), the formulations were reconstituted to the original concentration with ultrapure water. Then, their size, PDI, and zeta-potential were determined, as described in section 2.4. The amount of antigen associated to the nanocapsules was determined as described in section 2.7.

2.9.2 Cell culture and simulated biological media

The stability of monolayer (chitosan) and bilayer (dextran sulfate/chitosan) nanocapsules in PBS - Tween® 80 0.02% (dilution 1:20) and cell culture medium (RPMI supplemented with 10% FBS) at 37 ºC was followed for up to 24 h, and the evolution of particle size and PDI was carefully monitored.

2.10. Fluorescent labelling of nanocapsules, encapsulation efficiency and stability in cell culture medium

Nile Red-loaded nanocapsules were obtained by replacing 0.15 mL of ethanol in the organic phase with 0.15 mL of Nile Red solution in ethanol (0.5 mg/mL), as described in 2.3.2. The theoretical final concentration of Nile Red after centrifugation and resuspension was 50 µg/mL. Encapsulation efficiency was determined with the fluorescence ratio of the isolated nanocapsules (82,435 g, 1 h, 15 ºC) and non-isolated nanocapsules. Aliquots of these formulations were first diluted in water (1:10) and then in ethanol (1:10), and analyzed with a fluorometer (Envision Multilabel plate reader 2104-0010A, Perkin Elmer, Waltham, MA, US).

To check the stability and release of the labeled formulation in supplemented RPMI, nanocapsules were diluted in this medium (1:10), and placed at 37 ºC in a horizontal shaker. At different time points, samples were ultracentrifuged (82,435 g, 1 h, 15 ºC), the undernatant diluted in ethanol (1:10), and the amount of free Nile Red calculated after measuring the fluorescence intensity.

2.11. Cells and culture

The *in vitro* assays were performed in primary human cells and in the mouse macrophage cell line RAW 264.7 (RAW). RAW cell line was purchased from ATCC (American Type Culture Collection, Middlesex, UK) and cultured in complete medium (RPMI 1640 culture medium supplemented with 10% (v/v) of heated-inactivated fetal bovine serum (FBS from PAA Laboratories, Pasching, Austria), 2 mM glutamine and 100 U/mL of penicillin/streptomycin (Gibco, Life Technologies, Scotland, UK), at 37 ºC in 5% CO_2 atmosphere. Cells were split every other day with the aid of Accutase® (PAA Laboratories, Pasching, Austria) to maintain 70-80% confluent cultures.

Human peripheral blood mononuclear cells (hPBMCs) were obtained from 3 healthy voluntary donors. Mononuclear cells were isolated by Ficoll gradient. 7 mL of heparine-anticoagulated blood diluted 1:1 in PBS were carefully added over 3 mL of Ficoll-Hypaque, and centrifuged at 600 g, 30 min, at 20 ºC. Mononuclear cells were collected from the white interface between Ficoll and plasma, and washed with complete medium by centrifugation (300 g, 5 min, 20 ºC).

2.12. Cell viability studies

In order to study the effect of the nanoparticles on cell viability, xCELLigence® and MTS tests were performed.

The xCELLigence® test measures the impedance caused by cell growth using the RTCA DP Instrument (Roche Diagnostics, Penzberg, Germany). For the experiments, 25000 RAW cells in 200 µL of complete RPMI medium were seeded on each well, grown during 18 h, at 37 ºC and 5% CO_2, until they reached the exponential phase. At this point, 5 different concentrations of the tested nanoparticles were added (25, 50, 100, 200, and 400 µg/mL). Samples containing cells (without nanoparticles), or the highest concentration of nanoparticles used in the experiment (without cells), were included as positive and negative controls, respectively. Wells just with cell culture media were used as a blank. The impedance was monitored at 15 min intervals for 72 h.

For MTS assays, 25000 RAW cells were seeded into 96 well culture plates with 200 µL of complete RPMI medium, and let stand during 18 h, at 37 ºC and 5% CO_2. At this point, this medium was replaced with medium containing five different concentrations of the tested nanoparticles (25, 50, 100, 200, and 400 µg/mL). Samples with the same concentration of nanoparticles specified above but without cells, were included to check the possible background caused by the nanomaterial on the measurements. Cells with no nanoparticles and cells with Triton X-100 10% were included as positive and negative controls, respectively. Wells containing only cell culture media were used as blank. Incubation with nanoparticles was allowed for 6 or 24 h. In the first case, after 6 h, the stimulus was removed, replacing it with 200 µL of

fresh complete medium and leaving the cells for another 18 h. For both time points, culture medium was removed after 24 h and cells were rinsed with PBS. 120 µL of MTS solution (Promega, Madison, WI, USA) were added and, after two hours of incubation with this solution, the conversion of MTS to the soluble formazan product was measured by absorbance at 490 nm. The absorbance at 490 nm thus obtained is directly proportional to the number of living cells in culture. The viability of the adherent cells was then calculated as follows (Eq. 2):

$$Viability\ (\%) = \frac{(Abs\ cell\&NPs - Abs\ NPs)}{(Abs\ cells - Abs\ RPMI)} \cdot 100$$

where Abs cell&NPs is the absorbance of the cells treated with different amounts of NPs; Abs NPs is the absorbance of the nanocapsules diluted in the cell culture medium (without cells); Abs cells is the absorbance of the non-treated cells, and Abs RPMI is the absorbance of the cell culture medium.

2.13. Cellular uptake studies

Internalization studies using the mouse macrophage cell line RAW 264.7 were performed by flow cytometry and fluorescence microscopy. For both techniques, Nile Red-labeled nanoparticles were used.

To evaluate by flow cytometry the percentage of the nanosystems that interact with the cells, 5×10^5 RAW cells were plated into a 24-well plate with 1 mL of complete medium, and cultured for 24 h. Nile Red-labeled nanoparticles were added at a concentration of either 50 or at 100 µg/mL. After 30 min of incubation, cells were washed with PBS and detached by adding 250 µL of Accutase® (PAA laboratories, Pasching, Austria) and incubating them for 10 min at room temperature (RT). Finally, the cells were washed with complete medium in order to inactivate Accutase®, and the suspension was analyzed by flow cytometry (Accuri Cytometers, Ann Arbor, MI, USA).

To evaluate by fluorescence microscopy the percentage of internalization, 1×10^5 cells (RAW 264.7) were seeded in a NUNC 96-Well Optical-Bottom Plate with Coverglass Base (Thermo Fisher Scientific, Waltham, MA, USA) containing RPMI 10% FBS, and let grow for 24 h. Then, Nile Red-labeled nanoparticles were added at a concentration of either 50 or 100 µg/mL. After 30 minutes, the cells were washed with PBS to remove the excess of nanoparticles, and the cells were observed under an inverted fluorescent microscope (IX50, Olympus Optical Co GmbH; Hamburg, Germany). Confirmation of nanoparticle internalization was done using confocal microscopy. To do this, 5×10^5 RAW cells were seeded on a 24-well plate, over a glass cover slip (Menzel-Gläser; Braunschweig, Germany). As in the other techniques, after 24 h, the cells were incubated with the labeled nanoparticles at 50 µg/mL for 30 min. After washing the cells with PBS, they were fixed with formaldehyde 4% for 10 min and

permeabilized with Triton x100 0.1%. The cytoskeleton was stained with phalloidin conjugated to Alexa Fluor 488 (Molecular Probes Invitrogen, Eugene, OR, USA) for 20 min. Finally the samples were mounted on a slide using the ProLong®Gold Antifade mounting medium with DAPI (Invitrogen; Eugene, OR, USA). The cells were observed and images were captured using a Confocal Laser Scanning Microscopy (Leica SP5, Mannheim, Germany).

2.14. Cytokine secretion studies

The *in vitro* cytokine secretion was evaluated using human PBMCs from 3 healthy donors. 2×10^5 mononuclear cells/well were seeded on a 96 well-plate with 100 µL complete RPMI, and left for 24 h at 37 ºC, 5% CO_2. Then, nanoparticles were added to 100 µL of complete medium at 100 and 200 µg/mL (50 and 100 µg/mL final concentration), and incubated for 24 h. Cells in complete medium with no stimulus or with lipopolysaccharide (LPS)-phytohaemagglutinin (PHA) (1 µg/mL and 10 µg/mL) (InvivoGen; San Diego, CA, USA) were used as negative and positive controls, respectively. After 24 h, the plate was centrifuged (300 g, 5 min, 4 ºC) and the supernatants were kept at -20 ºC until analysis.

Cytokine detection in those supernatants was done using the FlowCytomix Human Th1/Th2 11plex Kit BMS810FF (Bender MedSystems, Vienna, Austria), including IFN-γ, IL-1β, IL-2, IL-4, IL-5, IL-6, IL-8, IL-10, IL-12 p70, TNF-α and TNF-β), following manufacturer's instructions. Briefly, 25 µL of antibody-coated microspheres were incubated with 25 µL of the supernatants and 50 µL of biotin-conjugated secondary antibodies. After 2 h shaking at room temperature, the plate was washed and incubated with 50 µL of streptavidin-phycoerythrin for 1 h on the microplate shaker, at room temperature, and protected from the light. Samples were measured on a FC500 flow cytometer (Beckman-Coulter; Miami, FL, USA) and data were analyzed using the FlowCytomix Pro 3.0 Software (Bender MedSystems, Vienna, Austria).

A similar assay using a higher concentration of the tested nanoparticles (200 and 400 µg/mL final concentration) was performed with other 3 donors. Cytokine detection in the supernatants was performed using the Luminex HCYTOMAG-60K kit from Merck Millipore (Darmstadt, Germany). In this case, the measured cytokines are almost the same, but this kit includes IL-17A, and not IL-5 nor TNF-β.

2.15. Immunization studies

To evaluate the systemic humoral immune response of our prototypes, the levels of serum antigen-specific antibodies generated by vaccinated mice were compared to those generated by the control mice. For this purpose, 50 outbred female Swiss mice (3–4 weeks old) were obtained from Janvier Laboratories (France), acclimated for 1

week prior to the initiation of experiments and provided food and water *ad libitum*. All animal experimentation was conducted following European (Directive 2010/63/EU on the protection of animals used for scientific purposes) and National (RD 53/2013) regulations for transport, housing and care of laboratory animals. The protocol used was approved by the Animal Welfare Committee of the Veterinary Faculty in Lugo, Universidade de Santiago de Compostela (AE-LU-002/14-1).

Groups of 10 mice were immunized 3 times with the loaded NCs (freshly prepared) or with the protein alone or in the presence of Alum as adjuvant. Control groups of 5 mice each were non-immunized, or immunized only with the adjuvant.

Mice were subcutaneously immunized on days 1, 21, and 35 by injection in the neck with a 25G needle of 200 µL of a suspension containing 5 µg IutA (4 groups of 10 animals) either alone, adsorbed onto Alum or loaded into CS or DS/CS NCs (total of 15 µg IutA per animal).

2.16. IgG detection by ELISA

One week after the last immunization, serum samples were collected from mice. Blood was drawn from the maxillary vein and let to clot. Then, it was centrifuged at 16000 g for 10 min, and the serum was collected and frozen at -20 ºC until use.

The titer of IgG against IutA was determined by ELISA. IutA was coated overnight on NUNC MaxiSorp 96-well ELISA (Nalge Nunc International, Roskilde, Denmark) plates at 2 µg/mL in 50 µL PBS. Wells were blocked with 150 µL PBS-BSA 1% for 1 h at 37 ºC, and then washed 4 times with PBS-Tween® 20 0.15% before the addition of the serum samples (50 µL), which were serially diluted from 1/2000 to 1/128000 in PBS-BSA 1%, and incubated for 1 hour at 37 ºC. After 4 more washes, 50 µL of secondary anti-mouse IgG antibodies conjugated to HRP (Southern Biotech 1030-05) and diluted 1/4000 in PBS-BSA 1% were added and incubated for another hour at 37 ºC. After the incubation, the samples were washed 4 times and the ELISA was developed with TMB for 15 min, and the reaction was stopped with 50 µL H_2SO_4. The signal was read in a microtiter plate reader at 450 nm. Titers were calculated from the highest dilutions that gave a signal higher than the blank + 3SD.

2.17. Statistical analysis

Unless otherwise indicated, all the experiments were repeated at least 3 times. Results are presented as mean ± standard deviation. A Mann-Whitney Test was used to determine the statistical significance of the *in vivo* experiment. Differences were considered significant for * $p < 0.05$, and very significant for ** $p < 0.01$. The statistical analyses were carried out with GraphPad Prism Version 6.0 and SPSS software.

3. Results and discussion

Progress in vaccine research towards the use of safer and purer antigens, such as isolated proteins or synthetic peptides, has grown in parallel with the development of effective adjuvants, necessary to compensate for their low immunogenicity [46]. In this context, nanoparticulated carriers by offering protection and a controlled delivery of antigens to the immune system, are strong candidates to help improve the immune response against soluble antigens used alone [47]. The performance of these nanosystems is significantly influenced by their physicochemical properties, their composition, and the structural organization of their associated antigen cargo. Because of this, an efficient entrapment of the antigen to the nanosystem is a prerequisite in the formulation of a nanovaccine [48]. For this reason, we first focused on the selection of the nanosystem components that would potentially promote antigen association efficiency, and that would, ultimately, influence the performance of the nanocarrier. Hence, based on a molecular level design, an adequate architectural organization that consisted of a protein antigen held between two polymers with opposite charge was built, thus creating a bilayer nanosystem (Fig. 1).

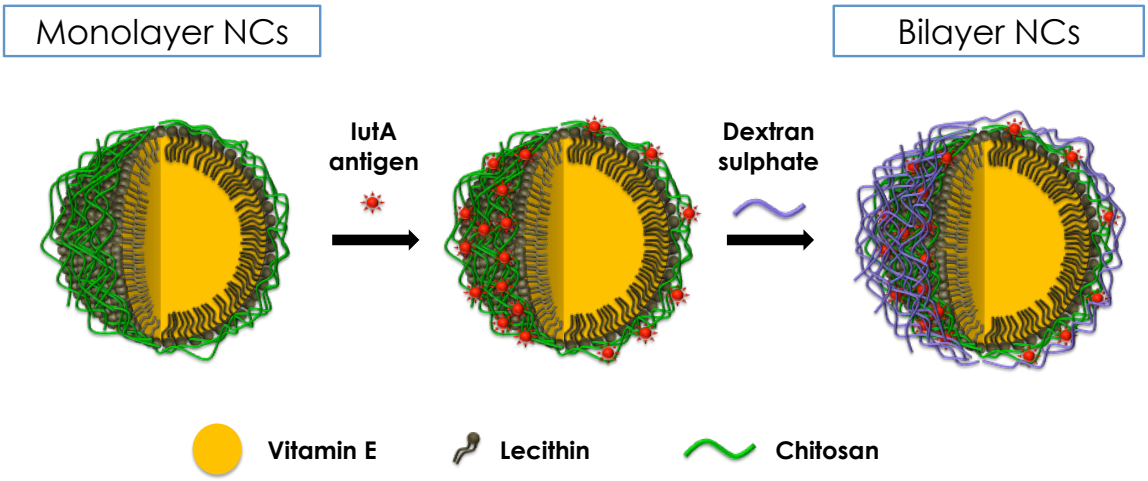

Figure 1. Scheme of the preparation of bilayer nanocapsules (NCs). In the bilayer nanosystem the antigen is entrapped between two polymer layers: chitosan and dextran sulfate.

3.1. Development of bilayer nanocapsules: entrapment of IutA antigen

We have previously developed polymeric nanocapsules as antigen delivery systems [27,29,31–33]. In addition to their appropriate and adjustable particle size (typically between 100–300 nm), nanocapsules can be designed to have multiple functions. Their oily core makes them adaptable for the encapsulation of hydrophobic

immunoestimulants [27], whereas their polymeric shell may constitute a good template for the association of protein antigens [32].

The first step in the formulation of a nanovaccine is the assessment of the antigen loading. In this regard, the physical adsorption of the protein onto the surface of the NCs does not involve the alteration of the antigen [5]. Besides, the small particle size of the NCs provides more surface available for antigen adsorption, which allows loadings hardly possible when using antigens entrapped in monolithic nanoparticles. Below, we describe, step-by-step, the formulation screening performed in order to produce the rationally designed nanocarrier. The screening started with the selection of a potentially immunostimulant oily core, and with a study of its affinity towards the antigen, and continued with the association of a first layer of polymer. The formation of a second polymeric layer that would coat the antigen-loaded NCs was intended to further protect the antigen and achieve its controlled release.

3.1.1. The selection of the immunostimulant oily core

We selected different oils, based on their potential adjuvant effect [49–51]: squalene, vitamin E, Miglyol® 812 and oleic acid, and formulated them as nanoemulsions with the help of the surfactant PEG-stearate and the co-surfactant sodium cholate. We screened these nanoemulsions according to their surface capacity to associate IutA, and observed that, irrespective of the type of oil, their association efficiency was close to 50%.

3.1.2. The selection of the stabilizing surfactants

Considering the lack of influence of the oily core on the association efficiency of the antigen, and based on its immunostimulatory properties, we selected vitamin E as the oily core of our nanosystem. Then, we analyzed the influence of a variety of surfactants, namely PEG-stearate, TPGS, Tween® 80, lecithin and Poloxamer® 407, on the properties of the nanocapsules. In the case of PEG-stearate and TPGS, we found it necessary to add sodium cholate as a co-surfactant in order to preserve the stability of the oily core. The resulting nanoemulsions had a nanometric size (120 to 170 nm) and a negative surface charge (-45 to -20 mV). In this case, our results showed that the amount of protein associated with the nanoemulsion was influenced by the surfactant, varying between 30% for lecithin and 60% for TPGS, with the antigen association efficiency of the rest of the surfactants being between these two values.

3.1.3. The formation of a polymeric shell able to support antigen association

Finally, the influence of the polymeric shell on protein association was evaluated by preparing different NCs with a vitamin E/PEG-stearate/sodium cholate core. Based on our previous experience, chitosan [32,33,52], protamine [29] and polyarginine [30] were selected for the shell formation. The results showed that chitosan NCs were able to associate an important amount of protein (approximately 50%), whereas the association efficiency value for protamine and polyarginine was lower than 20%. Considering that the antigen studied (IutA) is an amphiphilic membrane protein, its association to the NCs may involve not only electrostatic but also hydrophobic forces. After incubation with the NCs, the protein would interact with the surfactant layer and the polymeric shell, being these two the components that have an impact on the association efficiency levels.

3.1.4. Optimization of chitosan nanocapsules

Based on the positive results obtained with chitosan NCs in terms of antigen association efficiency, and their reported potential as carriers for other antigens [27,32,33], new formulations were prepared using different surfactants, taking into consideration the previous screening performed for the nanoemulsions. Three prototypes were selected, all of them with a core of vitamin E and a shell made of chitosan. The possible surfactants chosen were PEG-stearate/sodium cholate, TPGS/sodium cholate and lecithin. In order to select the best prototype we considered their physicochemical properties (Fig. 2A), their short-term colloidal stability (Fig. 2B), and their antigen association efficiency. Our results showed that chitosan NCs containing either lecithin or a mixture of TPGS/sodium cholate exhibited the highest association efficiency (69 ± 8 and 73 ± 14%, respectively). Of all the NCs, those containing lecithin were the most stable showing no significant variation on their physicochemical properties after a one-week storage. Based on these results, we chose the lecithin-containing prototype for the next step of the development of the formulation.

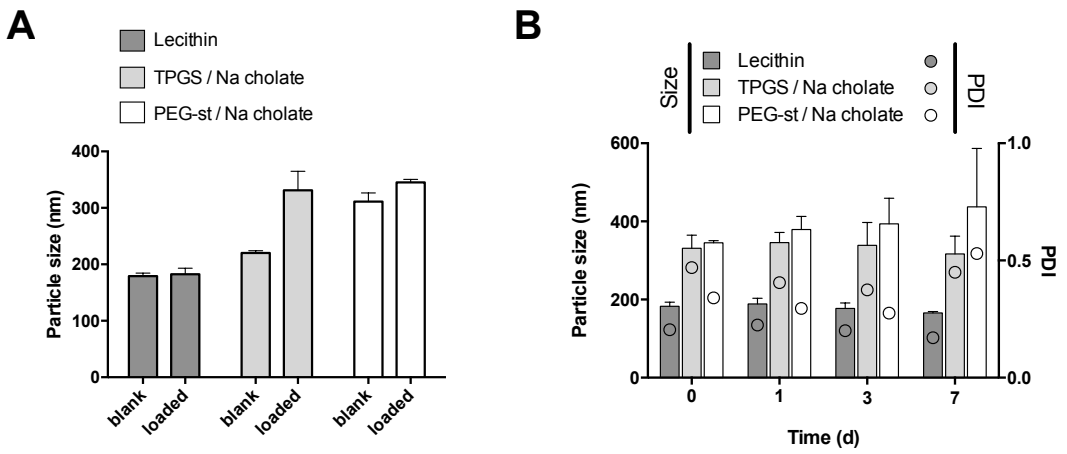

Figure 2. Particle size modification after antigen association, and short-term stability of different chitosan nanocapsules. Particle size of blank and IutA-loaded chitosan/vitamin E nanocapsules prepared with different surfactants: lecithin, D-α-Tocopherol polyethylene glycol 1000 succinate (TPGS), sodium cholate (Na cholate) and polyoxyethylene (40) stearate (PEG-st) (A). Prototypes stability, as function of their particle size and PDI, at storage conditions (4 ºC) for 1 week (B). Results are shown as the mean ± SD of 3 replicates.

3.1.5. Sandwich-like nanocapsules: antigen entrapment in bilayer nanocapsules

Proteins associated to the polymeric shell of the NCs may be prematurely exposed to the physiological environment leading to their inactivation or uncontrolled release. To prevent this potential problem, we propose here a sandwich-like structure in which the antigen is protected between a bilayer that surrounds the immunostimulating oily nanocore. For the bilayer formation we chose dextran sulfate, a negatively charged polymer that has been explored for the formation of nanocomplexes in association with chitosan [53–59]. The appropriate conditions for the formation of the dextran sulfate layer were determined empirically, using the saturation method [60,61]. For this determination, blank monolayer chitosan NCs (vitamin E/lecithin/chitosan) were incubated with different ratios of dextran sulfate (chitosan:dextran sulfate ratios 10:1 to 1:4 w/w) and the saturation of the NCs surface was determined by monitoring their zeta potential. As expected, the results in Fig. 3 illustrate the inversion of the zeta potential from positive (+ 50 mV) to highly negative values (-50 mV) upon addition of the dextran sulfate layer. This inversion happened at a chitosan:dextran sulfate ratio of 4:1, and reached a minimum value around the 2:1 ratio. A further increase of the amount of dextran sulfate did not cause an additional decrease of the zeta-potential. Benoit et al. obtained similar results on the optimal CS:DS ratio in a multilayer prototype [59].

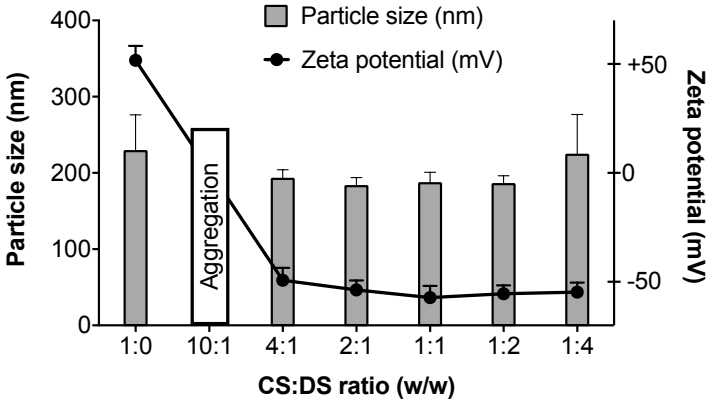

Figure 3. Evolution of the particle size and zeta potential of vitamin E/lecithin/chitosan nanocapsules upon formation of a second dextran sulfate layer. Results are shown as mean ± SD of 4 replicates.

Once we optimized the components of the coating of blank NCs, we applied the same experimental conditions to IutA-loaded NCs. We monitored the particle size and zeta potential after the addition of dextran sulfate, and concluded that, after the first 10 minutes, the forces that maintain dextran sulfate attached to the monolayer NCs were already established (Fig. S3). The properties of the bilayer chitosan/dextran sulfate NCs are shown in Table 1. The values of the monolayer system are indicated for comparison purposes. The addition of the second layer of dextran sulfate significantly reduced the NCs size down to 200 nm, from the 274 nm previously found for the IutA-loaded monolayer NCs. This change was attributed to the compacting of the loose chitosan shell due to its electrostatic interaction with dextran sulfate. As expected, the second polysulfated layer changed the surface charge of the nanoparticles from positive to highly negative. Finally, the antigen association efficiency was maintained after the addition of the second layer of the polymer, confirming that dextran sulfate does not displace the antigen, but keeps it protected in a polymeric sandwich-like structure, as we envisaged.

Table 1. Physico-chemical properties and antigen association efficiency (AE) of selected prototypes for *in vivo* experiments. Results are shown as mean ± SD of, at least, three replicates. n/a not applicable.

Nanosystems	Particle size (nm)	PDI	Z-potential (mV)	AE (%)
Blank CS NCs	166 ± 7	0.2	+ 35 ± 4	n/a
Loaded CS NCs	274 ± 19	0.2	+ 44 ± 2	67 ± 5
Blank DS/CS NCs	196 ± 5	0.1	- 52 ± 3	n/a
Loaded DS/CS NCs	200 ± 2	0.1	- 42 ± 4	71 ± 8

3.2. Morphological characterization of the mono and bilayer nanocapsules

According to the electron microscopy images presented in Fig. 4A, the chitosan NCs showed a structure consisting of a dense oily core surrounded by a light layer of entangled polymer. This structure was already described for similar prototypes of NCs [29,33,62]. However, in agreement with the decrease in particle size observed by DLS, in the case of the bilayer NCs, the loose chitosan layer seems to be compacted due to the electrostatics forces generated by the second layer of dextran sulfate (Fig. 4B). The particle size of the NCs observed by TEM is lower than the one observed by DLS, probably because, for TEM imaging, the NCs are dehydrated, whereas DLS measures the hydrodynamic ratio. FESEM images (Fig. 4C and 4D) also confirmed the spherical shape of the NCs, and showed a disperse population ranging from 100-500 nm, as commonly observed for this kind of systems. In this case, the hydration of the NCs seems to be higher than the one observed by TEM.

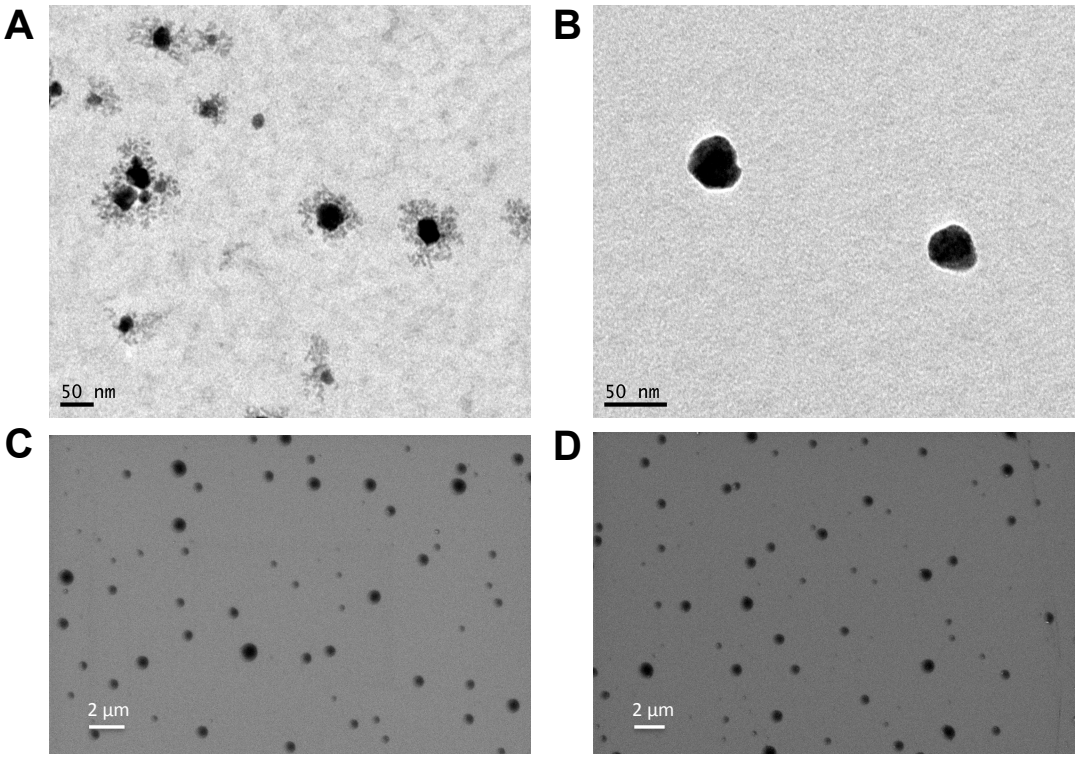

Figure 4. Electron microscopy images of the nanocapsules. TEM (A, B) and FESEM (C, D) images of monolayer chitosan nanocapsules (A, C) and bilayer chitosan/dextran sulfate nanocapsules (B, D).

Apart from the inversion in the Z-potential, an elemental microanalysis performed on individual NCs during the microscopy studies confirmed the presence of the second layer of dextran sulfate. Although carbon is the predominant element, phosphorus from lecithin could be detected in both the monolayer and bilayer nanosystems. Besides, in the bilayer NCs, sulfur and sodium were also detected, which can be explained by the presence of sulfate groups in the dextran.

3.3. Thermostability of antigen-loaded freeze-dried bilayer nanocapules

A freeze-drying process was developed to assure the long-term stability of the nanosystems. To maintain the physico-chemical properties of the NCs during the freeze-drying process different cryoprotectants were used. Sugars are among the most used cryoprotectants because during the freeze-drying process they produce an amorphous sugar glass matrix that protects nanoparticles from aggregation [63]. Besides, the sugar molecules interact with the polysaccharides of the NCs by hydrogen bonds, replacing the water molecules and stabilizing the whole system. Because of their specific molecular structure, different sugars can have different interactions with a particular nanosystem, so the common way to select the most appropriate cryoprotectant is making a screening of different compounds at different concentrations [64]. With that purpose, we selected a few sugars, i.e. mannitol, sucrose, trehalose and glucose, and we freeze-dried the NCs in their presence. The best result, in terms of preservation of the particle size upon freeze-drying and re-suspension, was obtained when sucrose was added to the suspension of NCs (10% sucrose concentration) (Fig. 5A). These conditions were used to freeze-dry antigen-loaded monolayer and bilayer NCs.

FESEM images of the freeze-dried formulations with 10% sucrose revealed a cheese-like structure with homogeneously distributed holes in the sugar matrix (Fig. 5B), similar to the one reported for PCL NCs freeze-dried with PVA [63]. Taking a closer look, shrunken NCs can be observed inside the holes. In the freeze-drying process, the originally hydrated NCs that occupy the entire volume of the holes are considerably reduced in size after the drying step, creating this pierced structure as the final product.

To check their thermostability, freeze-dried formulations were stored at room temperature and, at different times, resuspended in water and their particle size and antigen association measured. The results showed that the chitosan/dextran sulfate bilayer NCs maintained their particle size (≈ 200 nm) after storage in a freeze-dried form for the full duration of the experiment (12 weeks). However, an important increase in the particle size of the IutA-loaded monolayer chitosan NCs was observed: from 270 nm, before freeze-drying, to more than 400 nm after the process. These results support the premise that the additional dextran sulfate layer has a protective role. Noticeably, with regard to the association efficiency, the amount of the attached protein remained the same at least up to 90 days in the freeze-dried formulations (Fig. 5D). These remarkable results would make the potential nanovaccine a thermostable vaccine [65], overcoming the need for the cold chain, a feature particularly desirable when considering its use in developing countries.

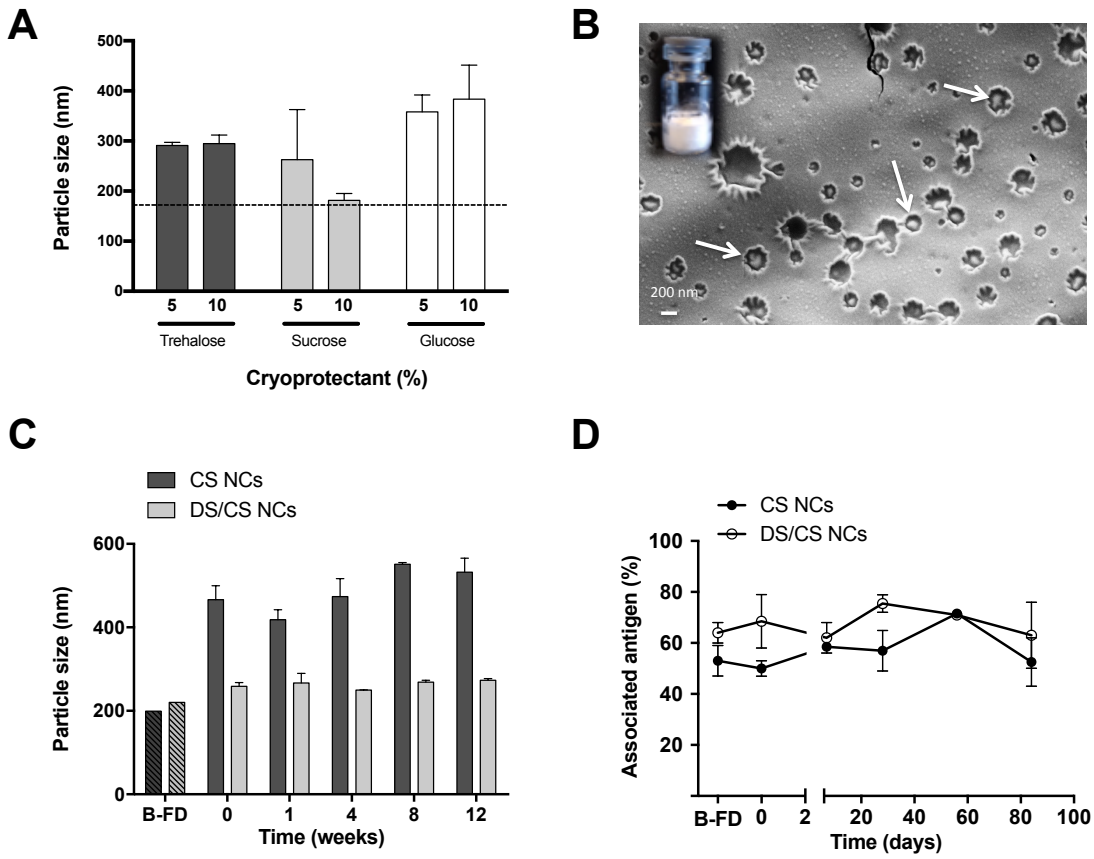

Figure 5. Microscopic structure, physicochemical properties and antigen association stability of freeze-dried antigen-loaded nanocapsules (NCs). Particle size of resuspended vitamin E/lecithin/chitosan NCs after freeze-drying with different percentages of cryoprotectant sugars. Dashed line represents particle size before freeze-drying (B-FD) (A). FESEM image of freeze-dried bilayer NCs with 10% sucrose. Arrows point out some shrunken NCs (B). Stability of freeze-dried monolayer and bilayer NCs after up to 3 months of storage at room temperature regarding particle size (C) and antigen association (D) after resuspension. Results are shown as mean ± SD of 3 replicates.

3.4. Stability and release in simulated physiological media

NCs prepared as a suspension or as a freeze-dried powder were incubated in PBS-Tween® 80 (0.02% w/w) and kept at 37 ºC. The results, shown in Figure 6, indicate that, when the antigen is associated with the bilayer NCs, it has a more sustained release than when it is associated with the monolayer NCs. This difference is even greater in the freeze-dried formulations. In this last case, monolayer NCs release around 100% of the antigen during the first 4 hours, while the bilayer nanosystem releases less than 35% within the same timeframe (Fig. 6). As a control, the particle size of the formulations was monitored in the same conditions. The freeze-dried monolayer chitosan NCs suffered an important increase in their particle size, whereas the double layer NCs were stable for at least 24 hours (Fig. S4).

Despite the abundant information about the release profiles from micro and nanoparticle formulations intended to work as single-dose formulations [52,66–69], in the case of nanocarriers intended to target the antigen to dendritic cells and achieve a

subsequent adjuvant effect, i.e. nanoemulsions, NCs, the information is very limited. In fact, we have found (data not published) that polymeric nanocapsules can freely drain to the closest lymph nodes where different subpopulations of immune cells are concentrated ready to process and present antigens. This drainage normally occurs in a few hours. Hence, a NC that releases the antigen for a number of hours could be adequate. Although these *in vitro* release data cannot be extrapolated to *in vivo* conditions, they are meaningful in the sense that they allow us to exclude the possibility of an uncontrolled and premature release upon injection.

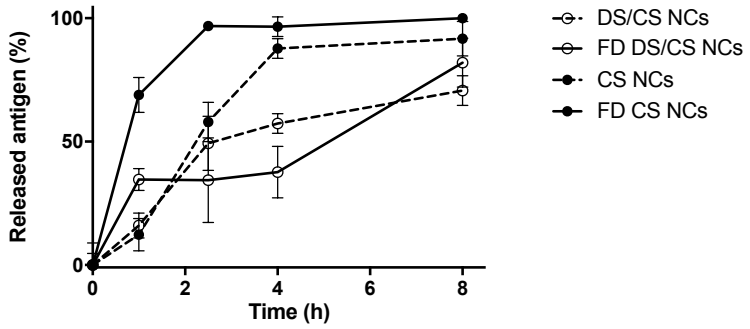

Figure 6. Antigen release from the nanocapsules (NCs). The study of the release of the antigen IutA from freeze-dried (FD) and non freeze-dried chitosan (CS) monolayer and dextran sulfate/chitosan (DS/CS) bilayer lecithin/vitamin E NCs was performed in PBS Tween® 80 0.02 % (w/w) at 37 ºC. Results are shown as mean ± SD of 3 replicates.

3.5. *In vitro* cell studies

3.5.1. Cytotoxicity

Prior to *in vivo* studies, the cytotoxicity of the nanosystems was evaluated *in vitro* using the murine macrophage cell line RAW 264.7. Two different methods were used to calculate viability: the colorimetric assay MTS, and the xCELLigence® system.

First, the stability of the nanosystems in cell culture media was verified under the conditions and for the duration planned for the *in vitro* experiments. The particle size of the NCs increased slightly upon contact with supplemented RPMI, and, then, remained stable for the duration of the experiment (Fig. S5).

NCs at different concentrations (from 25 to 400 µg/mL) were incubated with the cells in RPMI for up to either 6 or 24 hours, and the cytotoxicity was measured at 24 h using a MTS assay and compared with non-treated cells. A dose-dependent reduction of the viability was observed for both, the monolayer and bilayer NCs, whereas the incubation time did not have a relevant impact on the cytotoxicity values. In the case of CS NCs, at concentrations higher than 150 µg/mL, the macrophages viability was incrementally reduced, and this toxicity value was higher for the bilayer

DS/CS NCs, where signs of toxicity were observed starting at 100 µg/mL (Fig. 7A). However the differences between the toxicity values of both prototypes were not significant. The calculated DL50 are approximately 300 µg/mL for CS NCs, and 200 µg/mL for DS/CS NCs. These values are within the range of those previously reported in the literature for chitosan [27] and protamine NCs [29].

Similar results were observed using xCELLigence® (Fig. 7B and 7C). DS/CS NCs reduce macrophages viability in a slightly higher degree than CS NCs.

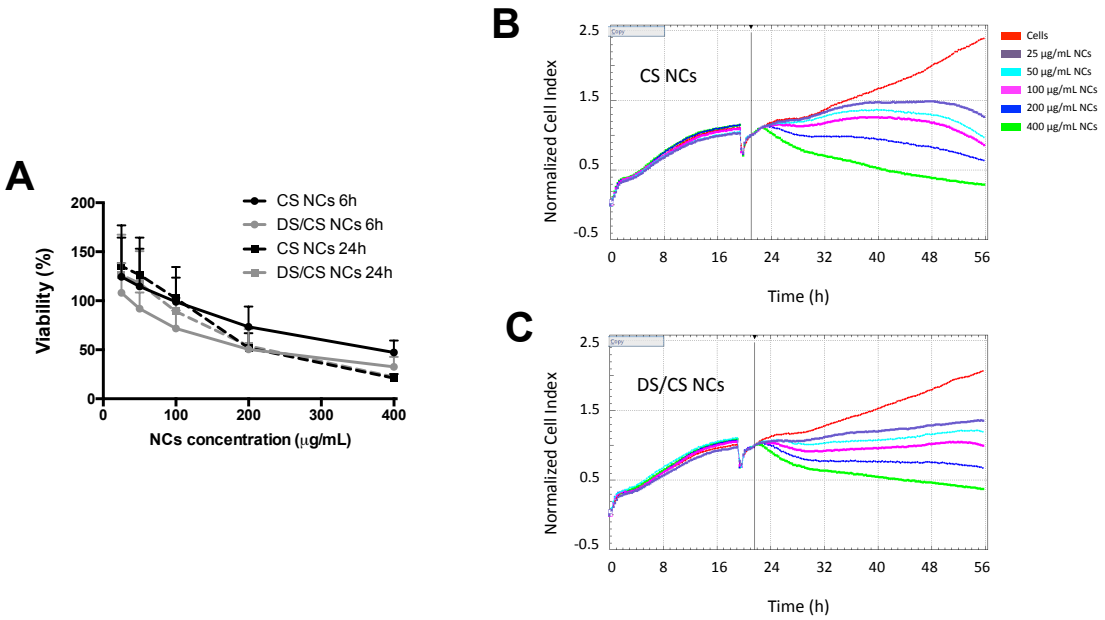

Figure 7. Viability of RAW 264.7 cells treated with different concentrations of NCs. The cell viability was measured by MTS (A) 24 h after adding the nanocapsules (NCs). The cells were left in contact with the NCs for either 6 or 24 h, as indicated in the graph. A different viability experiment for monolayer and bilayer NCs was performed using the xCELLigence® technique (B, C). Results are shown as mean ± SD of 3 replicates.

3.5.2. Internalization of the nanocapsules and cytokine production

The first step that triggers the immune response cascade is the recognition and internalization of the nanovaccine by antigen presenting cells (APCs), in order to properly process and present the antigen to T cells. Internalization studies were performed upon loading the NCs with the lipophilic marker Nile Red, and confirmed the absence of significant release of the marker in cell culture medium at 37 ºC (release less than 10% in 4 h). Macrophages were exposed to two different concentrations of fluorescent NCs, 50 and 100 µg/mL, for up to 30 minutes; then the cells were washed and NCs-cells interaction was analyzed by FACS. The FACS data (Fig. 8A) revealed that both, single and bilayer NCs strongly interact with macrophages, as shown by the clear shift of the peaks in the histogram when compared to the control

(red line). The fluorescence intensity associated to the macrophages increases as the NCs concentration in the incubation step increases, implying that the NCs-cell interaction was not saturated at the lower concentration (Fig. 8B). An evidence of the internalization of the NCs in macrophages was achieved using confocal microscopy (Fig. 8C-E). Images were acquired after treating the macrophages with 50 µg/mL of Nile Red-labeled NCs for 30 minutes. Again, the internalization of the mono and bilayer NCs was observed, with a noticeable contrast between the blue nuclei of the macrophages, and the cytoplasm that becomes stained in red due to the presence of fluorescent NCs.

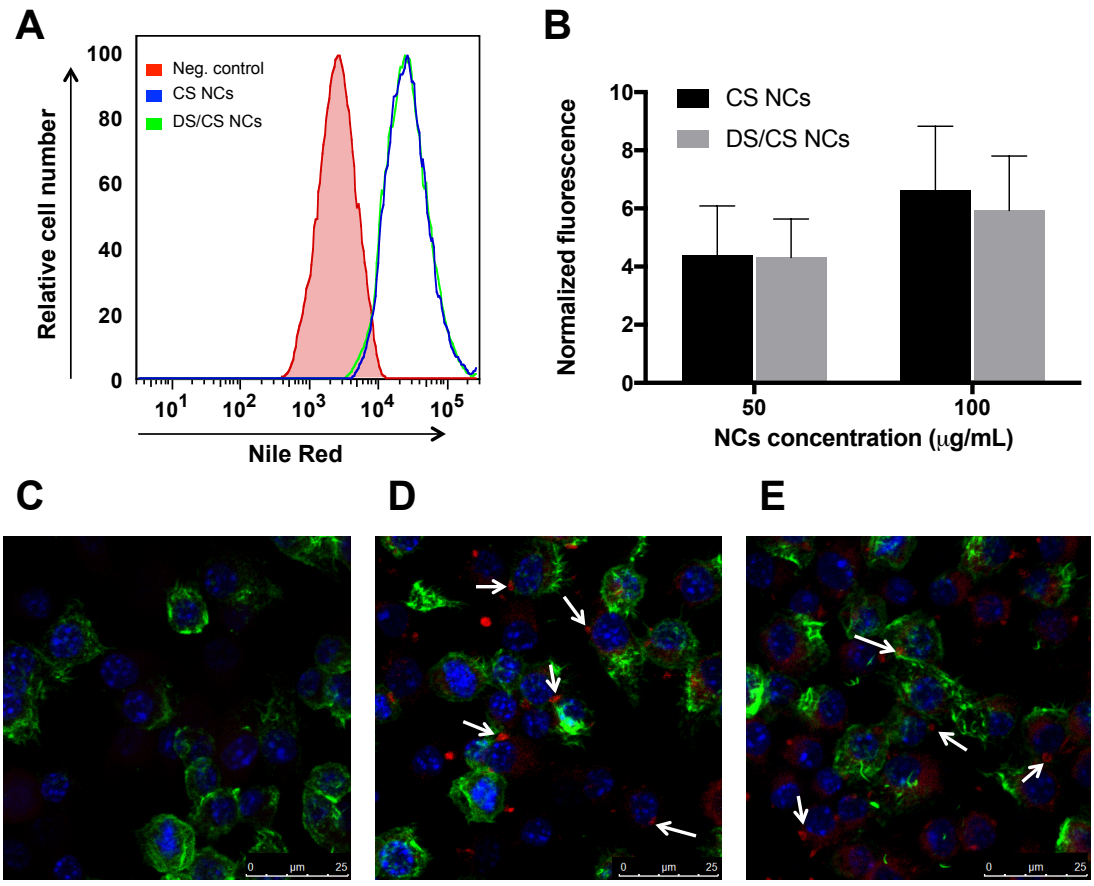

Figure 8. Internalization of the nanocapsules (NCs) in macrophages. Representative flow cytometry histograms showing the interaction with macrophages of monolayer (blue line) and bilayer NCs (green line) at 50 µg/mL after 30 minutes incubation. The red line shows untreated macrophages (A). Interaction with both prototypes at different concentrations obtained by FACS (B). Confocal microscopy images of macrophages incubated without (C) or with monolayer (D) and bilayer (E) Nile Red-loaded NCs (50 µg/mL for 30 minutes). White arrows point out an acumulation of NCs inside cells. Red channel: NCs; blue channel: cell nuclei; green channel: cytoskeleton.

Cytokine production (IFN-γ, IL-1β, IL-2, IL-4, IL-5, IL-6, IL-8, IL-10, IL-12 p70, TNF-α and TNF-β) was assessed in peripheral blood mononuclear cells (PBMCs) from healthy donors, after their exposure to a range of NCs concentrations, from 50 to 400 µg/mL for up to 24 h. The results of this study show that the blank NCs do not stimulate the production of cytokines. Similar results were previously reported for

chitosan NCs, despite the fact that they showed a specific and significant adjuvant effect *in vivo* for the hepatitis B antigen associated to them [27]. Finally, regarding the intrinsic immunostimulatory properties of chitosan and dextran, the results published are still inconclusive. Although some reports suggest that high molecular weight dextran sulfate (500 kDa) has immunostimulant properties [70,71], this effect has been associated with a certain toxicity. To avoid this, in this study, we have chosen low molecular weight dextran sulfate (6-8 kDa), which has a good safety profile, as underlined by the fact that it has been approved by the European Medicines Agency (EMA) as an orphan drug for stem cell and pancreatic transplantation. On the other hand, regarding chitosan, a few reports have been published that cover its immunostimulatory properties. The results indicate that the deacetylation degree, molecular weight, polydispersity, chitosan dosage and the cellular model determine the type of response, with the release of pro- and anti-inflammatory factors depending on these parameters [72]. However, in our experience, highly purified chitosan *per se* has not shown immunostimulatory response *in vitro,* whereas it is expected to enhance the immune response of specific antigens when presented in a nanoparticulated form. This observation is in agreement with the results of Villiers et al., which showed an activation of DCs by chitosan at the membrane level, via a TLR4-dependent mechanism, up-regulating CD80 and CD86 markers [73]. However, chitosan *per se* did not generate a robust cytokine response and could not activate T-cells. When combined with an antigen, chitosan stimulates the expression of MHC-I, eliciting the secretion of cytokines and leading to a $CD8^+$ cells proliferation and a cellular response.

3.6. *In vivo* assays

Ideally, the rational design of a new nanovaccine would translate into positive *in vivo* results. To test the influence of the composition and architectural disposition (monolayer *vs.* bilayer NCs) of the nanosystems *in vivo*, we measured the humoral immune response elicited by the different antigen-loaded compositions in mice. Groups of 10 mice were immunized subcutaneously 3 times with freshly prepared loaded NCs (monolayer and bilayer), or with the *E. coli* derived IutA protein alone. As a positive control, the protein was administered in the presence of Alum adjuvant. Additional control groups consisted of non-immunized (PBS) or Alum-immunized animals. The immunizations were done subcutaneously, and 2 boosts were applied at 3 and 5 weeks after the first dose. One week after the last immunization boost, serum levels of IgG were analyzed (Fig. 9). As expected, purified IutA protein alone could not generate significant levels of IgG, similar to what happened with the groups treated only with Alum or PBS. On the other hand, IutA-loaded monolayer NCs elicited an immune response similar to the one generated when the protein was adjuvanted with

Alum, the gold standard for subcutaneous vaccination. These results agree with previous data showing that CS NCs have an adjuvant behaviour comparable to Alum [33]. The results of our rational design experiments indicate that bilayer NCs further improved the performance of both monolayer NCs and Alum, and cause significantly higher levels of serum IgGs. Although some authors have claimed that a positive surface charge produces stronger immune responses than neutral or negative nanoparticles [33,74,75], in our experiments, negatively charged bilayer NCs performed better than positively charged monolayer NCs. Therefore, our results indicate that the protection of the antigen with a second polymeric layer, which was found not to reduce their uptake by macrophages, favors the processing and presentation of the antigen when compared with monolayer NCs, in which the antigen is adsorbed onto their surface. The benefits of an increased stability together with the adequate physicochemical properties, allows the antigen to be efficiently processed and presented by APCs.

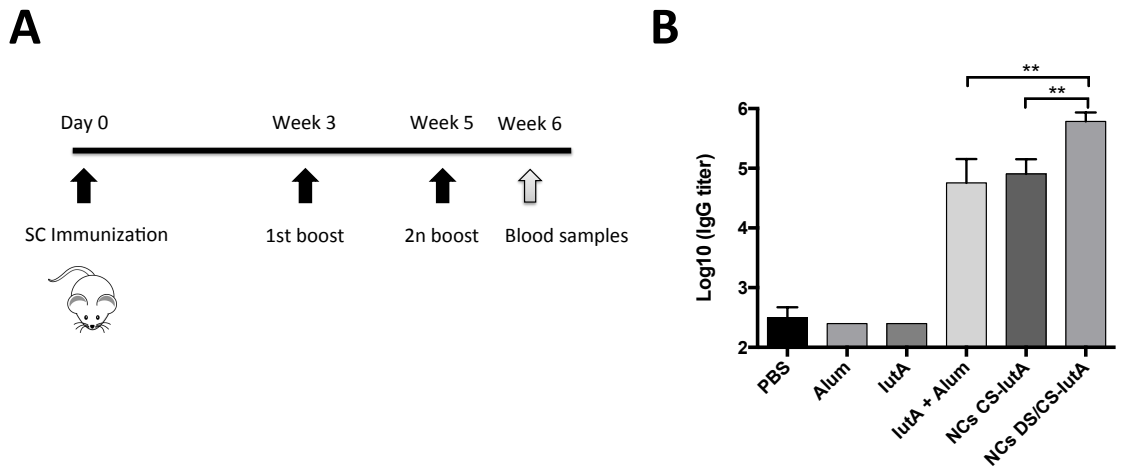

Figure 9. *In vivo* evaluation of the performance of antigen-loaded bilayer nanocapsules (NCs). Timeline of the immunization protocol for testing humoral response generated by these prototypes in mice (A). IgG levels observed upon subcutaneous (0, 3, and 5 weeks) immunization with IutA antigen, IutA adsorbed on Alum or IutA-loaded monolayer (CS) and bilayer (DS/CS) NCs (total of 15 μg of IutA per animal). PBS and Alum were used as controls (B). Results are shown as mean ± standard deviation (n = 5 for PBS and Alum, n = 10 for the rest of the groups). * and ** denote significant differences between groups (for $p < 0.05$, and $p < 0.01$ respectively).

Despite being the most frequently used adjuvant for parenteral administration, Alum has several disadvantages. Apart from its well-known local reactions [76], Alum is highly sensitive to temperature changes, particularly to freezing, requiring the maintenance of a cold chain of storage [76,77]. The thermostability of freeze-dried bilayer NCs (section 3.3) would give them a remarkable competitive advantage, allowing its use when the cold chain cannot be guaranteed. Moreover, the 10-fold increase in the IgG levels of the group treated with IutA-loaded bilayer NCs compared with the group treated with IutA adsorbed into Alum is expected to confer a better protection against infections by UPEC.

4. Conclusions

In this article, we described, for the first time, the preparation and characterization of bilayer NCs, composed by an oil with immunoregulatory properties, and two biodegradable polymers forming a sandwich-like structure with an antigen entrapped between them. The double-shell nanosystem was able to protect the IutA *E. coli* antigen and to control its release in simulated physiological media more efficiently than monolayer NCs. Furthermore, the resulting nanovaccine candidate showed a very good thermostability profile in a freeze-dried form (stable for 3 months at room temperature). Finally, the positive results observed *in vivo* in terms of the specific IgG response directed against the IutA a protein, highlight the value of the developed technology as a potential vaccine candidate against UPEC strains.

References

[1] J. Crecente-Campo, S. Lorenzo-Abalde, A. Mora, J. Marzoa, N. Csaba, J. Blanco, et al., Bilayer polymeric nanocapsules: A formulation approach for a thermostable and adjuvanted E. coli antigen vaccine, J. Control. Release. 286 (2018) 20–32. doi:10.1016/j.jconrel.2018.07.018.

[2] I. Toth, M. Skwarczynski, The immune system likes nanotechnology, Nanomedicine. 9 (2014) 2607–2609. doi:10.2217/nnm.14.199.

[3] J.V. Gonzalez-Aramundiz, A.S. Cordeiro, N. Csaba, M. de la Fuente, M.J. Alonso, Nanovaccines : nanocarriers for antigen delivery, Biol. Aujourdhui. 206 (2012) 249–261. doi:10.1051/jbio/2012027.

[4] Y. Liu, Y. Xu, Y. Tian, C. Chen, C. Wang, X. Jiang, Functional Nanomaterials Can Optimize the Efficacy of Vaccines, Small. 10 (2014) 4505–4520. doi:10.1002/smll.201401707.

[5] H. Yue, G. Ma, Polymeric micro / nanoparticles : Particle design and potential vaccine delivery applications, Vaccine. 33 (2015) 5927–5936. doi:10.1016/j.vaccine.2015.07.100.

[6] M.-L. De Temmerman, J. Rejman, J. Demeester, D.J. Irvine, B. Gander, S.C. De Smedt, Particulate vaccines: on the quest for optimal delivery and immune response., Drug Discov. Today. 16 (2011) 569–82. doi:10.1016/j.drudis.2011.04.006.

[7] A.C. Rice-ficht, A.M. Arenas-gamboa, M.M. Kahl-mcdonagh, T.A. Ficht, Polymeric particles in vaccine delivery, Curr. Opin. Microbiol. 13 (2010) 106–112. doi:10.1016/j.mib.2009.12.001.

[8] D.M. Smith, J.K. Simon, J.R. Baker, Applications of nanotechnology for immunology., Nat. Rev. Immunol. 13 (2013) 592–605. doi:10.1038/nri3488.

[9] P. Sahdev, L. Ochyl, J. Moon, Biomaterials for Nanoparticle Vaccine Delivery Systems, Pharm. Res. (2014). doi:10.1007/s11095-014-1419-y.

[10] T.G. Dacoba, A. Olivera, D. Torres, J. Crecente-Campo, M.J. Alonso, Modulating the immune system through nanotechnology., Semin. Immunol. 34 (2017) 78–102. doi:10.1016/j.smim.2017.09.007.

[11] Y. Liu, B. Workalemahu, X. Jiang, The Effects of Physicochemical Properties of Nanomaterials on Their Cellular Uptake In Vitro and In Vivo, Small. 13 (2017) 1–13. doi:10.1002/smll.201701815.

[12] H. Jiang, Q. Wang, X. Sun, Lymph node targeting strategies to improve vaccination efficacy, J. Control. Release. 267 (2017) 47–56. doi:10.1016/j.jconrel.2017.08.009.

[13] J.J. Richardson, J. Cui, M. Björnmalm, J.A. Braunger, H. Ejima, F. Caruso, Innovation in Layer-by-Layer Assembly, Chem. Rev. 116 (2016) 14828–14867. doi:10.1021/acs.chemrev.6b00627.

[14] B.M. Wohl, J.F.J. Engbersen, Responsive layer-by-layer materials for drug delivery, J. Control. Release. 158 (2012) 2–14. doi:10.1016/j.jconrel.2011.08.035.

[15] L.J. De Cock, S. De Koker, B.G. De Geest, J. Grooten, C. Vervaet, J.P. Remon, et al., Polymeric Multilayer Capsules in Drug Delivery, Angew. Chemie - Int. Ed. (2010) 6954–6973. doi:10.1002/anie.200906266.

[16] R.R. Costa, M. Alatorre-meda, J.F. Mano, Drug nano-reservoirs synthesized using layer-by-layer technologies, Biotechnol. Adv. 33 (2015) 1310–1326. doi:10.1016/j.biotechadv.2015.04.005.

[17] S. Correa, E.C. Dreaden, L. Gu, P.T. Hammond, Engineering nanolayered particles for modular drug delivery, J. Control. Release. 240 (2016) 364–386. doi:10.1016/j.jconrel.2016.01.040.

[18] O.S. Sakr, G. Borchard, Encapsulation of enzymes in layer-by-layer (LbL) structures: Latest advances and applications, Biomacromolecules. 14 (2013) 2117–2135. doi:10.1021/bm400198p.

[19] A.C. Anselmo, K.J. McHugh, J. Webster, R. Langer, A. Jaklenec, Layer-by-Layer Encapsulation of Probiotics for Delivery to the Microbiome, Adv. Mater. 28 (2016) 9486–9490. doi:10.1002/adma.201603270.

[20] M.T. Speth, U. Repnik, G. Griffiths, Layer-by-layer nanocoating of live Bacille-Calmette-Guérin mycobacteria with poly(I:C) and chitosan enhances pro-inflammatory activation and bactericidal capacity in murine macrophages, Biomaterials. 111 (2016) 1–12. doi:10.1016/j.biomaterials.2016.09.027.

[21] S. Pejawar-gaddy, J.M. Kovacs, D.H. Barouch, B. Chen, D.J. Irvine, Design of Lipid Nanocapsule Delivery Vehicles for Multivalent Display of Recombinant Env Trimers in HIV Vaccination, Bioconjug. Chem. 25 (2014) 1470–1478. doi:10.1021/bc5002246.

[22] K. van der Maaden, E. Sekerdag, P. Schipper, G. Kersten, W. Jiskoot, J. Bouwstra, Layer-by-Layer Assembly of Inactivated Poliovirus and N -Trimethyl Chitosan on pH-Sensitive Microneedles for Dermal Vaccination, Langmuir. 31 (2015) 8654–8660. doi:10.1021/acs.langmuir.5b01262.

[23] X. Su, B.-S. Kim, S.R. Kim, P.T. Hammond, D.J. Irvine, Layer-by-Layer-Assembled Multilayer Films for Transcutaneous Drug and Vaccine Delivery, ACS Nano. 3 (2009) 3719–3729. doi:10.1021/nn900928u.

[24] P.C. Demuth, J.J. Moon, H. Suh, P.T. Hammond, D.J. Irvine, Releasable Layer-by-Layer Assembly of Stabilized Lipid Nanocapsules on Microneedles for Enhanced Transcutaneous Vaccine Delivery, ACS Nano. 6 (2013) 8041–8051. doi:10.1021/nn302639r.Releasable.

[25] B.G. De Geest, Engineering the immune system with particles, step-by-step, Mol. Immunol. 98 (2018) 25–27. doi:10.1016/j.molimm.2018.02.015.

[26] R. Abellan-Pose, M. Rodríguez-Évora, S. Vicente, N. Csaba, C. Évora, M.J. Alonso, et al., Biodistribution of radiolabeled polyglutamic acid and PEG-polyglutamic acid nanocapsules, Eur. J. Pharm. Biopharm. 112 (2017) 155–163. doi:10.1016/j.ejpb.2016.11.015.

[27] S. Vicente, M. Peleteiro, B. Díaz-Freitas, A. Sanchez, Á. González-Fernández, M.J. Alonso, Co-delivery of viral proteins and a TLR7 agonist from polysaccharide nanocapsules: A needle-free vaccination strategy, J. Control. Release. 172 (2013) 773–781. doi:10.1016/j.jconrel.2013.09.012.

[28] S. Reimondez-troitiño, I. Alcalde, N. Csaba, A. Íñigo-portugués, M. De Fuente, F. Bech, Polymeric nanocapsules : a potential new therapy for corneal wound healing, Drug Deliv. Transl. Res. (2016) 708–721. doi:10.1007/s13346-016-0312-0.

[29] J.V. González-Aramundiz, E. Presas, I. Dalmau-Mena, S. Martínez-Pulgarín, C. Alonso, J.M. Escribano, et al., Rational design of protamine nanocapsules as antigen delivery carriers, J. Control. Release. 245 (2017) 62–69. doi:10.1016/j.jconrel.2016.11.012.

[30] G. Lollo, A. Gonzalez-Paredes, M. Garcia-Fuentes, P. Calvo, D. Torres, M.J. Alonso, Polyarginine Nanocapsules as a Potential Oral Peptide Delivery Carrier, J. Pharm. Sci. 106 (2017) 611–618. doi:10.1016/j.xphs.2016.09.029.

[31] S. Vicente, B.A. Goins, A. Sanchez, M.J. Alonso, W.T. Phillips, Biodistribution and lymph node retention of polysaccharide-based immunostimulating nanocapsules, Vaccine. 32 (2014) 1685–1692. doi:10.1016/j.vaccine.2014.01.059.

[32] S. Vicente, M. Peleteiro, J.V. González-Aramundiz, B. Díaz-Freitas, S. Martínez-Pulgarín, J.I. Neissa, et al., Highly versatile immunostimulating nanocapsules for specific immune potentiation., Nanomedicine (London). 9 (2014) 2273–2289. doi:10.2217/nnm.14.10.

[33] S. Vicente, B. Diaz-Freitas, M. Peleteiro, A. Sanchez, D.W. Pascual, A. Gonzalez-Fernandez, et al., A Polymer/Oil Based Nanovaccine as a Single-Dose Immunization Approach, PLoS One. 8 (2013) e62500. doi:10.1371/journal.pone.0062500.

[34] C.G. Venturini, E. Jäger, C.P. Oliveira, A. Bernardi, A.M.O. Battastini, S.S. Guterres, et al., Formulation of lipid core nanocapsules, Colloids Surfaces A Physicochem. Eng. Asp. 375 (2011) 200–208. doi:10.1016/j.colsurfa.2010.12.011.

[35] C.E.E. Mora-Huertas, H. Fessi, A. Elaissari, Polymer-based nanocapsules for drug delivery, Int. J. Pharm. 385 (2010) 113–142. doi:10.1016/j.ijpharm.2009.10.018.

[36] S. Salinthone, A.R. Kerns, V. Tsang, D.W. Carr, α-Tocopherol (vitamin E) stimulates cyclic AMP production in human peripheral mononuclear cells and alters immune function, Mol. Immunol. 53 (2013) 173–178. doi:10.1016/j.molimm.2012.08.005.

[37] R.P. Tengerdy, Vitamin E, Immune Response, and Disease Resistance, Ann. N. Y. Acad. Sci. 570 (1989) 335–344. doi:10.1111/j.1749-6632.1989.tb14932.x.

[38] S.N. Han, S.N. Meydani, Impact of vitamin E on immune function and its clinical implications., Expert Rev. Clin. Immunol. 2 (2006) 561–7. doi:10.1586/1744666X.2.4.561.

[39] S. Morel, A. Didierlaurent, P. Bourguignon, S. Delhaye, B. Baras, V. Jacob, et al., Adjuvant System AS03 containing α-tocopherol modulates innate immune response and leads to improved adaptive immunity, Vaccine. 29 (2011) 2461–2473. doi:10.1016/j.vaccine.2011.01.011.

[40] H. Mobley, C. Alteri, Development of a Vaccine against Escherichia coli Urinary Tract Infections, Pathogens. 5 (2015) 1. doi:10.3390/pathogens5010001.

[41] L.A. Mike, S.N. Smith, C.A. Sumner, K.A. Eaton, H.L.T. Mobley, Siderophore vaccine conjugates protect against uropathogenic Escherichia coli urinary tract infection, Proc. Natl. Acad. Sci. 113 (2016) 13468–13473. doi:10.1073/pnas.1606324113.

[42] D.T. Uehling, W.J. Hopkins, J.E. Elkahwaji, D.M. Schmidt, G.E. Leverson, Phase 2 Clinical Trial of a Vaginal Mucosal Vaccine for Urinary Tract Infections, J. Urol. 170 (2003) 867–869. doi:10.1097/01.ju.0000075094.54767.6e.

[43] H.W. Bauer, V.W. Rahlfs, P.A. Lauener, G.S.. Bleßmann, Prevention of recurrent urinary tract infections with immuno-active E. coli fractions: a meta-analysis of five placebo-controlled

double-blind studies, Int. J. Antimicrob. Agents. 19 (2002) 451–456. doi:10.1016/S0924-8579(02)00106-1.

[44] N.K. Burgess, T.P. Dao, A.M. Stanley, K.G. Fleming, -Barrel Proteins That Reside in the Escherichia coli Outer Membrane in Vivo Demonstrate Varied Folding Behavior in Vitro, J. Biol. Chem. 283 (2008) 26748–26758. doi:10.1074/jbc.M802754200.

[45] P. Calvo, C. Remuñán-López, J.L. Vila-Jato, M.J. Alonso, Development of positively charged colloidal drug carriers: Chitosan-coated polyester nanocapsules and submicron-emulsions, Colloid Polym. Sci. 275 (1997) 46–53. doi:10.1007/s003960050050.

[46] E. De Gregorio, R. Rappuoli, From empiricism to rational design: a personal perspective of the evolution of vaccine development, Nat Rev Immunol. 14 (2014) 505–514. doi:10.1038/nri3694.

[47] L. Zhao, A. Seth, N. Wibowo, C. Zhao, N. Mitter, C. Yu, et al., Nanoparticle vaccines, Vaccine. 32 (2014) 327–337. doi:10.1016/j.vaccine.2013.11.069.

[48] B. Slütter, P.C. Soema, Z. Ding, R. Verheul, W. Hennink, W. Jiskoot, Conjugation of ovalbumin to trimethyl chitosan improves immunogenicity of the antigen, J. Control. Release. 143 (2010) 207–214. doi:10.1016/j.jconrel.2010.01.007.

[49] S.G. Reed, S. Bertholet, R.N. Coler, M. Friede, New horizons in adjuvants for vaccine development, Trends Immunol. 30 (2009) 23–32. doi:10.1016/j.it.2008.09.006.

[50] N. Garçon, D.W. Vaughn, A.M. Didierlaurent, Development and evaluation of AS03, an Adjuvant System containing α-tocopherol and squalene in an oil-in-water emulsion, Expert Rev. Vaccines. 11 (2012) 349–366. doi:10.1586/erv.11.192.

[51] A.C. Allison, Squalene and Squalane Emulsions as Adjuvants, Methods. 19 (1999) 87–93. doi:10.1006/meth.1999.0832.

[52] C. Prego, P. Paolicelli, B. Díaz, S. Vicente, A. Sánchez, Á. González-Fernández, et al., Chitosan-based nanoparticles for improving immunization against hepatitis B infection, Vaccine. 28 (2010) 2607–2614. doi:10.1016/j.vaccine.2010.01.011.

[53] S. Sharma, T.K.S. Mukkur, H.A.E. Benson, Y. Chen, Enhanced Immune Response Against Pertussis Toxoid by IgA-Loaded Chitosan–Dextran Sulfate Nanoparticles, J. Pharm. Sci. 101 (2012) 233–244. doi:10.1002/jps.22763.

[54] S. Sharma, H. a E. Benson, T.K.S. Mukkur, P. Rigby, Y. Chen, Preliminary studies on the development of IgA-loaded chitosan-dextran sulphate nanoparticles as a potential nasal delivery system for protein antigens., J. Microencapsul. 30 (2013) 283–94. doi:10.3109/02652048.2012.726279.

[55] D.P. Gnanadhas, M. Ben Thomas, M. Elango, A.M. Raichur, D. Chakravortty, Chitosan-dextran sulphate nanocapsule drug delivery system as an effective therapeutic against intraphagosomal pathogen Salmonella, J. Antimicrob. Chemother. 68 (2013) 2576–2586. doi:10.1093/jac/dkt252.

[56] T. Delair, Colloidal polyelectrolyte complexes of chitosan and dextran sulfate towards versatile nanocarriers of bioactive molecules., Eur. J. Pharm. Biopharm. 78 (2011) 10–8. doi:10.1016/j.ejpb.2010.12.001.

[57] P. Zaman, J. Wang, A. Blau, W. Wang, T. Li, D.S. Kohane, et al., Incorporation of heparin-binding proteins into preformed dextran sulfate-chitosan nanoparticles, Int. J. Nanomedicine. 11 (2016) 6149–6159. doi:10.2147/IJN.S119174.

[58] W. Chaiyasan, S.P. Srinivas, W. Tiyaboonchai, Mucoadhesive Chitosan–Dextran Sulfate Nanoparticles for Sustained Drug Delivery to the Ocular Surface, J. Ocul. Pharmacol. Ther. 29 (2013) 200–207. doi:10.1089/jop.2012.0193.

[59] S. Hirsjärvi, Y. Qiao, A. Royere, J. Bibette, J. Benoit, Layer-by-layer surface modification of lipid nanocapsules, Eur. J. Pharm. Biopharm. 76 (2010) 200–207. doi:10.1016/j.ejpb.2010.07.010.

[60] K. Szczepanowicz, D. Dronka-Góra, G. Para, P. Warszyński, Encapsulation of liquid cores by layer-by-layer adsorption of polyelectrolytes, J. Microencapsul. 27 (2010) 198–204. doi:10.3109/02652040903052069.

[61] K. Szczepanowicz, U. Bazylińska, J. Pietkiewicz, L. Szyk-Warszyńska, K.A. Wilk, P. Warszyński, Biocompatible long-sustained release oil-core polyelectrolyte nanocarriers: From controlling physical state and stability to biological impact, Adv. Colloid Interface Sci. 222 (2015) 678–691. doi:10.1016/j.cis.2014.10.005.

[62] R. Abellan-Pose, C. Teijeiro-Valiño, M.J. Santander-Ortega, E. Borrajo, A. Vidal, M. Garcia-Fuentes, et al., Polyaminoacid nanocapsules for drug delivery to the lymphatic system: Effect of the particle size, Int. J. Pharm. 509 (2016) 107–117. doi:10.1016/j.ijpharm.2016.05.034.

[63] W. Abdelwahed, G. Degobert, S. Stainmesse, H. Fessi, Freeze-drying of nanoparticles:

Formulation, process and storage considerations, Adv. Drug Deliv. Rev. 58 (2006) 1688–1713. doi:10.1016/j.addr.2006.09.017.

[64] P. Fonte, S. Reis, B. Sarmento, Facts and evidences on the lyophilization of polymeric nanoparticles for drug delivery, J. Control. Release. 225 (2016) 75–86. doi:10.1016/j.jconrel.2016.01.034.

[65] D. Chen, D. Kristensen, Opportunities and challenges of developing thermostable vaccines, Expert Rev. Vaccines. 8 (2009) 547–557. doi:10.1586/erv.09.20.

[66] M.M. Tobío, J. Nolley, Y. Guo, J. McIver, M.J. Alonso, A Novel System Based on a Poloxamer/PLGA Blend as a Tetanus Toxoid Delivery Vehicle, Pharm. Res. 16 (1999) 682–688. doi:10.1023/a:1018820507379.

[67] M. Tobio, S.P. Schwendeman, Y. Guo, J. McIver, R. Langer, M.J. Alonso, Improved immunogenicity of a core-coated tetanus toxoid delivery system, Vaccine. 18 (1999) 618–622. doi:10.1016/S0264-410X(99)00313-8.

[68] A. Vila, A. Sánchez, C. Évora, I. Soriano, O. McCallion, M.J. Alonso, PLA-PEG particles as nasal protein carriers: The influence of the particle size, Int. J. Pharm. 292 (2005) 43–52. doi:10.1016/j.ijpharm.2004.09.002.

[69] A. Vila, A. Sánchez, K. Janes, I. Behrens, T. Kissel, J.L. V Jato, et al., Low molecular weight chitosan nanoparticles as new carriers for nasal vaccine delivery in mice, Eur. J. Pharm. Biopharm. 57 (2004) 123–131. doi:10.1016/j.ejpb.2003.09.006.

[70] R.E. McCarthy, L.W. Arnold, G.F. Babcock, Dextran sulphate: an adjuvant for cell-mediated immune responses., Immunology. 32 (1977) 963–974.

[71] T. Diamantstein, H. Rühl, W. Vogt, G. Bochert, Stimulation of B-cells by dextran sulphate in vitro., Immunology. 25 (1973) 743–7.

[72] D. Fong, C.D. Hoemann, Chitosan immunomodulatory properties: perspectives on the impact of structural properties and dosage, Futur. Sci. OA. 4 (2018) FSO225. doi:10.4155/fsoa-2017-0064.

[73] C. Villiers, M. Chevallet, H. Diemer, R. Couderc, H. Freitas, A. Van Dorsselaer, et al., From Secretome Analysis to Immunology, Mol. Cell. Proteomics. 8 (2009) 1252–1264. doi:10.1074/mcp.M800589-MCP200.

[74] J. Gasparri, L. Speroni, N.S. Chiaramoni, S. del Valle Alonso, Relationship between the adjuvant and cytotoxic effects of the positive charges and polymerization in liposomes, J. Liposome Res. 21 (2011) 124–133. doi:10.3109/08982104.2010.491073.

[75] C. a Fromen, G.R. Robbins, T.W. Shen, M.P. Kai, J.P.Y. Ting, J.M. DeSimone, Controlled analysis of nanoparticle charge on mucosal and systemic antibody responses following pulmonary immunization., Proc. Natl. Acad. Sci. U. S. A. 112 (2015) 488–93. doi:10.1073/pnas.1422923112.

[76] E.B. Lindblad, Aluminium adjuvants—in retrospect and prospect, Vaccine. 22 (2004) 3658–3668. doi:10.1016/j.vaccine.2004.03.032.

[77] D.M. Matthias, J. Robertson, M.M. Garrison, S. Newland, C. Nelson, Freezing temperatures in the vaccine cold chain: A systematic literature review, Vaccine. 25 (2007) 3980–3986. doi:10.1016/j.vaccine.2007.02.052.

Supplementary information

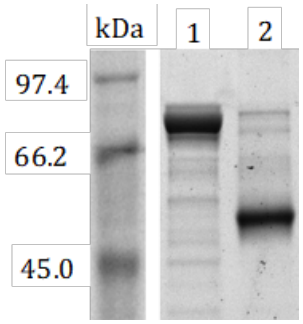

Figure S1. Detergent-mediated refolding of IutA. Polyacrilamide gel showing, Lane 1, IutA after the refolding process in presence of zwitterionic detergents followed by incubation at 95 ºC for 10 min before electrophoresis; Lane 2, IutA after the refolding process without heat treatment before electrophoresis.

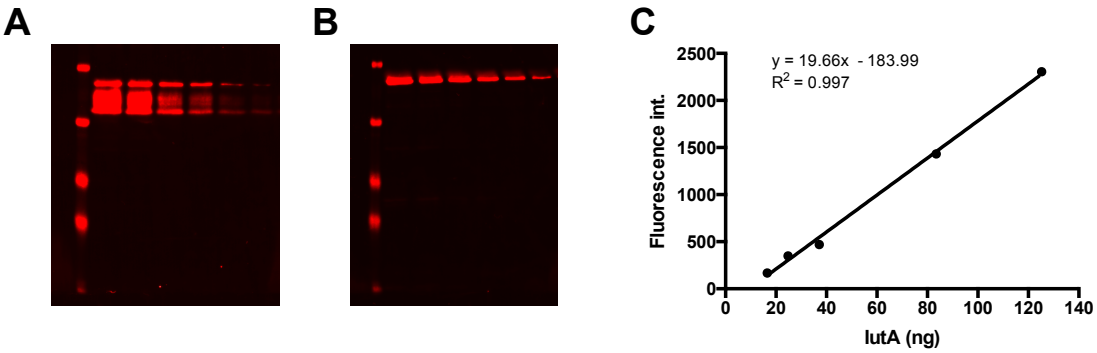

Figure S2. Western-blot for IutA determination. Gels containing standards of different concentrations of the IutA protein after native (A) and denaturing (B) electrophoresis and fluorescent western blotting. Representative calibration curve of the antigen IutA obtained with this technique (C).

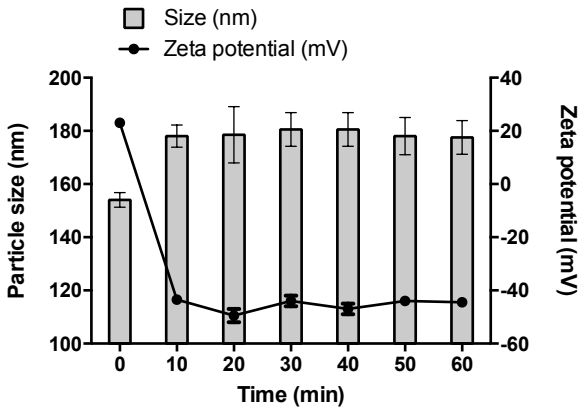

Figure S3. Evolution of the nanocapsules physicochemical properties after dextran sulfate coating. The particle size and zeta potential of bilayer DS/CS/lecithin/vitamin E nanocapsules were monitored after the addition of dextran sulfate (DS) to the monolayer chitosan (CS) nanocapsules (t=0).

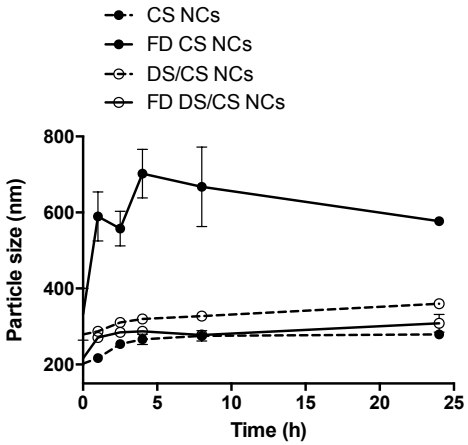

Figure S4. Nanocapsules stability in PBS. Particle size of freeze-dried (FD) and non freeze-dried monolayer and bilayer lecithin/vitamin E NCs was evaluated after incubation in PBS Tween 80® 0.02 % (w/w) at 37 ºC. Results are shown as mean ± SD of 3 replicates.

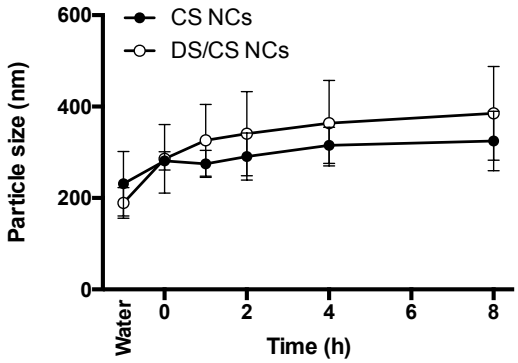

Figure S5. Nanocapsules stability in RPMI. Particle size of monolayer and bilayer lecithin/vitamin E NCs was evaluated after incubation in supplemented RPMI at 37 ºC. Results are shown as mean ± SD of 3 replicates.

Chapter 2

Engineering, on-demand manufacturing, and scaling-up of polymeric nanocapsules

Chapter 2

Engineering, on-demand manufacturing, and scaling-up of polymeric nanocapsules

The results from this chapter have already been published in [1].

Abstract

Polymeric nanocapsules are versatile delivery systems with the capacity to load lipophilic drugs in their oily nucleus and hydrophilic drugs in their polymeric shell. These nanocapsules have been extensively explored in various fields, such as oncology, vaccinology, and infectious diseases, among others. However, despite their reported therapeutic potential, a deeper knowledge of their manufacturing possibilities is still needed to propel their advance from bench to clinic. In this work, our aim was to expand the technological possibilities that the solvent displacement method offers to prepare customized nanocapsules at different scales. More precisely, we have produced nanocapsules with a shell made of one or multiple polymer layers, i.e. chitosan, dextran sulfate, hyaluronate, chondroitin sulfate, and alginate. For specific compositions, we have systematically studied the influence of different formulation parameters (i.e. components concentration in the organic and aqueous phases, and way of mixing these two phases) on the particle size and surface properties of the nanocapsules. The size of the nanocapsules, prepared by the solvent displacement technique, could be modulated in the 50 - 500 nm range. The preparation technique could be translated into a miniaturized HTS-adaptable method that enables the tailor-made fabrication of different prototypes and their subsequent screening. Finally, the production of the nanocapsules was scaled up both in a batch production (up to 1 L), and also using, for the first time, a continuous microfluidics preparation method. The versatility of the properties of these nanocapsules and their fabrication technologies is expected to contribute to their translational development and commercialization.

Graphical abstract

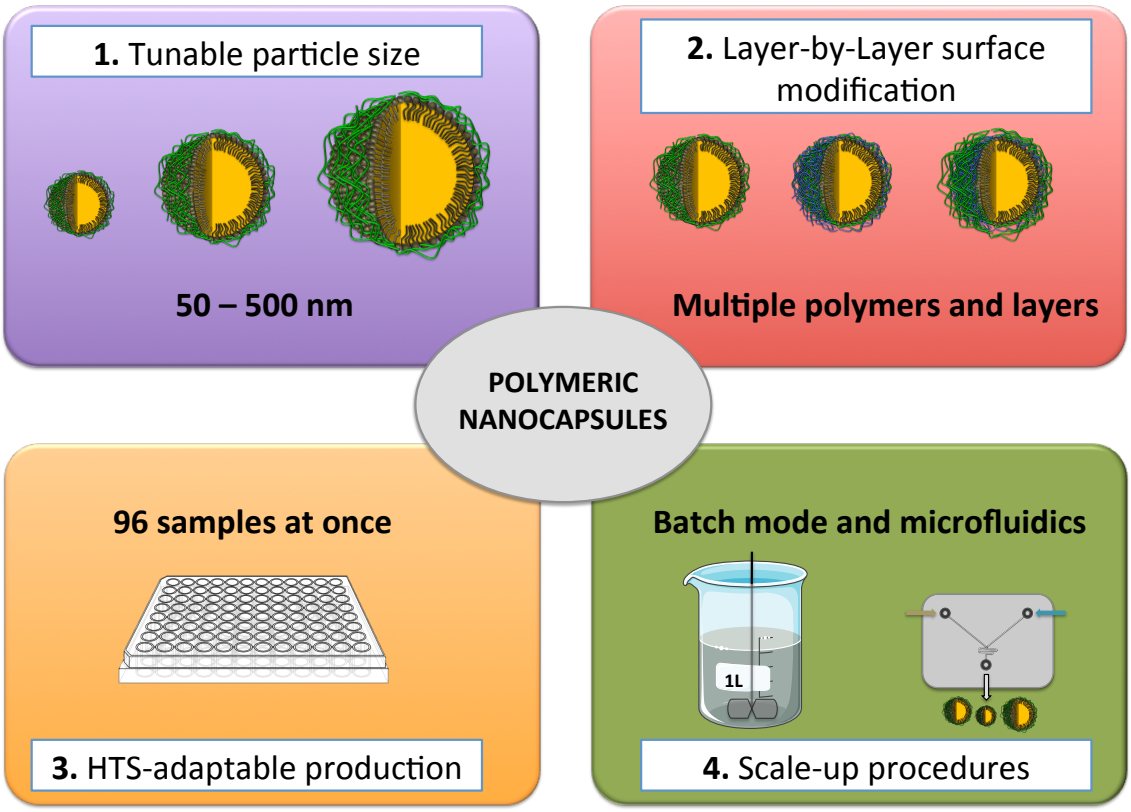

1. Introduction

Nanocapsules (NCs) are nanometric systems with an inner core and an external shell. Depending on their composition, NCs have been named as lipidic NCs, consisting of an oily core stabilized by PEGylated amphiphilic molecules; and polymeric NCs, when the oily nucleus is stabilized by a polymeric shell. Al-Kouri *et al.* described in 1986 the first polymeric NCs, made of polyisobutylcyanoacrylate (PACA) [2]. In 1989, Fessi *et al.* reported the preparation of poly-(D,L-lactide) (PLA) NCs by the solvent displacement technique [3]. Subsequently, our group extended the application of this technology to the production of NCs with a hydrophobic shell, i.e. poly-ε-caprolactone (PCL) NC [4–6], and a variety of hydrophilic polymer shells consisting of chitosan (CS) [7], hyaluronic acid [8], poly-L-asparagine [9], polyglutamic acid [10], polyarginine [11], and protamine [12].

Due to their lipidic core, NCs were, originally, conceived as suitable carriers for lipophilic drugs. However, our lab has expanded this technology to allow NCs to carry hydrosoluble macromolecules, such as proteins [13,14], peptides [15–17], and polynucleotides [11], using them in different therapeutic areas. For example, in the oncology field, we have developed different polymeric NCs containing the cytotoxic drugs, plitidepsin and docetaxel [11,18–22], which were able to prolong the blood circulation time of these drugs and reduce their toxicity. In addition, an important accumulation of the drugs in the lymphatic system was observed. In the vaccinology field, we have successfully associated different types of protein antigens, such as tetanus toxoid [14], influenza antigen [23], recombinant hepatitis B surface antigen [24], and IutA *E. coli* antigen[25] to different NCs. The overall result observed, when using these antigens, was an increased immunogenic response following either, intramuscular o nasal immunization. Finally, we have also found that polymeric NCs can increase the bioavailability of different drugs administered through different mucosal routes. For example, our results have shown the possibility of increasing the corneal penetration of drugs associated to the NCs [7,26]. Similarly, we have found that polymeric NCs led to an enhancement of the systemic absorption of peptide and protein drugs administered by the oral [12,16,17], or nasal[15,27] routes.

Apart from these uses, and due to their versatile nature, NCs have also been loaded with compounds with different activities: anti-inflammatory [28–30], antibacterial [31,32], antifungal [33–36], antioxidant [29,37,38], and immunosuppressant [39], among many others [40].

Besides the solvent displacement technique, two other widely used NCs preparation methods are: high energy-homogenization, and phase inversion temperature [41–44]. In general, it is known that the ratio between the different phases (solvent and non-solvent) [40], the type of oil and polymers used, and their relative concentration[45] may influence the size and surface properties of NCs obtained by solvent displacement. However, the influence of other technological

parameters, such as the way and rate of mixing of the two phases has not been systematically investigated. A better understanding of the impact of these variables would allow a more precise control over the particle size when engineering NCs. On the other hand, a combination of the solvent displacement technique with the layer-by-layer approach offers interesting possibilities to modify the NCs surface properties and, hence, to influence the stability of the NCs and their interaction with the biological systems. Moreover, the nature of the multiple shell polymers may facilitate the loading of different drugs, and their controlled release [25,46,47].

Taking all this into consideration, our goal in this work was to design formulation and technological approaches in order to produce tailor-made polymeric NCs, and to do so according to different scale-down (microliters) and scale-up (litter) techniques. The knowledge generated during these studies will hopefully contribute to a more straightforward translation of polymeric NCs from bench to clinic.

2. Materials and methods

2.1. Materials

2.1.1. Oils

DL-α-tocopherol (Calbiochem®) and squalene (density: 0.855 g/mL) were obtained from Merck Millipore (Darmstadt, Germany). Miglyol 812 was kindly gifted by Cremer Oleo GmbH & Co. KG (Hamburg, Germany).

2.1.2. Surfactants

Deoiled phosphatidylcholine-enriched L-α-lecithin (Epikuron 145V) was a gift from Cargill (Barcelona, Spain). Poloxamer 407 (Pluronic® 127) was obtained from BASF (Ludwigshafen, Germany). D-α-Tocopherol polyethylene glycol 1000 succinate (TPGS) was purchased to Antares Health Products Inc. (Jonesborough, TN, USA). Polyethylene glycol sorbitan monooleate (Tween® 80), hexadecyltrimethylammonium bromide (CTAB), and sodium cholate hydrate were purchased from Sigma-Aldrich (MO, USA).

2.1.3. Polymers

Ultrapure chitosan (CS) hydrochloride salt (Protasan UP CL 113, Mw 125 kDa, deacetylation degree of 86%) was purchased from Novamatrix (Sandvika, Norway). Dextran sulfate sodium salt (Mw 6-8 kDa) was bought to MP Biomedicals (Illkirch, France). For the preparation of the nanocapsules in the 96-well plate pharmaceutical

grade chitosan hydrochloride with a Mw of 47 kDa and a 80-95% deacetylation degree was acquired from Heppe Medical Chitosan GmbH (Halle, Germany), and dextran sulfate sodium salt pharmaceutical grade, with a Mw 8 kDa was purchased from Sigma-Aldrich SAFC® (Madison, Wisconsin, US). Polyarginine (Mw 29 kDa was obtained from PTS (Valencia, Spain). Sodium alginate ULV-L3 (viscosity 10% solution 27 mPa·s) was purchased from Kimica Corporation (Tokyo, Japan). Carboxymethyl-β-glucan sodium salt, obtained from *Saccharomyces cerevisae* and modified with carboxymethyl groups at an 85% substitution degree, was a kind donation from Mibelle AG Biochemistry (Buchs, Switzerland). Sodium hyaluronate (HA) (Mw 57 KDa) was purchased from Lifecore Biomedical (Chaska, MN, USA). Poly-L-glutamic acid sodium salt (Mw 15-50 kDa), and chondroitin-6-sulfate sodium salt were obtained from Sigma-Aldrich (MO, USA).

2.1.4. Others

All other chemicals used were of reagent grade or higher purity.

2.2. Design of experiments

The Statgraphics Centurion XVI.I software was used to design the experiments. Two response variables (size and PDI) and 3 experimental factors: i) rate of addition of the organic phase over the aqueous phase (pouring *vs* injection), ii) volume of the organic phase (ethanol volume from 0.25 to 5 mL), and iii) volume of aqueous phase (from 5 to 15 mL) were specified. A factorial 2^3 design was performed, with 4 centerpoints per block and a random centerpoint placement. The selected design had 12 runs, with 1 sample to be taken each run. The default model was 2-factor interactions with 7 coefficients.

Regarding the experimental procedure, the nanocapsules were prepared by the solvent displacement technique, using a modification of the method previously developed by us.[48] Briefly, an organic phase containing 30 mg of vitamin E and 10 mg of lecithin in the required amount of ethanol was added over an aqueous phase containing 5 mg of chitosan in the required amount of water. After the addition of the organic phase over the aqueous phase by either the pouring or the injecting procedure the sample was stirred at 300 rpm for 10 minutes. Finally, without removing the solvent, size and PDI were measured by DLS.

2.3. Nanocapsules preparation by either pouring or injecting the organic phase over the aqueous phase

The organic phase of these formulations consisted of 0.5 mL solution of the oil (60 mg/mL) and 0.5 mL of the surfactant (20 mg/mL), both in ethanol. In those cases where a co-surfactant was included, 25 µL of an aqueous solution of this component (sodium cholate 200 mg/mL or CTAB 66,67 mg/mL) were added. Finally, the volume was adjusted with pure ethanol up to 2.5 mL. The aqueous phase was prepared dissolving 5 mg of the polymer in 10 mL of ultrapure water, or just water for nanoemulsions. The addition of the organic phase over the aqueous phase was made in two different ways: by pouring one phase over the other, or by injecting the organic phase through a needle (100 Sterican®, Ø 0.60 x 60 mm, 23G x $2^{3/8}$”, Braun, Melsungen, Germany) applying high manual pressure. In both cases, the aqueous phase was maintained under stirring. After ten minutes of agitation at 300 rpm, samples were characterized by DLS.

2.4. Preparation of larger sizes nanocapsules

The solvent displacement technique was readjusted to modulate the nanocapsules particle size. Thus, 0.5 mL of a solution of vitamin E 60 mg/mL and 0.5 mL of a solution of lecithin 20 mg/mL, both in ethanol, were mixed in a test tube. Upon stirring at 700 rpm, an initial volume of water was added with a micropipette. The emulsion was maintained under these conditions for a specific time. After that time, 4 mL of an aqueous solution of chitosan 1.25 mg/mL were added, and the suspension stirred for 10 minutes. Finally, the nanocapsules were characterized by DLS.

2.5. Layer-by-Layer coating of nanocapsules

Different volumes of nanocapsules were placed in glass HPLC vials. To these samples, and under stirring at 300 rpm, different volumes of a second polymer solution were added up to a total of 1 mL, while keeping the ratio polymer layer 1:polymer layer 2 (w/w) constant. The mixture was stirred for 30 minutes and characterized by DLS. Once the ratio of volumes was selected, a fixed volume of nanocapsules was placed in a glass HPLC vial. To this solution, and under stirring at 300 rpm, a fixed volume of a second polymer solution was added up to 1 mL, testing different ratios polymer layer 1:polymer layer 2 (w/w). The mixture was stirred for 30 minutes and then characterized by DLS. This procedure was repeated for each consecutive layer.

2.6. Nanocapsules preparation by a HTS-adaptable procedure

Nanocapsules composed of different materials (see Table S1) were prepared adapting the solvent displacement method to a 96-multiwell plate. Briefly, an organic phase was prepared mixing 50 µL of a 72 mg/mL ethanolic solution of the selected oil, 40 µL of a 37.5 mg/mL ethanolic solution of the surfactant and 10 µL of the co-surfactant solution (if needed). As a co-surfactant an aqueous solution of sodium cholate 30 mg/ml or CTAB 10 mg/mL were used for positive and negatively charged nanocapsules, respectively. For the nanoemulsions and the combinations containing a positive polymer and lecithin, or a positive polymer and squalene, the co-surfactant was not included. The organic phase was poured with a micropipette into the corresponding well of a 96-multiwell plate containing 200 µL of 1.5 mg/mL aqueous solution of the polymer or just water in the case of nanoemulsions. The addition was made under horizontal shaking (300 rpm) and samples were incubated for 10 minutes before characterization by DLS.

2.7. Preparation of nanocapsules with different volumes of ethanol

30 mg of vitamin E and 10 mg of lecithin were dissolved in different volumes of ethanol. This solution was added over 10 mL of an aqueous solution of chitosan (0.5 mg/mL). The addition was done by either pouring the organic phase over the aqueous phase or by injecting it through a needle (100 Sterican®, Ø 0.60 x 60 mm, 23G x $2^{3/8}$”, Braun, Melsungen, Germany) applying high manual pressure. In both cases the aqueous phase was maintained under stirring. After ten minutes of agitation at 300 rpm the excess of ethanol was removed using a rotary evaporator (Büchi, Switzerland) and the volume was adjusted to 5 mL with ultrapure water.

2.8. Batch scale-up of nanocapsules

For a 100 mL batch: an organic solution was prepared mixing 2 mL of lecithin 50 mg/mL, and 0.5 mL of vitamin E 600 mg/mL both in ethanol. The final volume was adjusted with ethanol to 10 mL. This solution was poured into 100 mL of an aqueous solution of chitosan 0.5 mg/mL under agitation at 500 min^{-1}, using a propeller stirrer IKA® RW 20 (Staugen, Germany) (4-bladed, stir diameter 50 mm, shaft diameter 8 mm, shaft length 350 mm).

For a 1L batch: an organic solution containing 1 g of lecithin and 3 g of vitamin E in 100 mL of ethanol was prepared. This solution was poured into 1 L of an aqueous solution of chitosan 0.5 mg/mL under agitation at 500 min^{-1}, using a propeller stirrer IKA® RW 20 (Staugen, Germany) (4-bladed, stir diameter 10 cm, shaft diameter 8 mm, shaft length 350 mm). After 10 min of stirring sample was characterized by DLS.

2.9. Nanocapsules preparation by microfluidics

A NanoAssemblr Benchtop (Precision nanosystems, Vancouver, Canada) system was used to prepare the nanocapsules. The cartridge channels dimensions were 200 μm wide and 79 μm high, with herringbone structures formed by 31 μm high and 50 μm thick in the mixer area. To check the influence of the total flow rate this flow was varied from 2.5 to 15 mL/min. The organic phase was a mixture of 0.5 ml of vitamin E 60 mg/mL and 0.5 mL of lecithin 20 mg/mL, both in ethanol. The aqueous phase was prepared by dissolving 5 mg of chitosan in 9 mL of water. The total concentration in this case was 4.5 mg/mL. To check the influence of the components concentration, a total flow rate of 10 mL/min was selected. While the ratio of the components was constant, their concentration varied from 2.25 mg/ml to 22.50 mg/mL. After the samples were prepared, their particle size and PDI was characterized by DLS.

2.10. Physicochemical characterization

Particle size, polydispersity index, and zeta-potential were measured by photon correlation spectroscopy using a Zetasizer Nano-S (Malvern Instruments; Malvern, UK). If not indicated, analyses were performed at 25 ºC with a detection angle of 173 º in distilled water.

The morphology of the nanocapsules was examined by field emission scanning electron microscopy (FESEM) (ZEISS, ULTRA Plus, Germany). For the analysis, the nanocapsules were diluted in water 1:1000 and mixed with the same volume of 2% (w/v) phosphotungstic acid solution. 1 μL of this mixture was placed on copper grids with carbon films. The grids were left to dry in the open air and then they were washed with 1 mL of water. Once the grids were dried they were observed in the microscope using both STEM and InLens detectors.

2.11. Statistical analysis

Unless otherwise indicated, the experiments were repeated at least three times. The results are presented as mean ± standard deviation. For the comparison of the nanocapsules particles sizes by pouring or injecting the organic phase over the aqueous phase (section 3.1.1) a multiple t test was performed meanwhile for the comparison of the particles sizes in section 3.1.2 a one-way ANOVA was performed. The differences were considered significant for * $p < 0.05$, ** $p < 0.01$ and *** $p < 0.001$ and **** $p < 0.0001$. All the statistical analyses were carried out with Graph- Pad Prism Version 6.0 software.

3. Results and discussion

Polymeric NCs can be easily prepared using the solvent-displacement technique (Fig. S1). The lipids are dissolved in a solvent phase (also referred to as organic phase), which spontaneously forms NCs when poured into a non-solvent phase (usually an aqueous phase). Molecules that were soluble in the solvent phase exceed their thermodynamic solubility limit when the solvent and non-solvent phases mixes, which results in the formation of oily nanodroplets. Simultaneously, the polymer solubilized in the aqueous phase gets adsorbed onto the oily droplets surface due to its electrostatic interaction with surfactants of opposite charge. Finally, the excess of organic solvent, if any, is eliminated by evaporation.

From a technological point of view, it is crucial to have versatile methods that enable the control of the nanosystem's size, as this property is known to influence their interaction with the biological systems [49–51]. Moreover, from a quality control point of view, the accuracy of this parameter is essential for the high scale production and the clinical development of a formulation. Having this in mind, in this work, we studied systematically the influence of the composition and technological parameters on the size of NCs prepared by the solvent displacement technique.

3.1. Modification of the nanocapsules particle size

3.1.1. Preparation of nanocapsules with particle size < 100 nm

The production of nanosystems with particle sizes smaller than 100 nm may be of interest for specific applications. For example, in the area of oncology, a small size is critical for improving the penetration across the tumor [52,53]. Similarly, in vaccinology, the small size may favor the lymphatic drainage [54,55].

Previous studies by our research group showed that the dilution of Miglyol® 812 and lecithin in the organic phase, and the dropwise addition of this phase over an aqueous one lead to a significant decrease in the average size of the obtained oily nanodroplets, from approximately 200 to 100 nm [56]. Based on this result, we adopted an experimental design in which we kept constant the mass and ratio of the NCs components, and we varied the following parameters: i) the volume of the organic phase (ethanol), ii) the volume of the aqueous phase, and iii) the way the organic phase was added over the aqueous phase (pouring *vs* injecting). As a standard NC composition, we chose one previously reported by our group, that consisted on a combination of CS and vitamin E with lecithin as a surfactant [25]. The response surface, presented in Fig. 1, shows that the smallest particle sizes were obtained with the highest volumes of ethanol (5 mL) and water (15 mL), confirming that, as expected, the dilution of lipophilic and hydrophilic components in their respective phases favors the formation of smaller particle sizes. On the other hand, the injection of the organic

phase over the aqueous phase through a needle has a clear impact in the NCs particle size when compared with the technique consisting on just pouring one phase over the other, even when the concentration of the starting solutions remains the same.

The molecular mechanisms behind the nanodispersion achieved by the solvent displacement technique have been attributed to interfacial turbulences between the solvent and non-solvent phases, known as the Marangoni effect, which leads to the separation of the system into two phases [57,58]. Other authors attribute the formation of the nanoprecipitates to the "ouzo effect" [59,60]. In the case of polymeric NCs this means that the local supersaturation of the oil drives a spontaneous nucleation in the form of small oily nanodroplets. The already formed nuclei grow by aggregation or by diffusion of oil molecules from the surroundings. The growth continues until the oil concentration reaches the equilibrium saturation concentration [61]. Experimentally, to obtain small particles sizes we should favor rapid nuclei formation and little or no particle growth. This can be achieved, as indicated in Fig. 1, by decreasing the concentration of the oil, to avoid particle growth, and/or injecting the non-solvent into the solvent phase, which produces turbulences that create multiple small nuclei of oily nanodroplets.

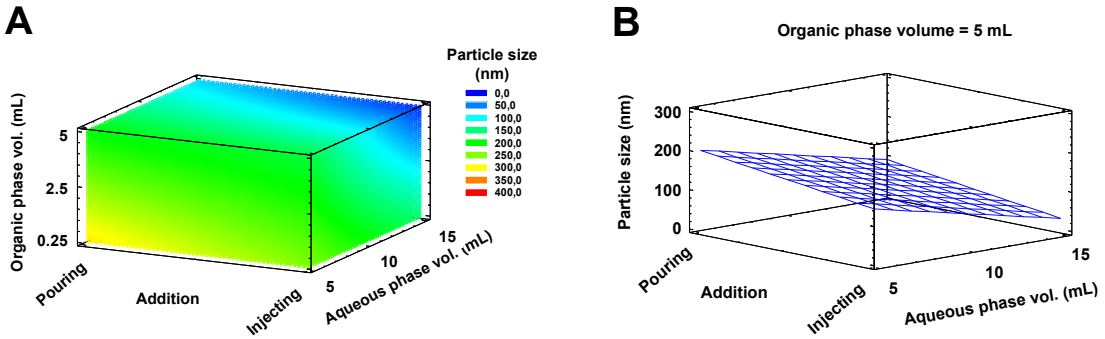

Figure 1. Response surface indicating the impact of different parameters on the nanocapsules particle size. The volumes of both the organic and aqueous phase, and the way the first phase was added over the second (by pouring or injecting through a needle) were varied. The particle size of the resulting nanocapsules was plotted against these three parameters (A). In (B), the influence of the aqueous phase volume and the rate of addition over the particle size were represented. The volume of organic phase was kept constant at 5 mL.

Considering that, with a simple injection of the organic phase over the aqueous phase the NCs particle size could be efficiently reduced, we wanted to know whether this result was composition-dependent. To do so, we tested different combinations of components from a panel of nanosystems (Fig. 2B). Positive and negative nanoemulsions (NEs) and NCs were prepared either by pouring or by injecting the organic phase over the aqueous phase (Fig. 2A), at a fixed concentration of the components.

A considerable reduction in the particle size was observed for all the formulations when using the injection method (between 50 and 115 nm of size

variation) (Fig. 2C). For lecithin/squalene NE (NE 4) this decrease was particularly obvious, with a drop in the particle size from 171 ± 3 to 56 ± 7 nm. This decrease in size was also noticeable when the particles were analyzed by electron microscopy (Fig. 2A). However, it is important to mention that the formulations obtained through injection tended to have slightly higher polydispersity index (PDI), especially for NEs, a fact that reflects the stabilizing property of the polymer shell.

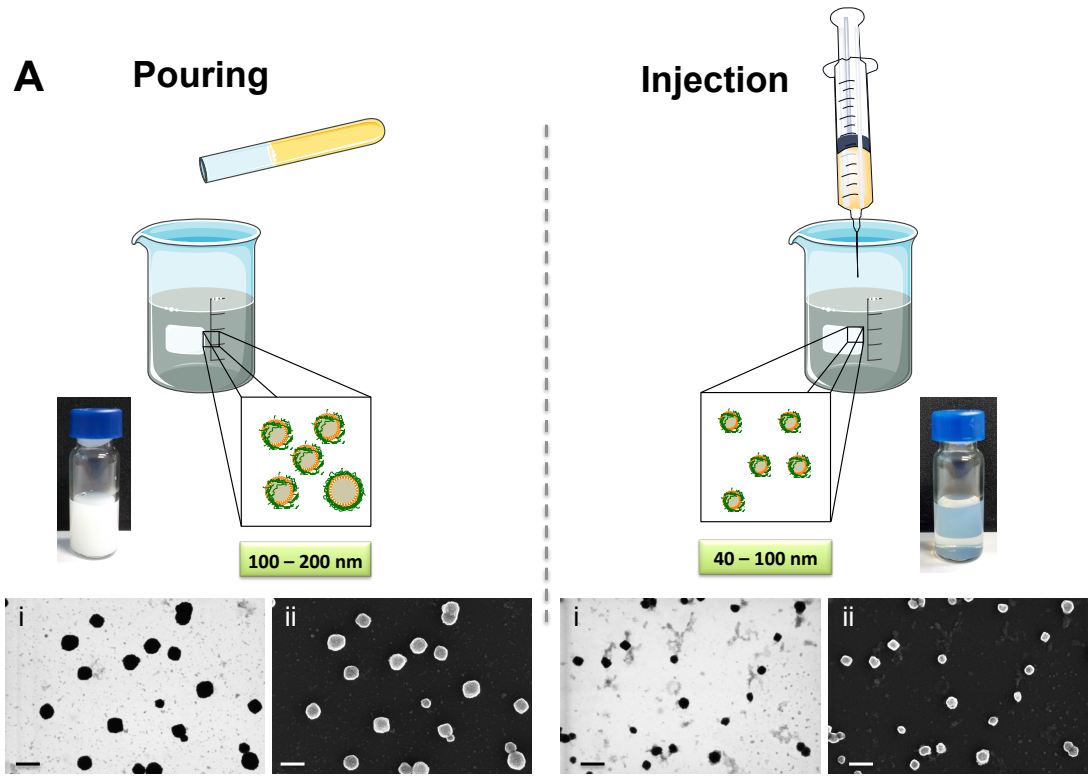

B

Sample	Polymer	Surfactant	Co-surfactant	Oil
NE 1	-	Lecithin	-	Vitamin E
NE 2	-	TPGS	Sodium cholate	Vitamin E
NE 3	-	Tween® 80	-	Vitamin E
NE 4	-	Lecithin	-	Squalene
NE 5	-	Lecithin	-	Miglyol® 812
NE 6	-	Lecithin	CTAB	Vitamin E
NC 1	Alginate	Lecithin	CTAB	Vitamin E
NC 2	Hyaluronate	Lecithin	CTAB	Vitamin E
NC 3	Chitosan	Lecithin	-	Vitamin E
NC 4	Polyarginine	Lecithin	-	Vitamin E

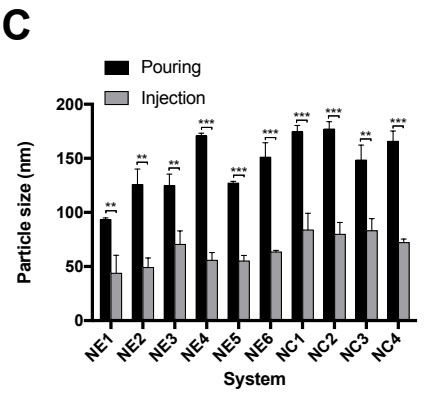

Figure 2. Reduction of the nanocapsules particle size following the injection of the organic phase over the aqueous phase. The injection of the organic phase over the aqueous phase in the preparation of nanoemulsions (NEs) and nanocapsules (NCs) by the solvent displacement technique remarkably reduced the particle size compared with just pouring one phase over the other. FESEM images, using STEM (i) and InLens (ii) detectors, of the CS/lecithin/vitamin E NCs prepared by the two methods. Scale bar 200 nm (A). Different combination of oils, surfactants and polymers were tested to produce NEs and NCs upon pouring or injecting the organic phase over the aqueous phase (B). Differences in the particle size of the NCs and NEs obtained with this modification in the preparation procedure are shown in (C). ** and *** denote significant differences between samples ($P < 0.01$ and $P < 0.001$ respectively).

3.1.2. Preparation of nanocapsules with particle size > 400 nm

In the same way that there is a reduction in the size of the NCs when the concentrations of their components in the organic and the aqueous phases are decreased, when their concentrations are higher there is a substantial increase in the NCs size. However, with the standard preparation protocols, there is a limit beyond which, aggregation and/or free oil are observed. In our hands, particle sizes higher than 400 nm were difficult to achieve with the previously reported procedures. In order to obtain higher particle sizes, we developed a new 2-step method for the preparation of NCs consisting of CS/lecithin/vitamin E. The method is described below.

3.1.2.1. Formation of an unstable nanoemulsion

After the addition of a small volume of water to a concentrated solution of lecithin and vitamin E in ethanol, the spontaneous formation of a dynamic colloidal system was observed. The system evolved during the first two minutes giving rise to an increase in the particle size and, eventually, to the formation of macroscopic oily droplets, probably due to the concentration and the size of the formed nanodroplets.

3.1.2.2. Stabilizing the nanoemulsion

After the addition of water to the organic phase and, prior to the aggregation phase (within the first 2 minutes), the system could be stabilized by adding a second, and larger, volume of water containing CS. By adjusting the elapsed time between the addition of the initial volume of water added to the ethanolic phase and the addition of the polymer solution, it was possible to modulate the NCs particle size in the 200 - 500 nm range.

To evaluate the influence of the initial volume of water added to the organic phase, (step 1, Fig. 3A), the elapsed time between the initial addition of water and the addition of the CS solution was kept constant. The results showed that when the initial volume was small (0.1 – 0.2 mL) compared with the ethanol volume (0.5 mL), the oil remained solubilized in the mixture and only after adding a second and larger volume of polymer aqueous solution (step 2 to 4), NCs with a size in the 250 - 350 nm range were formed. When the initial volume of water increased up to 0.3 - 0.5 mL, we detected the formation of large nanodroplets, which after addition of the CS aqueous solution produced stable NCs with average particle sizes between 400 and 500 nm. Finally, when the initial volume of water in step 1 was ≥ 0.6 mL, the size of the NCs particles was similar to the size of those obtained with the previously reported preparation procedures (around 350 nm). In Fig. 3B, the particle sizes of the obtained NCs by this procedure are compared with the standard protocol of NCs preparation,

with only one addition of water with the polymer dissolved in it over the organic phase.

On the other hand, the elapsed time between the two additions of water is also crucial because of the dynamic nature of the resulting nanoemulsion, as discussed before. For that reason, time is another of the variables that can be used to modulate the final particle size, being a 30 – 60 seconds range appropriate to obtain particles sizes greater than 300 nm (Fig. 3C).

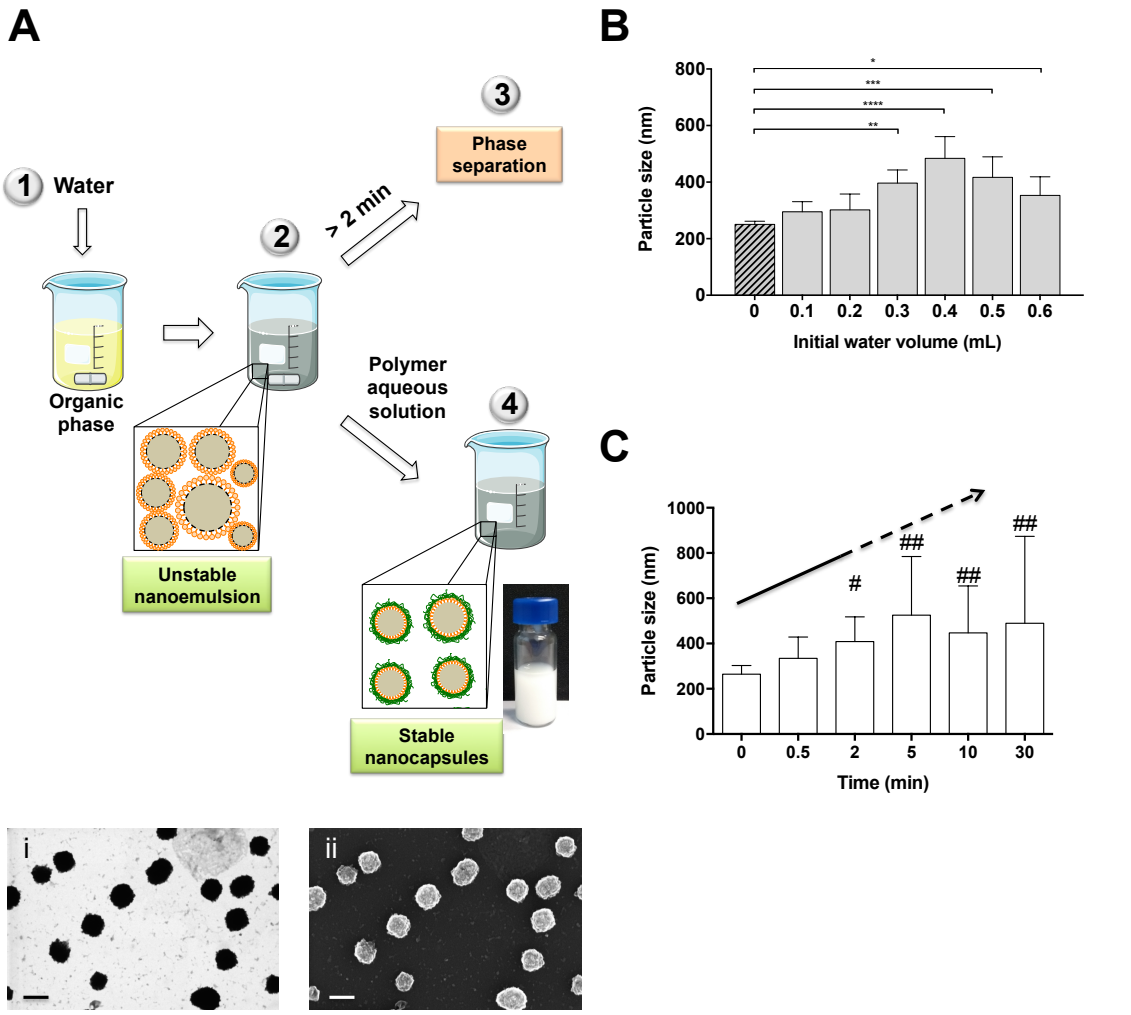

Figure 3. **Preparation method of nanocapsules with particle sizes > 400 nm**. (A) Schematic representation of the procedure to prepare nanocapsules with a particle size > 400 nm. This method consists of 2 steps: in a first step a dynamic nanoemulsion is formed by adding a small volume of water over an organic phase; in a second step, the primary nanoemulsion is diluted with a larger volume of a polymer aqueous solution to form stable nanocapsules. FESEM images, using STEM (i) and InLens (ii) detectors, of the resulting nanocapsules. Scale bar 200 nm (A). Influence of the initial volume of aqueous phase in the final particle size of the nanocapsules (B). Evolution of the nanoemulsion particle size after the initial volume of water was added, showing its dynamic nature (C). # indicates the presence of large particles in some replicates, ## indicates the presence of large particles in all replicates.

3.2. Layer-by-Layer surface modification of nanocapsules

Besides their particle size, the surface charge and composition of the nanosystems are also important parameters that influence their final fate *in vivo* [62,63]. In this regard, the layer-by-layer (LbL) technique allows the modification of the nanosystem's surface and the incorporation of new compounds in the formulation [64–66]. We previously reported the interest in combining the LbL technique with the solvent displacement method, to produce bilayer dextran sulfate (DS)-CS NCs for antigen protection and a controlled delivery [25]. The goal of the following experiments was to assess the applicability of the assembling process to a variety of polymers (bilayer NCs), and to determine the maximum number of layers that can be assembled around the oily cores (multilayer NCs).

3.2.1. Bilayer nanocapsules

CS/lecithin/vitamin E monolayer NCs, used as a model template, were incubated with different ratios of sulfated and carboxylated polyanions: hyaluronate (HA), alginate (Alg) and chondroitin sulfate (ChS) (Fig. 4A). The coating with a bilayer is considered effective when an inversion in the ζ-potential occurs, which indicates that the positive charge of CS has been completely masked by the negative charges of the polyanion. The mass/mass ratio at which this inversion happens is, ultimately, determined by the relative charge of the second polymer. In the case of the tested polymers, the charges per monomer at pH = 7 are: HA (0.5) < Alg (1) = ChS (1). These charges explain why with a small amount of ChS (ratio CS:ChS 1:0.25), an important inversion in the ζ-potential was already observed (Fig. 4B), an inversion similar to the one found with Alg (ratio CS:Alg 1:0.25) (Fig. 4C), and significantly smaller compared with the needed amount of HA (ratio CS:HA 1:1) (Fig. 4D). These results are in agreement with those previously reported for the bilayer CS/DS where a ratio CS:DS of 1:0.1 inverted the ζ-potential [25], due to the high negative charge per monomer of DS (2.3).

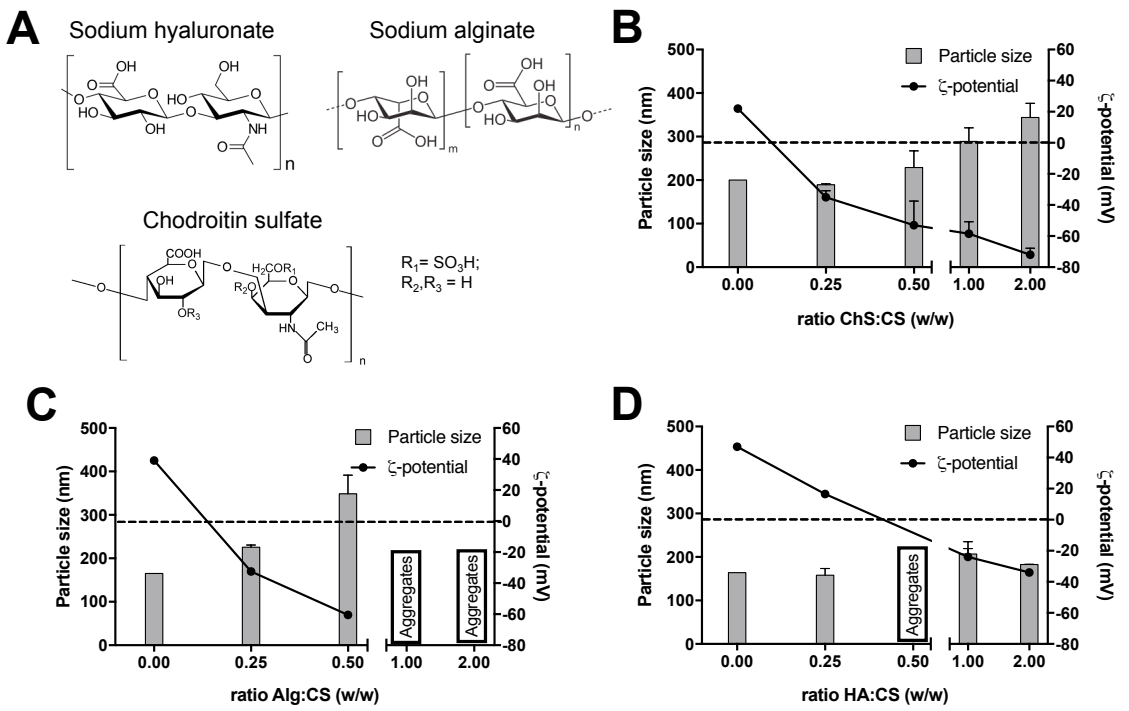

Figure 4. **Screening of the ratio of positive:negative polymer used to prepare bilayer nanocapsules.** (A) Structure of the different polysaccharides used to prepare bilayer nanocapsules of chitosan (CS) and sodium hyaluronate (HA) (B), sodium alginate (Alg) (C), and sodium chondroitin sulfate (ChS) (D), in their acid form. Dot line indicates neutral ζ-potential.

3.2.2. Multilayer nanocapsules

Multilayer NCs can increase the formulation load, and modify or delay the release of drug through the multiple polymeric shells. Based on the bilayer NCs described above, we extended this methodology to the engineering of multilayer NCs. Santos et al. followed a similar approach using a washless LbL polyelectrolyte assembly to encapsulate low solubility drugs [67]. In their case, the deposition of the polymers was assisted by sonication. This could be a problem when working with labile biomolecules. The group of Prof. Benoit, an expert in lipid NCs [68,69], developed multilayer CS/DS NCs (6 layers) using the phase inversion method, which needed a purification step by tangential flow filtration between the deposition of each layer [47]. Our goal was to determine the maximum number of layers that could be built over the oily core, without purification steps, and without high-energy inputs that could denature labile molecules.

In the process of engineering a multilayer NC, the key parameter to be considered was the mass ratio between the polymers with opposite charges (CS and DS). This mass ratio had to be empirically calculated to ensure an efficient coating with the minimum amount possible of free polymer [25]. We did this to avoid the presence of any soluble polymer in the colloidal suspension that could contribute to the formation of undesired subpopulations of polymeric nanocomplexes, through the

interaction with the polymer added to build the next layer. Other important parameter to consider was the ratio between the volume of the NCs suspension and the polymer solution added to form the new layer (Fig. S2). Using this technique, up to 5 layers of polymers could be built over the NE, without the need of purification steps (Fig. 5A-C). The chosen ratio DS:CS was 0.5:1 for the first two layers, for the 3th (CS), 4th (DS) and 5th (CS) layers the ratio polymer:CS-1st-layer was 1:1 with a final ratio $CS_{5th}/DS_{4th}/CS_{3rd}/DS_{2nd}/CS_{1st}$ 1:1:1:05:1. An inversion of the ζ-potential was observed with each new polymer layer added: from highly positive, when the CS was in the external layer, to highly negative, when the DS was the external polymer (Fig. 5D). Moreover, the addition of chitosan increased the particle size when it coated the NE or NCs, as expected. On the contrary, DS slightly reduced the particle size when added over CS NCs, probably because its highly negative charge caused a contraction of the polymers.

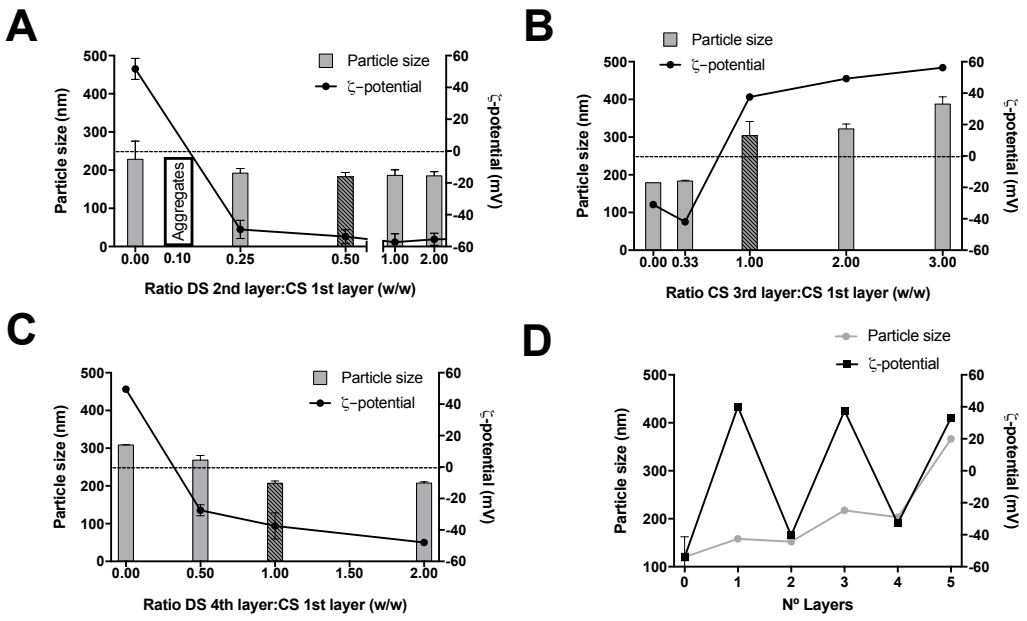

Figure 5. **Screening of different chitosan:dextran sulfate polymer ratios to study the formation of multilayer nanocapsules.** Different chitosan (CS)/ dextran sulfate (DS) ratios were used to form the bilayer nanocapsules (NCs) (A). For the following layers, the mass ratio referred to the first layer of CS was varied to form the 3rd-layer and 4th-layer of NCs (B and C, respectively). The 5th layer was achieved directly using a ratio 1:1 between the CS of the 1st and 5th layers. For the rest of the layers the ratio of election is indicated with the striped bar. Evolution of the particle size and ζ-potential depending on the number of layers is shown in (D).

3.3. Scale-down of the nanocapsules preparation: a HTS-adaptable procedure

The high-throughput screening (HTS), using robotics and automatic processes, has allowed the production and testing of a huge number of compounds in a very short

period of time,[70–72] leading to unprecedented advances in the pharmacology field [73]. Apart from saving time, a HTS-adaptable procedure allows the preparation of multiple nanosystems at once, with different composition or ratio between components, thus multiplying exponentially the possibilities of success when screening nanosystems.

In this work, a 96 multi-well plate was used to prepare NCs in a HTS-adaptable procedure, with a reduced batch volume (300 µL). For this purpose, a selection of 3 different oils, 4 surfactants, 2 co-surfactants, and 7 polymers were combined to produce 12 different NEs and 84 different NCs in the same multi-well plate (Fig. 6). Such an on-demand screening of formulation conditions has never been reported before. Taking into consideration that some of the tested compounds are present in marketed vaccines (such us vitamin E, squalene and Tween® 80) [74], and that most of the polymers have shown immunostimulant properties when associated to antigens in a nanoparticulated form,[75] we envisage that these nanoformulations might have a real potential as nanovaccines once loaded with the required antigen.

Apart from showing the feasibility of miniaturizing the NCs preparation procedure, and thus facilitating a fast screening of multiple nanosystems at the same time, this experiment allowed us to draw some conclusions that are rather specific for the nanosystems described here (Table S1). For example, although most of the nanosystems had a particle size between 150-250 nm, squalene NEs/NCs tended to have larger sizes and, in some cases, a wider distribution (PDI > 0.3). The combination of vitamin E in the oily core and poloxamer 407 (P407) as a surfactant rendered the smallest nanosystems. On the other hand, NCs with carboxymethyl beta glucan (CM-β-glucan) as polymer tended to have larger sizes and higher PDI.

A

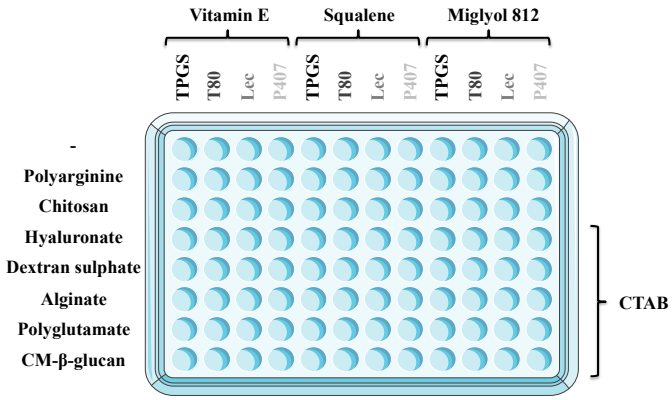

B

	Vitamin E				Squalene				Miglyol 812			
	TPGS	T80	Lec	P407	TPGS	T80	Lec	P407	TPGS	T80	Lec	P407
-	-	-	--	0	-	0	--	-	0	0	--	0
Polyarginine	++	++	++	++	+	0	++	+	0	0	++	++
Chitosan	+	+	++	+	0	0	++	+	+	0	++	+
Hyaluronate	--	--	--	-	--	--	--	--	--	--	-	--
Dextran sulphate	-	-	--	-	--	--	--	--	--	--	--	--
Alginate	--	--	--	--	--	--	--	--	--	--	--	--
Polyglutamate	--	--	--	-	-	-	--	-	-	-	--	--
CM-β-glucan	--	--	--	--	-	--	--	--	-	-	--	--

Particle size		Zeta potential
< 150 nm	++	> +30 mV
150 – 200 nm	+	+10 – +30 mV
200 – 250 nm	0	+10 – -10 mV
250 – 300 nm	-	-10 – -30 mV
> 300 nm	--	< -30 mV

Figure 6. **Miniaturization of the nanocapsules preparation procedure in an adaptable-HTS method.** Different combinations of polymers, oils and surfactants were used to prepare a variety of nanocapsules in a 96-multiwell plate (A). A schematic representation of the particle size and ζ-potential of the resulting nanosystem (B). CM-β-glucan: carboxymethyl-β-glucan, T80: Tween® 80, Lec: lecithin, P407: poloxamer 407, CTAB: cetyl trimethylammonium bromide.

3.4. Scale-up of the nanocapsules preparation

The standard procedure for the preparation of NCs by solvent displacement usually involves an organic phase, frequently ethanol, at half the volume of the water phase;[40] however, our results show that reducing the percentage of ethanol from 33.33% to 4.76%, did not affect the stability of the NCs (Fig. S3). Apart from minimizing/avoiding the use of solvents, another challenge the industry faces when developing a nanoformulation is the scalability of the technology [76]. In this work, we investigated the possibility of scaling-up the formulation both by a discontinuous and a continuous method.

3.4.1. Batch production process

Thomas and his co-workers scaled-up the fabrication of lipid NCs by phase inversion temperature up to approximately 870 mL, by increasing the amount of the components and using special reactors [77]. With this in mind, we scaled-up the production of polymeric NCs by increasing the volume of both phases, while maintaining the concentration of the reagents, and substituting the magnetic stirring for mechanical stirring, which is a more controllable way of mixing larger volumes of liquids. First, we increased the water volume from 10 mL to 100 mL (10x), and then, to 1 L (100x). The results shown in Fig. 7A indicate that the particle size, PDI and ζ-potential were maintained in the scaled-up batches. Interestingly, we also found that when using large volumes of water, the volume of the organic phase could be reduced without any change in the physicochemical properties of the final product. More specifically, for small volumes, we used a 33,33% v/v of ethanol, while for 100 mL and 1 L batches we were able to reduce this percentage to 9%. This result is particularly important as this amount of ethanol could be acceptable in a final product and, therefore, these conditions would preclude the need for solvent evaporation at the end of the process.

3.4.2. Production of nanocapsules by microfluidics

Microfluidics has been applied to the preparation of different types of nanosystems, such as metallic nanoparticles [78], polymer nanoparticles [79], and liposomes [80], among others. However, to the best of our knowledge, it has never been used to produce polymeric NCs. The continuous flow guarantees the same quality over time, and the adjustable parameters allow the control of the final system characteristics. However, this technique still faces some limitations mainly due to the incompatibility of some devices with solvents, high temperatures and sticky materials, and its higher cost when compared with the batch production [81].

We used the CS/vitamin E NCs as a model system to be prepared by this technique. Both phases, organic and aqueous, were pumped into the cartridge while keeping a controllable flow. Inside the cartridge the two phases were mixed, by passing through a mixing area (Fig. 7B). We kept constant the amount of each component to have a final concentration of NCs of 4.5 mg/mL. Then, we varied the flow, observing that, the higher the total flow rate, the smaller the NCs particle size (Fig. 7C). The size decreased from more than 200 nm, at a flow rate of 2.5 mL/min, to around 100 nm at a flow rate of 15 mL/min, which is in agreement with the results shown in *Section 3.1.1,* where we illustrated the influence of the addition rate of the organic phase over the aqueous phase in the NCs particle size. The PDI was maintained at around 0.3, which is slightly higher than the PDI of the batch production. The ζ-potential was highly positive (> +40 mV) in all cases. As expected, the particle size also

increased as the concentration of the phases increased (Fig. 7D). Finally, high concentrations (22.5 mg/mL) also produced polydispersed systems, which lead, finally, to aggregation.

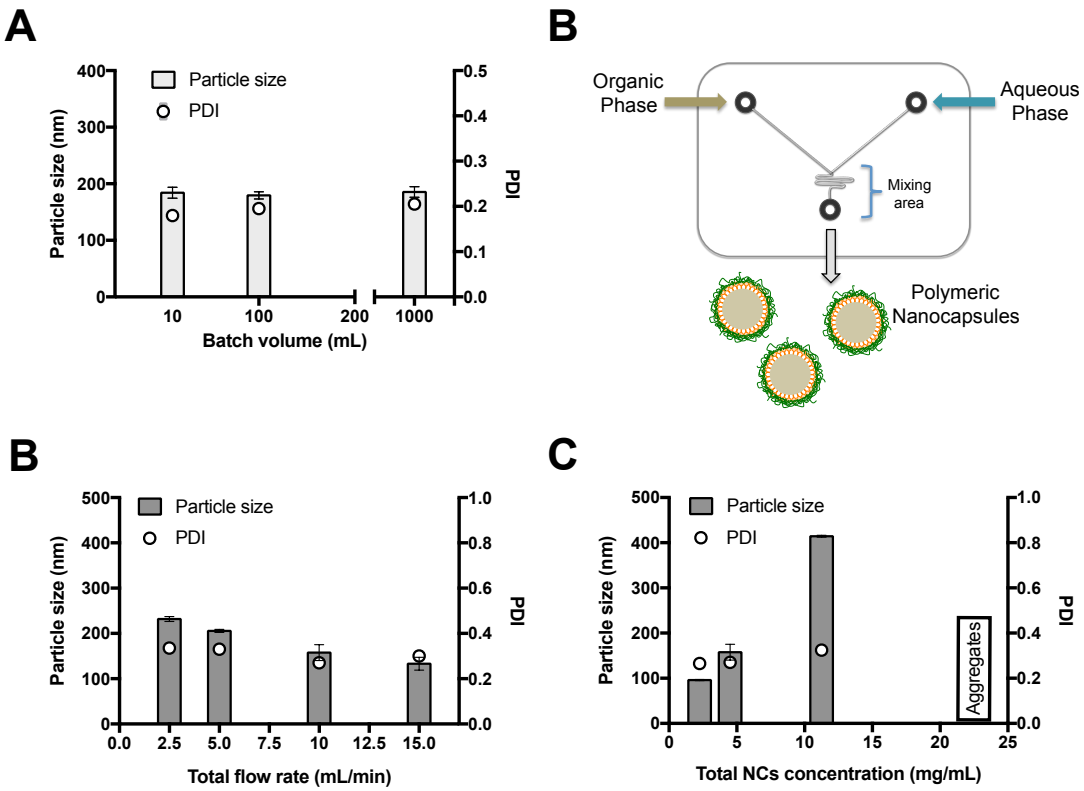

Figure 7: Scale-up of polymeric nanocapsules preparation. Influence of the batch volume in the particle size and PDI of the nanocapsules (NCs) prepared by a discontinuous procedure (A). Schematic representation of the chip used to prepare the polymeric NCs by microfluidics (B). Increasing the flow rate produces a faster mixing of the solvent and non-solvent phases inside the channels, leading to smaller NCs (C). In contrast, increasing the concentration of the components increases the particle sizes of the resulting nanosystems (D).

4. Conclusions

Here we show the versatility of the polymeric NCs delivery platform in terms of physicochemical properties and composition. In particular, NCs with one or multiple polymer layers and different surface charge can be produced with a tunable size ranging from 50 nm to 500 nm, approximately. Importantly, these NCs can be produced by the solvent displacement technique, using a minimum amount of ethanol, thus precluding the need for its elimination. In addition, the preparation can be miniaturized and adapted to a HTS procedure, and scaled-up using a batch mode, or in a continuous process using microfluidics. This information is particularly relevant as a forward step towards scaling the formation of NCs from bench to clinic.

References

[1] J. Crecente-Campo, M.J. Alonso, Engineering, on-demand manufacturing, and scaling-up of polymeric nanocapsules, Bioeng. Transl. Med. (2018). doi:10.1002/btm2.10118.

[2] N. Al Khouri Fallouh, L. Roblot-Treupel, H. Fessi, J.P. Devissaguet, F. Puisieux, Development of a new process for the manufacture of polyisobutylcyanoacrylate nanocapsules, Int. J. Pharm. 28 (1986) 125–132. doi:10.1016/0378-5173(86)90236-X.

[3] H. Lboutounne, J.-F. Chaulet, C. Ploton, F. Falson, F. Pirot, Sustained ex vivo skin antiseptic activity of chlorhexidine in poly(epsilon-caprolactone) nanocapsule encapsulated form and as a digluconate., J. Control. Release. 82 (2002) 319–34. doi:10.1016/0378-5173(89)90281-0.

[4] C. Losa, L. Marchal-Heussler, F. Orallo, J.L. Vila Jato, M.J. Alonso, Design of new formulations for topical ocular administration: polymeric nanocapsules containing metipranolol., Pharm. Res. 10 (1993) 80–7. doi:10.1023/A:1018977130559.

[5] P. Calvo, J.L. Vila-Jato, M.J. Alonso, Comparative in vitro evaluation of several colloidal systems, nanoparticles, nanocapsules, and nanoemulsions, as ocular drug carriers, J. Pharm. Sci. 85 (1996) 530–536. doi:10.1021/js950474+.

[6] P. Calvo, A. Sánchez, J. Martínez, M.I. López, M. Calonge, J.C. Pastor, et al., Polyester Nanocapsules as New Topical Ocular Delivery Systems for Cyclosporin A, Pharm. Res. 13 (1996) 311–315. doi:10.1023/A:1016015803611.

[7] F.A. Oyarzun-Ampuero, M. Garcia-Fuentes, D. Torres, M.J. Alonso, Chitosan-coated lipid nanocarriers for therapeutic applications, J. Drug Deliv. Sci. Technol. 20 (2010) 259–265. doi:10.1016/S1773-2247(10)50043-1.

[8] F.A. Oyarzun-Ampuero, G.R. Rivera-Rodríguez, M.J. Alonso, D. Torres, G.R. Rivera-Rodriguez, M.J. Alonso, et al., Hyaluronan nanocapsules as a new vehicle for intracellular drug delivery, Eur. J. Pharm. Sci. 49 (2013) 483–490. doi:10.1016/j.ejps.2013.05.008.

[9] G.R. Rivera-Rodriguez, G. Lollo, T. Montier, J.P. Benoit, C. Passirani, M.J. Alonso, et al., In vivo evaluation of poly-l-asparagine nanocapsules as carriers for anti-cancer drug delivery, Int. J. Pharm. 458 (2013) 83–89. doi:10.1016/j.ijpharm.2013.09.038.

[10] T. Gonzalo, G. Lollo, M. Garcia-Fuentes, D. Torres, J. Correa, R. Riguera, et al., A new potential nano-oncological therapy based on polyamino acid nanocapsules, J. Control. Release. 169 (2013) 10–16. doi:10.1016/j.jconrel.2013.03.037.

[11] M. V. Lozano, G. Lollo, M. Alonso-Nocelo, J. Brea, A. Vidal, D. Torres, et al., Polyarginine nanocapsules: A new platform for intracellular drug delivery, J. Nanoparticle Res. 15 (2013). doi:10.1007/s11051-013-1515-7.

[12] L.N. Thwala, A. Beloqui, N.S. Csaba, D. González-Touceda, S. Tovar, C. Dieguez, et al., The interaction of protamine nanocapsules with the intestinal epithelium: A mechanistic approach, J. Control. Release. 243 (2016) 109–120. doi:10.1016/j.jconrel.2016.10.002.

[13] S. Vicente, B. Diaz-Freitas, M. Peleteiro, A. Sanchez, D.W. Pascual, A. Gonzalez-Fernandez, et al., A Polymer/Oil Based Nanovaccine as a Single-Dose Immunization Approach, PLoS One. 8 (2013) e62500. doi:10.1371/journal.pone.0062500.

[14] M. Tobio, S.P. Schwendeman, Y. Guo, J. McIver, R. Langer, M.J. Alonso, Improved immunogenicity of a core-coated tetanus toxoid delivery system, Vaccine. 18 (1999) 618–622. doi:10.1016/S0264-410X(99)00313-8.

[15] C. Prego, D. Torres, M.J. Alonso, Chitosan nanocapsules: a new carrier for nasal peptide delivery, J. Drug Deliv. Sci. Technol. 16 (2006) 331–337. doi:10.1016/S1773-2247(06)50061-9.

[16] C. Prego, D. Torres, M.J. Alonso, Chitosan Nanocapsules as Carriers for Oral Peptide Delivery: Effect of Chitosan Molecular Weight and Type of Salt on the In Vitro Behaviour and In Vivo Effectiveness, J. Nanosci. Nanotechnol. 6 (2006) 2921–2928. doi:10.1166/jnn.2006.429.

[17] Z. Niu, E. Tedesco, F. Benetti, A. Mabondzo, I.M. Montagner, I. Marigo, et al., Rational design of polyarginine nanocapsules intended to help peptides overcoming intestinal barriers, J. Control. Release. 263 (2017) 4–17. doi:10.1016/j.jconrel.2017.02.024.

[18] D. Torrecilla, M. V. Lozano, E. Lallana, J.I. Neissa, R. Novoa-Carballal, A. Vidal, et al., Anti-tumor efficacy of chitosan-g-poly(ethylene glycol) nanocapsules containing docetaxel: Anti-TMEFF-2 functionalized nanocapsules vs. non-functionalized nanocapsules, Eur. J. Pharm. Biopharm. 83 (2013) 330–337. doi:10.1016/j.ejpb.2012.10.017.

[19] G.R. Rivera-Rodríguez, M.J. Alonso, D. Torres, Poly-l-asparagine nanocapsules as anticancer drug

delivery vehicles, Eur. J. Pharm. Biopharm. 85 (2013) 481–487. doi:10.1016/j.ejpb.2013.08.001.

[20] G. Lollo, P. Hervella, P. Calvo, P. Aviles, M.J. Guillen, M. Garcia-Fuentes, et al., Enhanced in vivo therapeutic efficacy of plitidepsin-loaded nanocapsules decorated with a new poly-aminoacid-PEG derivative, Int. J. Pharm. 483 (2015) 212–219. doi:10.1016/j.ijpharm.2015.02.028.

[21] E. Borrajo, R. Abellan-Pose, A. Soto, M. Garcia-Fuentes, N. Csaba, M.J. Alonso, et al., Docetaxel-loaded polyglutamic acid-PEG nanocapsules for the treatment of metastatic cancer, J. Control. Release. 238 (2016) 263–271. doi:10.1016/j.jconrel.2016.07.048.

[22] R. Abellan-Pose, M. Rodríguez-Évora, S. Vicente, N. Csaba, C. Évora, M.J. Alonso, et al., Biodistribution of radiolabeled polyglutamic acid and PEG-polyglutamic acid nanocapsules, Eur. J. Pharm. Biopharm. 112 (2017) 155–163. doi:10.1016/j.ejpb.2016.11.015.

[23] J.V. González-Aramundiz, E. Presas, I. Dalmau-Mena, S. Martínez-Pulgarín, C. Alonso, J.M. Escribano, et al., Rational design of protamine nanocapsules as antigen delivery carriers, J. Control. Release. 245 (2017) 62–69. doi:10.1016/j.jconrel.2016.11.012.

[24] S. Vicente, M. Peleteiro, J.V. González-Aramundiz, B. Díaz-Freitas, S. Martínez-Pulgarín, J.I. Neissa, et al., Highly versatile immunostimulating nanocapsules for specific immune potentiation., Nanomedicine (London). 9 (2014) 2273–2289. doi:10.2217/nnm.14.10.

[25] J. Crecente-Campo, S. Lorenzo-Abalde, A. Mora, J. Marzoa, N. Csaba, J. Blanco, et al., Bilayer polymer nanocapsules: a formulation approach for a thermostable and adjuvanted E. coli antigen vaccine, J. Control. Release. Submitted (2018).

[26] M. de la Fuente, M. Raviña, P. Paolicelli, A. Sanchez, B. Seijo, M.J. Alonso, Chitosan-based nanostructures: a delivery platform for ocular therapeutics., Adv. Drug Deliv. Rev. 62 (2010) 100–17. doi:10.1016/j.addr.2009.11.026.

[27] S. Vicente, M. Peleteiro, B. Díaz-Freitas, A. Sanchez, Á. González-Fernández, M.J. Alonso, Co-delivery of viral proteins and a TLR7 agonist from polysaccharide nanocapsules: A needle-free vaccination strategy, J. Control. Release. 172 (2013) 773–781. doi:10.1016/j.jconrel.2013.09.012.

[28] A. Umerska, C.R.A. Mouzouvi, A. Bigot, P. Saulnier, Formulation and nebulization of fluticasone propionate-loaded lipid nanocarriers, Int. J. Pharm. 493 (2015) 224–232. doi:10.1016/j.ijpharm.2015.07.008.

[29] A. Beloqui, P.B. Memvanga, R. Coco, S. Reimondez-Troitiño, M. Alhouayek, G.G. Muccioli, et al., A comparative study of curcumin-loaded lipid-based nanocarriers in the treatment of inflammatory bowel disease, Colloids Surfaces B Biointerfaces. 143 (2016) 327–335. doi:10.1016/j.colsurfb.2016.03.038.

[30] F.S. Poletto, E. Jäger, L. Cruz, A.R. Pohlmann, S.S. Guterres, The effect of polymeric wall on the permeability of drug-loaded nanocapsules, Mater. Sci. Eng. C. 28 (2008) 472–478. doi:10.1016/j.msec.2007.04.015.

[31] Y. Il Jeong, H.S. Na, D.H. Seo, D.G. Kim, H.C. Lee, M.K. Jang, et al., Ciprofloxacin-encapsulated poly(dl-lactide-co-glycolide) nanoparticles and its antibacterial activity, Int. J. Pharm. 352 (2008) 317–323. doi:10.1016/j.ijpharm.2007.11.001.

[32] S. Khoee, M. Yaghoobian, An investigation into the role of surfactants in controlling particle size of polymeric nanocapsules containing penicillin-G in double emulsion, Eur. J. Med. Chem. 44 (2009) 2392–2399. doi:10.1016/j.ejmech.2008.09.045.

[33] S.S. Santos, A. Lorenzoni, N.S. Pegoraro, L.B. Denardi, S.H. Alves, S.R. Schaffazick, et al., Formulation and in vitro evaluation of coconut oil-core cationic nanocapsules intended for vaginal delivery of clotrimazole, Colloids Surfaces B Biointerfaces. 116 (2014) 270–276. doi:10.1016/j.colsurfb.2014.01.011.

[34] A. Ćurić, J.P. Möschwitzer, G. Fricker, Development and characterization of novel highly-loaded itraconazole poly(butyl cyanoacrylate) polymeric nanoparticles, Eur. J. Pharm. Biopharm. 114 (2017) 175–185. doi:10.1016/j.ejpb.2017.01.014.

[35] D.N. de Assis, V.C.F. Mosqueira, J.M.C. Vilela, M.S. Andrade, V.N. Cardoso, Release profiles and morphological characterization by atomic force microscopy and photon correlation spectroscopy of 99mTechnetium-fluconazole nanocapsules, Int. J. Pharm. 349 (2008) 152–160. doi:10.1016/j.ijpharm.2007.08.002.

[36] Z. Zili, S. Sfar, H. Fessi, Preparation and characterization of poly-ε-caprolactone nanoparticles containing griseofulvin, Int. J. Pharm. 294 (2005) 261–267. doi:10.1016/j.ijpharm.2005.01.020.

[37] B. Carletto, J. Berton, T.N. Ferreira, L.F. Dalmolin, K.S. Paludo, R.M. Mainardes, et al., Resveratrol-loaded nanocapsules inhibit murine melanoma tumor growth, Colloids Surfaces B Biointerfaces. 144 (2016) 65–72. doi:10.1016/j.colsurfb.2016.04.001.

[38] S.R. Schaffazick, I.R. Siqueira, A.S. Badejo, D.S. Jornada, A.R. Pohlmann, C.A. Netto, et al., Incorporation in polymeric nanocapsules improves the antioxidant effect of melatonin against lipid peroxidation in mice brain and liver, Eur. J. Pharm. Biopharm. 69 (2008) 64–71. doi:10.1016/j.ejpb.2007.11.010.

[39] T. Nassar, A. Rom, A. Nyska, S. Benita, Novel double coated nanocapsules for intestinal delivery and enhanced oral bioavailability of tacrolimus, a P-gp substrate drug, J. Control. Release. 133 (2009) 77–84. doi:10.1016/j.jconrel.2008.08.021.

[40] C.E.E. Mora-Huertas, H. Fessi, A. Elaissari, Polymer-based nanocapsules for drug delivery, Int. J. Pharm. 385 (2010) 113–142. doi:10.1016/j.ijpharm.2009.10.018.

[41] P. Kothamasu, H. Kanumur, N. Ravur, C. Maddu, R. Parasuramrajam, S. Thangavel, Nanocapsules: the weapons for novel drug delivery systems., Bioimpacts. 2 (2012) 71–81. doi:10.5681/bi.2012.011.

[42] L. Zhao, G. Shen, G. Ma, X. Yan, Engineering and delivery of nanocolloids of hydrophobic drugs, Adv. Colloid Interface Sci. 249 (2017) 308–320. doi:10.1016/j.cis.2017.04.008.

[43] N. Anton, J.P. Benoit, P. Saulnier, Design and production of nanoparticles formulated from nano-emulsion templates-A review, J. Control. Release. 128 (2008) 185–199. doi:10.1016/j.jconrel.2008.02.007.

[44] I. Santalices, A. Gonella, D. Torres, M.J. Alonso, Advances on the formulation of proteins using nanotechnologies, J. Drug Deliv. Sci. Technol. 42 (2017) 155–180. doi:10.1016/j.jddst.2017.06.018.

[45] K. Mäder, W. Mehnert, Solid lipid nanoparticles: production, characterization and applications., Adv. Drug Deliv. Rev. 47 (2001) 165–96. doi:10.1016/S0169-409X(01)00105-3.

[46] J. Szafraniec, A. Błazejczyk, E. Kus, M. Janik, G. Zajac, J. Wietrzyk, et al., Robust oil-core nanocapsules with hyaluronate-based shells as promising nanovehicles for lipophilic compounds, Nanoscale. 9 (2017). doi:10.1039/c7nr05851a.

[47] S. Hirsjärvi, Y. Qiao, A. Royere, J. Bibette, J. Benoit, Layer-by-layer surface modification of lipid nanocapsules, Eur. J. Pharm. Biopharm. 76 (2010) 200–207. doi:10.1016/j.ejpb.2010.07.010.

[48] P. Calvo, C. Remuñán-López, J.L. Vila-Jato, M.J. Alonso, Development of positively charged colloidal drug carriers: Chitosan-coated polyester nanocapsules and submicron-emulsions, Colloid Polym. Sci. 275 (1997) 46–53. doi:10.1007/s003960050050.

[49] U. Bilati, E. Allémann, E. Doelker, Development of a nanoprecipitation method intended for the entrapment of hydrophilic drugs into nanoparticles, Eur. J. Pharm. Sci. 24 (2005) 67–75. doi:10.1016/j.ejps.2004.09.011.

[50] D. Moinard-Chécot, Y. Chevalier, S. Briançon, L. Beney, H. Fessi, Mechanism of nanocapsules formation by the emulsion-diffusion process., J. Colloid Interface Sci. 317 (2008) 458–68. doi:10.1016/j.jcis.2007.09.081.

[51] J.W. Hickey, J.L. Santos, J.M. Williford, H.Q. Mao, Control of polymeric nanoparticle size to improve therapeutic delivery, J. Control. Release. 219 (2015) 535–547. doi:10.1016/j.jconrel.2015.10.006.

[52] L. Tang, X. Yang, Q. Yin, K. Cai, H. Wang, I. Chaudhury, et al., Investigating the optimal size of anticancer nanomedicine, Proc. Natl. Acad. Sci. 111 (2014) 15344–15349. doi:10.1073/pnas.1411499111.

[53] H. Cabral, Y. Matsumoto, K. Mizuno, Q. Chen, M. Murakami, M. Kimura, et al., Accumulation of sub-100 nm polymeric micelles in poorly permeable tumours depends on size, Nat. Nanotechnol. 6 (2011) 815–823. doi:10.1038/nnano.2011.166.

[54] K.T. Gause, A.K. Wheatley, J. Cui, Y. Yan, S.J. Kent, F. Caruso, Immunological Principles Guiding the Rational Design of Particles for Vaccine Delivery, ACS Nano. 11 (2017) 54–68. doi:10.1021/acsnano.6b07343.

[55] D.J. Irvine, M.A. Swartz, G.L. Szeto, Engineering synthetic vaccines using cues from natural immunity, Nat. Mater. 12 (2013) 978–990. doi:10.1038/nmat3775.

[56] R. Abellan-Pose, C. Teijeiro-Valiño, M.J. Santander-Ortega, E. Borrajo, A. Vidal, M. Garcia-Fuentes, et al., Polyaminoacid nanocapsules for drug delivery to the lymphatic system: Effect of the particle size, Int. J. Pharm. 509 (2016) 107–117. doi:10.1016/j.ijpharm.2016.05.034.

[57] D. Quintanar-Guerrero, E. Allémann, H. Fessi, E. Doelker, Preparation techniques and mechanism of formation of biodegradable nanoparticles from preformed polymers, Drug Dev. Ind. Pharm. 24 (1998) 1113–1128. doi:10.3109/03639049809108571.

[58] S. Galindo-rodriguez, E. Alle, H. Fessi, E. Doelker, Physicochemical Parameters Associated with

Nanoparticle Formation in the Salting-out , Nanoprecipitation Methods, Pharm. Res. 21 (2004) 1428–1439. doi:10.1023/B:PHAM.0000036917.75634.be.

[59] F. Ganachaud, J.L. Katz, Nanoparticles and nanocapsules created using the ouzo effect: Spontaneous emulsification as an alternative to ultrasonic and high-shear devices, ChemPhysChem. 6 (2005) 209–216. doi:10.1002/cphc.200400527.

[60] M. Beck-Broichsitter, E. Rytting, T. Lebhardt, X. Wang, T. Kissel, Preparation of nanoparticles by solvent displacement for drug delivery: A shift in the " ouzo region" upon drug loading, Eur. J. Pharm. Sci. 41 (2010) 244–253. doi:10.1016/j.ejps.2010.06.007.

[61] W.S. Saad, R.K. Prud'Homme, Principles of nanoparticle formation by flash nanoprecipitation, Nano Today. 11 (2016) 212–227. doi:10.1016/j.nantod.2016.04.006.

[62] S. Hirsjärvi, S. Dufort, G. Bastiat, P. Saulnier, C. Passirani, J.L. Coll, et al., Surface modification of lipid nanocapsules with polysaccharides: From physicochemical characteristics to in vivo aspects, Acta Biomater. 9 (2013) 6686–6693. doi:10.1016/j.actbio.2013.01.038.

[63] H.X. Wang, Z.Q. Zuo, J.Z. Du, Y.C. Wang, R. Sun, Z.T. Cao, et al., Surface charge critically affects tumor penetration and therapeutic efficacy of cancer nanomedicines, Nano Today. 11 (2016) 133–144. doi:10.1016/j.nantod.2016.04.008.

[64] J. Cui, M.P. Van Koeverden, M. Müllner, K. Kempe, F. Caruso, Emerging methods for the fabrication of polymer capsules, Adv. Colloid Interface Sci. 207 (2014) 14–31. doi:10.1016/j.cis.2013.10.012.

[65] E. Guzmán, A. Mateos-Maroto, M. Ruano, F. Ortega, R.G. Rubio, Layer-by-Layer polyelectrolyte assemblies for encapsulation and release of active compounds, Adv. Colloid Interface Sci. 249 (2017) 290–307. doi:10.1016/j.cis.2017.04.009.

[66] S. Correa, E.C. Dreaden, L. Gu, P.T. Hammond, Engineering nanolayered particles for modular drug delivery, J. Control. Release. 240 (2016) 364–386. doi:10.1016/j.jconrel.2016.01.040.

[67] A.P. Pandey, S.S. Singh, G.B. Patil, P.O. Patil, C.J. Bhavsar, P.K. Deshmukh, Sonication-assisted drug encapsulation in layer-by-layer self-assembled gelatin-poly (styrenesulfonate) polyelectrolyte nanocapsules : process optimization, 405 (2014) 1–12. doi:10.3109/21691401.2014.898646.

[68] B. Heurtault, P. Saulnier, B. Pech, J. Proust, J. Benoit, A Novel Phase Inversion-Based Process for the Preparation of Lipid Nanocarriers, Pharm. Res. 19 (2002) 875–880. doi:10.1023/A:1016121319668.

[69] N.T. Huynh, C. Passirani, P. Saulnier, J.P. Benoit, Lipid nanocapsules: A new platform for nanomedicine, Int. J. Pharm. 379 (2009) 201–209. doi:10.1016/j.ijpharm.2009.04.026.

[70] A.E. Kusi-Appiah, N. Vafai, P.J. Cranfill, M.W. Davidson, S. Lenhert, Lipid multilayer microarrays for in vitro liposomal drug delivery and screening, Biomaterials. 33 (2012) 4187–4194. doi:10.1016/j.biomaterials.2012.02.023.

[71] R. Damoiseaux, S. George, M. Li, S. Pokhrel, Z. Ji, B. France, et al., No time to lose—high throughput screening to assess nanomaterial safety, Nanoscale. 3 (2011) 1345. doi:10.1039/c0nr00618a.

[72] J.L. Fraikin, T. Teesalu, C.M. McKenney, E. Ruoslahti, A.N. Cleland, A high-throughput label-free nanoparticle analyser, Nat. Nanotechnol. 6 (2011) 308–313. doi:10.1038/nnano.2011.24.

[73] R. Macarron, M.N. Banks, D. Bojanic, D.J. Burns, D.A. Cirovic, T. Garyantes, et al., Impact of high-throughput screening in biomedical research, Nat. Rev. Drug Discov. 10 (2011) 188–195. doi:10.1038/nrd3368.

[74] P. Pellegrino, E. Clementi, S. Radice, On vaccine's adjuvants and autoimmunity: Current evidence and future perspectives, Autoimmun. Rev. 14 (2015) 880–888. doi:10.1016/j.autrev.2015.05.014.

[75] A.S. Cordeiro, M.J. Alonso, M. de la Fuente, Nanoengineering of vaccines using natural polysaccharides, Biotechnol. Adv. 33 (2015) 1279–1293. doi:10.1016/j.biotechadv.2015.05.010.

[76] Q. Sun, M. Radosz, Y. Shen, Challenges in design of translational nanocarriers, J. Control. Release. 164 (2012) 156–169. doi:10.1016/j.jconrel.2012.05.042.

[77] O. Thomas, F. Lagarce, Lipid nanocapsules: A nanocarrier suitable for scale-up process, J. Drug Deliv. Sci. Technol. 23 (2013) 555–559. doi:10.1016/S1773-2247(13)50084-0.

[78] P.R. Makgwane, S.S. Ray, Synthesis of Nanomaterials by Continuous-Flow Microfluidics: A Review, J. Nanosci. Nanotechnol. 14 (2014) 1338–1363. doi:10.1166/jnn.2014.9129.

[79] X. Li, X. Jiang, Microfluidics for producing poly (lactic- co -glycolic acid)-based pharmaceutical nanoparticles, Adv. Drug Deliv. Rev. (2017). doi:10.1016/j.addr.2017.12.015.

[80] D. Carugo, E. Bottaro, J. Owen, E. Stride, C. Nastruzzi, Liposome production by microfluidics: Potential and limiting factors, Sci. Rep. 6 (2016) 1–15. doi:10.1038/srep25876.

[81] P.M. Valencia, O.C. Farokhzad, R. Karnik, R. Langer, Microfluidic technologies for accelerating the clinical translation of nanoparticles, Nat. Nanotechnol. 7 (2012) 623–629. doi:10.1038/nnano.2012.168.

Supplementary information

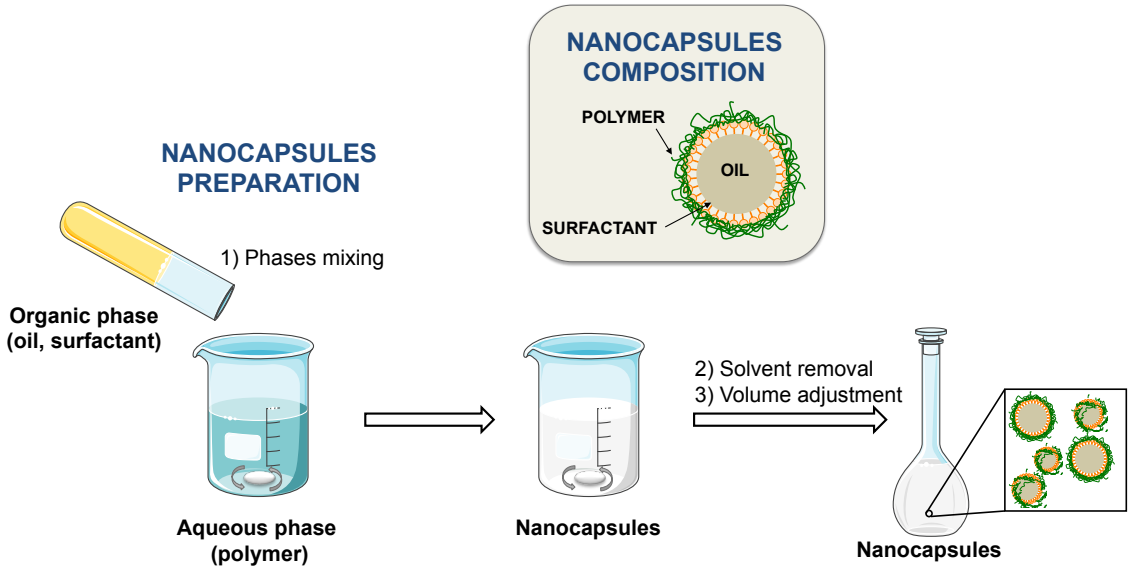

Figure S1. Scheme of nanocapsules composition and of their preparation by the solvent displacement technique.

Table S1. Particle size, polydispersity index (PDI), and ζ-potential of the nanocapsules prepared in a 96 multi-well plate. PArg: polyarginine, CS: Chitosan, HA: hyaluronate, DS: dextran sulphate, Alg: alginate, PGA: polyglutamic acid, CMβG: carboxymethyl-β-glucan, T80: Tween® 80, Lec: lecithin, P407: poloxamer 407. n=1.

	Vitamin E				Squalene				Miglyol 812			
	TPGS	T80	Lec	P407	TPGS	T80	Lec	P407	TPGS	T80	Lec	P407
-	168 nm PDI 0.1 -13 mV	185 nm PDI 0.1 -12 mV	150 nm PDI 0.2 - 55 mV	135 nm PDI 0.1 +5 mV	265 nm PDI 0.3 -14 mV	324 nm PDI 0.3 -9 mV	280 nm PDI 0.3 -59 mV	266 nm PDI 0.2 -15 mV	189 nm PDI 0.1 -2 mV	240 nm PDI 0.2 -1 mV	182 nm PDI 0.2 -46 mV	215 nm PDI 0.3 -10 mV
PArg	201 nm PDI 0.1 +61 mV	253 nm PDI 0.1 +63 mV	218 nm PDI 0.1 +59 mV	178 nm PDI 0.1 +43 mV	308 nm PDI 0.2 +14 mV	370 nm PDI 0.3 +1 mV	257 nm PDI 0.2 +65 mV	253 nm PDI 0.2 +18 mV	192 nm PDI 0.2 +3 mV	234 nm PDI 0.2 +1 mV	188 nm PDI 0.1 +53 mV	230 nm PDI 0.2 +48 mV
CS	193 nm PDI 0.2 +21 mV	262 nm PDI 0.2 +15 mV	210 nm PDI 0.2 +54 mV	163 nm PDI 0.1 +19 mV	281 nm PDI 0.3 -2 mV	391 nm PDI 0.3 +1 mV	273 nm PDI 0.3 +51 mV	255 nm PDI 0.3 +18 mV	195 nm PDI 0.2 +19 mV	440 PDI 0.5 +10 mV	196 nm PDI 0.1 +49 mV	232 nm PDI 0.2 +30 mV
HA	191 nm PDI 0.2 -33 mV	260 nm PDI 0.2 -40 mV	336 nm PDI 0.3 -55 mV	145 nm PDI 0.2 -28 mV	328 nm PDI 0.3 -43 mV	401 nm PDI 0.3 -36 mV	345 nm PDI 0.3 -48 mV	287 nm PDI 0.2 -31 mV	193 nm PDI 0.2 -34 mV	244 nm PDI 0.2 -31 mV	237 nm PDI 0.1 -26 mV	223 nm PDI 0.2 -48 mV
DS	161 nm PDI 0.1 -28 mV	222 nm PDI 0.2 -30 mV	252 nm PDI 0.2 -57 mV	133 nm PDI 0.1 -28 mV	254 nm PDI 0.2 -59 mV	304 nm PDI 0.3 -58 mV	193 nm PDI 0.1 -65 mV	211 nm PDI 0.2 -52 mV	169 nm PDI 0.1 -50 mV	194 nm PDI 0.2 -59 mV	187 nm PDI 0.1 -62 mV	187 nm PDI 0.1 -48 mV
Alg	183 nm PDI 0.1 -35 mV	207 nm PDI 0.2 -39 mV	259 nm PDI 0.2 -59 mV	137 nm PDI 0.2 -35 mV	278 nm PDI 0.3 -34 mV	297 nm PDI 0.2 -41 mV	276 nm PDI 0.2 -40 mV	252 nm PDI 0.2 -54 mV	175 nm PDI 0.1 -33 mV	199 nm PDI 0.1 -42 mV	203 nm PDI 0.2 -52 mV	203 nm PDI 0.2 -48 mV
PGA	187 nm PDI 0.1 -37 mV	221 nm PDI 0.2 -37 mV	280 nm PDI 0.2 -46 mV	134 nm PDI 0.1 -29 mV	255 nm PDI 0.2 -19 mV	287 nm PDI 0.3 -19 mV	230 nm PDI 0.2 -46 mV	259 nm PDI 0.3 -37 mV	177 nm PDI 0.1 -27 mV	217 nm PDI 0.2 -27 mV	217 nm PDI 0.2 -31 mV	204 nm PDI 0.2 -42 nm
CMβG	213 nm PDI 0.3 -36 mV	293 nm PDI 0.3 -45 mV	424 nm PDI 0.2 -60 mV	176 nm PDI 0.2 -51 nm	369 nm PDI 0.4 -19 mV	355 nm PDI 0.4 -31 mV	377 nm PDI 0.3 -58 mV	283 nm PDI 0.3 -54 mV	194 PDI 0.2 -18 mV	281 nm PDI 0.3 -19 mV	335 nm PDI 0.3 -57 mV	260 nm PDI 0.3 -52 mV

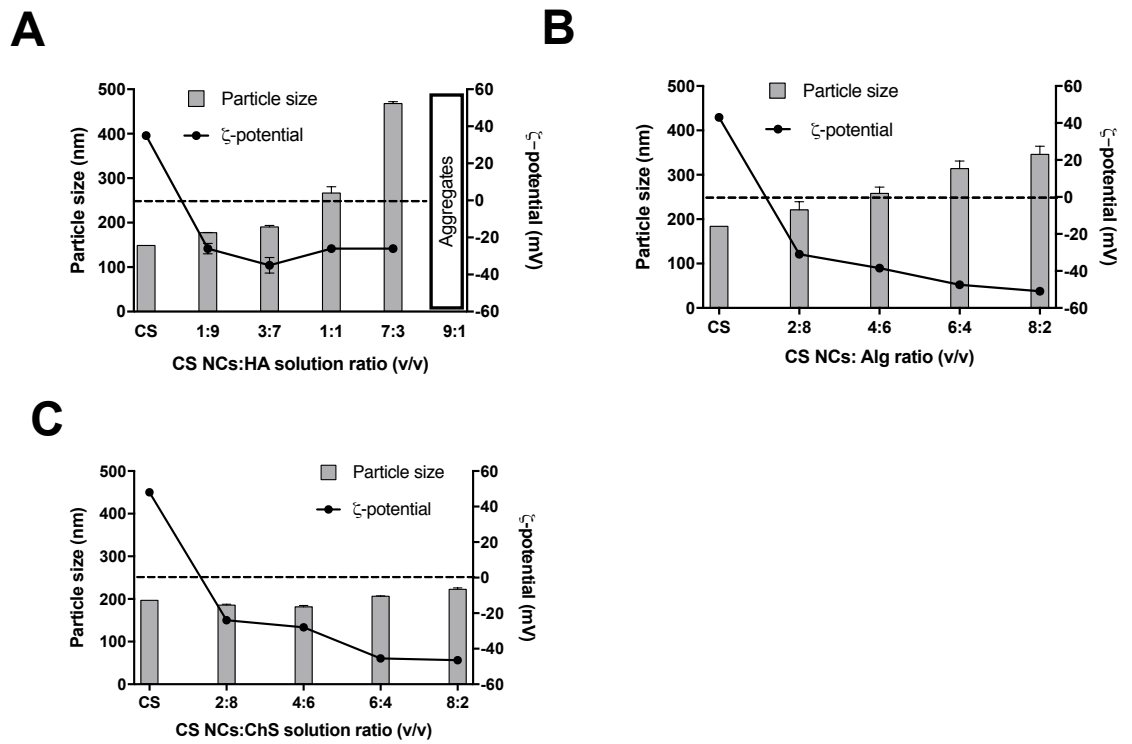

Figure S2. Screening of different polycation:polyanion volume ratios to form bilayer nanocapsules. The ratio between chitosan (CS) and hyaluronate (HA) (B), alginate (Alg) (B) and chondroitin sulphate (ChS) (C) aqueous solutions in monolayer nanocapsules (NCs) was modified to form bilayer NCs.

We investigated the effect of reducing the volume of the ethanolic phase on the particle size of the nanocapsules (NCs), after either pouring or injecting the organic phase over the aqueous phase, using chitosan/lecithin/vitamin E NCs as a model (Fig. S2). Remarkably, after reducing the percentage of ethanol from 33.33 to 4.76%, the NCs were still stable. Furthermore, using the injection method we could reduce the final amount of ethanol up to 2.44%. Other important observation was that there was an optimal volume of solvent, between 2.5–5 mL, that led to a minimum particle size. The PDI was in all cases below 0.3.

Besides, we confirmed the influence of the addition rate of the organic phase over the water phase on the particle size. However, this influence was only significant for volumes < 5 mL (% ethanol < 33.3%). In the case of larger volumes (> 5 mL), since the diffusion of the components is already favored by the high dilution, the application of high pressure did not provide any extra advantage in terms of size reduction.

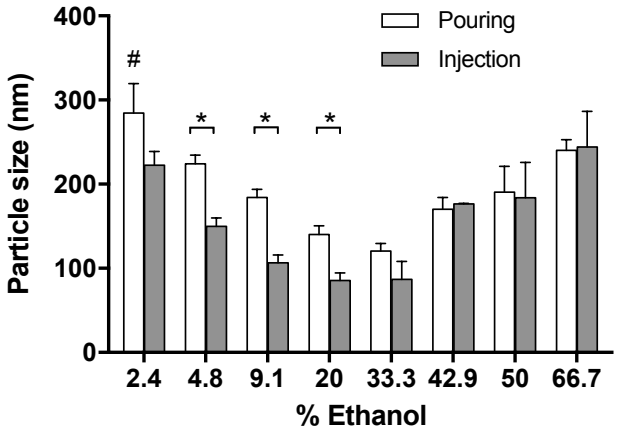

Figure S3: Influence of the percentage of ethanol in the particle size of the nanocapsules. The amount of ethanol in the organic phase, and the way it is added over the aqueous phase (pouring *vs* injecting) have a clear impact on the particle size of the nanocapsules prepared by the solvent displacement technique (A), (* P<0.05; # macroscopic aggregation).

Chapter 3

New inulin nanocapsules: size-dependent interaction with macrophages and biodistribution in zebrafish

Chapter 3

New inulin nanocapsules: size-dependent interaction with macrophages and biodistribution in zebrafish

This work was done in collaboration with Department of Zoology, Genetics & Physical Anthropology (USC) and Centro de Investigaciones Biomédicas (Universidade de Vigo).

Abstract

Despite the reported role of Inulin microparticles as adjuvant carriers for a variety of antigens, recent studies suggest that the reduction of the particle size of these carriers could positively influence their biodistribution and, hence, their adjuvant capacity. Therefore, the main objective of this work was to develop for the first time inulin nanocapsules (NCs) and to evaluate their interaction with macrophages *in vitro* and *in vivo*, using a transgenic zebrafish model (GFP-expressing macrophages). Inulin NCs were prepared with two different sizes, small (≈ 70 nm) and medium (≈ 250 nm) size, and a negative charge, and their biological behavior was evaluated in comparison with that of chitosan NCs, with similar sizes but positively charged. The *in vitro* results showed that both, inulin and chitosan NCs, of smaller size interacted more efficiently with macrophages that the larger ones. Chitosan NCs were slightly more taken-up by macrophages than inulin ones, however they also showed a higher toxicity. Similarly, *in vivo*, inulin NCs resulted significantly less toxic than the chitosan ones. With regard to their biodistribution in zebrafish, after intravenous and intramuscular administration, both, inulin and chitosan NCs, of smaller size (≈ 70 nm) drained and disseminated considerably faster than the medium size ones (≈ 250 and 170 nm, respectively). Besides, after intramuscular injection, chitosan NCs favored the recruitment of macrophages with high clearance after 24 h post injection, especially for the medium size. In contrast, inulin NCs did not show this “pull-off” effect. These results highlight the fact that small changes in the nanometric region may lead to a remarkably different *in vitro* an *in vivo* behavior. Moreover, this report presents inulin NCs as a new nanocarrier for antigens and drugs and emphasizes the interest of zebrafish as a model for studying the biodistribution and interaction of nanoparticles with macrophages.

Graphical abstract

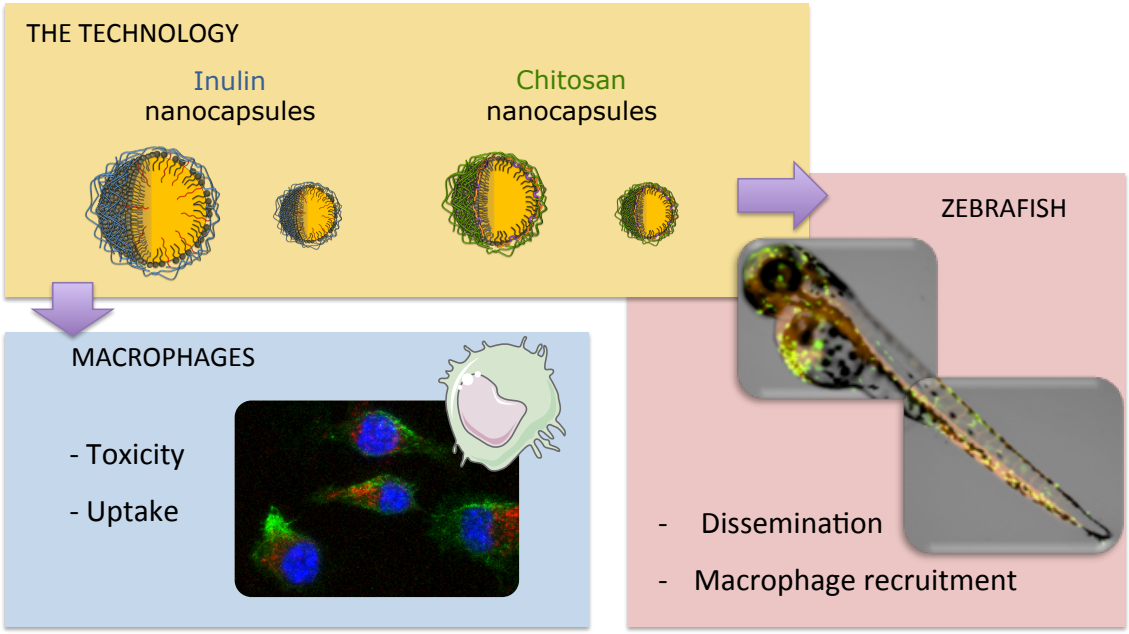

1. Introduction

Polysaccharides are excellent biomaterials for the design of antigen/drug delivery carriers. Apart from their biocompatibility and biodegradability, their versatility in terms of chemical modification and self-assembling make them particularly attractive in the nanopharmaceutical field [1,2]. Among them, inulin (INU), composed by polyfructose chains with a terminal glucose, has been used in the food and pharmaceutical industry as a stabilizing agent, and has a GRAS status [3]. Moreover, INU is being used at the clinical level as a marker to determine the glomerular filtration rate [4]. In vaccination, INU microparticles have been shown to enhance humoral and cellular immune responses against different antigens [5]. In fact, Advax™, composed by delta-INU in microcrystalline form, has been tested in human clinical trials, including hepatitis B, influenza and allergy vaccines [6,7]. In contrast with other adjuvants, INU microparticles have not shown the capacity to activate innate immune receptors such as Dectin-1, TLRs or the inflammasome. Instead, they were found to modulate directly the dendritic cells function, resulting in an improved antigen presentation to T and B cells through a non-inflammatory mechanism [8,9]. The particle size of Advax® (1-2 µm) and its low solubility favor a depot effect when injected either subcutaneously or intramuscularly. Then, macrophages engulf the microparticles and transport them to secondary lymphoid organs [10]. Besides the potential value of this microparticulate vaccine delivery system, recent knowledge in the vaccine field suggests that the direct drainage of the antigen-loaded nanoparticles (NPs) towards the lymphatics might be a better strategy to improve the performance of nanovaccines than the depot mechanism [11–15].

Interestingly, despite the fact that INU has been used for a long time as a pharmaceutical excipient to increase the solubility of lipophilic drugs, and also as an adjuvant, its use as a biomaterial in the design of drug delivery nanocarriers, has been so far hardly explored [16–22]. Therefore, bearing in mind this background information and our extensive experience in the design of polymeric nanocapsules (NCs) [23–28], the first goal of this study was to design and characterize INU NCs. Based on the premise that the nanometric size could increase the dissemination of the particles to the lymphatics [29–31], INU NCs were produced with two different sizes (70 and 250 nm). In addition, chitosan (CS) NCs of similar sizes were also produced for comparative purposes. The two types of nanocarriers were first studied *in vitro* using macrophage cultures, and then, *in vivo,* using the zebrafish (*Danio rerio*) model. This model is particularly suitable as the transparency of the embryos allows the visualization of the interaction of nanosystems with the biological environment [32–35]. Moreover the transgenic lines of zebrafish possessing fluorescently labeled macrophages [36] allow us to investigate, in a living organism, the interaction of nanoparticles with one of the key players of the innate immune system [37].

2. Materials and Methods

2.1. Materials

DL-α-tocopherol (vitamin E) (Calbiochem®) was obtained from Merck Millipore (Billerica, MA, USA), and Pluronic® 127 (Poloxamer 407) from BASF (Ludwigshafen, Germany). Sodium glycocholate was purchased from to Dextra (Reading, UK). Benzethonium chloride was obtained from Spectrum Chemical Mgf. Corp. (NJ, US). Ultrapure chitosan (CS) hydrochloride salt (Mw 42.7 kDa, deacetylation degree of 88%) was purchased from Heppe Medical Chitosan GmbH (Saale, Germany). Inutec® SL1 (25% modified inulin suspension in glycerol) was a kind gift from CreaChem (Tienen, Belgium). DiD (DiIC18(5) oil) was obtained from Invitrogen (CA, USA), and sucrose was purchased from Acofarma (Madrid, Spain).

Materials from *in vitro* studies

Cell culture media RPMI 1640 and the antibiotics (penicillin/streptomycin) were supplied by Gibco (Life Technologies, Scotland). Heat inactivated fetal bovine serum (FBS) and Accutase® were purchased from PAA Laboratories (Austria). CellTiter 96® AQueous One Solution Cell Proliferation Assay used to perform MTS assays was supplied by Promega (USA). Phalloidin conjugated to Alexa Fluor 488 and ProLong®Gold Antifade mounting medium were purchased by Invitrogen (USA).

Materials from *in vivo* studies

Breeding stocks of wild type and Tg(mpeg1:EGFP) (mpeg-individuals present green fluorescent macrophages) adult zebrafish were maintained independently at 28 ºC in a controlled environment of recirculating water system, in a 14h light/10h dark cycle following Westerfield (2007) [38]. Embryos were obtained by massive spawning and maintained at 28 ºC during the experiments. Those discarded were euthanized by tricaine (MS-222) overdose. Care, use and treatment of zebrafish were done following the 3R's principles (replacement, reduction and refinement [39]) and the procedures were approved by competent authorities.

All other chemicals were of reagent grade or high purity. For *in vitro* and *in vivo* experiments endotoxin free water and sterile/autoclaved materials were used.

2.2. Preparation of the nanosystems

2.2.1. Screening of different ratios inulin:vitamin E and incorporation of co-surfactants

Nanocapsules (NCs) were prepared by the solvent displacement technique [40]. Briefly, 60 mg of vitamin E dissolved in 2 mL of ethanol were poured over 4 mL of an aqueous solution of Inutec® SL1 (60 mg, 30 mg and 15 mg, for a ratio Inutec®:vitamin E of 1:1, 0.5:1 and 0.25:1, respectively). The addition was performed under stirring, then

kept for 10 minutes before proceeding with the characterization of the nanosystems. In the case of NCs containing a co-surfactant, sodium glycocholate or benzethonium chloride, the co-surfactant was added to the ethanolic phase as an aqueous solution (50 µL of sodium glycocholate 200 mg/mL or 100 µL of benzethonium chloride 20 mg/mL).

2.2.2. Preparation of medium (M) and small (S) size chitosan (CS) and inulin (INU) nanocapsules

The NCs were prepared following a protocol similar to the one described in section 2.2.1. The vitamin E was dissolved in ethanol (table 1), and the glycocholate was added to this phase as a 200 mg/mL aqueous solution. The polymers (CS or INU) were added to the aqueous phase. For CS NCs, poloxamer 407 was used as a surfactant in the aqueous phase. The different amounts of compounds and solvents used are shown in Table 1. To obtain the S NCs the organic phase was injected into the aqueous phase through a needle (100 Sterican®, Ø 0.60 x 60 mm, 23G x $2^{3/8}$", Braun, Melsungen, Germany), applying high manual pressure (approximate flow 2 mL/s). In both cases, the aqueous phase was maintained under stirring. After 10 minutes of incubation, the excess of ethanol was removed under vacuum using a rotary evaporator (Büchi, Switzerland), and the volume adjusted with ultrapure water.

Table 1. Different composition and preparation parameters of the nanosystems developed in this study

	INU NCs S	**INU NCs M**	**CS NCs S**	**CS NCs M**
Vitamin E (mg)	30	60	30	60
Sodium glycocholate (mg)	5	10	5	10
Ethanol (mL)	2.5	2	2.5	3
Poloxamer 407 (mg)	-	-	5	10
Chitosan (mg)	-	-	5	10
Inutec® SL1 (mg)	15	30	-	-
Water (mL)	10	4	10	4
Stirring speed (rpm)	*900*	*500*	*900*	*500*
Addition	*High pressure (injecting)*	*Low pressure (pouring)*	*High pressure (injecting)*	*Low pressure (pouring)*
Final volume (mL)	*5*	*10*	*5*	*10*
Final concentration (mg/mL)	*10*	*10*	*9*	*9*

2.2.3. DiD-labeled nanocapsules

For *in vitro* and *in vivo* studies, the NCs were labeled with the fluorescent marker DiD. For this purpose, DiD-loaded NCs were obtained by replacing an equivalent amount of ethanol with the required amount of an ethanolic solution of DiD 2.5 mg/mL. The final theoretical concentration of DiD went from 10 to 100 µg/mL, depending on the experiment.

2.3. Physicochemical characterization

Particle size, polydispersity index, and zeta-potential were measured by photon correlation spectroscopy using a Zetasizer Nano-S (Malvern Instruments; Malvern, UK). The S NCs were diluted 1:10, and the M NCs 1:20 in water prior to their measurement. Unless otherwise indicated, analyses were performed at 25 ºC with a detection angle of 173 º in distilled water.

The pH of the formulations was determined with a Sartorius Docu-pH Benchtop Meter (Thermo Fisher Scientific, Waltham, MA, USA).

The morphology of the NCs was examined by different electron microscopy techniques:

- *Transmission electron microscopy (TEM)*

For the negative staining, a 4 µL drop of each sample was left to dry for 15 min on a 200-mesh copper grid covered with a formvar-carbon film. Then, the excess liquid was removed with a filter paper, serially washed with three drops of ultrapure water, followed by incubation during 30 s with a drop of 1% uranyl acetate solution. Afterwards, the excess of uranyl solution was removed with a filter paper and the grids were left to dry before observing them under the microscope (Thermo-Fisher (MA, USA) Tecnai G2 20 Twin) operating at 120 kV.

- *Sample vitrification and Cryo-TEM*

For Cryo-TEM visualization, samples were vitrified by adding 4 µL of the NCs solution over a previously glow-discharged Quantifoil R2/2 200-mesh copper grid and using a Vitrobot Mark IV (Thermo-Fisher (MA, USA)). Grids were observed in the TEM under cryo-conditions, mounting the grids on a GATAN 626 cryo-holder, and operating at 120 kV under low-dose conditions.

- *Wet Scanning Transmission Electron Microscopy (Wet-STEM)*

Liquid samples were visualized under a scanning electron microscope (Thermo-Fisher (MA, USA) Quanta 250 FEG), using a Peltier stage to keep the humidity of the sample around 80-100%, the temperature at 5 ºC, and the pressure inside the chamber at 700-800 Pa. A 3 µL sample drop was applied onto a Quantifoil holey carbon film-covered 200-mesh copper grid, previously mounted on the Peltier stage, and visualized at 20 kV.

2.4. Freeze-drying studies

NCs were freeze-dried in the presence of sucrose as the cryoprotectant at different final concentrations of 10% and 15% (w/v). NCs and the sugar solution were mixed 1:1 (v/v) to 1 mL in a 5 mL freeze-drying glass vials. Vials were quickly frozen at -80 ºC and then transferred to the freeze-drier Genesis 25 ES, VirTis Model-Wizard 2.0 (SP Industries, USA). During the primary drying step, that lasted for 35 h, the temperature increased from -40 to -20 ºC. In the secondary drying step, the temperature of the samples was raised gradually up to +20 ºC.

2.5. Colloidal stability

2.5.1. Stability at storage conditions

Suspensions of the different NCs were stored at 4 ºC for 1 month. At fixed time points their size, PDI, and zeta-potential were determined, as described in section 2.4.

2.5.2 Stability in cell culture media

The stability of the NCs diluted 1:10 in cell culture medium (RPMI supplemented with 10% FBS) at 37 ºC was followed for up to 24 h, and the evolution of particle size and PDI was carefully monitored.

2.5.3 Stability in water for zebrafish

The stability at 37 ºC of the NCs diluted 1:10 in water, and purified by osmosis before performing the zebrafish experiments was followed for up to 4 days. The particle size and PDI were evaluated at fixed time points for the duration of the experiment.

2.6. Cells and culture

RAW 264. 7 (mouse macrophage cell line) were purchased from ATCC (American Type Culture Collection, Middlesex, UK) and cultured in RPMI supplemented with 10% (v/v) of heat-inactivated FBS, 2 mM glutamine, and 100 U/mL of penicillin/streptomycin, at 37 ºC in 5% CO_2 atmosphere. Cells were split every other day using Accutase® (PAA Laboratories, Pasching, Austria) to maintain 70-80% confluent cultures.

2.7. Cell viability studies

In order to study the effect of the NCs on cell viability, xCELLigence® and MTS tests were performed.

The xCELLigence® system provides cell viability data through the measurement of the impedance of cells attached to special wells with gold electrodes at the bottom using the RTCA DP Instrument (Roche Diagnostics, Penzberg, Germany). For these experiments, 2.5×10^4 cells/well were cultured with 200 µL of RPMI supplemented with 10% FBS during 20 h, at 37 ºC and 5% CO2, until they reached the exponential phase. The different prototypes were then added at five different concentrations (25, 50, 100, 200, and 400 µg/mL). Samples containing cells (without NCs) were included as controls. Cell culture media alone and the highest concentration of NCs used in the experiment (without cells), were evaluated to discard a possible interference with the xCELLigence system. The impedance was monitored at 15 min intervals for 72 h.

For the colorimetric MTS assays, the same protocol was followed, but 96 wells plates (Corning, USA) were used in this case. In addition, Triton X-100 10% was included as a positive control when measuring cell death. After 24 h of incubation with NCs, culture medium was removed, cells were rinsed with PBS, and 120 µL of a MTS solution was added. After a 2h incubation period, the conversion of MTS to the soluble formazan product was measured by absorbance at 490 nm. The absorbance obtained, proportional to the number of living cells, was used to calculate cell viability using the following equation:

$$Viability\ (\%) = \frac{(Abs\ cell\&NCs - Abs\ NCs)}{(Abs\ cells - Abs\ RPMI)} \cdot 100$$

where Abs cell&NCs is the absorbance of the cells treated with different amount of NCs; Abs NCs is the absorbance of the NCs diluted in the cell culture medium (without cells); Abs cells is the absorbance of the non-treated cells, and Abs RPMI is the absorbance of the cell culture medium.

2.8. Cellular uptake studies

To evaluate the process of cell internalization of the NCs, RAW 264.7 cells - as a model of phagocytic cell- and DiD labeled NCs were used and the uptake process was followed by flow cytometry and fluorescence microscopy.

For flow cytometry analysis, 5×10^5 RAW 264.7 cells were plated into a 24-well plate (Corning, USA) with 1 mL of complete medium, and cultured for 24 h. At this point, fluorescently labeled NCs were added (50 and 100 µg/mL) and after 1 h of incubation, cells were washed with PBS and detached with Accutase®. After a final

wash with complete medium in order to inactivate Accutase®, the cell suspension was analyzed by flow cytometry (Accuri Cytometers, Ann Arbor, MI, USA).

To evaluate the degree of NC internalization, confocal microscopy studies were performed. For this purpose, 5×10^5 cells were seeded on 24-well plate (Corning, USA), over a glass cover slip (Menzel-Gläser; Braunschweig, Germany). After 24 h, cells were incubated with NCs (50 μg/mL) for 1 h. In this case, cells were then washed and fixed with formaldehyde 4% and the cytoskeleton stained with phalloidin conjugated to Alexa Fluor 488 for 20 min. Finally, the cover-slips with the attached cells were mounted over slides in the presence of ProLong®Gold Antifade mounting medium containing DAPI, and cells were observed and images captured using a Confocal Laser Scanning Microscopy (Leica SP5, Mannheim, Germany).

2.9. *In vivo* studies in zebrafish

Studies in zebrafish embryos were done in Lugo in the animal facilities EA-LU-003 following European and National regulations. The procedures were approved by the ethical committee of the USC and Xunta de Galicia (MR110250).

2.9.1. Toxicity of the nanocapsules in zebrafish embryos

Newly fertilized wild type zebrafish embryos (0 hours post fertilization, hpf) were exposed to 5 different concentration solutions of the four nanosystems under study. Basic design was modified from Test No. 236: *Fish Embryo Toxicity* (FET) *test* (OECD, 2013). 3 replicates of 20 embryos were used per concentration. Mortality was recorded every 24 h until 96 hpf. Following preliminary results, zebrafish embryos were exposed to 15, 30, 60, 120, and 240 μg/mL of CS NCs and 0.5, 1, 2 and 3 mg/mL of INU NCs.

Lethal concentration 50 (LC_{50}) was calculated by Probit regression, whereas *lowest observed effect concentration* (LOEC) and *no observed effect concentration* (NOEC) were calculated by Fisher´s exact test using the software ToxRat Professional v3.2 (ToxRat Solutions GmbH®) software.

2.9.2. Biodistribution of the nanocapsules in zebrafish after intramuscular and intravenous injection

Prior to biodistribution experiments, toxicity tests were carried out by injecting one of the different nanosystems in the circulatory system (caudal vein and Cuvier's duct) or the yolk of 48 hpf wild type embryos.

Afterwards, in order to evaluate the biodistribution of these NCs, microinjections were carried out intramuscularly (in the trunk region) and intravenously (in the Cuvier's duct) in 48 hpf Tg(mpeg1:EGFP) zebrafish embryos. In addition, this experiment also gives information about retention time in the place of injection (especially interesting in intramuscular tests) and NCs-macrophages interaction. NCs visualization was possible because they were DiD-labeled (DU® 730, Beckman Coulter, USA; λ = 646 nm exc. – 655 nm em.). Non-injected embryos were used as blank and embryos injected with DiD-Trehalose solution were used as controls. Embryos were photographed at 0.5, 4, and 24 h post-injection with a fluorescence zoom microscope (Nikon AZ100) and at 2 and 25 h with a confocal microscope (Leica DMi-8).

2.10. Statistical analysis

Unless otherwise indicated, all the experiments were repeated at least 3 times. Results are presented as mean ± standard deviation. The differences were considered significant for * $p < 0.05$, ** $p < 0.01$ and *** $p < 0.001$ and **** $p < 0.0001$. All statistical analyses were carried out with Graph- Pad Prism Version 7.0 software.

3. Results and discussion

Inulin (INU) microparticles have reached the clinical development status as an adjuvant for vaccination [5–7]. Yet, despite this achievement and the extensive use of INU in pharmaceutical industry, this neutral polysaccharide, has barely been explored as drug/antigen delivery nanocarrier. Here, we envisaged that Inutec® SL1, a non-ionic INU-based polymeric surfactant dispersed in glycerin (25%), could be used to make the NCs shell, a versatile nanosystem that we have extensively explored as a vaccine carrier [41–44]. As the oil for the NC's core, we selected vitamin E based on its reported immunoregulatory properties [45]. The *in vitro* and *in vivo* behaviour of this novel nanocarrier was evaluated in a comprehensive manner and compared to that of CS NCs, a nanocarrier originally developed in our laboratory and that has been shown to have the capacity to enhance the immunogenicity of specific antigens [46,47]. *In vitro* experiments were performed in murine macrophages (MΦs), and for the *in vivo* experiments we selected the zebrafish model, with labelled MΦs, being the NCs administered both intramuscularly and intravenously.

3.1. Development and characterization of inulin-based nanosystems

During the first step in the development of INU NCs, we evaluated different ratios of vitamin E:INU to check the particle size and polydispersity of the resulting nanosystems (Fig. S1A). All the ratios of vitamin E:Inutec® tested, from 4:1 to 1:1, rendered low polydisperse nanometric size particles with an almost neutral zeta potential.

The use of a neutral polysaccharide, such as INU, allowed us to specifically modulate the charge of the nanosystem using ionic co-surfactants. Thus, the use of sodium glycocholate, which is negatively charged, allowed us to prepare INU NCs with a negative charge of approximately – 40 mV. On the other hand, by using positively charged benzethonium chloride as a co-surfactant, we obtained NCs with a highly positive surface charge of approximately + 40 mV (Fig. S1B and S1C). After this exploratory study, we selected sodium glycocholate as the co-surfactant for further studies, because negatively charged NCs tend to be less toxic than positive ones, and to have better dissemination capacity in the organism. The resulting INU NCs had a particle size of approximately 250 nm and a negative surface charge (Table 2, INU NCs M).

Different electron microscopy techniques were used to characterize this new nanosystem. The Wet-STEM technique (Fig. 1A), in which the humidity of the sample is maintained to simulate the behavior of the system in the liquid state, revealed particle sizes comprised between 200 nm and 1 μm. Probably, the high concentration required to do the analysis favored partial aggregation of the system. This result was confirmed using cryo-TEM, which retains the conformation of the nanosystem in the liquid state after its vitrification. The images obtained revealed round-shape structures with particle sizes between 150 and 300 nm (Fig. 1B), in agreement with the values obtained by DLS. Finally, using conventional transmission electron microscopy (TEM) (Fig. 1C), it was possible to confirm the globular structure of the NCs. Besides, unlike other types of nanoparticles (NPs), these nanosystems, due to their oily liquid core, show a certain flexibility, which is expected to favor their interaction with the cell membranes.

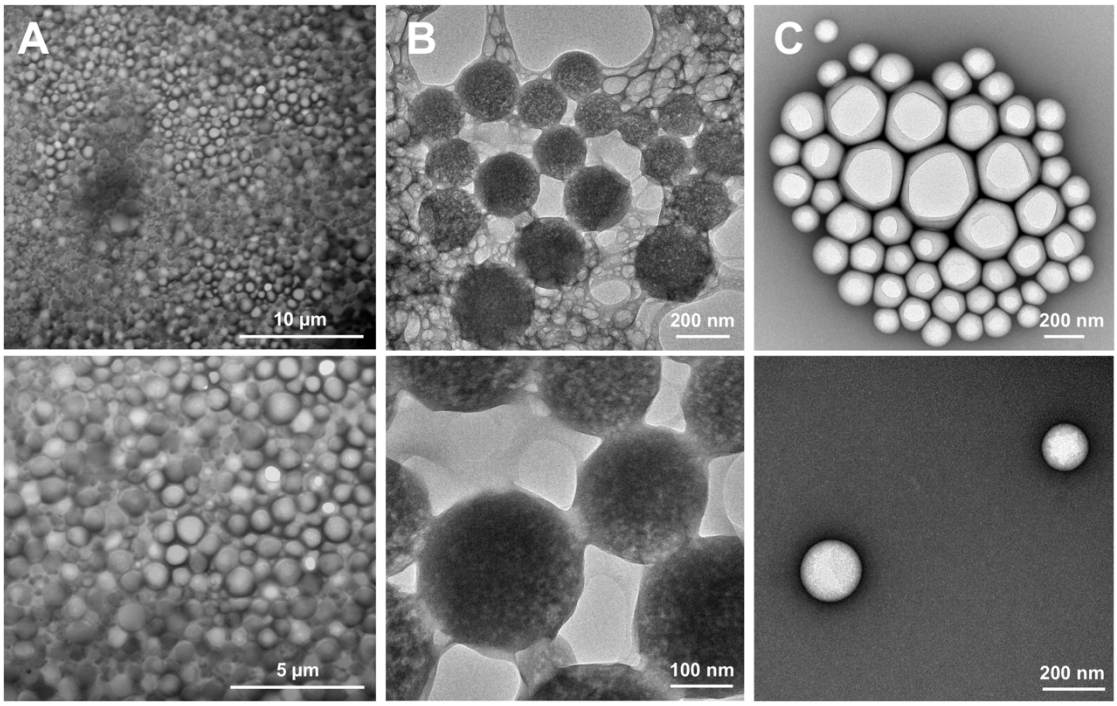

Figure 1. Electron microscopy images of inulin nanocapsules. Different techniques were used to visualize the size and shape of the nanocapsules: Wet-STEM (A), Cryo-TEM (B) and TEM with a negative staining (C).

A second step in the process to develope INU NCs involved the reduction of their size below 100 nm. The rational behind this step is that 100 nm is considered the threshold for an adequate access of nanoparticulated materials to the lymphatics [29,30]. A reduction in the particle size, without a modification of the final concentration of each component, was accomplished by following a modification of the solvent displacement technique, as previously described in chapter 2. As shown in Table 2, the resulting NCs had a size of around 70 nm and a negative surface charge. Based on our previous experience [47–49], and the results obtained in chapter 1, CS NCs, with a vitamin E and glycocholate core, were produced and adopted as a reference of positively charged NCs. The selected NCs exhibited a size of 170 and 70 nm, both with a highly positive surface charge (between + 30 and + 40 mV) (Fig. 2, Table 2).

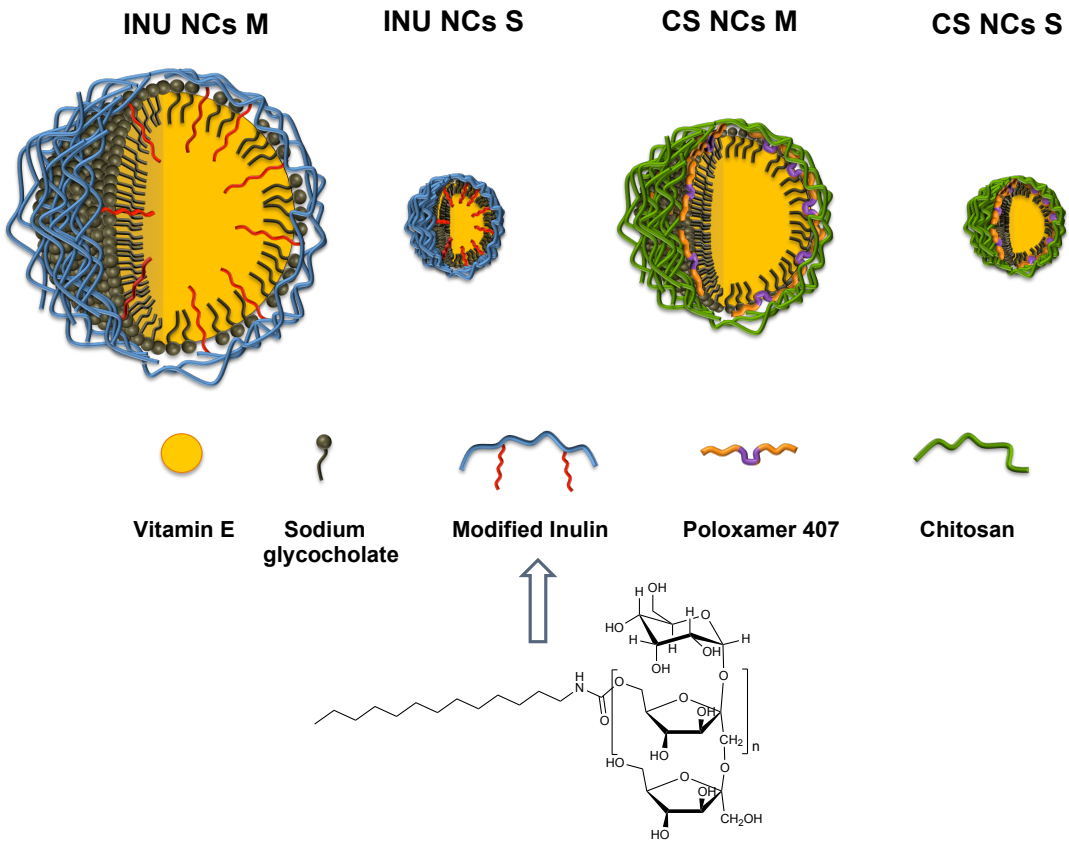

Figure 2. Illustration of the different polymeric nanocapsules (NCs) developed for this work. Inulin nanocapsules (INU NCs) and chitosan nanocapsules (CS NCs): two different particle sizes, small (S < 100 nm) and medium (M > 100 nm) size. The structure of the modified inulin is also shown. The size of the prototypes is drawn to scale.

Table 2: Physicochemical properties of the developed nanosystems. INU: inulin; CS: chitosan; NCs: nanocapsules; S: small size; M: medium size (n ≥ 10)

Nanosystem	Particle size (nm)	PDI	Z-potential (mV)	pH
INU NCs S	69 ± 6	0.18	- 33 ± 8	6.3 ± 0.2
INU NCs M	246 ± 16	0.12	- 25 ± 11	6.4 ± 0.2
CS NCs S	72 ± 5	0.16	+ 37 ± 4	4.5 ± 0.1
CS NCs M	172 ± 11	0.11	+ 34 ± 4	4.5 ± 0.1

When developing a new nanosystem, apart from obtaining the adequate physicochemical properties, a minimum stability, for operational purposes, has to be guaranteed. For this purpose, the colloidal stability of the nanosystems at 4 ºC was monitored over time, being stable at least for 1 month (Fig. 3A). Nevertheless, to guarantee long-term stability, a freeze-drying process was developed. The use of sucrose at a concentration of a 15% allowed the preservation of the particle size, when resuspended in water (Fig. 3B). Similar results were already reported in chapter 1.

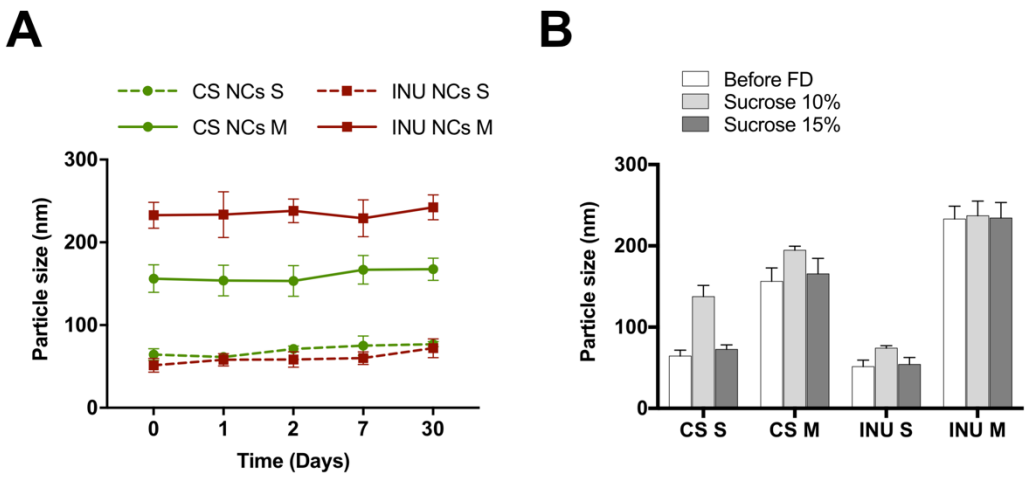

Figure 3. Colloidal stability of the different nanosystems at 4 ºC (A). To guarantee the long-term stability of the systems a freeze-drying process was optimized, using sucrose as cryoprotectant (B). CS: chitosan; INU: inulin; NCs: nanocapsules, S: small size (< 100 nm), M: medium size (> 100 nm); FD: freeze-drying.

3.2. *In vitro* cell studies

The understanding of the capture and subsequent processing of NPs by MΦs is important as it concers their use as carriers for antigens and immunological compounds. In the following sections we describe the *in vitro* interaction of the developed prototypes with MΦs, in terms of toxicity and uptake.

3.2.1. Cytotoxicity of the NCs

Prior to the evaluation of the toxicity, we tested the stability of the systems in cell culture media (Fig. S2). The incubation of the cells with the NCs revealed that both, the polymer in the shell and the particle size influenced the toxicity of the systems (Fig. 4). More precisely, CS NCs showed the highest toxicity, while INU NCs M maintained more viable cells at high concentrations. On the other hand, a size-dependent cytotoxicity tendency was observed; the S prototypes (< 100 nm) were more toxic than their counterparts with larger sizes (M). We speculated that the more pronounced differences on the toxicity of the two INU prototypes, compared to those observed for CS prototypes, could be due to their larger differences in particle size (a difference of 180 nm in the case of INU NCs *vs* 100 nm in the case of CS NCs). The results were obtained using two different methods, MTS (Fig. 4A), that measures the metabolic activity, and xCELLigence® test (Fig. 4B-F), that measures the impedance caused by cell growth. Starting at NCs concentrations higher than 200 μg/mL there is a reduction on the MΦs viability for all prototypes, expect for INU NCs M, which presented low toxicity up to 400 μg/mL. These values are in agreement with previously reported data for CS [43], including those shown in chapter 1, and protamine [50] NCs.

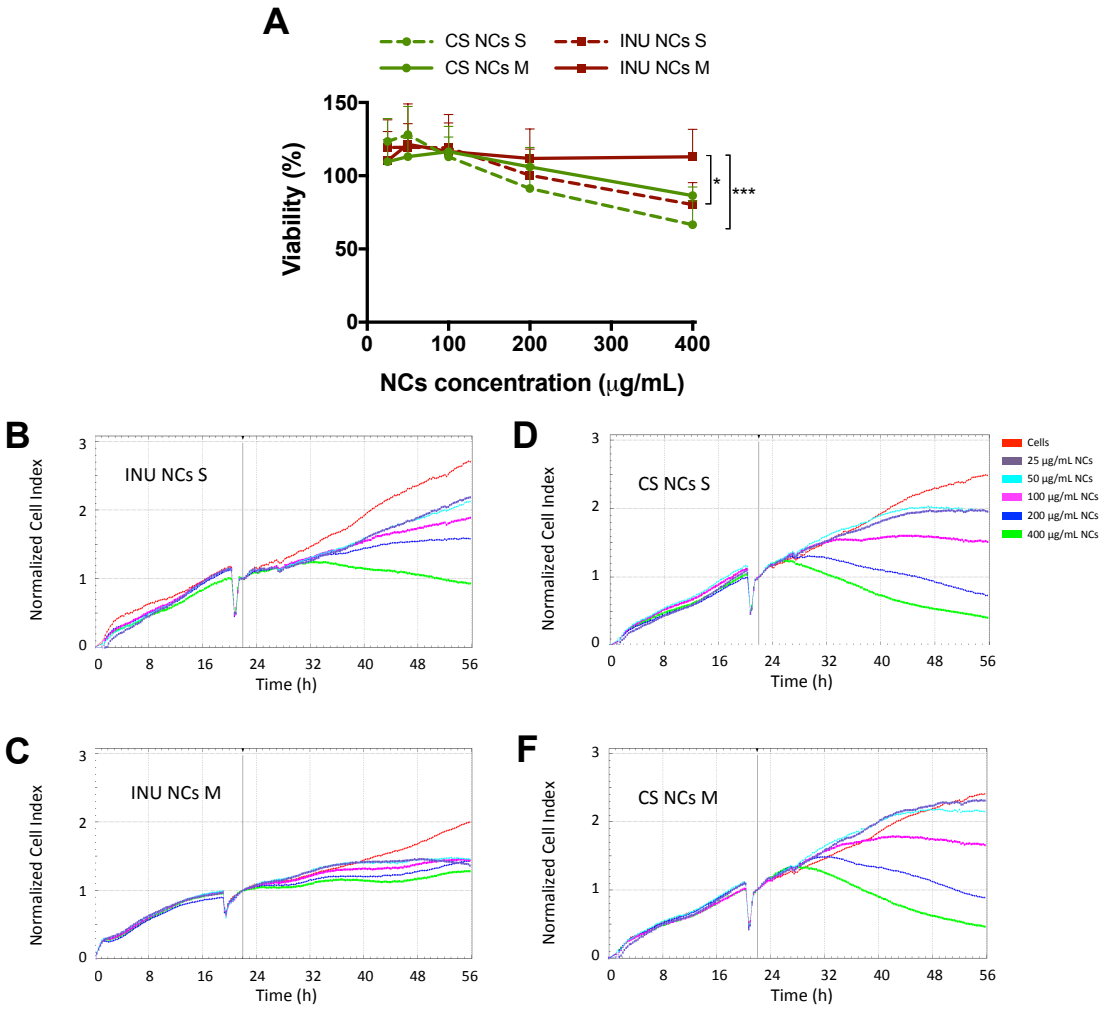

Figure 4. *In vitro* cytotoxicity of the different nanosystems. Inulin (INU) and chitosan (CS) nanocapsules (NCs) in two different sizes: small (S < 100 nm) and medium (M > 100 nm). The toxicity was evaluated in murine macrophages RAW 264.7 by MTS (A) and by xCELLigence® (from B to E) (red color corresponds to untreated cells). For the statistical analysis, the area under the curve for each nanosystem was calculated and analyzed using a One-way ANOVA followed by a Tukey test. Significance levels * $p < 0.05$ and *** $p < 0.001$.

3.2.2. Interaction of the nanocapsules with macrophages

In order to determine if the toxicity was quantitatively related to the cellular interaction, MΦs were analyzed by flow cytometry after their incubation with DiD-labeled nanosystems at a non-toxic dose. The incorporation of DiD did not alter the particle size of the NCs (Fig. S3). Flow cytometry analyses indicated that the toxicity results correlate with the fact that small sizes and positively charged NCs interacted in a greater extent with MΦs (Fig. 5A-C). In fact, at the dose of 50 μg/mL almost all MΦs were DiD+ after incubation with both CS and INU NCs of small size (S). On the contrary, with medium size particles, a dose of 100 μg/mL of INU NCs was necessary in order to achieve a significant interaction with MΦs (60%) (Fig. 5A). On the other hand, the

results of the mean fluorescence intensity (Fig. 5B) indicate that CS NCs exhibited a higher degree of interaction than INU NCs. In addition, for both types of NCs, a decrease in the particle size resulted in a greater interaction with MΦs. This behavior was also observed by confocal microscopy (Fig. 5D).

The greater interaction observed with positively charged NCs is in agreement with previously reported data [51–53]. This result is explained by a stronger interaction between the negative surface of MΦs with the positive particles. On the other hand, the literature reports have been sometimes contradictory regarding the contribution of the particle size. For instance, the uptake of CS NPs by murine MΦs was found to be slightly higher for 300 nm than for 150 nm particles [52]. In the same study, 500 nm carboxymethylchitosan NPs (negatively charged) were phagocytized slightly better (40% *vs* 30% uptake percentage) than their 150 nm counterparts. For PLGA NPs, a size-dependent uptake was found in the range 200 – 1000 nm, with bigger NPs being internalized at a higher degree [54]. However, this difference was not observed with lipid NCs of very small sizes (25, 50, and 100 nm), where internalization was similar irrespective of the size [55]. On the other hand, other authors have reported that the maximal uptake of polypyrrole NPs [56] and PVP-coated iron oxide NPs [57] was around 10-100 nm. Overall, it maybe be concluded that not only the particle size but also the composition of the NPs and probably other properties, i.e. the shape and elasticity/rigidity, may influence their interaction with MΦs and, therefore, a general rule in terms of size threshold for MΦs interaction is difficult to establish.

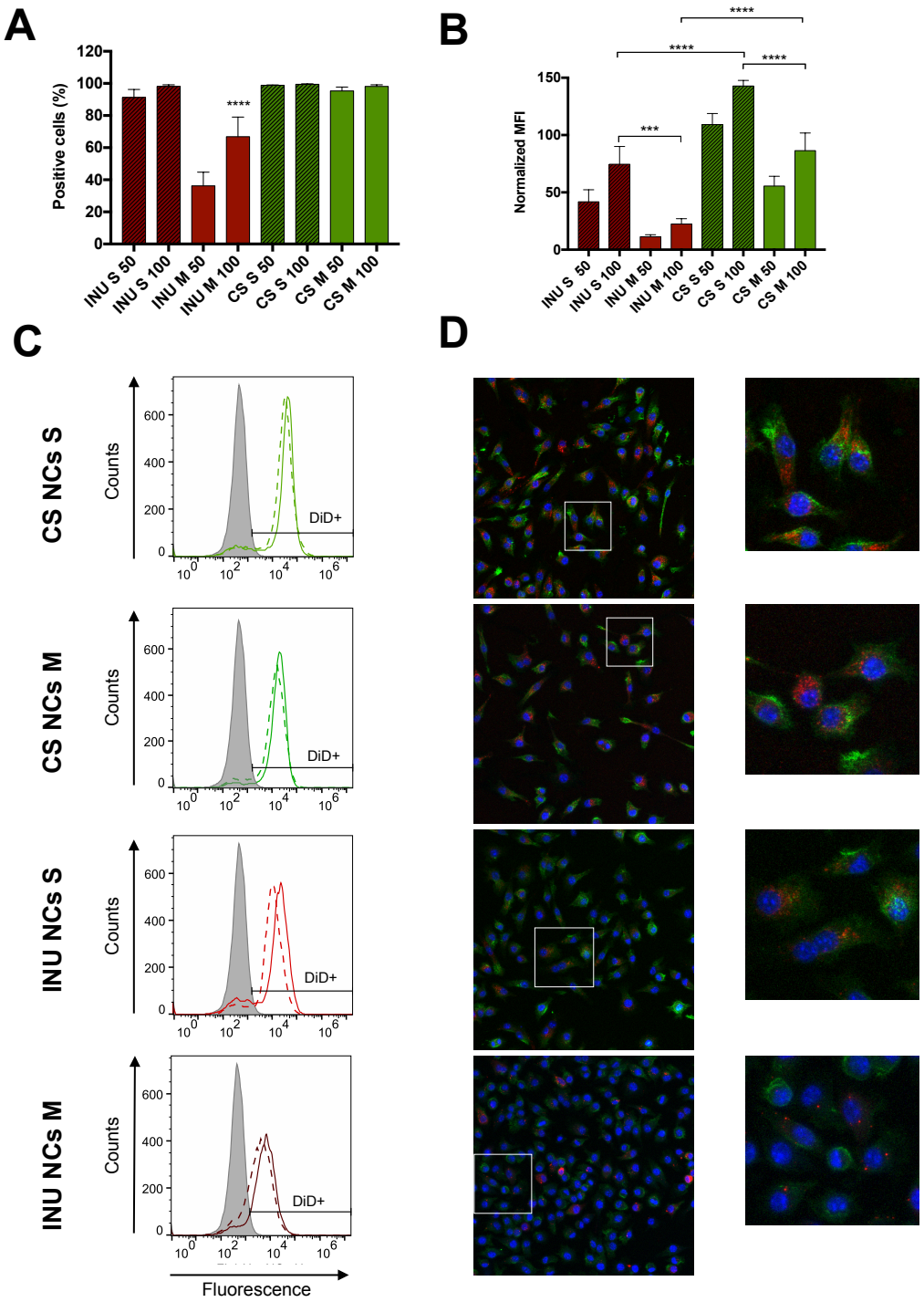

Figure 5. Interaction of different labeled nanosystems with macrophages. Nanocapsules (NCs), at a concentration of 50 and 100 µg/mL (indicated in the X axis) were incubated with RAW macrophages and the interaction analyzed in terms of percentage of positive cells (A) and normalized mean fluorescence intensity, compared with the cellular autofluorescence (B). Representative flow cytometry histograms showing the interaction of the nanosystems at 50 µg/mL after 1 h incubation with macrophages (C). Confocal microscopy images of macrophages incubated with the different nanosystems (50 µg/mL for 1 h). Inulin nanocapsules (INU NCs) and chitosan nanocapsules (CS NCs) of two different sizes, small (S < 100 nm) and medium (M > 100 nm). Red channel: DiD-labeled NCs; blue channel: cell nuclei; green channel: cytoskeleton. One-way ANOVA followed by a Tukey test were applied for the statistical analysis (only for 100 µg/mL, and comparing S *vs* M and CS *vs* INU); significance level *** $p \leq 0.001$ and **** $p \leq 0.0001$.

3.3. *In vivo* studies in zebrafish

3.3.1. Toxicity of the NCs in zebrafish embryos

In vitro studies merely reflect the interaction of NPs with isolated cells but the *in vivo* scenario is much more complex, being the biodistribution of the nanosystems, in most cases, a limiting factor for their adequate performance in the target site. Based on previous studies from our group and others [35,58–60], we chose the zebrafish model to assess the toxicity, the diffusion through biological media and the access to MΦs.

3.3.1.1. Toxicity of the NCs by incubation

Our first step was to ensure the stability of the nanosystems in the water where zebrafish embryos were growing (Fig. S2B). After the NCs incubation with the zebrafish embryos, the results showed that, as expected, the toxicity values of CS NCs prototypes were notoriously higher than those of INU NCs (Fig. 6A). More precisely, the calculated LC_{50} was 68 and 63 μg/mL for CS NCs S and M, respectively. At the lowest concentrations (15 and 30 μg/mL), the toxicity of CS NCs S was slightly higher than that of the CS NCs M (LOEC and NOEC values of 15 and ≤ 15 μg/mL respectively for CS NCs S; and 30 and 15 μg/mL for CS NCs M). These results were in agreement with the ones observed in the *in vitro* studies. On the other hand, the toxicity observed for CS NCs was in the range of previously reported values for CS NPs in zebrafish embryos [61,62]. The mechanisms behind this toxicity seem to be the oxidative stress caused by the reactive oxygen species produced by CS. On the other hand, the toxicity of INU NCs was remarkably lower than that of CS NCs, showing high viability (> 80%) even at doses as high as 3 mg/mL. This could be attributed in part to the negative surface charge of these NCs which would be in agreement with the low toxicity we have previously observed for hyaluronic acid NCs [33]. Similarly, different negatively charged NPs, such as Au NPs, Ag NPs and PAMAM dendrimers, presented significantly less toxicity in zebrafish than their positive counterparts [35].

3.3.1.1. Toxicity of the injected NCs

Prior to performing the biodistribution studies, we studied the toxicity of the NCs upon injection in 48 hpf zebrafish. About 5 nL of each nanosystem were injected in either the yolk sac, the caudal vein, or the ventral area of Cuvier's duct (anterior to the heart). Our results (Tables S1, S2 and S3) indicated that the dose was non-toxic when injected in all locations, except on the caudal vein (Fig. 6B), where the injection of CS NCs caused some toxicity (75% survival for CS NCs S, and 90 % survival for CS NCs M).

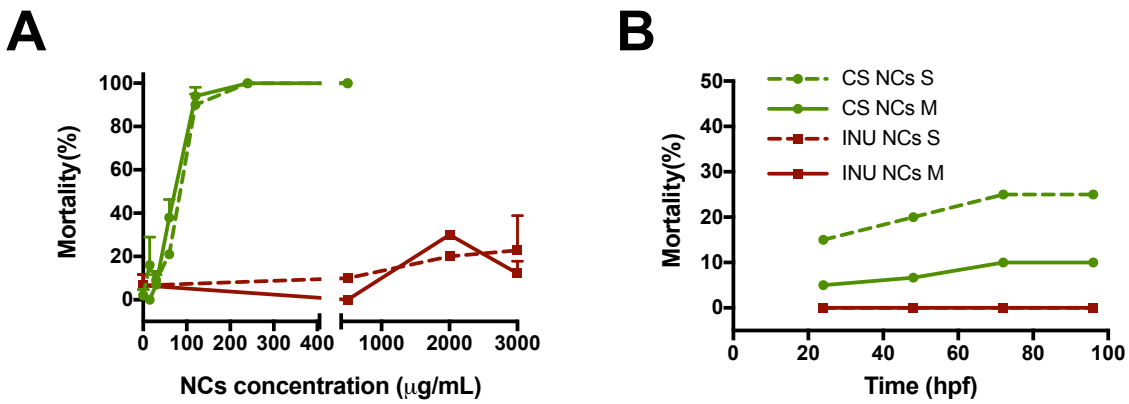

Figure 6. Toxicity of the nanosystems in zebrafish embryos. The *in vivo* toxicity was assessed after incubation with several nanocapsules (NCs) concentrations (A), and after injection of 5 nL in the caudal vein (B). Inulin (INU) and chitosan (CS) nanocapsules (NCs) of two different sizes, small (S < 100 nm) and medium (M > 100 nm); hpf: hours post-fertilization.

3.3.2. Biodistribution of the NCs in zebrafish after intramuscular and intravenous injection

During the first 4 weeks of their life, zebrafish have yet to develop their adaptive immunity, which allows the study of their innate immune system, exclusively [63,64]. In addition, zebrafish MΦs have a morphology and functions similar to those of their mammalians counterparts [65]. For that reason, the use of MΦ-labeled zebrafish offers a powerful system to monitor *in vivo* nanoparticles-immune cells interaction.

To assess the influence of the nanosystems particle size and polymer shell composition in their biodistribution, fluorescently labeled NCs were injected into 48 hpf Tg(mpeg1:EGFP) zebrafish embryos either intramuscularly or intravenously (Cuvier's duct) (Fig. 7A). Non-injected and DiD-injected embryos were used as controls to ensure that the intrinsic fluorescence of the animals and the free fluorescent marker did not interfere with the signal from labeled-NCs (Fig. S4).

Figures 7 and 8 show the microscopy images of zebrafish receiving the formulations by intramuscular and intravenous injection, respectively. In both injection modalities, clear differences were found between the behavior of NCs with different particle size (S and M). Regardless of the composition and modality of administration, small NCs (S) disseminated further and faster than medium size NCs (M).

When injected intramuscularly (Fig. 7B, magnified view in Fig. S5), the higher degree of dissemination of CS and INU NCs S, regardless of their composition, led to their spreading all along the myomere and clearly limited by myosepta, a dense membrane of collagen fibrils. In addition, they were still found in the muscle at 25 h post-injection, both inside MΦs, seen as bright spots, and outside them, seen as more diffuse fluorescence (yellow dotted area in the confocal microscope). This retention at longer times seem to be more pronounced for INU NCs S. On the contrary, CS and INU

NCs M hardly spread from the injection point at 2 - 4 h (Fig.7B, red dashed circles), and at 24 h only residual fluorescence was observed at the site of injection. It might be hypothesized that this clearance is mediated by MΦs, since the NCs remaining fluorescence at 24 h was mainly co-localized with MΦs.

With regard to the influence of the NCs polymer shell, both CS NCs, S and M, exhibited a high capacity to recruit MΦs at the injection site (Fig. 7B, indicated as "MΦ", with green fluorescence from the MΦs and also yellow fluorescence due to the co-localization of MΦs and NCs, in red). On the contrary, INU NCs showed a lower capacity to attract MΦs. In this sense, it is well documented that chitosan implants and scaffolds cause inflammatory cells infiltration with an important accumulation of neutrophils and macrophages [71].

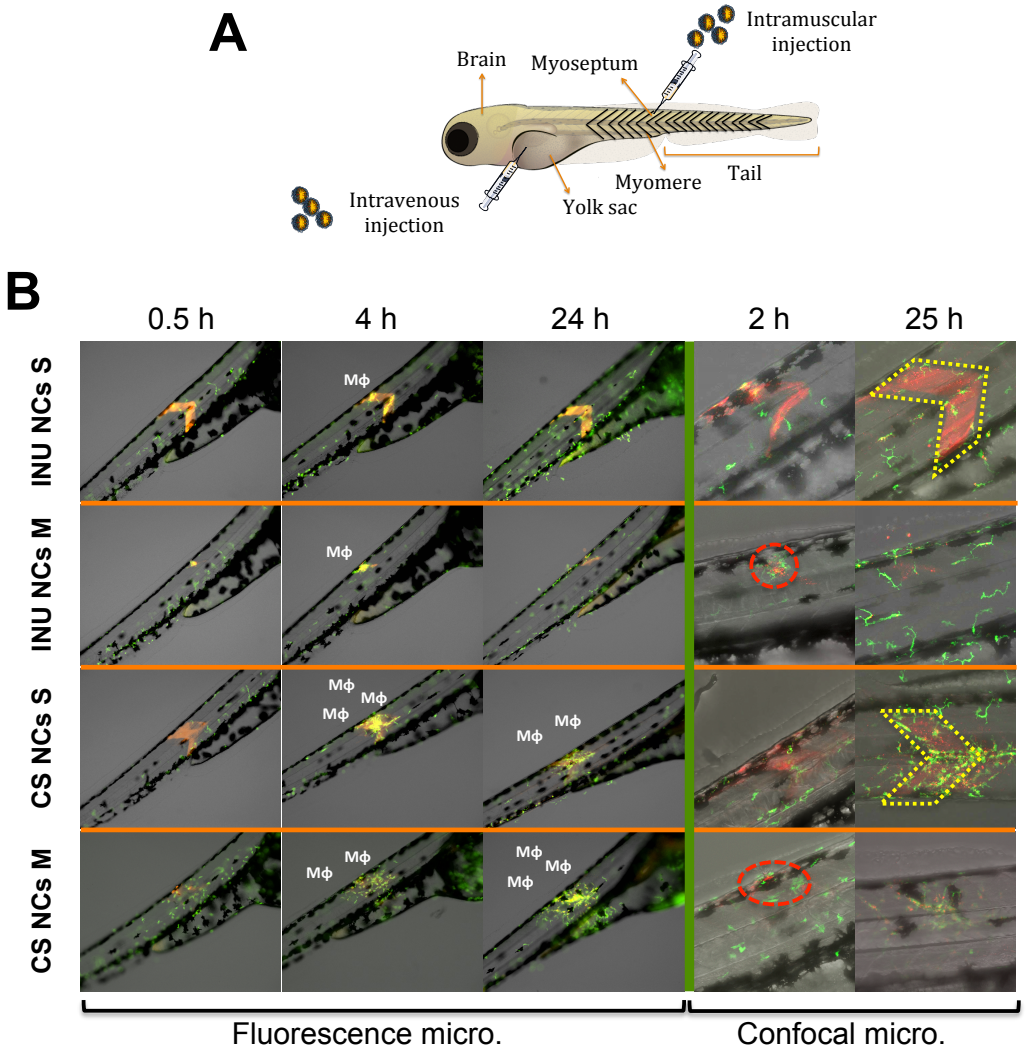

Figure 7. Nanocapsules (NCs) biodistribution in zebrafish after intramuscular injection. Representative scheme of the administration routes and relevant anatomical regions in the biodistribution studies of zebrafish embryos (A). Chitosan (CS) and inulin (INU) NCs of two different particle sizes (S <100 nm and M >100 nm) were administered intramuscularly in 48 hours post fertilization (hpf) zebrafish embryos. Images were taken with a fluorescence zoom microscope and with a confocal microscope at different hours post-injection (B). Red channel: NCs, green channel: macrophages, red dashed circles: low dissemination from the injection site; yellow dotted area: dissemination along the myomere; MΦ: macrophages recruitment. Zebrafish embryo drawing adapted from Lizzy Griffiths http://zebrafishart.blogspot.com/.

On the other hand, following intravenous injection (Fig. 8, magnified view in Fig. S6 and S7), it is possible to evaluate the interaction of NCs with endothelial cells and MΦs [72,73]. Regarding NCs size, similarly to what happened in the intramuscular route, CS and INU NCs S, regardless of their polymeric shell composition, spread faster and at a higher extent than their M counterparts. The higher dissemination of NCs S was particularly noticeable in the vasculature of the tail with the intersegmental vessels (ISV), surrounding the myomeres, and the caudal vein (CV) visible due to their fluorescence (Fig. 8, confocal images, at 2 h, CS and INU NCs S; and Fig. S7). Considering the composition, CS NCs, were found to be slightly more attached to the endothelial cells of the blood vessels at a higher degree than INU NCs. In fact, among all the prototypes, CS NCs S ultimately showed highest intensity within the circulatory system and, also, seemed to have reached tissues, such as the brain and visceral organs (Fig. 8, fluorescence microscope, at 4-24 h, head region). This difference was also noticeable in the ventral region of the tail, where CS NCs S showed the higher fluorescence in the caudal hematopoietic tissue (CHT) when compared with other NCs (Fig. 8, fluorescence microscope, at 4 h, tail region; Fig. S7). On the contrary, INU NCs M showed limited fluorescence in this region, mainly associated to MΦs (Fig. 8, yellow dots in the tail indicated by white arrows; Fig. S7).

Regarding the interaction with MΦs, the four prototypes of NCs injected into the circulatory system were found to be internalized by the MΦs (Fig. 8, white arrows), at a higher degree in the case of CS NCs. In relation to the particle size, both NCs M interacted with MΦs from early time points (Fig. 8 and S7, 0.5 h) and for all the duration of the experiment, whereas CS and INU NCs S presented less interaction at 0.5 h and this interaction increased with time.

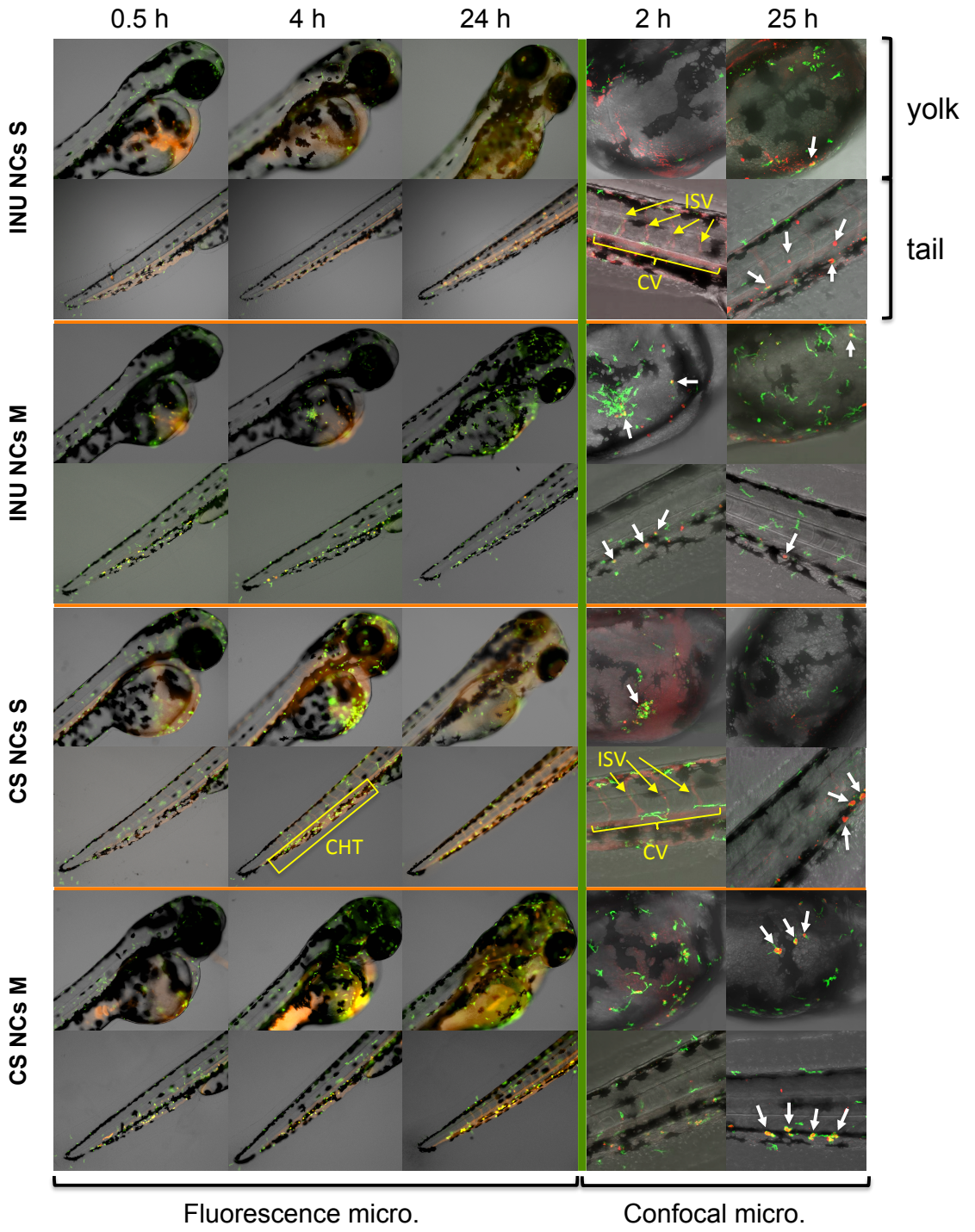

Figure 8. Nanocapsules (NCs) biodistribution in zebrafish after intravenous administration. Biodistribution of two different particle sizes (S <100 nm and M >100 nm) of chitosan (CS) and inulin (INU) NCs in 48 h zebrafish embryos after intravenous administration trough the duct of Cuvier. Images were taken at 0.5, 4, and 24 h with a fluorescence zoom microscope and at 2 and 25 h with a confocal microscope. Red channel: NCs, green channel: macrophages. White arrows point out colocalization of NCs and macrophages in the confocal images. ISV = intersegmental vessels; CV = caudal vein; CHT = caudal hematopoietic tissue.

4. Conclusions

During the course of this work, we have developed new polymeric nanocapsules based on modified inulin, with a tunable particles size (70 and 250 nm). When compared with chitosan nanocapsules of similar size, the inulin nanocapsules presented a lower interaction with macrophages *in vitro,* but considerably less toxicity. Moreover, we have studied the potential of macrophage-labeled zebrafish as a model to understand the interactions between nanosystems with different physicochemical properties and the immune cells in a dynamic and living environment. Specifically, particle sizes smaller than 100 nm allowed for a faster and deeper dissemination of the nanocapsules in the tissues compared with 170 – 250 nm nanocapsules, both after intravenous and intramuscular injection. Besides, the smaller nanocapsules were retained longer in the muscle, whereas medium size NCs suffered a higher clearance rate mediated by macrophages. In this sense, although both types of nanocapsules were captured by macrophages, chitosan seemed to play an important role in phagocytes recruitment. However, due to its non-inflammatory mechanism of adjuvancy, proved safety and good capacity to disseminate, we believe that small inulin nanocapsules should be further explored as new nanovaccines with the potential to drain and accumulate in the lymphatic system.

References

[1] A.S. Cordeiro, M.J. Alonso, M. de la Fuente, Nanoengineering of vaccines using natural polysaccharides, Biotechnol. Adv. 33 (2015) 1279–1293. doi:10.1016/j.biotechadv.2015.05.010.
[2] J. Yang, S. Han, H. Zheng, H. Dong, J. Liu, Preparation and application of micro/nanoparticles based on natural polysaccharides, Carbohydr. Polym. 123 (2015) 53–66. doi:10.1016/j.carbpol.2015.01.029.
[3] M.A. Mensink, H.W. Frijlink, K. Van Der Voort Maarschalk, W.L.J. Hinrichs, Inulin, a flexible oligosaccharide. II: Review of its pharmaceutical applications, Carbohydr. Polym. 134 (2015) 418–428. doi:10.1016/j.carbpol.2015.08.022.
[4] M. Walser, D.G. Davidson, J. Orloff, The renal clearance of alkali-stable inulin, J. Clin. Invest. 34 (1955) 1520–1523. doi:10.1172/JCI103204.
[5] M. Skwarczynski, Inulin: A New Adjuvant With Unknown Mode of Action, EBioMedicine. 15 (2017) 8–9. doi:10.1016/j.ebiom.2016.11.019.
[6] D.G. Silva, P.D. Cooper, N. Petrovsky, Inulin-derived adjuvants efficiently promote both Th1 and Th2 immune responses, Immunol. Cell Biol. 82 (2004) 611–616. doi:10.1111/j.1440-1711.2004.01290.x.
[7] N. Petrovsky, P.D. Cooper, Advax™, a novel microcrystalline polysaccharide particle engineered from delta inulin, provides robust adjuvant potency together with tolerability and safety, Vaccine. 33 (2015) 5920–5926. doi:10.1016/j.vaccine.2015.09.030.
[8] L. Li, Y. Honda-Okubo, C. Li, D. Sajkov, N. Petrovsky, Delta inulin adjuvant enhances plasmablast generation, expression of activation-induced cytidine deaminase and B-cell affinity maturation in human subjects receiving seasonal influenza vaccine, PLoS One. 10 (2015) 1–18. doi:10.1371/journal.pone.0132003.
[9] M. Hayashi, T. Aoshi, Y. Haseda, K. Kobiyama, E. Wijaya, N. Nakatsu, et al., Advax, a delta inulin microparticle, potentiates in-built adjuvant property of co-administered vaccines, EBioMedicine. 15 (2017) 127–136. doi:10.1016/j.ebiom.2016.11.015.
[10] L. Wang, T. Barclay, Y. Song, P. Joyce, I.G. Sakala, N. Petrovsky, et al., Investigation of the biodistribution, breakdown and excretion of delta inulin adjuvant, Vaccine. 35 (2017) 4382–4388. doi:10.1016/j.vaccine.2017.06.045.
[11] H. Jiang, Q. Wang, X. Sun, Lymph node targeting strategies to improve vaccination efficacy, J. Control. Release. 267 (2017) 47–56. doi:10.1016/j.jconrel.2017.08.009.
[12] S.T. Reddy, M.A. Swartz, J.A. Hubbell, Targeting dendritic cells with biomaterials: developing the next generation of vaccines, Trends Immunol. 27 (2006) 573–579. doi:10.1016/j.it.2006.10.005.
[13] T.J. Moyer, A.C. Zmolek, D.J. Irvine, Beyond antigens and adjuvants: formulating future vaccines, J. Clin. Invest. 126 (2016) 799–808. doi:10.1172/JCI81083.
[14] N. Hoshyar, S. Gray, H. Han, G. Bao, The effect of nanoparticle size on in vivo pharmacokinetics and cellular interaction, Nanomedicine. (2016). doi:10.2217/nnm.16.5.
[15] N. Benne, J. van Duijn, J. Kuiper, W. Jiskoot, B. Slütter, Orchestrating immune responses: How size, shape and rigidity affect the immunogenicity of particulate vaccines, J. Control. Release. 234 (2016) 124–134. doi:10.1016/j.jconrel.2016.05.033.
[16] C. V. Stevens, A. Meriggi, K. Booten, Chemical modification of inulin, a valuable renewable resource, and its industrial applications, Biomacromolecules. 2 (2001) 1–16. doi:10.1021/bm005642t.
[17] C. V. Stevens, A. Meriggi, M. Peristeropoulou, P.P. Christov, K. Booten, B. Levecke, et al., Polymeric surfactants based on inulin, a polysaccharide extracted from chicory. 1. Synthesis and interfacial properties, Biomacromolecules. 2 (2001) 1256–1259. doi:10.1021/bm015570l.
[18] G. Van den Mooter, I. Weuts, T. De Ridder, N. Blaton, Evaluation of Inutec SP1 as a new carrier in the formulation of solid dispersions for poorly soluble drugs, Int. J. Pharm. 316 (2006) 1–6. doi:10.1016/j.ijpharm.2006.02.025.
[19] P. Srinarong, S. Hämäläinen, M.R. Visser, W.L.J. Hinrichs, J. Ketolainen, H.W. Frijlink, Surface-Active Derivative of Inulin (Inutec® SP1) Is a Superior Carrier for Solid Dispersions with a High Drug Load, J. Pharm. Sci. 100 (2011) 2333–2342. doi:10.1002/jps.22471.
[20] P.R. Mishra, L. Al Shaal, R.H. Müller, C.M. Keck, Production and characterization of Hesperetin nanosuspensions for dermal delivery, Int. J. Pharm. 371 (2009) 182–189. doi:10.1016/j.ijpharm.2008.12.030.
[21] P. Muley, S. Kumar, F. El Kourati, S.S. Kesharwani, H. Tummala, Hydrophobically modified inulin as an amphiphilic carbohydrate polymer for micellar delivery of paclitaxel for intravenous route, Int. J.

Pharm. 500 (2016) 32–41. doi:10.1016/j.ijpharm.2016.01.005.
[22] T.F. Tadros, A. Vandamme, K. Booten, B. Levecke, C. V. Stevens, Stabilisation of emulsions using hydrophobically modified inulin (polyfructose), Colloids Surfaces A Physicochem. Eng. Asp. 250 (2004) 133–140. doi:10.1016/j.colsurfa.2004.03.041.
[23] C. Losa, L. Marchal-Heussler, F. Orallo, J.L. Vila Jato, M.J. Alonso, Design of new formulations for topical ocular administration: polymeric nanocapsules containing metipranolol., Pharm. Res. 10 (1993) 80–7. doi:10.1023/A:1018977130559.
[24] C. Prego, D. Torres, M.J. Alonso, Chitosan Nanocapsules as Carriers for Oral Peptide Delivery: Effect of Chitosan Molecular Weight and Type of Salt on the In Vitro Behaviour and In Vivo Effectiveness, J. Nanosci. Nanotechnol. 6 (2006) 2921–2928. doi:10.1166/jnn.2006.429.
[25] F.A. Oyarzun-Ampuero, G.R. Rivera-Rodríguez, M.J. Alonso, D. Torres, G.R. Rivera-Rodriguez, M.J. Alonso, et al., Hyaluronan nanocapsules as a new vehicle for intracellular drug delivery, Eur. J. Pharm. Sci. 49 (2013) 483–490. doi:10.1016/j.ejps.2013.05.008.
[26] G. Lollo, P. Hervella, P. Calvo, P. Aviles, M.J. Guillen, M. Garcia-Fuentes, et al., Enhanced in vivo therapeutic efficacy of plitidepsin-loaded nanocapsules decorated with a new poly-aminoacid-PEG derivative, Int. J. Pharm. 483 (2015) 212–219. doi:10.1016/j.ijpharm.2015.02.028.
[27] L.N. Thwala, A. Beloqui, N.S. Csaba, D. González-Touceda, S. Tovar, C. Dieguez, et al., The interaction of protamine nanocapsules with the intestinal epithelium: A mechanistic approach, J. Control. Release. 243 (2016) 109–120. doi:10.1016/j.jconrel.2016.10.002.
[28] G. Lollo, A. Gonzalez-Paredes, M. Garcia-Fuentes, P. Calvo, D. Torres, M.J. Alonso, Polyarginine Nanocapsules as a Potential Oral Peptide Delivery Carrier, J. Pharm. Sci. 106 (2017) 611–618. doi:10.1016/j.xphs.2016.09.029.
[29] K.T. Gause, A.K. Wheatley, J. Cui, Y. Yan, S.J. Kent, F. Caruso, Immunological Principles Guiding the Rational Design of Particles for Vaccine Delivery, ACS Nano. 11 (2017) 54–68. doi:10.1021/acsnano.6b07343.
[30] D.J. Irvine, M.A. Swartz, G.L. Szeto, Engineering synthetic vaccines using cues from natural immunity, Nat. Mater. 12 (2013) 978–990. doi:10.1038/nmat3775.
[31] K. Siram, G. Marslin, C.V. Raghavan, K. Balakumar, H. Rahman, G. Franklin, A brief perspective on the diverging theories of lymphatic targeting with colloids, Int. J. Nanomedicine. 11 (2016) 2867–2872. doi:10.2147/IJN.S105852.
[32] K.Y. Lee, G.H. Jang, C.H. Byun, M. Jeun, P.C. Searson, K.H. Lee, Zebrafish models for functional and toxicological screening of nanoscale drug delivery systems: promoting preclinical applications, Biosci. Rep. 37 (2017) BSR20170199. doi:10.1042/BSR20170199.
[33] C. Teijeiro-Valiño, E. Yebra-Pimentel, J. Guerra-Varela, N. Csaba, M.J. Alonso, L. Sánchez, Assessment of the permeability and toxicity of polymeric nanocapsules using the zebrafish model, Nanomedicine. 12 (2017) 2069–2082. doi:10.2217/nnm-2017-0078.
[34] V.E. Fako, D.Y. Furgeson, Zebrafish as a correlative and predictive model for assessing biomaterial nanotoxicity, Adv. Drug Deliv. Rev. 61 (2009) 478–486. doi:10.1016/j.addr.2009.03.008.
[35] S. Lin, Y. Zhao, A.E. Nel, S. Lin, Zebrafish: An In Vivo Model for Nano EHS Studies, Small. 9 (2013) 1608–1618. doi:10.1002/smll.201202115.
[36] V. Torraca, S. Masud, H.P. Spaink, A.H. Meijer, Macrophage-pathogen interactions in infectious diseases: new therapeutic insights from the zebrafish host model, Dis. Model. Mech. 7 (2014) 785–797. doi:10.1242/dmm.015594.
[37] G. Arango Duque, A. Descoteaux, Macrophage Cytokines: Involvement in Immunity and Infectious Diseases, Front. Immunol. 5 (2014) 1–12. doi:10.3389/fimmu.2014.00491.
[38] M. Westerfield, The zebrafish book : a guide for the laboratory use of zebrafish (Danio rerio), 5th ed., Oregon, 2007.
[39] W.M.S. Russell, R.L. Burch, The principles of humane experimental technique, Mehuen, London. UK, 1959.
[40] P. Calvo, C. Remuñán-López, J.L. Vila-Jato, M.J. Alonso, Development of positively charged colloidal drug carriers: Chitosan-coated polyester nanocapsules and submicron-emulsions, Colloid Polym. Sci. 275 (1997) 46–53. doi:10.1007/s003960050050.
[41] S. Vicente, B. Diaz-Freitas, M. Peleteiro, A. Sanchez, D.W. Pascual, A. Gonzalez-Fernandez, et al., A Polymer/Oil Based Nanovaccine as a Single-Dose Immunization Approach, PLoS One. 8 (2013) e62500. doi:10.1371/journal.pone.0062500.
[42] S. Vicente, M. Peleteiro, J.V. González-Aramundiz, B. Díaz-Freitas, S. Martínez-Pulgarín, J.I. Neissa, et al., Highly versatile immunostimulating nanocapsules for specific immune potentiation.,

Nanomedicine (London). 9 (2014) 2273–2289. doi:10.2217/nnm.14.10.
[43] S. Vicente, M. Peleteiro, B. Díaz-Freitas, A. Sanchez, Á. González-Fernández, M.J. Alonso, Co-delivery of viral proteins and a TLR7 agonist from polysaccharide nanocapsules: A needle-free vaccination strategy, J. Control. Release. 172 (2013) 773–781. doi:10.1016/j.jconrel.2013.09.012.
[44] J. Crecente-Campo, S. Lorenzo-Abalde, A. Mora, J. Marzoa, N. Csaba, J. Blanco, et al., Bilayer polymeric nanocapsules: A formulation approach for a thermostable and adjuvanted E. coli antigen vaccine, J. Control. Release. 286 (2018) 20–32. doi:10.1016/j.jconrel.2018.07.018.
[45] S. Moriguchi, M. Kaneyasu, Role of Vitamin E in Immune System, Ser. Rev. J.Clin. Biochem. 34 (2003) 97–109.
[46] S. Vicente, M. Peleteiro, B. Díaz-Freitas, A. Sanchez, Á. González-Fernández, M.J. Alonso, Co-delivery of viral proteins and a TLR7 agonist from polysaccharide nanocapsules: A needle-free vaccination strategy, J. Control. Release. 172 (2013) 773–781. doi:10.1016/j.jconrel.2013.09.012.
[47] F.A. Oyarzun-Ampuero, M. Garcia-Fuentes, D. Torres, M.J. Alonso, Chitosan-coated lipid nanocarriers for therapeutic applications, J. Drug Deliv. Sci. Technol. 20 (2010) 259–265. doi:10.1016/S1773-2247(10)50043-1.
[48] M. V Lozano, H. Esteban, J. Brea, M.I. Loza, D. Torres, M.J. Alonso, Intracellular delivery of docetaxel using freeze-dried polysaccharide nanocapsules., J. Microencapsul. 30 (2013) 181–8. doi:10.3109/02652048.2012.714411.
[49] A.C. Pinheiro, A.I. Bourbon, M.A. Cerqueira, É. Maricato, C. Nunes, M.A. Coimbra, et al., Chitosan / fucoidan multilayer nanocapsules as a vehicle for controlled release of bioactive compounds, Carbohydr. Polym. 115 (2015) 1–9. doi:10.1016/j.carbpol.2014.07.016.
[50] J.V. González-Aramundiz, E. Presas, I. Dalmau-Mena, S. Martínez-Pulgarín, C. Alonso, J.M. Escribano, et al., Rational design of protamine nanocapsules as antigen delivery carriers, J. Control. Release. 245 (2017) 62–69. doi:10.1016/j.jconrel.2016.11.012.
[51] T. Nakanishi, J. Kunisawa, A. Hayashi, Y. Tsutsumi, K. Kubo, S. Nakagawa, et al., Positively Charged Liposome Functions as an Efficient Immunoadjuvant in Inducing Immune Responses to Soluble Proteins, Biochem. Biophys. Res. Commun. 240 (1997) 793–797.
[52] C. He, Y. Hu, L. Yin, C. Tang, C. Yin, Effects of particle size and surface charge on cellular uptake and biodistribution of polymeric nanoparticles, Biomaterials. 31 (2010) 3657–3666. doi:10.1016/j.biomaterials.2010.01.065.
[53] L. Thiele, B. Rothen-Rutishauser, S. Jilek, H. Wunderli-Allenspach, H.P. Merkle, E. Walter, Evaluation of particle uptake in human blood monocyte-derived cells in vitro. Does phagocytosis activity of dendritic cells measure up with macrophages?, J. Control. Release. 76 (2001) 59–71.
[54] J.S. Choi, J. Cao, M. Naeem, J. Noh, N. Hasan, H.K. Choi, et al., Size-controlled biodegradable nanoparticles: Preparation and size-dependent cellular uptake and tumor cell growth inhibition, Colloids Surfaces B Biointerfaces. 122 (2014) 545–551. doi:10.1016/j.colsurfb.2014.07.030.
[55] S. Hirsjärvi, S. Dufort, J. Gravier, I. Texier, Q. Yan, J. Bibette, et al., Influence of size, surface coating and fine chemical composition on the in vitro reactivity and in vivo biodistribution of lipid nanocapsules versus lipid nanoemulsions in cancer models, Nanomedicine Nanotechnology, Biol. Med. 9 (2013) 375–387. doi:10.1016/j.nano.2012.08.005.
[56] S. Kim, W.K. Oh, Y.S. Jeong, J.Y. Hong, B.R. Cho, J.S. Hahn, et al., Cytotoxicity of, and innate immune response to, size-controlled polypyrrole nanoparticles in mammalian cells, Biomaterials. 32 (2011) 2342–2350. doi:10.1016/j.biomaterials.2010.11.080.
[57] J. Huang, L. Bu, J. Xie, K. Chen, Z. Cheng, X. Li, et al., Effects of nanoparticle size on cellular uptake and liver MRI with polyvinylpyrrolidone-coated iron oxide nanoparticles, ACS Nano. (2010). doi:10.1021/nn101643u.
[58] H.J. Johnston, R. Verdon, S. Gillies, D.M. Brown, T.F. Fernandes, T.B. Henry, et al., Adoption of in vitro systems and zebrafish embryos as alternative models for reducing rodent use in assessments of immunological and oxidative stress responses to nanomaterials, Crit. Rev. Toxicol. 48 (2018) 252–271. doi:10.1080/10408444.2017.1404965.
[59] I. Paatero, E. Casals, R. Niemi, E. Özliseli, J.M. Rosenholm, C. Sahlgren, Analyses in zebrafish embryos reveal that nanotoxicity profiles are dependent on surface-functionalization controlled penetrance of biological membranes, Sci. Rep. 7 (2017) 1–13. doi:10.1038/s41598-017-09312-z.
[60] M.F. Cordeiro, F.A. Girardi, C.O.F. Gonçalves, C.S. Peixoto, L. Dal Bosco, S.K. Sahoo, et al., Toxicological assessment of PEGylated single-walled carbon nanotubes in early developing zebrafish, Toxicol. Appl. Pharmacol. 347 (2018) 54–59. doi:10.1016/j.taap.2018.03.031.
[61] Y.-L. Hu, W. Qi, F. Han, J.-Z. Shao, J.-Q. Gao, Toxicity evaluation of biodegradable chitosan

nanoparticles using a zebrafish embryo model., Int. J. Nanomedicine. 6 (2011) 3351–9. doi:10.2147/IJN.S25853.
[62] Y. Wang, J. Zhou, L. Liu, C. Huang, D. Zhou, L. Fu, Characterization and toxicology evaluation of chitosan nanoparticles on the embryonic development of zebrafish, Danio rerio, Carbohydr. Polym. 141 (2016) 204–210. doi:10.1016/j.carbpol.2016.01.012.
[63] S.H. Lam, H.L. Chua, Z. Gong, T.J. Lam, Y.M. Sin, Development and maturation of the immune system in zebrafish, Danio rerio: a gene expression profiling, in situ hybridization and immunological study., Dev. Comp. Immunol. 28 (2004) 9–28. doi:10.1016/S0145-305X(03)00103-4.
[64] C. Cui, E.L. Benard, Z. Kanwal, O.W. Stockhammer, M. van der Vaart, A. Zakrzewska, et al., Infectious Disease Modeling and Innate Immune Function in Zebrafish Embryos, Methods Cell Biol. 105 (2011) 273–308. doi:10.1016/B978-0-12-381320-6.00012-6.
[65] N.D. Meeker, N.S. Trede, Immunology and zebrafish: Spawning new models of human disease, Dev. Comp. Immunol. 32 (2008) 745–757. doi:10.1016/j.dci.2007.11.011.
[66] S. Ravindranathan, B.P. Koppolu, S.G. Smith, D.A. Zaharoff, Effect of chitosan properties on immunoreactivity, Mar. Drugs. 14 (2016). doi:10.3390/md14050091.
[67] M. Oliveira, S. Santos, M. Oliveira, A. Torres, M. Barbosa, Chitosan drives anti-inflammatory macrophage polarisation and pro-inflammatory dendritic cell stimulation, Eur. Cells Mater. 24 (2012) 136–153. doi:10.22203/eCM.v024a10.
[68] C.L. Bueter, C.K. Lee, J.P. Wang, G.R. Ostroff, C.A. Specht, S.M. Levitz, Spectrum and Mechanisms of Inflammasome Activation by Chitosan, J. Immunol. 192 (2014) 5943–5951. doi:10.4049/jimmunol.1301695.
[69] J. Crecente-Campo, S. Lorenzo-Abalde, A. Mora, J. Marzoa, N. Csaba, J. Blanco, et al., Bilayer polymer nanocapsules: a formulation approach for a thermostable and adjuvanted E. coli antigen vaccine, J. Control. Release. Submitted (2018).
[70] C. Nikapitiya, S.H.S. Dananjaya, B.C.J. De Silva, G.-J. Heo, C. Oh, M. De Zoysa, et al., Chitosan nanoparticles: A positive immune response modulator as display in zebrafish larvae against Aeromonas hydrophila infection, Fish Shellfish Immunol. 76 (2018) 240–246. doi:10.1016/j.fsi.2018.03.010.
[71] C.D. Hoemann, D. Fong, Immunological responses to chitosan for biomedical applications, in: Chitosan Based Biomater. Vol. 1, Elsevier, 2017: pp. 45–79. doi:10.1016/B978-0-08-100230-8.00003-0.
[72] F. Campbell, F.L. Bos, S. Sieber, G. Arias-Alpizar, B.E. Koch, J. Huwyler, et al., Directing Nanoparticle Biodistribution through Evasion and Exploitation of Stab2-Dependent Nanoparticle Uptake, ACS Nano. 12 (2018) 2138–2150. doi:10.1021/acsnano.7b06995.
[73] B. Yin, K.H.K. Li, L.W.C. Ho, C.K.W. Chan, C.H.J. Choi, Toward Understanding in Vivo Sequestration of Nanoparticles at the Molecular Level, ACS Nano. 12 (2018) 2088–2093. doi:10.1021/acsnano.8b00141.

Supplementary information

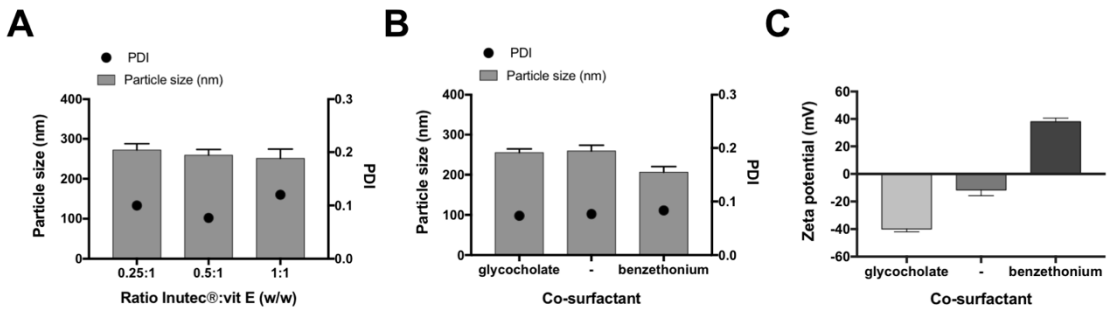

Figure S1. Influence of the ratio Inutec®:vitamin E (w/w) in the particle size of the resulting nanocapsules (A). The addition of a co-surfactant, such us sodium glycocholate or benzethonium chloride, rendered nanocapsules of similar particle size (B) but very different surface charge (C).

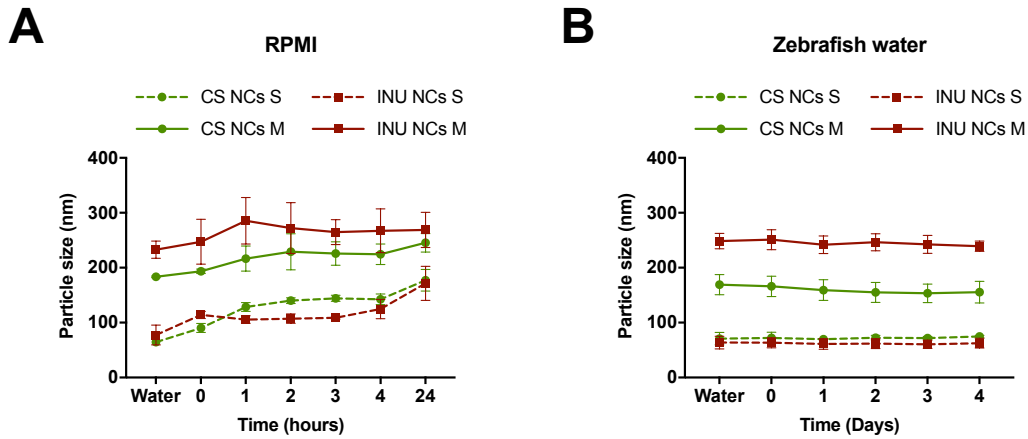

Figure S2. Stability of the nanosystems regarding their particle size in cell culture medium at 37 ºC (A) and in water for zebrafish growing at 32 ºC (B). Inulin-based nanocapsules (INU NCs) and chitosan nanocapsules (CS NCs) of two different sizes, small (S) and medium (M).

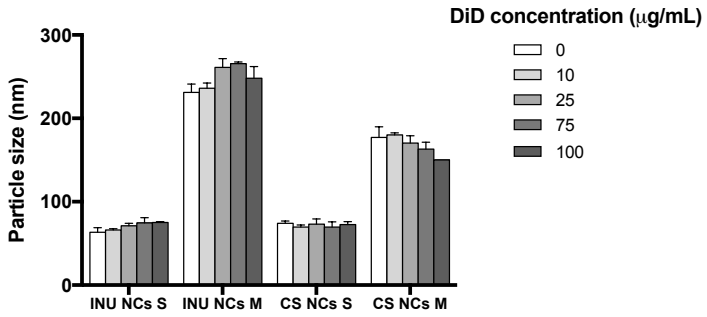

Figure S3. Influence of the fluorescent marker DiD concentration in the particle size of the different nanocapsules (NCs): inulin (INU) and chitosan (CS), small (S) and medium (M) size.

Table S1. Mortality of the nanocapsules (NCs) after injection in the caudal vein of zebrafish embryos.

	24h	48h	72h	96h
INU NCs S	0	0	0	0
INU NCs M	0	0	0	0
CS NCs S	9	12	15	15
CS NCs M	3	4	6	6

The number of dead embryos from a total of 60 embryos (three triplicates with 20 embryos each) is indicated. Inulin (INU) and chitosan (CS), small (S) and medium (M) size.

Table S2. Mortality of the nanocapsules after injection in the yolk sac of zebrafish embryos.

	24h	48h	72h	96h
INU NCs S	0	0	0	0
INU NCs M	0	0	0	0
CS NCs S	0	0	0	0
CS NCs M	0	0	0	0

The number of dead embryos from a total of 60 embryos (three triplicates with 20 embryos each) is indicated. Inulin (INU) and chitosan (CS), small (S) and medium (M) size.

Table S3. Mortality of the nanocapsules after injection in the Cuvier's duct of zebrafish embryos.

	24h	48h	72h	96h
INU NCs S	0	0	0	0
INU NCs M	0	0	0	0
CS NCs S	0	0	0	0
CS NCs M	0	0	0	0

The number of dead embryos from a total of 10 embryos is indicated. Inulin (INU) and chitosan (CS), small (S) and medium (M) size.

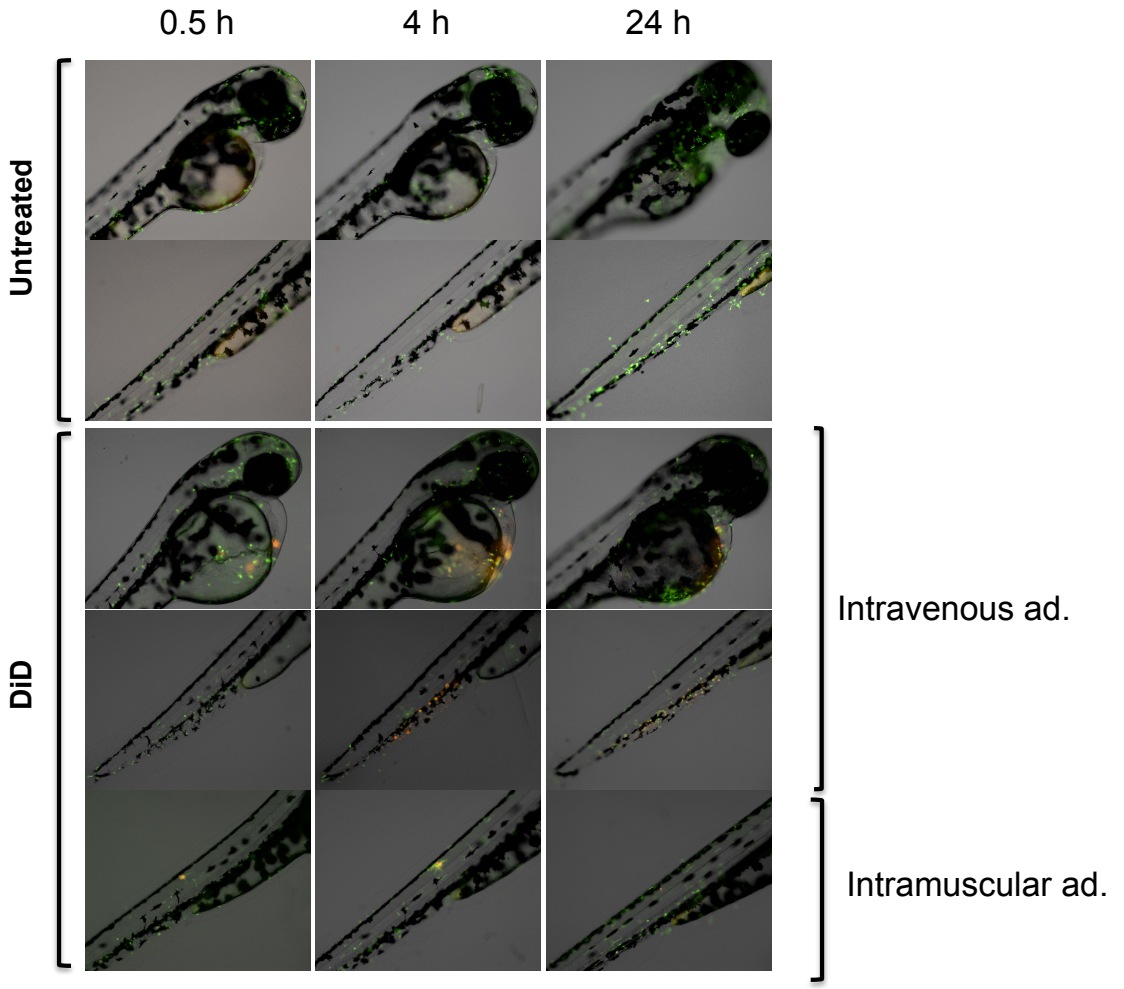

Figure S4. Photographs of untreated and DiD-treated zebrafish embryos (48 hours post fertilization). DiD was solubilized in trehalose for its administration through either intramuscular or intravenous route. Images were taken at 0.5, 4 and 24 h with a fluorescence zoom microscope. Red channel: NCs, green channel: macrophages.

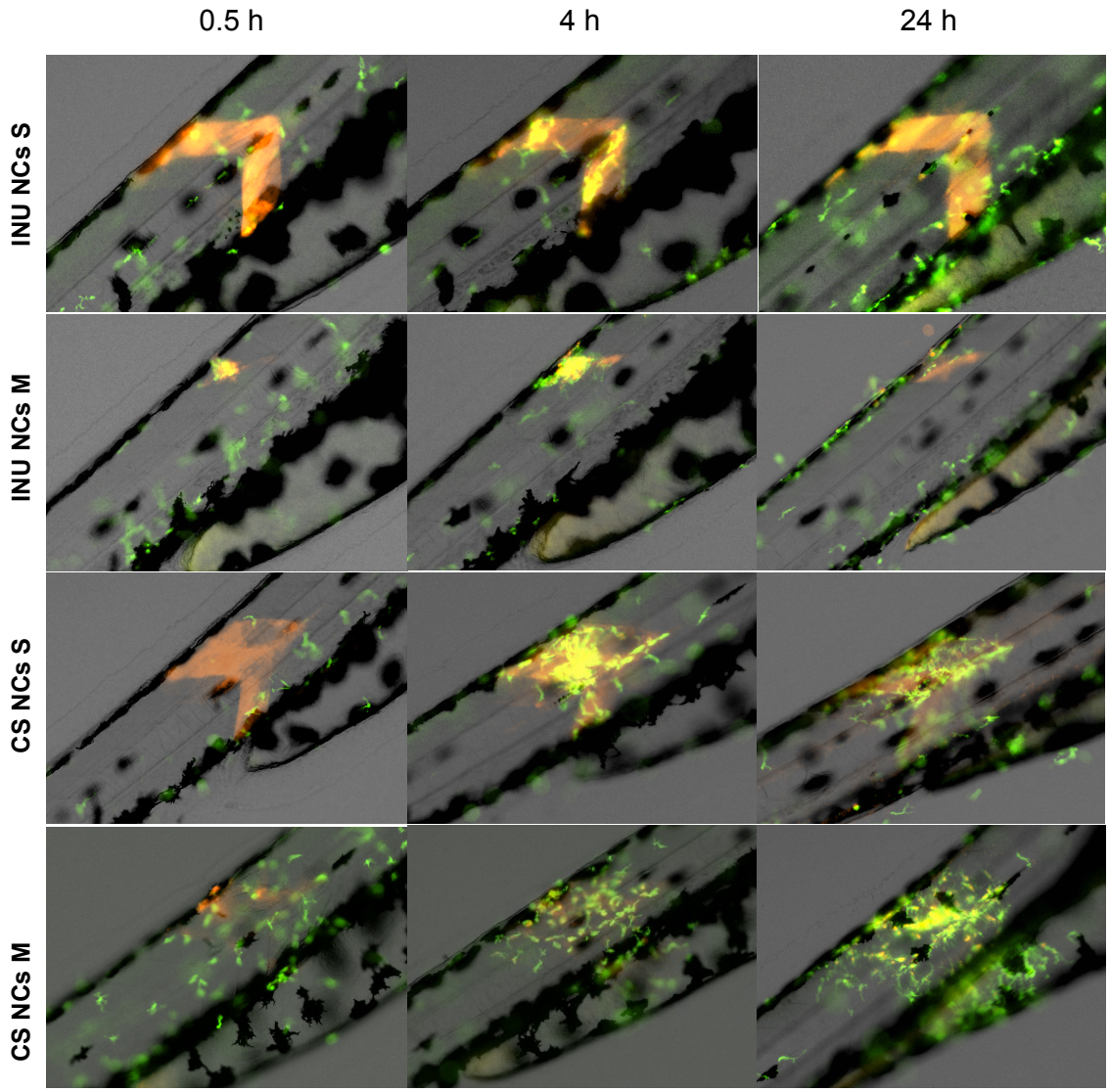

Figure S5. Nanocapsules (NCs) biodistribution in zebrafish after intramuscular injection. Chitosan (CS) and inulin (INU) NCs of two different particle sizes (S <100 nm and M >100 nm) were administered intramuscularly in 48 hours post fertilization (hpf) zebrafish embryos. Images were taken with a fluorescence zoom microscope (B). Red channel: NCs, green channel: macrophages.

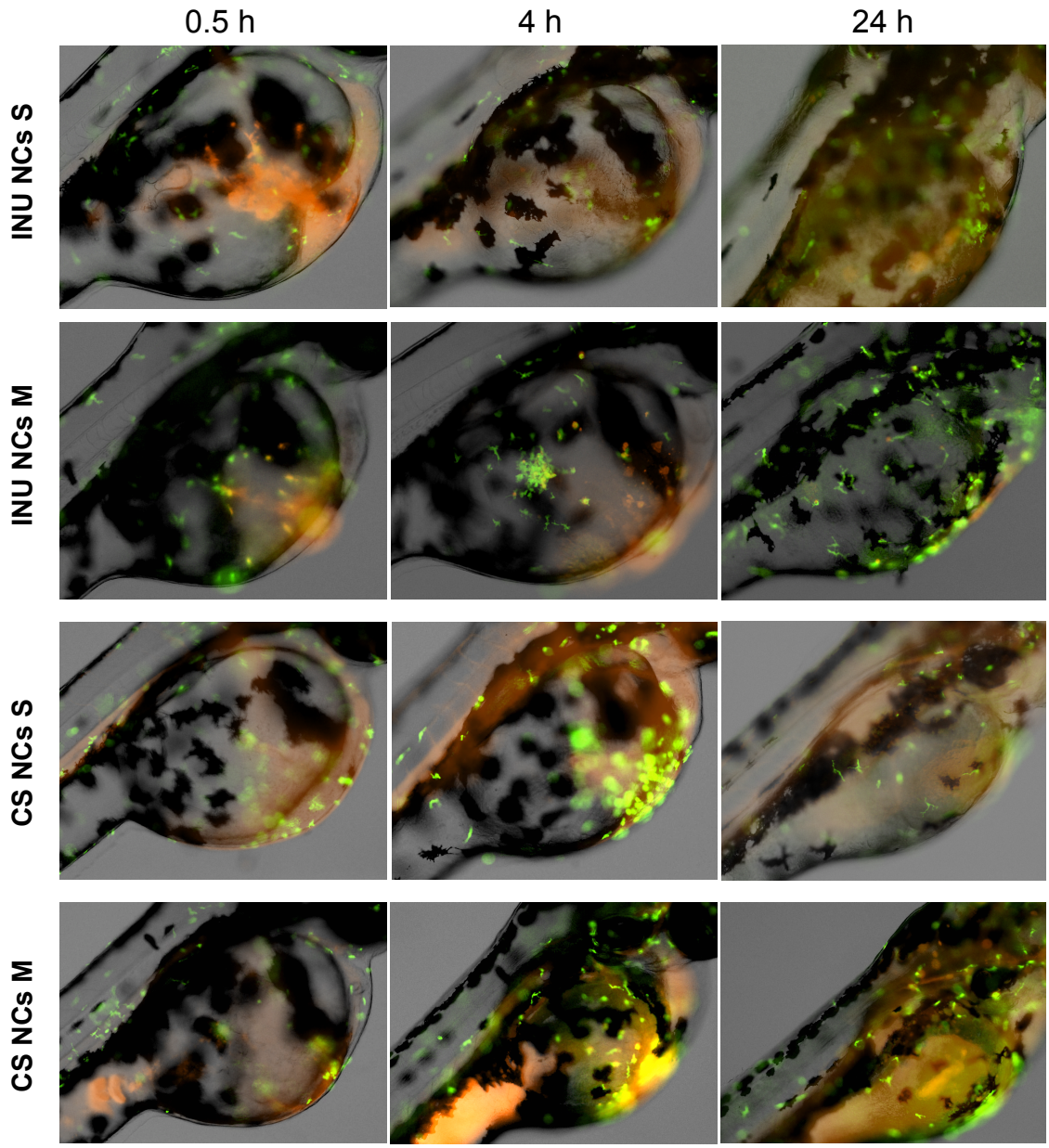

Figure S6. Nanocapsules (NCs) biodistribution in zebrafish in the yolk sac region after intravenous administration. Biodistribution of chitosan (CS) and inulin (INU) NCs of two different particle sizes (S <100 nm and M >100 nm) in 48 h zebrafish embryos after intravenous administration trough the duct of Cuvier. Images were taken at 0.5, 4 and 24 h with a fluorescence zoom microscope.

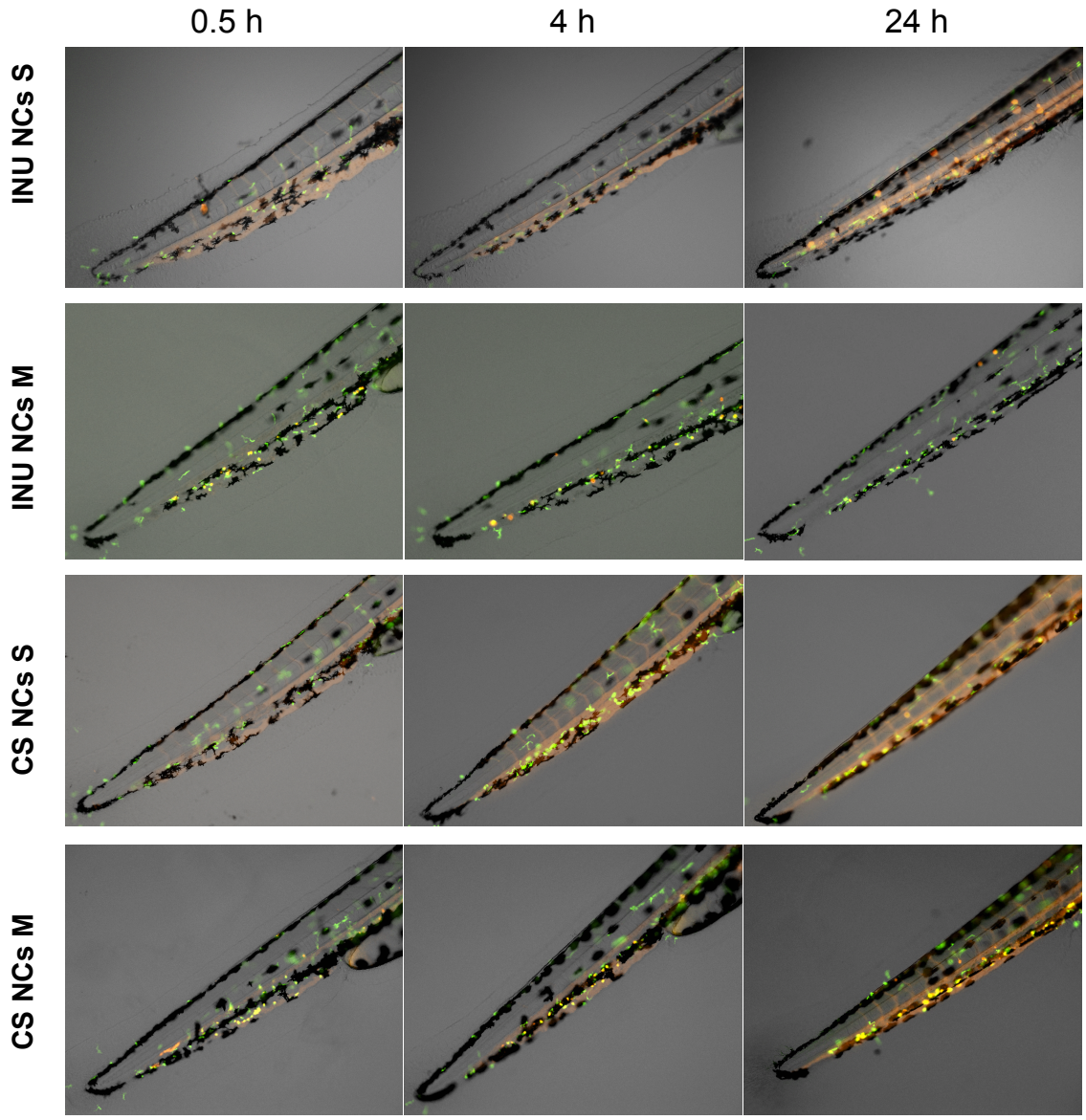

Figure S7. Nanocapsules (NCs) biodistribution in zebrafish in the tail region after intravenous administration. Biodistribution of chitosan (CS) and inulin (INU) NCs of two different particle sizes (S <100 nm and M >100 nm) in 48 h zebrafish embryos after intravenous administration trough the duct of Cuvier. Images were taken at 0.5, 4 and 24 h with a fluorescence zoom microscope.

Chapter 4

Polysaccharidic nanocapsules with lympho-targeting properties: simultaneous effect of size and composition

Chapter 4

Polysaccharidic nanocapsules with lympho-targeting properties: simultaneous effect of size and composition

This work was done in collaboration with Institute for Research in Biomedicine, (Università della Svizzera Italiana), Graduate School of Cellular and Molecular Sciences, Faculty of Medicine (University of Bern) and Department of Biochemistry and Molecular Biology, School of Pharmacy (USC).

Abstract

A key challenge of nanomedicine is to understand the interaction of the nanoparticles with the immune system, not only from the toxicological point of view but also because of its potential benefit to modulate immune responses and associated therapeutic actions. The objective of this work has been to bring light into how the composition and the particle size of polymeric nanocapsules (NCs) influence their lympho-targeting properties and subsequent interaction with lymph node resident immune cells. The selected polysaccharides were inulin and chitosan, which rendered negatively and positively charged NCs, respectively. The *in vitro* results indicated that small particle size (70 nm) NCs interacted in a higher extent with dendritic cells than the larger ones (170 - 250 nm). Besides, chitosan NCs caused a higher activation of dendritic cells, in terms of cytokines release and T cell stimulation, compared with inulin NCs. The biodistribution of the NCs, after subcutaneous administration to mice, was investigated using 2-photon microscopy, a technique that allowed the visualization of the nanoparticles behavior in living animals with high resolution. The results showed a higher accumulation of small particle size inulin NCs in the popliteal lymph node compared with the rest of prototypes, whereas chitosan NCs were more retained in the injection site. Within the lymph node, small inulin NCs were those that exhibited the greatest interaction with all the analyzed immune cells although small chitosan NCs were also highly captured by $CD11b^{+}$ dendritic cells, monocytes, neutrophils and NK cells. This work highlights the simultaneous influence of the size and surface composition of the nanosystems on the lymphatic drainage and their prior or subsequent interaction with immune cells, a mechanism that will be relevant in the design of new nanovaccines.

Graphical abstract

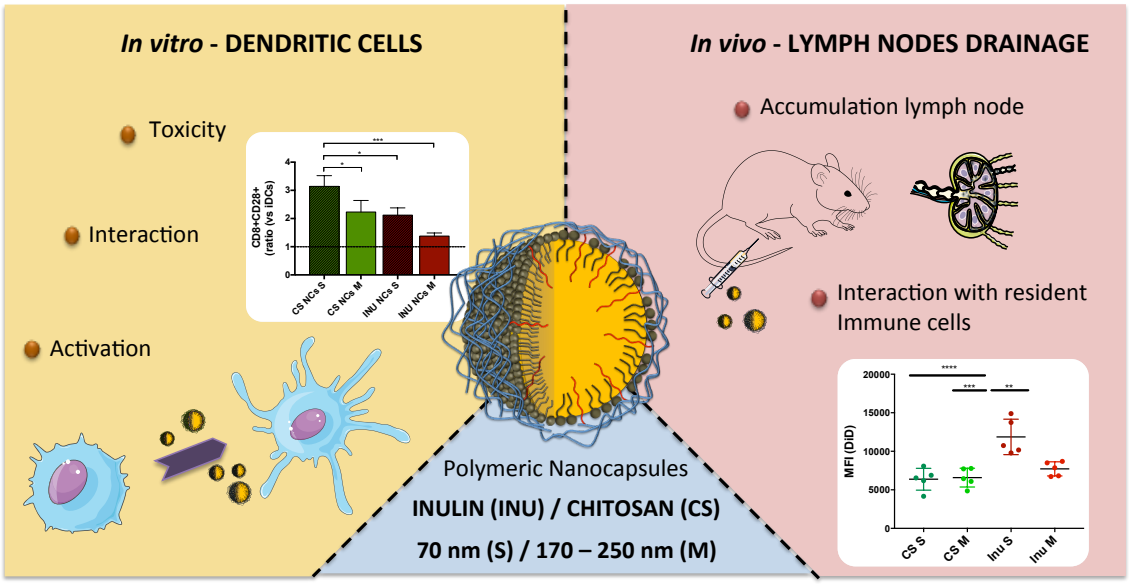

1. Introduction

Dendritic cells (DCs) are the most important antigen presenting cells (APCs), representing the connection between the innate and adaptive arms of the immune system [1–3]. DCs present exogenous and self-antigens to T-cells, thus being key elements in some of the most important human health disorders, such as autoimmune diseases, infectious diseases (malaria, tuberculosis, HIV, etc.) and cancer, among others. These diseases lack of a satisfactory treatment, reason why there is an enormous interest in developing new strategies to fight them. In this sense, important efforts have been made in the field of nanotechnology with the design of an armament of nanosystems intended to help, activate and re-educate the immune system [1].

On the other hand, polymeric nanocapsules (NCs), consisting of an oily core and a polymeric shell have shown a capacity to deliver drugs, antigens and immunomodulatory compounds. Our group has made relevant contributions to this field by developing a variety of NCs with different polymer shells, such as chitosan (CS) [4–6], hyaluronic acid [7], poly-L-Asparagine [8,9], polyarginine [10] and poly(glutamic acid) (PGA) [11–13]. We have also shown the possibility to ensemble multiple polymer layers within the polymer shell, as described in chapter 1, a configuration that allows the co-encapsulation of adjuvants and antigens and their prolonged release [14,15].

Nanotechnologist have aimed at finding the golden rules behind particles' design to maximize their uptake by DCs. Based on simple *in vitro* experiments, some authors have concluded that nanoparticles (NPs) are usually preferred than microparticles [16,17], and that cationic NPs are better than the anionic ones in terms of cellular uptake [17,18]. However, other authors have found that, in the nanometric region, larger PGA-based NPs (235 nm) could be more internalized than small ones (33 nm) [19].

Our view is that it is not possible to present general conclusions, specially based on *in vitro* data, and disregard the critical impact of the biodistribution of the particles in the final access to the targeted cells. In fact, beyond the potential effect of the particle size and surface charge in the interaction of the particles with the biological system, each type of particle will have a specific behavior in terms of biodistribution and cell uptake, which will be also determined by its composition. For example, in the case of cationic chitosan (CS) NCs, we have observed that they form a depot after subcutaneous administration [20], whereas in the case of negatively-charged PGA NCs, we found, in a mice cancer model, that they drained to the lymphatic system decreasing the metastatic load in the lymph nodes [21]. Overall, our view is that both, depot and lymphatic drainage may coexist, and the physicochemical properties of the nanosystems will dictate which one will predominate [22].

With regard to the biodistribution of marketed adjuvants, such as aluminium salts or MF59, it is known that they are recruited by the APCs from the injection site and transported to the lymph nodes (LNs) [23]. Based on the fact that the final

targeted cells are mainly DCs located in the lymphatics, we and others have speculated that the lympho-targeting of antigen-loaded NPs could provide them with a more direct way of interaction with a high number of DCs and, hence, an enhancement of the immune response. This increasingly evident theory has changed the paradigm of nanovaccine design, with modern nanosystems being engineered to have an efficient drainage to the lymphatics [24–26].

The generated knowledge about the influence of the size on the capacity of nanosystems to reach the lymphatic system indicates that a substantial accumulation in the LNs occurs for particles in the 20 – 200 nm range. Nevertheless, it is commonly agreed that a value of 100 nm is the threshold below which NPs may drain relatively easy along the lymphatic vessels without being assisted by immune cells and reach the LNs [27–29]. This also agrees with our recent finding that small (≈ 90 nm) CS NCs can reach the popliteal lymph node (PLN) after injection in the footpad of mice in a greater extent than the medium size ones (≈ 250 nm) (data not published).

The effect of the surface charge in the drainage to the LNs is not completely clear. Positive [18,30], negative [31,32] and neutral [33] small particles have shown accumulation in these organs, although, negative surface NPs seem to disseminate better along the lymphatic vessels [24]. However, what is broadly accepted is that the charge shielding, using PEGylated systems, favors their drainage towards the LNs [34,35]. Overall, the interplay between different physicochemical parameters will dictate the performance of the nanosystem.

The objective of this work was to perform a systematic study of the influence of the composition and physicochemical properties of polymeric NCs on their interaction with DCs, and also on their biodistribution. More precisely, we first analyzed the cytotoxicity and interaction of the NCs with DCs *in vitro,* as well as their capacity to activate the cells in terms of biomarkers activation and cytokine release. Then, the NCs drainage towards the LNs and accumulation in the different subset of resident immune cells was studied after their subcutaneous administration to rats, using two complementary techniques: flow cytometry and 2-photon microscopy (2PM). 2PM is a powerful technique that allows the *in vivo* visualization of the interactions between NPs and cells in the surroundings. It allows a deep penetration into the tissue with a minimum damage due to the low-energy photons employed. With this our final goal was to contribute to the rational design of new nanovaccines intended to freely drain to the lymphatic system triggering an enhanced immune response.

2. Materials and Methods

2.1. Materials

DL-α-tocopherol (vitamin E) (Calbiochem®) was obtained from Merck Millipore (Billerica, MA, USA). Pluronic® 127 was obtained from BASF (Ludwigshafen, Germany). Sodium glycocholate was bought to Dextra (Reading, UK). Benzethonium chloride was obtained from Spectrum Chemical Mgf. Corp. (NJ, US). Ultrapure chitosan (CS) hydrochloride salt (Mw 42.7 kDa, deacetylation degree of 88%) was purchased from Heppe Medical Chitosan GmbH (Saale, Germany). Inutec® SL1, 25% modified inulin (INU) suspension in glycerol, was a kind gift from CreaChem (Tienen, Belgium). DiD (DiIC18(5) oil) was obtained from Invitrogen (CA, USA) and sucrose was purchased to Acofarma (Madrid, Spain).

2.2. Nanocapsules preparation

The preparation of the nanocapsules was already described in chapter 3. Briefly, the vitamin E was dissolved in ethanol (table 1) and the glycocholate was added to this phase as a 200 mg/mL aqueous solution, making the organic phase. On the other hand, the polymers (CS or INU) were dissolved in water, making the aqueous phase. In the case of CS NCs, poloxamer 407 was used as surfactant in the aqueous phase. The different amount of compounds and solvents is shown in table 1. To prepare the S NCs the organic phase was injected into the aqueous phase through a needle (100 Sterican®, Ø 0.60 x 60 mm, 23G x $2^{3/8}$”, Braun, Melsungen, Germany) applying high manual pressure. In both cases, the aqueous phase was maintained under stirring. After 10 minutes of incubation the excess of ethanol was removed under vacuum using a rotary evaporator (Büchi, Switzerland) and the volume was adjusted with ultrapure water.

Table 1. Different composition and preparation parameters of the nanosystems developed in this study

	INU NCs S	**INU NCs M**	**CS NCs S**	**CS NCs M**
Vitamin E (mg)	30	60	30	60
Sodium glycocholate (mg)	5	10	5	10
Ethanol (mL)	2.5	2	2.5	3
Poloxamer 407 (mg)	-	-	5	10
Chitosan (mg)	-	-	5	10
Inutec® SL1 (mg)	15	30	-	-
Water (mL)	10	4	10	4
Stirring speed (rpm)	*900*	*500*	*900*	*500*
Addition	*High pressure (injecting)*	*Low pressure (pouring)*	*High pressure (injecting)*	*Low pressure (pouring)*
Final volume (mL)	*5*	*10*	*5*	*10*
Final concentration (mg/mL)	*10*	*10*	*9*	*9*

2.3. Particle size characterization

2.3.1. Electron microscopy

For FESEM studies (ZEISS FESEM ULTRA Plus, Germany) the NCs were diluted in water 1:1000 and mixed with the same volume of 2% (w/v) phosphotungstic acid solution. 1 µL of this mixture was placed on copper grids with carbon films. The grids were left to dry in the open air and then washed, drop-by-drop, with 1 mL of water. Once the grids were dried they were observed in the microscope using both STEM and InLens detectors.

2.3.2. Nanoparticle tracking Analysis

Nanoparticle tracking analysis (NTA) is a method to measure the particle size of nanoparticles based on imaging. The light scattered for individual nanoparticles is captured by the camera. The software (v3.3) uses the Stokes-Einstein equation to transform the Brownian movement into a particle size. The experiments were conducted after diluting the NCs (1:2000) in ultrapure water (MilliQ®) using a NanoSight NS3000 equipment (Malvern Panalytical Ldt, UK). 5 videos of each sample were captured over 90 s, maintaining the temperature stable at 25 ºC. All measurements were performed in triplicate.

2.4. Human Dendritic Cell (DC) generation

Peripheral blood mononuclear cells (PBMCs) were isolated by Ficoll centrifugation. Adherent monocytes were isolated by incubation of PBMCs in culture plates (2 h, 37 ºC) in R2 culture media (RPMI-1640 completed with 2% of fetal bovine serum, FBS). After the incubation period, non-adherent cells were washed three times with R2 media and adherent monocytes were cultured for 6 days in R10 media (RPMI-1640 completed with 10% FBS) containing GM-CSF and IL-4 (both at 100 ng/mL), renewing half of the media after 3 days. With this protocol, immature DCs (iDCs) were obtained. Non-adherent cells (peripheral blood lymphocytes, PBLs) were washed with PBS and stored in liquid nitrogen until use in allogenic stimulation experiments (see below).

Mature DCs (mDCs) were obtained by incubation of iDCs with bacterial lypopolysacharide (LPS) (10 ng/mL) and interferon-γ (IFN-γ) (100 U/mL) for 48 h. Tolerogenic DCs (tolDCs) were obtained using the same conditions indicated for mDCs but also adding 1α,25-dihidroxyvitamin D3 (50 nM) to the culture media.

2.5. Nanocapsules toxicity on immature DCs

iDCs were incubated for 24 h with the different NCs at increasing final concentrations (25, 50, 100, 200, 400 and 900 μg/mL). After the incubation period, cells were harvested, washed twice with PBS and stained with optimal quantities of vital marker eFluor™660 for 30 min (4 ºC). After washing 3 times with PBS containing bovine serum albumin (BSA) at 2 %, cells were analyzed by flow cytometry in a BD FACSCalibur^{TM} cytometer. Data was analyzed using the Flowing software (Cell Imaging Core, Turku Centre for Biotechnology, Finland). Data is shown as the ratio between dead cells incubated with the different NCs and dead cells obtained after iDC incubation in culture media alone.

2.6. Interaction of the nanocapsules with DCs

To evaluate by flow cytometry the percentage of the nanosystems that interact with the cells, 5x10^5 hDCs were plated into a 24-well plate with 0.5 mL of RPMI 10% FBS. Immediately, DiD-labelled nanosystems were added at a concentration of 100 µg/mL. After 1h of incubation, cells were washed with PBS and fixed in a flow cytometry tube with 200 µL of PBS containing 1% paraformaldehyde (PFA). For adquisition, samples were diluted with 500 µL of PBS and the suspension was analyzed by flow cytometry (Accuri Cytometers, Ann Arbor, MI, USA).

2.7. Human DCs phenotype analysis

To analyze the phenotype of iDCs after incubation with the different NCs, iDCs were incubated with the different nanosystems at a final concentration of 200 μg/mL for either 2 h or 24 h. After the activation period, cells were washed twice to eliminate the NCs and incubated up to a total period of 48 h. To determine the iDC phenotype, cells were washed twice with PBS containing BSA (0.1%) and stained with optimal amounts of different antibodies for 30 min, at 4 ºC, in the dark). Levels of maturation markers HLA class II, CD80 and CD83 were quantified by flow cytometry. CD1a was included as a DC marker to verify the correct monocyte differentiation. Cell viability was determined using the vital marker eFluor™660. After washing 3 times with PBS containing bovine serum albumin (BSA) at 2%, cells were analyzed by flow cytometry in a BD FACSCalibur™ cytometer. Data was analyzed using the Flowing software (Cell Imaging Core, Turku Centre for Biotechnology, Finland). Data is shown as the ratio between the mean fluorescent intensity (MFI) of the corresponding marker in iDCs incubated with the different NCs and the MFI of iDC incubated in culture media alone.

2.8. Indoleamine 2,3-dioxygenase (IDO) activity in iDCs

IDO activity was determined by quantification of kinurenin in culture media obtained from different DCs using described methods [36]. Briefly, 4 h before end of the culture period L-tryptophan (100 μM) was added. Culture media (100 μL) was mixed with 30% trifluoroacetic acid (TFA) (50 μL) to precipitate proteins and cell debris by centrifugation (10.000 xg, 5 min, room temperature). Supernatant (75 μL) was mixed with an identical volume of the Ehrlich Reagent and absorbance at 490 nm was determined using a BioRad 680 ELISA reader.

2.9. Lymphocyte activation capacity of iDCs pre-incubated with different NCs

The capacity of of iDCs pre-incubated with the different NCs to activate CD8+ T lymphocytes in an allogenic culture was determined by flow cytometry. Briefly, after incubation of iDCs with the different NCs for 24 h (200 μg/mL), cells were harvested, washed with PBS and plated with allogeneic T cells (non-adherent PBLs obtained after washing adherent monocytes, see above) at a 1:10 ratio (DC:T) for 7-10 days. After the activation and proliferation period, cells were harvested, washed and stained with optimal quantities of CD8 and CD28 antibodies and analyzed by flow cytometry as indicated above.

2.10. Cytokine secretion by iDCs incubated with different NCs

We used personalised MILLIPLEX®MAP kits containing microparticles to capture IFN-γ, IL-10, IL-12p70, IL-15, IL-1β, IL-2, IL-4, IL-23, IL-27, TNF-α, TNF-β, IL-5 and IL-8 present in culture media store at -80 ºC. The assay was using the manufacturer instructions (Millipore). Plates were read in a MAGPIX® analyzer (Merk Chemicals & Life Sciences) (Servicio de Citometría de Flujo, CINBIO, Vigo). Cytokine concentration was determined using calibration curves (variable ranges for the different cytokines) and calculated as pg/mL with the exception of IL-4, IL-23, IL-27 and TNF-β calculated as ng/mL.

2.11. *In vivo* studies

2.11.1. Animals

$CX_3CR_1^{+/gfp}$ [37] heterozygous mice were obtained from Jackson Laboratories and bred in-house. C57BL/6JRj were obtained from Janvier Laboratories. Mice were housed in the specific pathogen-free animal facility of the Institute for Research in Biomedicine, Bellinzona in individually ventilated cages and were used between 8 and 12 weeks of age. Experiments were performed in accordance with the Swiss Federal Veterinary Office guidelines, and animal protocols were approved by the veterinarian local authorities.

2.11.2. Footpad injection model

Mice were anesthetized with a mixture of ketamine (100 mg/kg bodyweight, Parke Davis) and xylazine (10 mg/kg bodyweight, Bayer), A volume of 15 µL of nanosystems was subcutaneously injected 12 hours before sample collection.

2.11.3. Two-Photon Microscopy

For follicular dendritic cells and subcapsular sinus macrophages labeling, $CX_3CR_1^{+/gfp}$ mice were injected in the footpad with 0.5 µg of αCD21/35-Pacific Blue (Biolegend) and αCD169-PE (Biolegend) respectively 2 hours before sample collection. Popliteal lymph nodes were then collected and mounted on a slide with PBS. Images were acquired with a LaVision Trimscope II upright two-photon microscope (LaVision Biotec) with a 10x (Plan Apo lambda NA 0.45, Nikon) dry objective. Excitation was performed with two Chameleon Vision Ti:Sa lasers (Coherent) tuned at 830 nm and 925 nm respectively. Images were z-stacks or mosaic reconstructions acquired with a pixel size

of 1.07 µm and z-step of 3 µm, for a total imaging depth of around 350 µm. Mosaic reconstructions and image analysis were conducted with Fiji-Imagej (ImageJ) and Image Stitching plugin.

2.11.4. Flow Cytometry

A single cell suspension of popliteal lymph nodes from NP-injected C57BL/6JRj was obtained by digestion for 10 minutes at 37°C with an enzyme mix of DNase I (0.28 mg/mL, Amresco), dispase (1 U/mL, Corning), and collagenase P (0.5 mg/ml, Roche) in calcium- and magnesium-free PBS (PBS -/-) followed by a stop solution composed of 2 mM EDTA (Sigma-Aldrich) and 2% heat-inactivated filter-sterilized fetal calf serum (Thermo Fisher Scientific) in PBS -/- (Sigma-Aldrich). Fc receptors were blocked (αCD16/32, BioLegend) followed by surface staining with αMHC II-Pacific Blue, αCD11b-Brilliant Violet 785, αCD11c-Brilliant Violet 711, αF4/80-Alexa 488, αCD169-Brilliant Violet 605 (Biolegend) and analyzed by flow cytometry on an LSRFortessa (BD Biosciences). Cells were gated as follows: CD11b+ DCs, MHC II+ CD11c+ CD11b+; CD11b- DCs, MHC II+ CD11c+ CD11b-; SSM, MHC II+ CD11c intlow CD11b+ CD169+ F4/80-; MM, MHC II+ CD11c intlow CD11b+ CD169+ F4/80+; Monocytes/Neutrophils/NK cells, MHC II- CD11b+. Data were analyzed using FlowJo software (TriStar).

2.12. Statistical analysis

Unless otherwise indicated, all the experiments were repeated at least 3 times. Results are presented as mean ± standard deviation. The differences were considered significant for * $p < 0.05$, ** $p < 0.01$ and *** $p < 0.001$ and **** $p < 0.0001$. All the statistical analyses were carried out with Graph- Pad Prism Version 7.0 software.

3. Results and discussion

Despite the evidences of the influence of the nanosystems particle size in the their lymphatic biodistribution [38,39], generally, these studies have made use of model non-biodegradable NPs and have not been performed in a systematic and comprehensive manner. In chapter 3, we described chitosan (CS) and inulin-based (INU) nanocapsules (NCs) of two different particles sizes (small, S < 100 nm and medium, M > 100 nm) (Fig. 1) and we studied their interaction with macrophages. In this chapter, we have made a deeper characterization of the nanosystems using complementary techniques for size determination, namely field emission scanning electron microscopy (FESEM) and nanoparticle tracking analysis (NTA). Besides, we have evaluated the interaction and the effect that the NCs cause in DCs, the major player in the generation of an immune response. Finally, the drainage of the different NCs to the LNs and their capture by the different subsets of the immune cells were analyzed.

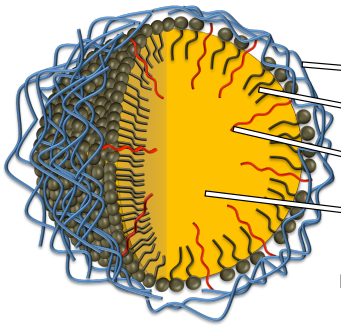

	NCs CS S	NCs CS M	NCs INU S	NCs INU M
POLYMER	Chitosan	Chitosan	Modified inulin	Modified inulin
SURFACTANT	Poloxamer 407	Poloxamer 407		
CO-SURFACTANT	Glycocholate	Glycocholate	Glycocholate	Glycocholate
OIL	Vitamin E	Vitamin E	Vitamin E/ glycerin	Vitamin E/ glycerin
Particle size (nm)	72 ± 5	172 ± 11	69 ± 6	246 ± 16
PDI	0.16	0.11	0.18	0.12
Zeta-Potential (mV)	+ 37 ± 4	+ 34 ± 4	- 33 ± 8	- 25 ± 11

Figure 1. Composition and main physico-chemical properties of the nanosystems studied in this work. Inulin-based nanocapsules (INU NCs) and chitosan nanocapsules (CS NCs) of two different particle sizes, small (S < 100 nm) and medium (M > 100 nm) size.

3.1. NCs physicochemical and morphological characterization

Different techniques were used to rigorously characterize the particle size of the nanosystems. FESEM images, using STEM and InLens detectors, corroborated the differences in the particle size of S and M NCs. The round-shape structure of CS and INU NCs was similar, independently of the nature of the polysaccharide shell (Fig. 2). NTA, which correlates the Brownian motion of individual particles recorded with a camera with their particle size, supplemented the measurements done by DLS, where an average of the fluctuations in the scattered light is related with that size. In our case, the particle size of the S NCs proved to be similar using both techniques (between 70 and 80 nm, approximately). However, the particle size of M NCs offered

unequal results, with particle sizes by NTA around 40 nm smaller than by DLS (246 *vs* 197 nm for INU NCs M, and 172 *vs* 128 nm for CS NCs M, respectively). In the case of INU NCs M, we have also observed a considerable polydisperse sample, with a population of nanoparticles in the range of 100 – 300 nm.

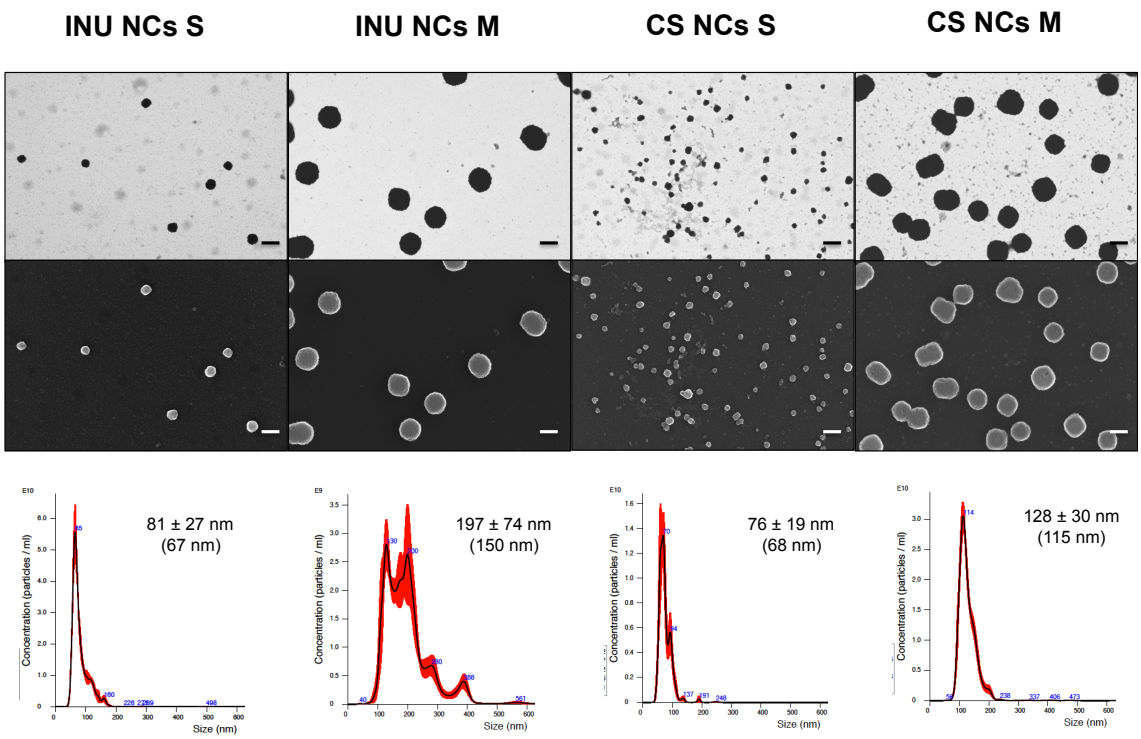

Figure 2. **Particle size by field emission scanning electron microscopy (FESEM) and nanoparticle tracking analysis (NTA) of the different nanosystems.** FESEM images, using STEM (first row) and InLens (second row) detectors, of inulin nanocapsules (INU NCs) (A and B) and chitosan nanocapsules (C and D) of two different particles sizes: small (S < 100 nm) and medium (M > 100 nm) size, respectively. All scale bars = 200 nm. In the third row, a representative image of the particle size distribution obtained for each system by NTA is shown. The mean particle size with the standard deviation and the mode (between brackets) are indicated in the figure (n=3).

3.2. Study of the interaction of NCs with primary human DCs

DCs are the main APCs in our immune system. In their immature state they patrol de body to capture pathogens and exogenous antigens, as it is the case of NPs. After antigen capture, DCs mature and go to LNs where they process and present the antigen to T cells generating an immune response. Thus, it is critical to know how to modulate the interaction between NPs and DCs to generate a specific immune response. In this section, firstly we describe the toxicity of the different nanosystems towards human DCs and, secondly, the type and degree of activation that the DCs suffer after incubation with the NCs. In chapter 3, we have already shown the stability of the nanosystems in cell culture media.

3.2.1. Cytotoxicity

Primary human immature DCs (iDCs) were differentiated from monocytes as described in section 2.4. Then, cells were incubated with different concentrations of either CS or INU NCs for 24 h and stained with a vital label to be analyzed by flow cytometry. As depicted in Fig. 3, CS NCs were more toxic compared to INU NCs, being INU NCs M the ones showing the lowest toxicity. At the highest concentration, small particle size NCs showed a tendency to be more toxic (ratios of 9.3 and 6.3 for CS NCs S and INU NCs S, respectively) than medium size NCs (ratios of 7.3 and 3.75 for CS NCs M and INU NCs M, respectively). Similar results were found in macrophages, with the small particles being more toxic than the medium size NCs (see chapter 3).

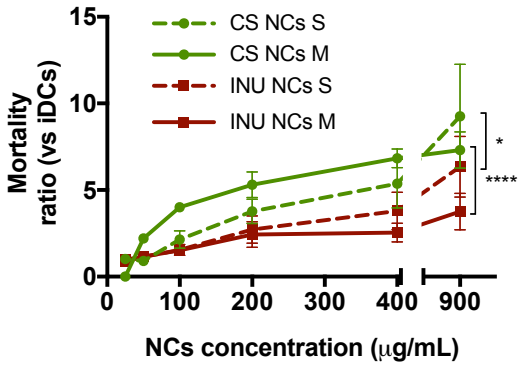

Figure 3. Chitosan (CS) and inulin (INU) nanocapsules (NCs) cytotoxicity on immature dendritic cells (iDCs). iDCs were incubated with either CS (green lines) or INU (red lines) NCs at different concentrations during 24 h. Small (S, <100 nm) (dashed lines) and medium (M, >100 nm)(continuous lines) size NCs were tested. After the incubation period, cells were harvested, washed and stained with a vital label. Results are the ratio between the percentage of dead iDCs incubated with NC *vs* the percentage of dead iDCs incubated in culture media. An average value of 5% was observed for the mortality of iDCs. Each point represents the mean of four different donors. For the statistical analysis the area under the curve for each nanosystem was calculated and the differences between the particles size (S vs M) and the polymer shell (CS vs INU) analyzed using a One-way ANOVA followed by a Tukey test. Significance levels * $p < 0.05$ and **** $p < 0.0001$.

3.2.2. Interaction cell-nanosystems

After establishing a non-toxic dose, NCs were labeled with DiD to evaluate their interaction with iDCs. The analysis by flow cytometry showed a size-dependent effect, where small particles (S < 100 nm) were found to interact with iDCs to a higher extent compared with medium size (M > 100 nm) particles (Fig. 4A), being significantly higher for INU NCs and following this tendency for CS NCs. These results are in agreement with the majority of the research regarding NPs uptake by DCs [16,17,40].

With regard to the influence of the polymer shell on the NCs interaction with DCs, based on the literature, we could speculate that positive particles would interact to a higher degree compared to the negative ones [17,18,41]. This was the case for NCs M (Fig. 4A), however, in the case of NCs S, the percentage of positive cells was

similar for INU and CS NCs. Surprisingly, in terms of mean fluorescence per cell, INU NCs S showed the highest mean fluorescence value (MFI) (Fig. 4B). The level of significance of this difference is low and, hence, we should take this value with caution. Irrespective of this, the higher uptake of INU NCs S as compared to small CS NCs highlights the fact that the surface charge is not the only factor -in addition to the size- influencing the uptake, and that the composition may ultimately drive particle-cell interaction.

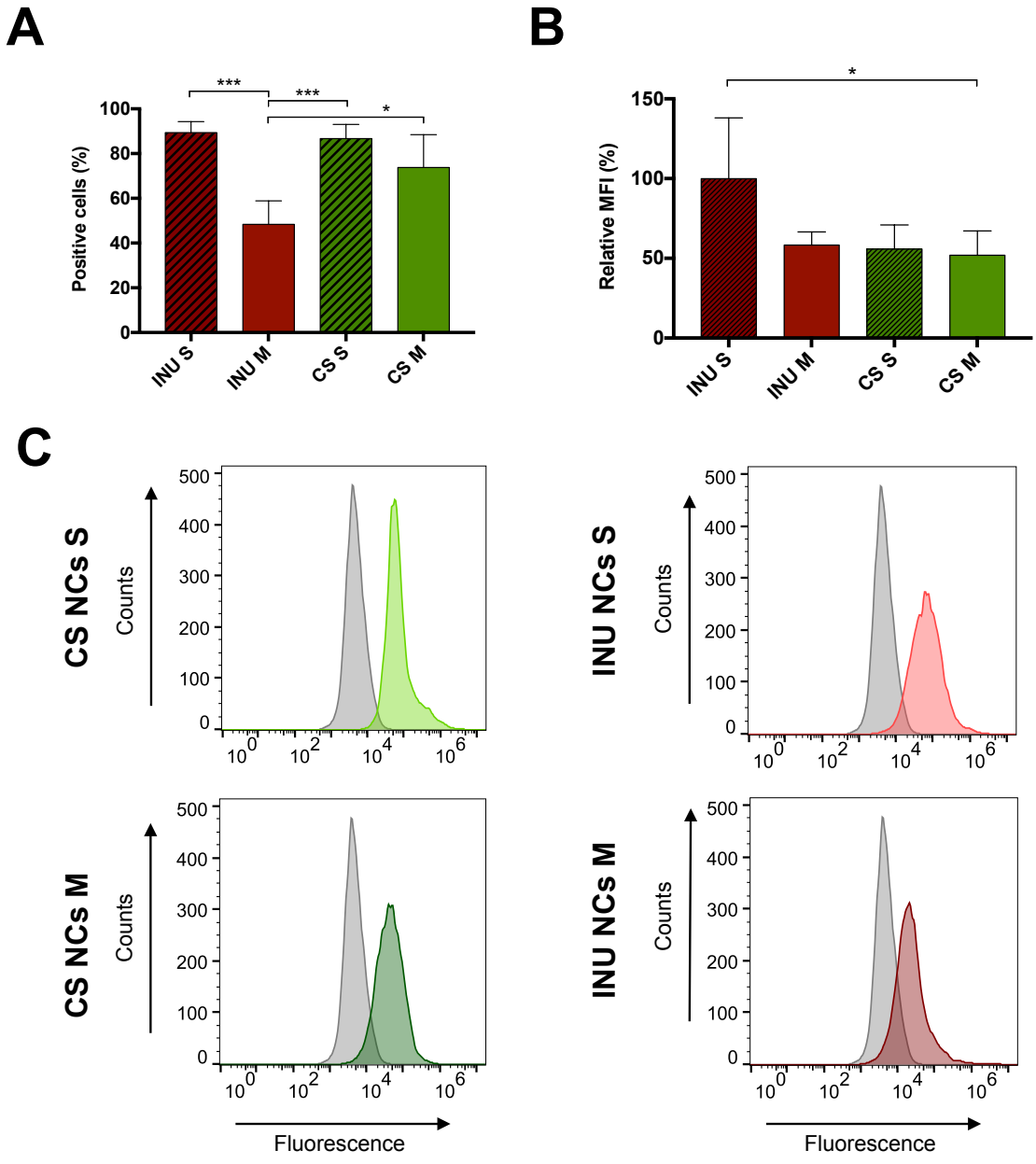

Figure 4. **Interaction of the different labeled nanosystems with iDCs.** After incubation of iDCs with the different NCs, the percentage of positive cells (A) and relative mean fluorescence intensity (B) were analyzed. Representative flow cytometry histograms showing the interaction of the four nanosystems at 100 µg/mL after 1 h incubation with iDCs is shown. In grey non-treated cells are represented. Inulin-based nanocapsules (INU NCs) and chitosan nanocapsules (CS NCs) of two different sizes, small (S) and medium (M) were tested. Statistical analysis was done using a one-way ANOVA followed by a Tukey test. Significance levels * $p < 0.05$ and *** $p < 0.001$.

3.2.3. Change in iDCs phenotype

To evaluate the effect that NCs have on iDC phenotype, different cell markers were analyzed by flow cytometry after incubation with the four different nanosystems. After 2 h incubation, both CS NCs, S and M (Fig. 5A), showed a higher capacity of DC activation compared to INU NCs (Fig. 5B) causing a greater increase in the expression of CD80 and CD83 activation markers. After 24 h, DCs incubated with CS NCs still showed a tendency of up-regulation of CD80 and CD83 but without reaching statistical significance (Fig. 5C). These results agree with previous studies that have shown the activation of these two markers in DCs by different CS NPs [42,43]. In the case of INU NCs, only the small particles showed slight increase in the upregulation of CD83 (Fig. 5D), with a similar tendency for INU NCs M. The activation by inulin nanosystems has hardly been reported, this is the case of INU acetate NPs, which have shown upregulation of CD80 [44]. The higher upregulation of activation markers caused by CS NCs as compared to INU NCs could be related to their higher toxicity, as shown in Fig. 4 [45]. Regarding the particle size, similar values were found for S and M NCs.

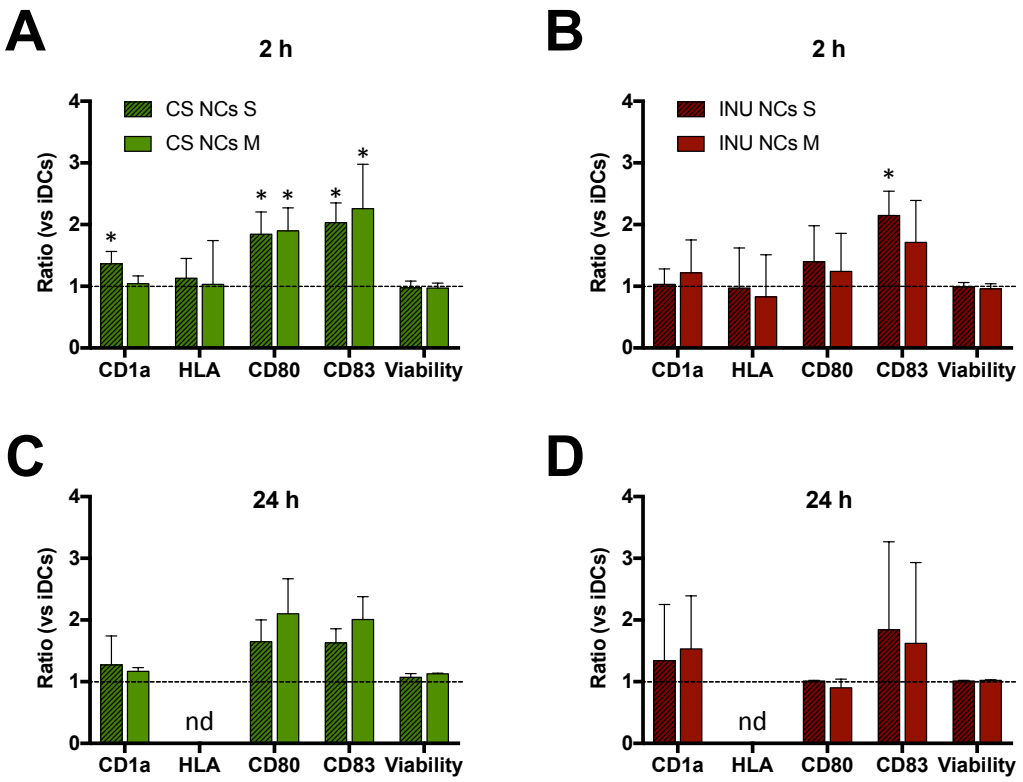

Figure 5. Dendritic cell (DC) phenotype induced by incubation with chitosan (CS) and inulin (INU) nanocapsules (NCs). Immature DCs were incubated with either CS (A, C) or INU (B, D) NCs at 200 µg/mL. Incubation was performed for 2 or 24 h. Small (S, <100 nm) and medium (M, >100 nm) size NCs were tested. After the incubation period, cells were stained with different antibodies and analyzed by flow cytometry. Results are shown as the ratio between the iDCs incubated with NC *vs* iDCs incubated in culture media. *: ratio significantly higher than 1 ($p<0.05$; Student´s T Test). No significant differences were found between the capacity of the four NCs to modify the expression of the different markers (one-way ANOVA). n.d. Not determined.

The fact that INU NCs hardly showed a capacity of DCs activation *in vitro*, led us to speculate about their potential to induce a tolerogenic phenotype on iDCs. To evaluate this hypothesis we quantified the 2,3-Indoleamine dioxigenase (IDO) enzymatic activity. IDO activity has been linked to suppression of both innate and adaptive immunity promoting immune tolerance through the catabolism of tryptophan and other indole compounds [46]. IDO activity in iDCs treated with the four different NCs was similar to that observed in both immature and mature DCs (Fig. 6A, iDCs and mDCs respectively) and significantly lower to that observed in DCs incubated with vitamin D3 (Fig. 6A, tolDCs), an agent known to induce IDO expression. These results clearly indicate that none of the evaluated NCs induced a tolerogenic DC phenotype.

3.2.4. Stimulation of CD8+ T lymphocytes

Next, we decided to evaluate the capacity of iDCs pre-incubated with each of the nanosystems to activate allogeneic CD8+ T lymphocytes *in vitro* (Fig. 6B). Pre-incubation of iDCs with the different NCs significantly increased the percentage of activated CD8+ T lymphocytes (determined as CD28+ cells) (Fig. 6B) with ratios *vs* iDCs significantly higher to 1 in all cases. Both, size and composition were found to influence this response. CS NCs S showed the highest level of CD8+ T lymphocyte responses compared to the other NCs evaluated.

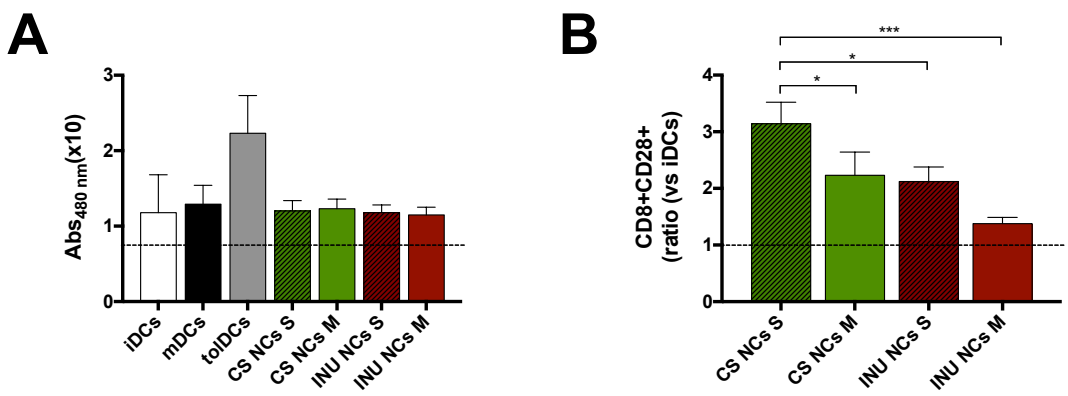

Figure 6. IDO activity and T cell activation capacity by iDCs incubated with different nanocapsules. (A) Immature dendritic cells (iDCs) from four different donors were incubated with either chitosan (CS) or inulin (INU) nanocapsules (NCs) at 100 µg/mL for 2 h. Small (S, <100 nm) and medium (M, >100 nm) size NCs were tested. The 2,3-Indoleamine dioxigenase (IDO) enzymatic activity was determined by the quantification of kinurenin in culture media [36]. Data is shown as the absorbance at 490 nm. Addition of vitamin D3 to iDCs was used to induce a tolerogenic phenotype (tolDCs). iDCs and mature DCs (mDCs) were used as controls. (B) The capacity of the treated iDCs to activate allogeneic CD8+ T lymphocytes is determined by flow cytometry quantifying the up-regulation of CD28. Results are shown as the ratio between the percentage of CD8+CD28+ T cells using iDCs incubated with NC *vs* percentage of CD8+CD28+ T cells using iDCs incubated in culture media. With the only exception of INU NCs M (p=1.0, one-way ANOVA, Bonferroni post hoc) all the NCs significantly increased the percentage of activated CD8+ T lymphocytes compared to non-treated iDCs (NCs CS S, p=0.0001; NCs CS M, p=0.006; NCs INU S, p=0.012; one-way ANOVA, Bonferroni post hoc)(data not shown in the graph). For all four NCs evaluated, CS NCs S showed the higher capacity of CD8 T lymphocyte stimulation (one-way ANOVA, Bonferroni post hoc). The differences were considered significant for * $p < 0.05$, ** $p < 0.01$ and *** $p < 0.001$ and **** $p < 0.0001$.

3.2.5. Cytokine secretion

To deeper analyze the kind of activation that the different nanosystems induce on iDCs, we quantified the amount of cytokines secreted to the culture media by iDCs incubated with the different NCs for 24 h. The human origin of the DCs led to a high variability of the results from different donors, reason why they were expressed as a ratio compared with cytokines released by non-treated DCs. The results, in Table 2, indicate that CS NCs induced a higher cytokine secretion (ratios >1) by iDCs compared to INU NCs, with the exceptions of IL-8 where similar secretion for both types of prototypes is seen. The induction of cytokines secretion by CS formulations has been previously reported [47,48]. However, it should be noted that in the case of highly purified CS, and in the absence of an antigen, the level of cytokines has generally been low [43]. The effects of INU over the DCs were mainly studied at gut level and associated to both pro- and anti-inflammatory cytokines, although at low levels [49].

Similarly to what we found for the activation markers, the particle size seemed not to have a strong influence in the secretion of the cytokines.

Table 2. Cytokine secretion by iDCs after incubation with different nanocapsules (NCs).

Cytokine*	CS NCs S	CS NCs M	INU NCs S	INU NCs M
IFN-γ	+	+	-	-
IL-10	+	++	-	-
IL-12p70	-	-	-	-
IL-5	+++	+++	-	-
IL-8	+	+	+	+
TNF-α	-	-	-	-
TNF-β	+++	+++	+	+

* Data is expressed as the ratio between cytokine secreted by iDCs after treatment with NCs and cytokine secreted by iDCs incubated in media alone. Symbols: -: ratio ≤ 1; +: ratio 1-2; ++: ratio 2-3; +++: ratio > 3.

In summary, the *in vitro* data suggest a clear difference between the CS and INU NCs in terms of DCs activation. Compared with INU NCs, CS NCs caused a higher up-regulation of different activation markers, stimulated the secretion of higher levels of cytokines and demonstrate a higher capacity of CD8+ T cell activation. These data reinforce the idea that CS NCs triggered a more prominent immune activation *in vitro* compared to INU NCs, and that this activation could be partially attributed to their higher toxicity. However, this does not necessarily mean that INU NCs cannot have and adjuvant effect *in vivo*. In fact, the marketed formulation, Advax®, did not show a capacity to activate DCs *in vitro*, however, *in vivo*, this formulation was efficient in terms of enhancing the antigen presentation to T and B cells [50,51]. Notably, delta-INU has shown to be safe in pregnant and very young animals [52,53], a feature that may be attributed to its non-inflammatory mode of action.

Regarding the particle size, although differences were found in terms of iDC interaction with S NCs rendering more positive cells than M size, these differences did not translated into a higher iDC biomarker up-regulation or cytokine production. However, in the case of CS, the small particles induced a higher proliferation of CD8+ T cells.

3.3. Lymphatic drainage of inulin and chitosan NCs in mice

As discussed above, recent data supports the hypothesis that free drainage of nanosystems to the LNs can improve the efficacy of vaccines [24]. These nanostructures, usually with particles sizes less than 100 nm, have shown to favor cross-presentation when interacting with the resident DCs in the LNs, triggering an important cellular response [27,28]. Besides, the direct interaction with B-cells can also improve the humoral branch of the immune response [54]. Based on this information and previous studies in our lab showing the faster lymphatic drainage of small CS NCs (90 nm) as compared to medium size ones (240 nm), after subcutaneous injection to

mice (data not published), in this work our objective was to make a systematic study of the influence of the particle size and the polymeric shell on the drainage of NCs to the LNs and their accumulation in different subsets of immune cells. Considering the prototypes described in chapter 3, we compared the behavior of CS NCs of 70 and 170 nm with that of negatively-charged INU NCs, also with two different particles sizes (70 and 250 nm).

Each of the four DiD-labeled nanosystems were injected in the footpad of mice and the arrival of the structures to the PLN (Fig. 7) was evaluated using two different techniques, flow cytometry (Fig. 8A), after the digestion of the lymph node and appropriate staining, and 2-photon microscopy (2PM) (Fig. 8B). 2PM is an emerging technique in the nanotechnology field, capable of showing with high resolution and in real time *in vivo* interactions at subcellular level. In this work, we benefit from this potent technique, mainly used for model or metallic NPs [55,56], to evaluate the lympho-targeting properties of NCs that have already shown their interest in the nanomedicine field [14,57–59].

The results in Fig. 8 indicate that 12 h after the injection of the NCs in the footpad of the mice the four nanosystems were capable of reaching the PLN, independently of their size and charge. However, using both, flow cytometry and the 2PM studies, it was observed that INU NCs S reached the PLN in a higher extent than the rest of the prototypes. The small size of INU NCs S (70 nm) might explain the difference in their drainage with respect to the medium size ones (INU NCs M, 250 nm). On the other hand, the higher lymphatic drainage with respect to that of CS NC S could be related to the positive charge of the latest ones. Finally, the behavior of CS NCs of different sizes was similar, probably because the differences in the size were not pronounced enough. Overall, we could conclude that both, small size together with negative charge (as compared to positive) where determinant factors of the improved lymphatic drainage of INU NCs S.

If we analyze the biodistribution inside the LN, the accumulation of the NCs mainly occurred in the medullar region (Fig. 8), probably associated with the presence of different population of highly phagocytic cells such as medullary macrophages (MM) and different subtypes of LN resident DCs. The images of the excised PLNs also showed this distribution (Fig. 8C): DiD-labeled NCs appear in white, the follicles can be discerned by the presence of subcapsular sinus macrophages (SSM) (red dots) covering these areas. In the green channel, cells of myeloid origin expressing CX3CR1 were visualized. These results are in accordance with previous experiments performed by us (data not published) and other groups [60], showing the accumulation of nanosystems in the medulla of the LN.

Comparably with what we found, other authors suggested the capacity to freely drain to LNs of particles in the range of 10 – 200 nm [22,61,62], and preferably bellow 100 nm [27,28]. Besides, some of these studies have pointed out that the optimum size would be between 20 - 50 nm. This was the case of 40 nm polyglutamic

acid NPs, which were found to migrate more rapidly to the LNs and captured more efficiently by resident DCs compared with 100 and 200 nm NPs [63]. Similarly, 20 - 40 nm polystyrene nanoparticles were found to drain more rapidly than larger NPs in the nanometric range [16,60]. Overall, these previous works would be in agreement with the results found for INU NCs.

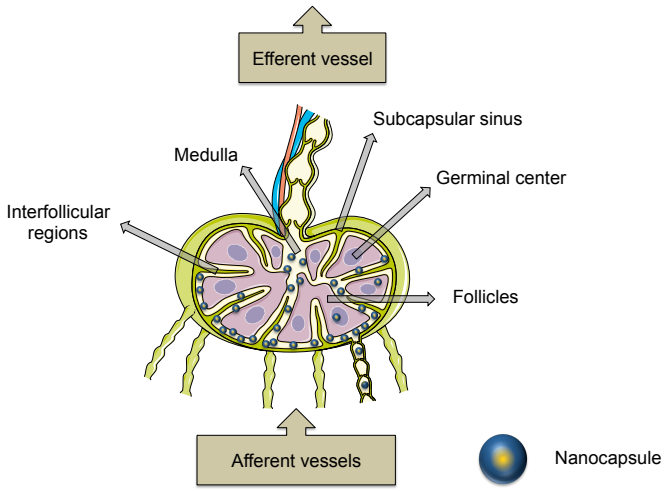

Figure 7. **Schematic illustration of the lymph node.** The different parts of the lymph node are indicated, as well as a simulated arrival of the polymer nanocapsules after subcutaneous injection. This schematic drawing has been modified from the original work provided by Servier Medical Art (https://smart.servier.com/)

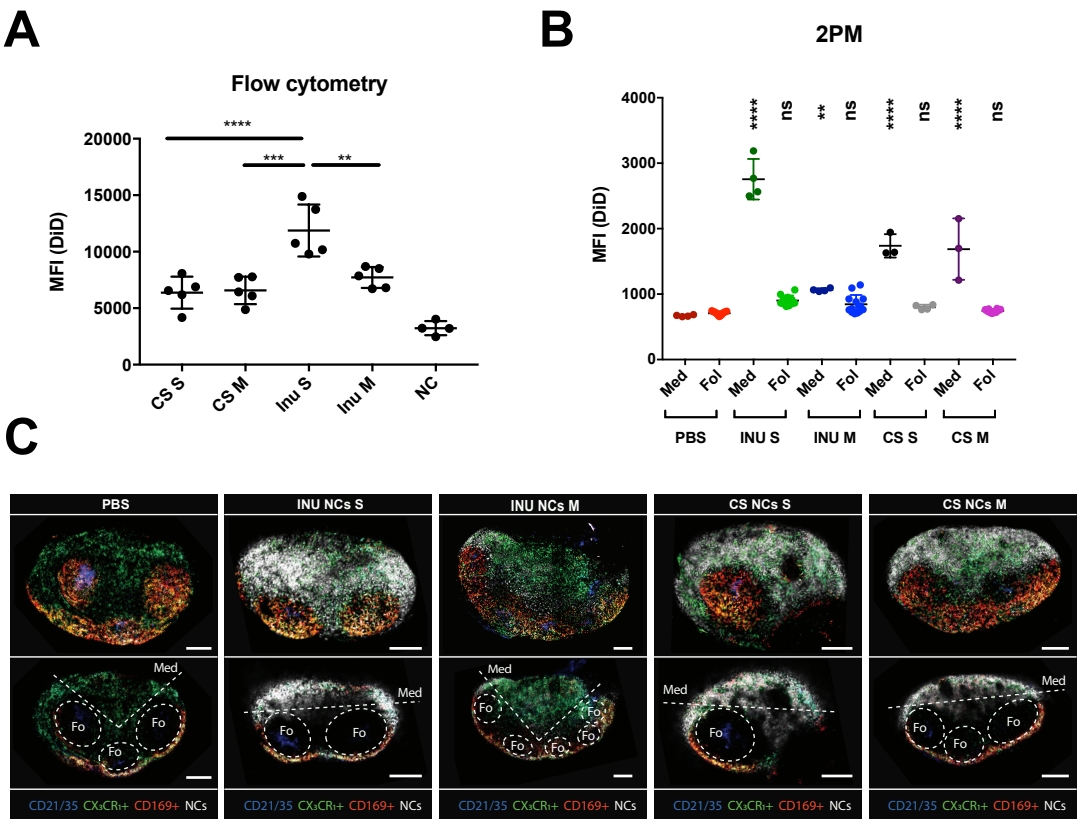

Figure 8. Accumulation of the different nanosystems in the popliteal lymph nodes (PLNs). Chitosan (CS) and inulin (INU) nanocapsules (NCs) of two different sizes (S, <100 nm and M, >100 nm) and labeled with DiD were injected in the footpad of $CX_3CR_1^{+/gfp}$ and C57BL/6JRj mice (5 animals per group). After 12 hours the PLNs from C57BL/6JRj were digested and the mean fluorescence intensity (MFI) evaluated by flow citometry (A). PLNs from $CX_3CR_1^{+/gfp}$ mice were evaluated using 2-photon microscopy (2PM). With this technique the MFI of each nanosytem in the medullar (Med) and the follicular (Fol) region was quantified (B). In C, a representative image of the PLNs. The upper row shows a maximum intensity projection of the whole z-stack of the lymph node, while lower row shows a slice with the different regions highlighted. Subcapsular sinus macrophages (CD169+) are shown in red, nanocapsules (NCs) in white, in blue the follicular dendritic cells (CD21/35+) and in green cells of myeloid origin expressing CX_3CR_1 receptor. One-way ANOVA, Brown-Forsythe test. The differences were considered significant for * $p < 0.05$, ** $p < 0.01$ and *** $p < 0.001$ and **** $p < 0.0001$.

3.3.1. NCs capture by different subsets of immune cells

The delivery of drugs to particular cell subsets can improve the therapeutic index by concentrating their action on the desired cells. Besides, the immune response induced by the different cell subsets after their interaction with an antigen or a NP system could be different, not only regarding its intensity but also the type of immune response (cellular *vs* humoral, activation *vs* tolerogenic, etc.) [64,65]. To detect which populations were mainly responsible for different NCs uptake, we measured the DiD mean fluorescence intensity (MFI) in cells subtypes of the innate compartment (Fig. 9). The results showed that the majority of MM and CD11b+ DCs were positive for DiD,

this meaning that they captured and/or interacted with the NCs. High percentages of positive cells were observed also in SSM, whereas lower percentages were detected in CD11b- DCs, monocytes, neutrophils and NK cells. Among the different NCs, INU NCs S were the ones that were captured to a higher extent by all the cell subtypes confirming the results showed in Fig. 8. On the other hand, CS NCs S showed higher counts (similar to INU NCs S) of positive CD11b+ DCs, monocytes, neutrophils and NK cells (Fig. 9D and 9E). Manolova *et al.* already evaluated the accumulation of model polystyrene beads in different subpopulations of immune cells, demonstrating that the beads were captured by both $CD11c^{+}$ and $CD11c^{-}$ DCs. Besides, similarly to our findings, they showed that the larger the particles the less they were captured by macrophages [60]. That is a remarkable result because, although the accumulation of CS NCs S and M was the same, the small particle sizes NCs were taken-up to a higher extent by specific subsets of immune cells. Probably, in these cells, the influence of the particle size in the uptake is more emphasized. At the same time, the results correlates with the *in vitro* data, showing a preference of DCs by small particle sizes.

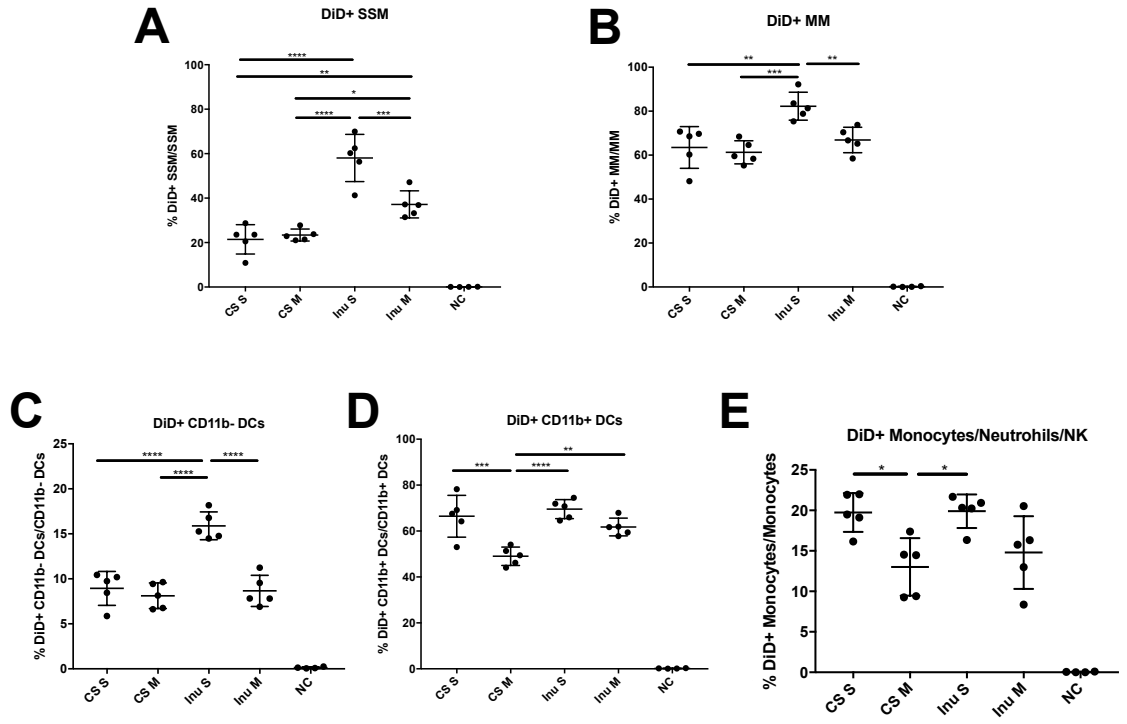

Figure 9: Percentage of the different subsets of immune cells in the popliteal lymph node (PLN) that interact with the nanocapsules (NCs). Chitosan (CS) and inulin (INU) nanocapsules (NCs) of two different sizes (S, <100 nm and M, >100 nm) were injected in the footpad of B6 mice (5 animals per group). After 12 hours the PLNs were collected, enzymatically digested and stained with an antibody panel specific to, macrophages (MHC II+, CD11b+, CD11c intlow, CD169+, and F4/80 positive in medullary macrophages, MM, and negative in subcapsular sinus macrophages, SSM), dendritic cells (DC, MHC II+, CD11c+, CD11b positive or negative population) and monocytes/neutrophils/NK cells (MHC II-, CD11b+). Analysis: all statistical analyses were performed assessing normal distribution of samples (Saphiro-Wilk test) and applying a one-way ANOVA test. *P < 0.05, **P < 0.01, ***P < 0.001, **** P < 0.0001.

To the best of our knowledge, this is the first systematic study intended to evaluate the preferential passive accumulation of NPs in the different subtypes of immune cells in the LNs depending on their size and composition. Overall, the *in vivo* results highlight the fact that small negatively charged NC have a more efficient drainage than positively charged NCs and that, depending on the particle size, the accumulation in the different subsets of immune cells can be passively targeted.

4. Conclusions

Achieving an effective lymphatic accumulation of nanoparticles could be of capital importance for designing modern vaccines. It is well known that the particle size of the nanosystems influences their uptake by the immune cells and the lymphatic drainage. However, the concomitant influence of the particle size and other factors, such as the surface charge inherent to the particle composition, makes it very difficult to withdraw general assertions. An overall conclusion from this work is that, irrespective of their composition (CS NCs vs. INU NCs), small particle sizes favored both, cell uptake and biodistribution. Nevertheless, the composition of the NCs did influence the activation of the immune cells, being those made of CS the ones leading to an upregulation of activation markers in dendritic cells and to a higher secretion of cytokines *in vitro*. However, these results do not mean that INU NCs cannot have an adjuvant effect. In fact, INU operates by a non-inflammatory mechanism, explaining its low reactogenicity. This makes this biomaterial of great interest. Besides, the lymphatic drainage after subcutaneous administration showed that small INU NCs accumulated in a higher extent in the lymph nodes as compared with the rest of the prototypes. All nanosystems were found in macrophages, dendritic cells and monocytes, neutrophils and NK cells but in different proportions depending on the size and the shell polymer. Finally, the two-photon microscopy allowed the visualization of the precise biodistribution of the NCs in the different regions of the lymph node, highlighting the potential of this technique to analyze the lymphatic targeting of the nanosystems. Future studies are needed to evaluate the therapeutic potential of drug-loaded inulin nanocapsules designed to maximize the accumulation in the lymph nodes and targeted to different subsets of immune cells.

References

[1] T.G. Dacoba, A. Olivera, D. Torres, J. Crecente-Campo, M.J. Alonso, Modulating the immune system through nanotechnology., Semin. Immunol. 34 (2017) 78–102. doi:10.1016/j.smim.2017.09.007.

[2] J.M. Tran Janco, P. Lamichhane, L. Karyampudi, K.L. Knutson, Tumor-Infiltrating Dendritic Cells in Cancer Pathogenesis, J. Immunol. 194 (2015) 2985–2991. doi:10.4049/jimmunol.1403134.

[3] K. Sehgal, K.M. Dhodapkar, M. V. Dhodapkar, Targeting human dendritic cells in situ to improve vaccines, Immunol. Lett. 162 (2014) 59–67. doi:10.1016/j.imlet.2014.07.004.

[4] M. V. Lozano, D. Torrecilla, D. Torres, A. Vidal, F. Domínguez, M.J. Alonso, Highly Efficient System To Deliver Taxanes into Tumor Cells: Docetaxel-Loaded Chitosan Oligomer Colloidal Carriers, Biomacromolecules. 9 (2008) 2186–2193. doi:10.1021/bm800298u.

[5] D. Torrecilla, M. V. Lozano, E. Lallana, J.I. Neissa, R. Novoa-Carballal, A. Vidal, et al., Anti-tumor efficacy of chitosan-g-poly(ethylene glycol) nanocapsules containing docetaxel: Anti-TMEFF-2 functionalized nanocapsules vs. non-functionalized nanocapsules, Eur. J. Pharm. Biopharm. 83 (2013) 330–337. doi:10.1016/j.ejpb.2012.10.017.

[6] M. V Lozano, H. Esteban, J. Brea, M.I. Loza, D. Torres, M.J. Alonso, Intracellular delivery of docetaxel using freeze-dried polysaccharide nanocapsules., J. Microencapsul. 30 (2013) 181–8. doi:10.3109/02652048.2012.714411.

[7] F.A. Oyarzun-Ampuero, G.R. Rivera-Rodríguez, M.J. Alonso, D. Torres, G.R. Rivera-Rodriguez, M.J. Alonso, et al., Hyaluronan nanocapsules as a new vehicle for intracellular drug delivery, Eur. J. Pharm. Sci. 49 (2013) 483–490. doi:10.1016/j.ejps.2013.05.008.

[8] G.R. Rivera-Rodríguez, M.J. Alonso, D. Torres, Poly-l-asparagine nanocapsules as anticancer drug delivery vehicles, Eur. J. Pharm. Biopharm. 85 (2013) 481–487. doi:10.1016/j.ejpb.2013.08.001.

[9] G.R. Rivera-Rodriguez, G. Lollo, T. Montier, J.P. Benoit, C. Passirani, M.J. Alonso, et al., In vivo evaluation of poly-l-asparagine nanocapsules as carriers for anti-cancer drug delivery, Int. J. Pharm. 458 (2013) 83–89. doi:10.1016/j.ijpharm.2013.09.038.

[10] M. V. Lozano, G. Lollo, M. Alonso-Nocelo, J. Brea, A. Vidal, D. Torres, et al., Polyarginine nanocapsules: A new platform for intracellular drug delivery, J. Nanoparticle Res. 15 (2013). doi:10.1007/s11051-013-1515-7.

[11] G. Lollo, G.R. Rivera-Rodriguez, J. Bejaud, T. Montier, C. Passirani, J.P. Benoit, et al., Polyglutamic acid-PEG nanocapsules as long circulating carriers for the delivery of docetaxel, Eur. J. Pharm. Biopharm. 87 (2014) 47–54. doi:10.1016/j.ejpb.2014.02.004.

[12] T. Gonzalo, G. Lollo, M. Garcia-Fuentes, D. Torres, J. Correa, R. Riguera, et al., A new potential nano-oncological therapy based on polyamino acid nanocapsules, J. Control. Release. 169 (2013) 10–16. doi:10.1016/j.jconrel.2013.03.037.

[13] G. Lollo, P. Hervella, P. Calvo, P. Aviles, M.J. Guillen, M. Garcia-Fuentes, et al., Enhanced in vivo therapeutic efficacy of plitidepsin-loaded nanocapsules decorated with a new poly-aminoacid-PEG derivative, Int. J. Pharm. 483 (2015) 212–219. doi:10.1016/j.ijpharm.2015.02.028.

[14] S. Vicente, M. Peleteiro, B. Díaz-Freitas, A. Sanchez, Á. González-Fernández, M.J. Alonso, Co-delivery of viral proteins and a TLR7 agonist from polysaccharide nanocapsules: A needle-free vaccination strategy, J. Control. Release. 172 (2013) 773–781. doi:10.1016/j.jconrel.2013.09.012.

[15] S. Vicente, M. Peleteiro, J.V. González-Aramundiz, B. Díaz-Freitas, S. Martínez-Pulgarín, J.I. Neissa, et al., Highly versatile immunostimulating nanocapsules for specific immune potentiation., Nanomedicine (London). 9 (2014) 2273–2289. doi:10.2217/nnm.14.10.

[16] T. Fifis, A. Gamvrellis, B. Crimeen-Irwin, G.A. Pietersz, J. Li, P.L. Mottram, et al., Size-dependent immunogenicity: therapeutic and protective properties of nano-vaccines against tumors, J. Immunol. 173 (2004) 3148–3154. doi:10.4049/jimmunol.173.5.3148.

[17] C. Foged, B. Brodin, S. Frokjaer, A. Sundblad, Particle size and surface charge affect particle uptake by human dendritic cells in an in vitro model, Int. J. Pharm. 298 (2005) 315–322. doi:10.1016/j.ijpharm.2005.03.035.

[18] C.A. Fromen, T.B. Rahhal, G.R. Robbins, M.P. Kai, T.W. Shen, J.C. Luft, et al., Nanoparticle surface charge impacts distribution, uptake and lymph node trafficking by pulmonary antigen-presenting cells, Nanomedicine Nanotechnology, Biol. Med. 12 (2016) 677–687. doi:10.1016/j.nano.2015.11.002.

[19] H. Kim, T. Uto, T. Akagi, M. Baba, M. Akashi, Amphiphilic Poly(Amino Acid) Nanoparticles Induce

Size-Dependent Dendritic Cell Maturation, Adv. Funct. Mater. 20 (2010) 3925–3931. doi:10.1002/adfm.201000021.

[20] S. Vicente, B.A. Goins, A. Sanchez, M.J. Alonso, W.T. Phillips, Biodistribution and lymph node retention of polysaccharide-based immunostimulating nanocapsules, Vaccine. 32 (2014) 1685–1692. doi:10.1016/j.vaccine.2014.01.059.

[21] R. Abellan-Pose, C. Teijeiro-Valiño, M.J. Santander-Ortega, E. Borrajo, A. Vidal, M. Garcia-Fuentes, et al., Polyaminoacid nanocapsules for drug delivery to the lymphatic system: Effect of the particle size, Int. J. Pharm. 509 (2016) 107–117. doi:10.1016/j.ijpharm.2016.05.034.

[22] M.F. Bachmann, G.T. Jennings, Vaccine delivery: a matter of size, geometry, kinetics and molecular patterns, Nat. Rev. Immunol. 10 (2010) 787–796. doi:10.1038/nri2868.

[23] R. Bastola, G. Noh, T. Keum, S. Bashyal, J.-E. Seo, J. Choi, et al., Vaccine adjuvants: smart components to boost the immune system, Arch. Pharm. Res. 40 (2017) 1238–1248. doi:10.1007/s12272-017-0969-z.

[24] H. Jiang, Q. Wang, X. Sun, Lymph node targeting strategies to improve vaccination efficacy, J. Control. Release. 267 (2017) 47–56. doi:10.1016/j.jconrel.2017.08.009.

[25] T.J. Moyer, A.C. Zmolek, D.D.J. Irvine, W. Koff, B. Walker, D. Burton, et al., Beyond antigens and adjuvants: formulating future vaccines, J. Clin. Invest. 126 (2016) 799–808. doi:10.1172/JCI81083.

[26] S.T. Reddy, M.A. Swartz, J.A. Hubbell, Targeting dendritic cells with biomaterials: developing the next generation of vaccines, Trends Immunol. 27 (2006) 573–579. doi:10.1016/j.it.2006.10.005.

[27] D.J. Irvine, M.C. Hanson, K. Rakhra, T. Tokatlian, Synthetic Nanoparticles for Vaccines and Immunotherapy, Chem. Rev. 115 (2015) 11109–11146. doi:10.1021/acs.chemrev.5b00109.

[28] K.T. Gause, A.K. Wheatley, J. Cui, Y. Yan, S.J. Kent, F. Caruso, Immunological Principles Guiding the Rational Design of Particles for Vaccine Delivery, ACS Nano. 11 (2017) 54–68. doi:10.1021/acsnano.6b07343.

[29] A. Gutjahr, C. Phelip, A.-L. Coolen, C. Monge, A.-S. Boisgard, S. Paul, et al., Biodegradable Polymeric Nanoparticles-Based Vaccine Adjuvants for Lymph Nodes Targeting, Vaccines 2016, Vol. 4, Page 34. 4 (2016) 34. doi:10.3390/VACCINES4040034.

[30] Q. Zeng, H. Jiang, T. Wang, Z. Zhang, T. Gong, X. Sun, Cationic micelle delivery of Trp2 peptide for efficient lymphatic draining and enhanced cytotoxic T-lymphocyte responses, J. Control. Release. 200 (2015) 1–12. doi:10.1016/j.jconrel.2014.12.024.

[31] D.A. DA Rao, M.L.M. Forrest, A.W. Alani, G.S. Kwon, J.R. Robinson, Biodegradable PLGA based nanoparticles for sustained regional lymphatic drug delivery, J. Pharm. Sci. 99 (2010) 2018–2031. doi:10.1002/jps.

[32] C.D. Kaur, M. Nahar, N.K. Jain, Lymphatic targeting of zidovudine using surface-engineered liposomes., J. Drug Target. 16 (2008) 798–805. doi:10.1080/10611860802475688.

[33] K. Siram, G. Marslin, C.V. Raghavan, K. Balakumar, H. Rahman, G. Franklin, A brief perspective on the diverging theories of lymphatic targeting with colloids, Int. J. Nanomedicine. 11 (2016) 2867–2872. doi:10.2147/IJN.S105852.

[34] S. De Koker, J. Cui, N. Vanparijs, L. Albertazzi, J. Grooten, F. Caruso, et al., Engineering Polymer Hydrogel Nanoparticles for Lymph Node-Targeted Delivery, Angew. Chemie Int. Ed. 55 (2016) 1334–1339. doi:10.1002/anie.201508626.

[35] X. Zhan, K.K. Tran, H. Shen, Effect of the Poly(ethylene glycol) (PEG) Density on the Access and Uptake of Particles by Antigen-Presenting Cells (APCs) after Subcutaneous Administration, Mol. Pharm. 9 (2012) 3442–3451. doi:10.1021/mp300190g.

[36] D. Braun, A two-step induction of indoleamine 2,3 dioxygenase (IDO) activity during dendritic-cell maturation, Blood. 106 (2005) 2375–2381. doi:10.1182/blood-2005-03-0979.

[37] S. Jung, J. Aliberti, P. Graemmel, M.J. Sunshine, G.W. Kreutzberg, A. Sher, et al., Analysis of Fractalkine Receptor CX3CR1 Function by Targeted Deletion and Green Fluorescent Protein Reporter Gene Insertion, Mol. Cell. Biol. 20 (2000) 4106–4114. doi:10.1128/MCB.20.11.4106-4114.2000.

[38] N. Benne, J. van Duijn, J. Kuiper, W. Jiskoot, B. Slütter, Orchestrating immune responses: How size, shape and rigidity affect the immunogenicity of particulate vaccines, J. Control. Release. 234 (2016) 124–134. doi:10.1016/j.jconrel.2016.05.033.

[39] N. Hoshyar, S. Gray, H. Han, G. Bao, The effect of nanoparticle size on in vivo pharmacokinetics and cellular interaction, Nanomedicine. (2016). doi:10.2217/nnm.16.5.

[40] A. Gamvrellis, D. Leong, J.C. Hanley, S.D. Xiang, P. Mottram, M. Plebanski, Vaccines that facilitate

antigen entry into dendritic cells, Immunol. Cell Biol. 82 (2004) 506–516. doi:10.1111/j.0818-9641.2004.01271.x.

[41] L. Thiele, B. Rothen-Rutishauser, S. Jilek, H. Wunderli-Allenspach, H.P. Merkle, E. Walter, Evaluation of particle uptake in human blood monocyte-derived cells in vitro. Does phagocytosis activity of dendritic cells measure up with macrophages?, J. Control. Release. 76 (2001) 59–71.

[42] C. Villiers, M. Chevallet, H. Diemer, R. Couderc, H. Freitas, A. Van Dorsselaer, et al., From Secretome Analysis to Immunology, Mol. Cell. Proteomics. 8 (2009) 1252–1264. doi:10.1074/mcp.M800589-MCP200.

[43] B. Koppolu, D.A. Zaharoff, The effect of antigen encapsulation in chitosan particles on uptake, activation and presentation by antigen presenting cells, Biomaterials. 34 (2013) 2359–2369. doi:10.1016/j.biomaterials.2012.11.066.

[44] M.K.S. Rajput, S.S. Kesharwani, S. Kumar, P. Muley, S. Narisetty, H. Tummala, Dendritic Cell-Targeted Nanovaccine Delivery System Prepared with an Immune-Active Polymer, ACS Appl. Mater. Interfaces. 10 (2018) 27589–27602. doi:10.1021/acsami.8b02019.

[45] K.L. Rock, H. Kono, The Inflammatory Response to Cell Death, Annu. Rev. Pathol. Mech. Dis. 3 (2008) 99–126. doi:10.1146/annurev.pathmechdis.3.121806.151456.

[46] A.L. Mellor, H. Lemos, L. Huang, Indoleamine 2,3-Dioxygenase and Tolerance: Where Are We Now?, Front. Immunol. 8 (2017) 1–6. doi:10.3389/fimmu.2017.01360.

[47] L. Jia, X. Gao, Y. Wang, N. Yao, X. Zhang, Structural, phenotypic and functional maturation of bone marrow dendritic cells (BMDCs) induced by Chitosan (CTS), Biologicals. 42 (2014) 334–338. doi:10.1016/j.biologicals.2014.07.004.

[48] M. Oliveira, S. Santos, M. Oliveira, A. Torres, M. Barbosa, Chitosan drives anti-inflammatory macrophage polarisation and pro-inflammatory dendritic cell stimulation, Eur. Cells Mater. 24 (2012) 136–153. doi:10.22203/eCM.v024a10.

[49] L. Vogt, D. Meyer, G. Pullens, M. Faas, M. Smelt, K. Venema, et al., Immunological Properties of Inulin-Type Fructans, Crit. Rev. Food Sci. Nutr. 55 (2015) 414–436. doi:10.1080/10408398.2012.656772.

[50] L. Li, Y. Honda-Okubo, C. Li, D. Sajkov, N. Petrovsky, Delta inulin adjuvant enhances plasmablast generation, expression of activation-induced cytidine deaminase and B-cell affinity maturation in human subjects receiving seasonal influenza vaccine, PLoS One. 10 (2015) 1–18. doi:10.1371/journal.pone.0132003.

[51] J. Tomar, H.P. Patil, G. Bracho, W.F. Tonnis, H.W. Frijlink, N. Petrovsky, et al., Advax augments B and T cell responses upon influenza vaccination via the respiratory tract and enables complete protection of mice against lethal influenza virus challenge, J. Control. Release. 288 (2018) 199–211. doi:10.1016/j.jconrel.2018.09.006.

[52] Y. Honda-Okubo, A. Kolpe, L. Li, N. Petrovsky, A single immunization with inactivated H1N1 influenza vaccine formulated with delta inulin adjuvant (Advax^{TM}) overcomes pregnancy-associated immune suppression and enhances passive neonatal protection, Vaccine. 32 (2014) 4651–4659. doi:10.1016/j.vaccine.2014.06.057.

[53] Y. Honda-Okubo, C.H. Ong, N. Petrovsky, Advax delta inulin adjuvant overcomes immune immaturity in neonatal mice thereby allowing single-dose influenza vaccine protection, Vaccine. 33 (2015) 4892–4900. doi:10.1016/j.vaccine.2015.07.051.

[54] S.N. Mueller, S. Tian, J.M. DeSimone, Rapid and Persistent Delivery of Antigen by Lymph Node Targeting PRINT Nanoparticle Vaccine Carrier To Promote Humoral Immunity, Mol. Pharm. 12 (2015) 1356–1365. doi:10.1021/mp500589c.

[55] B. Ballou, S.K. Andreko, E. Osuna-Highley, M. McRaven, T. Catalone, M.P. Bruchez, et al., Nanoparticle Transport from Mouse Vagina to Adjacent Lymph Nodes, PLoS One. 7 (2012). doi:10.1371/journal.pone.0051995.

[56] J.H. Park, J. Park, S. Kim, S.H. Kim, T.G. Lee, J.Y. Lee, et al., Characterization and application of porous gold nanoparticles as 2-photon luminescence imaging agents: 20-fold brighter than gold nanorods, J. Biophotonics. 11 (2018) 1–7. doi:10.1002/jbio.201700174.

[57] L.N. Thwala, A. Beloqui, N.S. Csaba, D. González-Touceda, S. Tovar, C. Dieguez, et al., The interaction of protamine nanocapsules with the intestinal epithelium: A mechanistic approach, J. Control. Release. 243 (2016) 109–120. doi:10.1016/j.jconrel.2016.10.002.

[58] S. Reimondez-troitiño, I. Alcalde, N. Csaba, A. Íñigo-portugués, M. De Fuente, F. Bech, Polymeric nanocapsules : a potential new therapy for corneal wound healing, Drug Deliv. Transl. Res. (2016) 708–721. doi:10.1007/s13346-016-0312-0.

[59] E. Borrajo, R. Abellan-Pose, A. Soto, M. Garcia-Fuentes, N. Csaba, M.J. Alonso, et al., Docetaxel-loaded polyglutamic acid-PEG nanocapsules for the treatment of metastatic cancer, J. Control. Release. 238 (2016) 263–271. doi:10.1016/j.jconrel.2016.07.048.

[60] V. Manolova, A. Flace, M. Bauer, K. Schwarz, P. Saudan, M.F. Bachmann, Nanoparticles target distinct dendritic cell populations according to their size., Eur. J. Immunol. 38 (2008) 1404–13. doi:10.1002/eji.200737984.

[61] M. Pitorre, G. Bastiat, E.M. dit Chatel, J.-P. Benoit, Passive and specific targeting of lymph nodes: the influence of the administration route, Eur. J. Nanomedicine. 7 (2015) 121–128. doi:10.1515/ejnm-2015-0003.

[62] R. Abellán-pose, N. Csaba, M.J. Alonso, Lymphatic Targeting of Nanosystems for Anticancer Drug Therapy, (2016) 1194–1209.

[63] F. Shima, T. Uto, T. Akagi, M. Baba, M. Akashi, Size effect of amphiphilic poly(γ-glutamic acid) nanoparticles on cellular uptake and maturation of dendritic cells in vivo., Acta Biomater. 9 (2013) 8894–901. doi:10.1016/j.actbio.2013.06.010.

[64] M. Rincon-Restrepo, A. Mayer, S. Hauert, D.K. Bonner, E.A. Phelps, J.A. Hubbell, et al., Vaccine nanocarriers: Coupling intracellular pathways and cellular biodistribution to control CD4 vs CD8 T cell responses, Biomaterials. 132 (2017) 48–58. doi:10.1016/j.biomaterials.2017.03.047.

[65] S.F. Gonzalez, V. Lukacs-Kornek, M.P. Kuligowski, L.A. Pitcher, S.E. Degn, Y.A. Kim, et al., Capture of influenza by medullary dendritic cells via SIGN-R1 is essential for humoral immunity in draining lymph nodes, Nat. Immunol. 11 (2010) 427–434. doi:10.1038/ni.1856.

Overall discussion

Nanotechnology is considered a useful tool for overcoming the limitations of newly developed and poorly immunogenic subunit vaccines [1–3]. Indeed, nanocarriers have been shown to protect the integrity of their associated antigens once in the body, and to modify their biodistribution, thereby offering the possibility to modulate the immune response towards either a Th1 or a Th2 profile [4–6].

In the scope of this work, we have focused on polymeric nanocapsules (NCs) as a carrier for purified protein antigens. NCs are nanometric systems with an inner core and an external polymeric shell. Due to their lipidic core, NCs were, originally, conceived as suitable carriers for lipophilic drugs. However, our lab has expanded this technology to allow NCs to carry hydrosoluble macromolecules, such as proteins [7,8], peptides [9–11], and polynucleotides [12], and their use in different therapeutic areas. In the vaccinology field, we have successfully associated protein antigens, such as tetanus toxoid [8] influenza antigen [13] and hepatitis B antigen [14] to different NCs. In the last two decades, we have gathered considerable knowledge regarding the preparation and behavior of different polymeric NCs, with especial interest in chitosan (CS) NCs, a system that was pioneered by our group [15]. In fact, we have previously reported that CS NCs were efficient vehicles for the delivery of a recombinant hepatitis B vaccine [7]. Furthermore, we additionally disclosed that the incorporation of the immunostimulant imiquimod to the oily core could further contribute to achieve a significant and long-lasting IgG response, following either nasal or intramuscular administration [14,16].

Considering this background, the first aim of this work was to develop bilayer polymeric NCs intended to protect and control the release of IutA antigen from uropathogenic *E. coli* (UPEC). The potential of this antigen for the treatment of urinary tract infections caused by UPEC has been reported in the literature [17,18].

1. Bilayer polymeric nanocapsules: a formulation approach for *E. coli* antigen vaccine

The performance of the nanovaccines is significantly influenced by their physicochemical properties, their composition, and the structural organization of their associated antigen cargo. Besides, an efficient entrapment of the antigen to the nanosystem is a prerequisite in the formulation of a nanovaccine [19]. For this reason, we first focused on the selection of the nanosystem components that could potentially promote antigen association efficiency, and that would, ultimately, influence the performance of the nanocarrier. Later, an adequate architectural organization that consisted of a protein antigen held between two polymers with opposite charge was built, thus creating a bilayer nanosystem (Fig. 1).

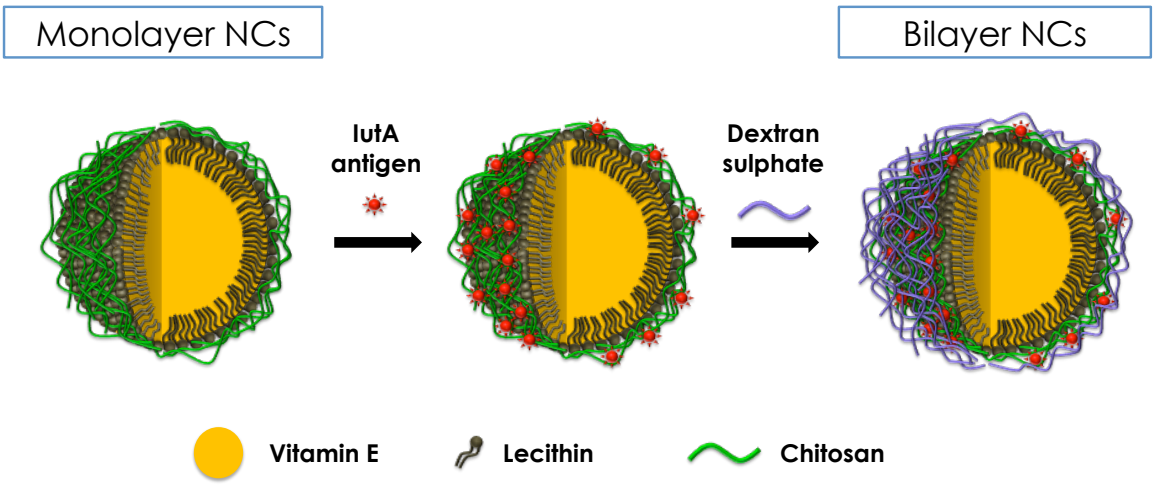

Figure 1. Scheme of the preparation of bilayer nanocapsules (NCs). In the bilayer nanosystem the antigen was entrapped between two polymer layers: chitosan and dextran sulfate.

A first screening, using compounds with interest in the vaccinology field, was performed in order to identify a composition that guaranteed an optimal IutA antigen loading while keeping adequate physicochemical properties. For this purpose, different oils (squalene, vitamin E, Miglyol® 812 and oleic acid), surfactants (PEG-stearate, TPGS, Tween® 80, lecithin, Poloxamer® 407 and sodium cholate) and polymers (CS, protamine and polyarginine) were used to prepare a panel of different polymeric NCs. After their characterization, the IutA antigen was associated to the NCs by simple incubation. The main conclusion was that, as expected, the surfactant and the polymer forming the shell had an important influence in the IutA association efficiency. Considering that IutA is an amphiphilic membrane protein, its association to the NCs may involve not only electrostatic but also hydrophobic forces. After incubation with the NCs, the protein would interact with the surfactant layer and the polymeric shell, being these two the components that have an impact on the association efficiency levels.

Based on the screening above mentioned, NCs with vitamin E in the oily core and a shell consisting of lecithin and CS in the polymeric shell were selected as adequate carriers for IutA (Table 1). Nevertheless, proteins associated to the polymeric shell of the NCs may be prematurely exposed to the physiological environment leading to their inactivation or uncontrolled release. To prevent this potential problem, we designed a sandwich-like structure in which the antigen was protected between a bilayer that surrounds the immunostimulating oily nanocore.

In a first step, the objective was to combine the layer-by-layer (LbL) approach with the solvent displacement method in order modify the surface composition of the NCs [20,21]. For the preparation of bilayer nanosystems, CS/lecithin/vitamin E monolayer NCs were incubated with different ratios of sulfated and carboxylated polyanions: hyaluronate (HA), alginate (Alg), chondroitin sulfate (ChS) and dextran sulfate (DS). The bilayer is formed when the surface charge of the NCs change from

positive (monolayer of CS) to negative (anionic polymer). The mass/mass ratio at which this inversion happens was, ultimately, determined by the relative charge of the second polymer. In the case of the tested polymers, the charges per monomer at pH = 7 are: HA (0.5) < Alg (1) = ChS (1) < DS (2.3). These charges explain why a small amount of DS (ratio CS:DS 1:01) led to an important inversion in the ζ-potential. In contrast, in the case of ChS, Alg and HA, a higher amount was required to achieve the surface charge inversion.

Secondly, the goal was to determine the maximum number of layers that could be built over the oily core, without purification steps, and without high-energy inputs that could denature labile molecules. For this purpose, we selected DS, a polymer that has been explored for the formation of nanocomplexes in association with CS [22–28]. The amount of DS needed to obtain an efficient coating was calculated empirically [29]. Using this technique, up to 5 layers of polymers could be built over the NE, without the need of purification steps. The chosen ratio DS:CS was 0.5:1 for the first two layers (bilayer NCs) and for the 3th (CS), 4th (DS) and 5th (CS) layers the ratio polymer:CS-1st-layer was 1:1 with a final ratio $CS_{5th}/DS_{4th}/CS_{3rd}/DS_{2nd}/CS_{1st}$ 1:1:1:05:1. An inversion of the ζ-potential was observed with each new polymer layer added: from highly positive, when the CS was in the external layer, to highly negative, when the DS was the external polymer.

In the process of loading IutA antigen it was found that the addition of the second layer of DS significantly reduced the NCs size down to 200 nm, from the 274 nm previously found for the IutA-loaded monolayer NCs. This change was attributed to the compacting of the loose CS shell due to its electrostatic interaction with DS. Finally, the antigen association efficiency was maintained after the addition of the second layer of the polymer, confirming that DS does not displace the antigen, but keeps it protected in a polymeric sandwich-like structure, as we envisaged.

Table 1. Physico-chemical properties and antigen association efficiency (AE) of selected prototypes for *in vivo* experiments. Results are shown as mean ± SD of, at least, three replicates. n/a not applicable.

Nanosystems	Particle size (nm)	PDI	Z-potential (mV)	AE (%)
Blank CS NCs	166 ± 7	0.2	+ 35 ± 4	n/a
Loaded CS NCs	274 ± 19	0.2	+ 44 ± 2	67 ± 5
Blank DS/CS NCs	196 ± 5	0.1	- 52 ± 3	n/a
Loaded DS/CS NCs	200 ± 2	0.1	- 42 ± 4	71 ± 8

One of the main challenges in vaccine development is to overcome the need for the cold-chain and to guarantee the long-term stability [30]. For that reason, we developed a freeze-drying process using different cryoprotectants (mannitol, sucrose, trehalose and glucose). The best results, in terms of preservation of the initial

physicochemical properties, were obtained using 10% (w/v) of sucrose. FESEM images of the freeze-dried formulations revealed a cheese-like structure with homogeneously distributed holes in the sugar matrix (Fig. 2A), similar to the one reported for PCL NCs freeze-dried with PVA [31].

CS/DS bilayer NCs maintained their particle size (≈ 200 nm) after storage in a freeze-dried form for the full duration of the experiment (12 weeks) (Fig. 2B). However, an important increase in the particle size of the IutA-loaded monolayer CS NCs was observed: from 270 nm, before freeze-drying, to more than 400 nm after the process. These results support the premise that the additional DS layer has a protective role. Noticeably, with regard to the association efficiency, the amount of the attached protein remained the same at least up to 90 days in the freeze-dried formulations (Fig. 2C). These remarkable results would make the potential nanovaccine a thermostable vaccine.

To assess the protective role of the second polymer layer the release from NCs was performed. The results, shown in Fig. 3D, indicate that, when the antigen was entrapped within the bilayer the release was more sustained than when it was simply associated to CS NCs. This difference is greater in the freeze-dried formulations. In this last case, monolayer NCs release around 100% of the antigen during the first 4 hours, while the bilayer nanosystem releases less than 35% within the same timeframe.

Despite the abundant information about the release profiles from micro and nanoparticle formulations intended to work as single-dose formulations [8,32–35], in the case of nanocarriers designed to target the antigen to dendritic cells and achieve a subsequent adjuvant effect, i.e. nanoemulsions and NCs, this information is very limited. Although these *in vitro* release data cannot be extrapolated to *in vivo* conditions, they are meaningful in the sense that they allow us to exclude the possibility of an uncontrolled and premature release upon injection.

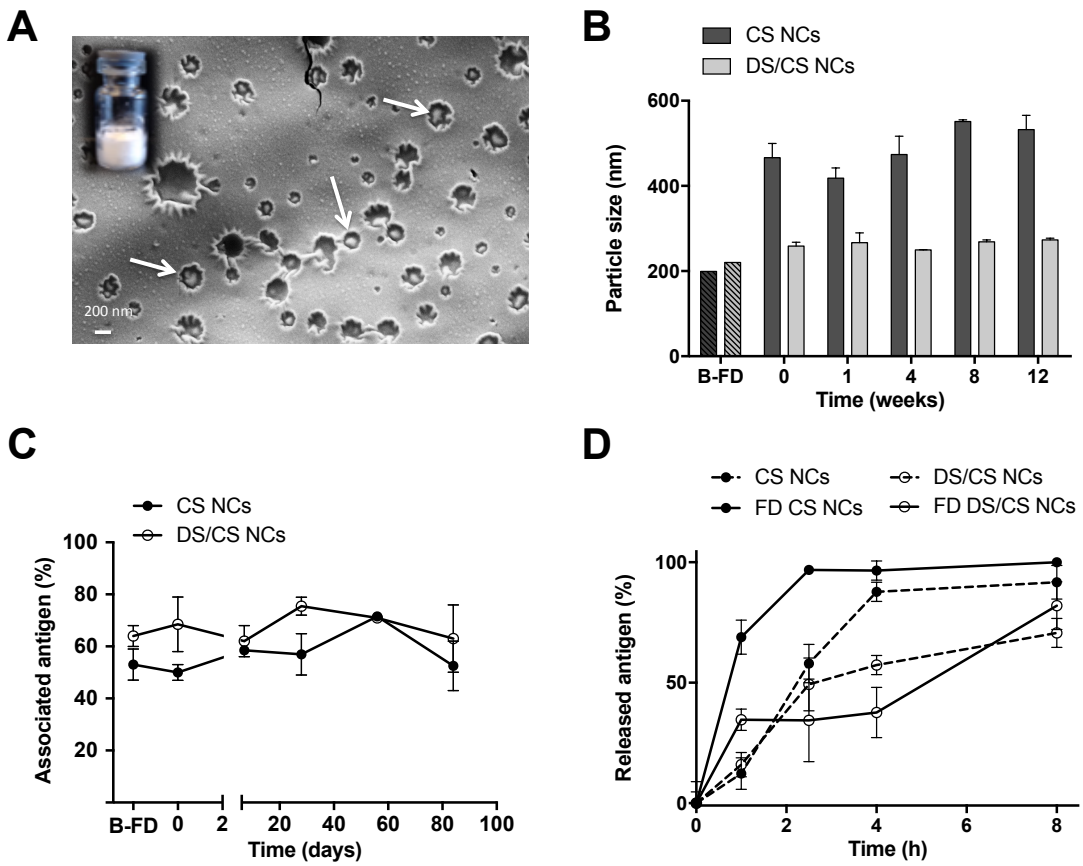

Figure 2. Microscopic structure, stability and IutA release from freeze-dried nanocapsules (NCs). FESEM image of freeze-dried bilayer NCs with 10% sucrose. Arrows point out some shrunken NCs (A). Stability of freeze-dried monolayer and bilayer NCs after up to 3 months of storage at room temperature regarding particle size (B) and antigen association (C) after resuspension. The study of the release of the antigen IutA from freeze-dried (FD) and non freeze-dried monolayer and bilayer NCs was performed in PBS Tween® 80 0.02 % (w/w) at 37 ºC (D). Results are shown as mean ± SD of 3 replicates.

Prior to *in vivo* studies, the cytotoxicity of the nanosystems was evaluated *in vitro* using the murine macrophages (RAW 264.7). A dose-dependent reduction of the viability was observed for both, the monolayer and bilayer NCs. The calculated DL50 were approximately 300 µg/mL for CS NCs, and 200 µg/mL for DS/CS NCs. These values are within the range of those previously reported in the literature for chitosan [16] and protamine NCs [13]. The flow cytometry data revealed that both, single and bilayer NCs strongly interact with macrophages, a result that was also confirmed using confocal microscopy. Cytokine production studies performed in peripheral blood mononuclear cells (PBMCs) from healthy donors indicated that the blank NCs do not stimulate the production of cytokines. Similar results were previously reported for chitosan NCs, despite the fact that they showed a specific and significant adjuvant effect *in vivo* for the hepatitis B antigen associated to them [16]. These results will be further discussed in section 3.

Finally, to test the influence of the composition and architectural disposition (monolayer *vs.* bilayer NCs) of the nanosystems *in vivo*, we measured the humoral immune response elicited by the different antigen-loaded compositions in mice. IutA-

loaded monolayer NCs elicited an immune response similar to the one generated when the protein was adjuvanted with Alum, the gold standard for subcutaneous vaccination (Fig. 3). These results indicate that, in agreement with previous data showing the adjuvant capacity of CS [7], the bilayer NCs further improved the performance of both monolayer NCs and Alum, and cause significantly higher levels of serum IgGs. The benefits of an increased stability together with the adequate physicochemical properties, allows the antigen to be efficiently processed and presented by APCs.

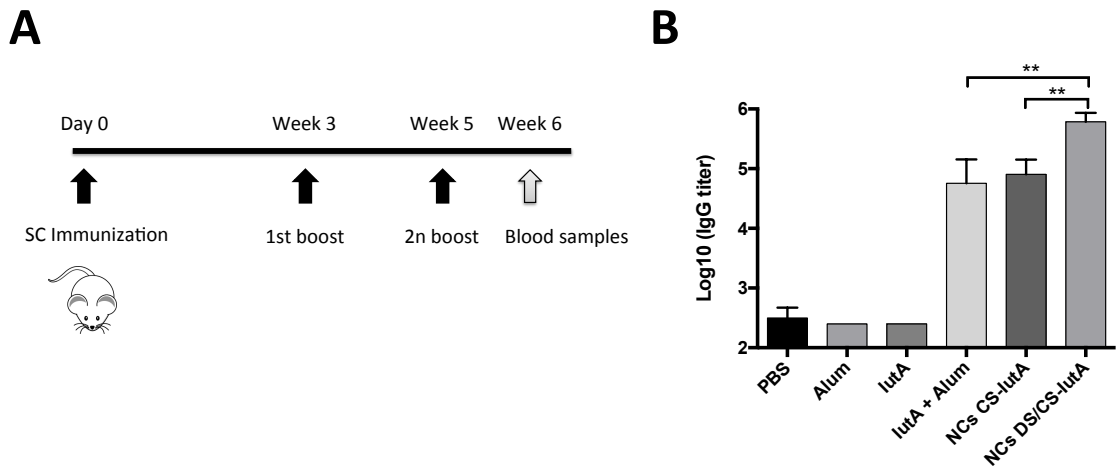

Figure 3. *In vivo* evaluation of the performance of antigen-loaded bilayer nanocapsules (NCs). Timeline of the immunization protocol for testing humoral response generated by these prototypes in mice (A). IgG levels observed upon subcutaneous (0, 3, and 5 weeks) immunization with IutA adsorbed on Alum or IutA-loaded monolayer (CS) and bilayer (DS/CS) NCs (total of 15 µg of IutA per animal). PBS and Alum were used as controls (B). Results are shown as mean ± standard deviation (n = 10). * and ** denote significant differences between groups (for $p < 0.05$, and $p < 0.01$ respectively).

To sum up, the double-shell nanosystem was able to protect the IutA *E. coli* antigen and to control its release more efficiently than monolayer NCs. Furthermore, the resulting nanovaccine candidate showed a very good thermostability profile in a freeze-dried form. The positive outcome observed *in vivo* in terms of the specific IgG response directed against the IutA protein, highlight the value of the developed technology. However, despite the good results obtained using these polymeric NCs, we believed that there was still space for improvement. In fact, the current understanding is that, in order to make significant progress in the vaccine formulation field, it is necessary to design the antigen nanocarriers in a more rational manner. Besides the composition, the physicochemical properties of the nanosystem, such as the particle size and the surface composition, have been shown to be critical for the nanovaccine final outcome, with even small changes in the nanometric region leading to significantly different biological behaviors [36–38]. Nevertheless, prior to any study about the influence of these parameters in the biological performance of the NCs we must develop new methods to be able to produce nanosystems with controllable

particle size. For that reason, the following aim of this work was to investigate the technological possibilities that the solvent displacement technique offers to prepare tailor-made NCs.

2. Expanding the technological possibilities of polymeric NCs

From a technological point of view, it is crucial to have versatile methods that enable the control of the nanosystem's size, as this property is known to influence their interaction with the biological systems [39–41]. Moreover, the production of nanosystems with particle sizes smaller than 100 nm may be of interest in vaccinology, since the small size may favor the lymphatic drainage [42,43].

In this study, in order to elucidate the technological variables the determine the size of the NCs we adopted an experimental design in which we kept constant the mass and ratio of the NCs components of a standard composition, reported in section 1, which consisted on a combination of CS and vitamin E with lecithin as a surfactant. The technological variables investigated were: i) the volume of the organic solvent (ethanol) used to dissolve vitamin E and lecithin, ii) the volume of the aqueous phase (CS aqueous solution), and iii) the way the organic phase was added over the aqueous phase (pouring *vs* injecting). The response surface, presented in Fig. 4, shows that the smallest particle sizes were obtained with the highest volumes of ethanol (5 mL) and water (15 mL), confirming that, as expected, the dilution of lipophilic and hydrophilic components in their respective phases favors the formation of smaller particle sizes. On the other hand, the injection of the organic phase into the aqueous phase has a clear impact in the NCs particle size when compared with the technique consisting on just pouring one phase over the other.

Having this into consideration, we wanted to prove if the particle size reduction effect was or not composition-dependent. For that, we tested different combinations of oils, surfactants and polymers (Fig. 4B). Positive and negative nanoemulsions (NEs) and NCs were prepared either by pouring or by injecting the organic phase over the aqueous phase, at a fixed concentration of the components. A considerable reduction in the particle size was observed for all the formulations when using the injection method (between 50 and 115 nm of size variation) (Fig. 4C) confirming that can be applied to different compositions.

The molecular mechanisms behind the nanodispersion achieved by the solvent displacement technique have been attributed to interfacial turbulences between the solvent and non-solvent phases, known as the Marangoni effect, which leads to the separation of the system into two phases [44,45]. Other authors attribute the formation of the nanoprecipitates to the "ouzo effect" [46,47], which refers to the fact that the local supersaturation of the oil drives a spontaneous nucleation in the form of small oily nanodroplets. The nuclei grow by aggregation or by diffusion of oil molecules

from the surroundings until the oil concentration reaches the equilibrium saturation concentration [48]. Experimentally, to obtain small particles sizes we should favor rapid nuclei formation and little or no particle growth. This can be achieved, as indicated in Fig. 4, by decreasing the concentration of the oil, to avoid particle growth, and/or injecting the non-solvent into the solvent phase, which produces turbulences that create multiple small nuclei of oily nanodroplets.

A

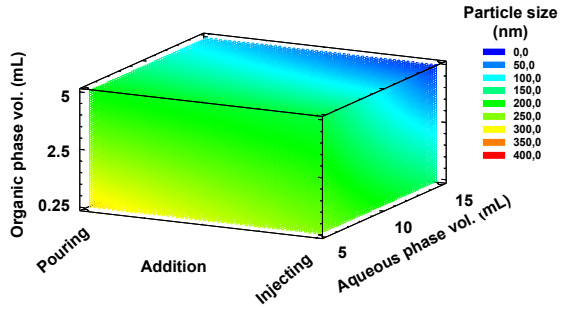

B

Sample	Polymer	Surfactant	Co-surfactant	Oil
NE 1	-	Lecithin	-	Vitamin E
NE 2	-	TPGS	Sodium cholate	Vitamin E
NE 3	-	Tween® 80	-	Vitamin E
NE 4	-	Lecithin	-	Squalene
NE 5	-	Lecithin	-	Miglyol® 812
NE 6	-	Lecithin	CTAB	Vitamin E
NC 1	Alginate	Lecithin	CTAB	Vitamin E
NC 2	Hyaluronate	Lecithin	CTAB	Vitamin E
NC 3	Chitosan	Lecithin	-	Vitamin E
NC 4	Polyarginine	Lecithin	-	Vitamin E

C

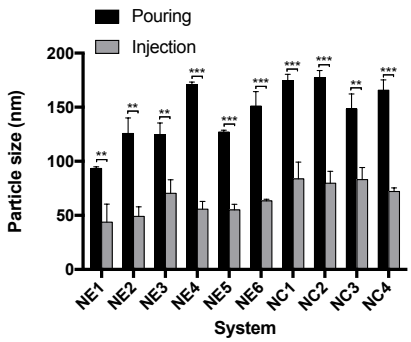

Figure 4. Influence of different production parameters on the particle size of polymeric nanocapsules (NCs). The volumes of both the organic and aqueous phase, and the way the first phase was added over the second (by pouring or injecting through a needle) were varied. The particle size of the resulting nanocapsules was plotted against these three parameters (A). Different combination of oils, surfactants and polymers were tested to produce NEs and NCs upon pouring or injecting the organic phase over the aqueous phase (B). Differences in the particle size of the NCs and NEs obtained with this modification in the preparation procedure are shown in (C). For the comparison a multiple t test was performed. ** and *** denote significant differences between samples ($p < 0.01$ and $p < 0.001$ respectively).

3. Comparative behavior of polymeric NCs with regard to their interaction with immune cells, biodistribution and lymphatic targeting. The case of inulin NCs

Taking advantage of the new technological possibilities we have developed for polymeric NCs (section 2), in particular the surface modification using the LbL technique and the controllable particle size in the 50 – 500 nm region, the next aim of this work was to understand the impact of the particle size and the polymeric shell of NCs in their interaction with immune cells, biodistribution and lymphatic targeting. In parallel, we wanted to compare the behavior of CS NC, developed in section 1, with that of those produced with hydrophobized inulin (INU) as a biomaterial hardly explored in the development of drug delivery nanocarriers.

INU, a polysaccharide composed by polyfructose chains with a terminal glucose, is currently being used in the food and pharmaceutical industry as an stabilizing agent and has a GRAS status [49]. In addition, there is a composition consisting of delta-INU in microcrystalline form, that has been tested, as adjuvant, in human clinical trials, including hepatitis B, influenza and allergy vaccines (Advax^{TM}) [50,51]. In contrast with other adjuvants, Advax^{TM} does not activate innate immune receptors such as TLRs or the inflammasome. Instead, delta-INU modulates directly the dendritic cells (DCs) function, resulting in an improved antigen presentation to T and B cells through a non-inflammatory mechanism [52,53]. Therefore, bearing in mind this background information and our extensive experience in the design of polymeric nanocapsules (NCs) [10,54–58], we aimed at designing and characterizing new INU NCs with two different sizes (70 and 250 nm) and to compare their *in vitro* and *in vivo* behavior with that of chitosan NCs of similar sizes. The *in vitro* studies were performed using the most important APCs: macrophages (MΦs) and DCs. On the contrary, the *in vivo* behavior was evaluated in terms of dissemination in zebrafish and lymphatic drainage in a murine model.

3.1. Development and characterization of inulin-based nanosystems

INU, modified with C12 chains, has been used at the research level to increase the solubility of lipophilic drugs [59–65]. However, its potential for the development of drug delivery nanocarriers has been hardly explored. Using vitamin E, a potential immunostimulator, as an oily core, a screening of different ratios INU:vitamin E was performed in order to select the best components combination to produce low polydispersed stable NCs. Then, based on the information disclosed in section 2 (injection of the organic phase over the aqueous phase), INU NCs with a size < 100 nm (S) were produced. For comparative purposes CS NCs with similar sizes and the same core composition were also obtained (Fig. 5).

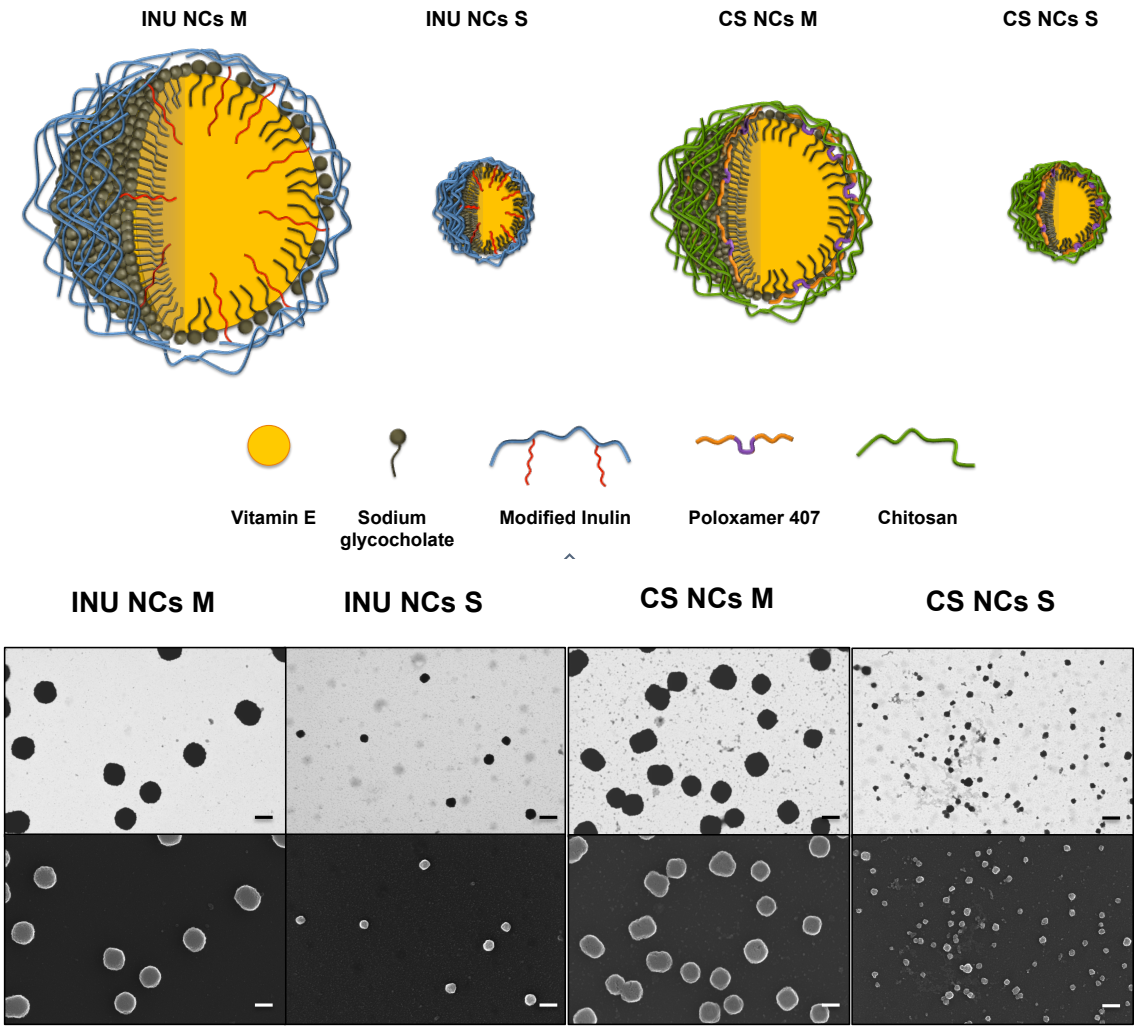

Figure 5. Different polymeric nanocapsules (NCs) developed in this study. Inulin nanocapsules (INU NCs) and chitosan nanocapsules (CS NCs) of two different particle sizes, small (S < 100 nm) and medium (M > 100 nm) size. The size scale between the prototypes was maintained in the draw. In the lower part, field emission scanning electron microscopy (FESEM) images of the different nanosystems using STEM (first row) and InLens (second row) detectors. All scale bars = 200 nm.

Different techniques were used to determine the particle size of the nanosystems (Table 2). FESEM images, using STEM and InLens detectors, corroborated the differences in the particle size of S and M NCs. The round-shape structure of CS and INU NCs was similar, independently of the nature of the polysaccharide shell (Fig. 7).

Table 2. Composition and physicochemical properties of chitosan (CS) and inulin (INU) nanocapsules (NCs) of two different particle sizes (small, S < 100 nm and medium, M > 100 nm)

Nanosystem	CS NCs S	CS NCs M	INU NCs S	INU NCs M
Polymer	Chitosan	Chitosan	Modified inulin	Modified inulin
Surfactant	P407	P407	Modified inulin	Modified inulin
Oil	Vit. E	Vit. E	Vit. E /glycerine	Vit. E /glycerine
Size (nm) by DLS	72 ± 5	172 ± 11	69 ± 6	246 ± 16
Size (nm) by NTA	76 ± 19	128 ± 30	81 ± 27	197 ± 74
PDI	0.16	0.11	0.18	0.12
Z-potential (mV)	+ 37 ± 4	+ 34 ± 4	- 33 ± 8	- 25 ± 11

* co-surfactante = glycocholate, in all cases. P407 = poloxamer 407

3.2. *In vitro* cell studies

DCs and MΦs are the main antigen presenting cells (APCs) in our immune system. MΦs are the key elements in the innate immune system. They are specialized in engulfing and destroying foreign substances, microbes and cellular debris. MΦs also help initiate the adaptive immunity by recruiting other immune cells and they can present antigens to T cells. The latter function is the main goal of DCs, which, in their immature state, patrol all over the body to capture pathogens or foreigner elements. After they are activated, they travel to the lymph nodes (LNs) where they process and present the antigen to T cells and B cells generating an immune response.

As depicted in Fig. 6, CS NCs were more toxic for both, macrophages and DCs, compared to INU NCs. In addition, a tendency was observed for S NCs to be more toxic than M NCs.

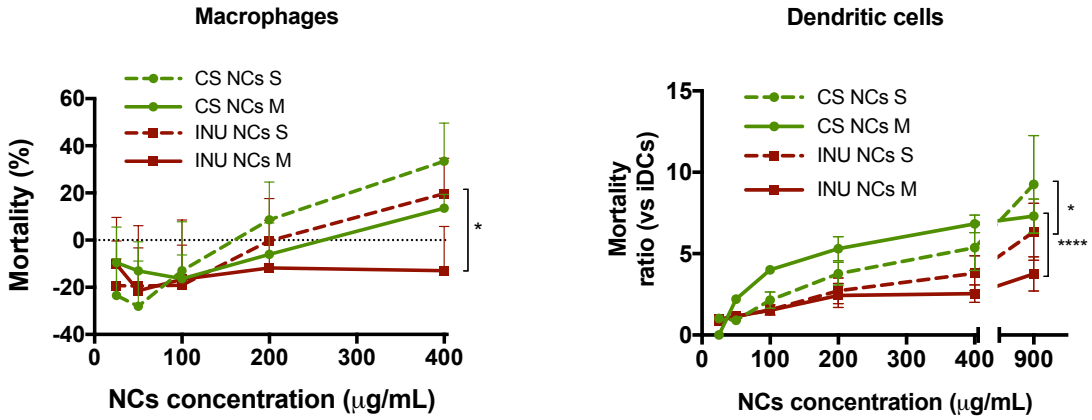

Figure 6. *In vitro* cytotoxicity of the different nanosystems. Inulin (INU) and chitosan (CS) nanocapsules (NCs) of two different sizes, small (S < 100 nm) and medium (M > 100 nm) size were tested. The toxicity was evaluated in murine macrophages RAW by MTS and in immature dendritic cells (iDCs) by flow cytometry, using a vital label. The results by flow cytometry are expressed as the ratio between the percentage of dead iDCs incubated with NC *vs* the percentage of dead iDCs incubated in culture media (for comparative purposes an average of 5% can be considered for mortality of iDCs incubated in culture media). For the statistical analysis the area under the curve for each nanosystem was calculated and the differences between the particles size (S vs M) and the polymer shell (CS vs INU) analyzed using a One-way ANOVA followed by a Tukey test. Significance levels * $p < 0.05$, *** $p < 0.001$ and **** $p < 0.0001$.

In order to determine if toxicity was quantitatively related to the cellular interaction, cells were analyzed by flow cytometry after their incubation with DiD-labeled nanosystems at a non-toxic dose. The results indicated that almost 100% of the MΦs and DCs incubated with the different NCs were DiD+, with the exception of INU NCs M in which this value was lower (Fig. 7). If we consider the mean fluorescence intensity (MFI), the analyses indicated different patterns for DCs and MΦs. Namely, in MΦs, the toxicity results correlate with the fact that small sizes and positively charge NCs interacted in a higher extent with them. Curiously, in the case of DCs, the behavior of all systems was similar, with INU NCs S showing the highest values of fluorescence.

The traditional approach regarding immune cells uptake of NPs, mainly based on *in vitro* studies, suggested that DCs preferentially ingested small NPs, in the viral size range (20 – 200 nm), while MΦs preferred the larger, bacterial-size particles (500 – 2000 nm) [66–68]. Nevertheless, recent studies have questioned this assertion and the current tendency is to believe that small NPs can be also very efficiently taken up by MΦs, and that their preference for smaller or larger particles could be counterbalanced by the composition of the nanosystem. For instance, the uptake of CS NPs by murine MΦs was found to be slightly higher for 300 nm than for 150 nm particles [69]. Similarly, in the case of PLGA NPs, a size-dependent uptake was found in the range 200 – 1000 nm, with bigger NPs being more internalized [70]. However, such a tendency was not observed when comparing lipid NCs of very small sizes (25, 50 and 100 nm), where internalization was similar irrespective of the size [71]. Other authors have reported that the maximal uptake of polypyrrole NPs [72] and PVP-coated iron

oxide NPs [73] was in the region of 10-100 nm compared with larger nanometric particles. This latest work would agree with our data showing the preference of small size in order to achieve a high uptake. In the case of DCs, the majority of the research regarding NPs uptake suggest that small particle sizes are internalized more easily than larger NPs [74,75], similar to what we found in this study.

Regarding the surface charge, we could presume that the positive particles interacted in a higher degree with the immune cells due to their negative surface [75–77]. However, in this study, the preference for positively-charged NCs was evident for MΦs, whereas in the case of DCs such effect was observed for medium size but not for the smallest ones. The higher uptake of small INU NCs as compared to small CS NCs highlights the fact that the surface charge is not the only factor -in addition to the size- influencing the uptake, and that the composition may ultimately drive particle-cell interaction. In this sense, it could be speculated that the presence of poloxamer 407, with polyethyleneglycol chains, in the CS NC's shell might neutralize cell uptake [78].

Overall, it maybe be concluded that the particle size is a critical parameter influencing cell uptake, especially in the case of DCs, and that the effect of the surface charge might be counterbalanced in the case of very small NCs, depending on their composition.

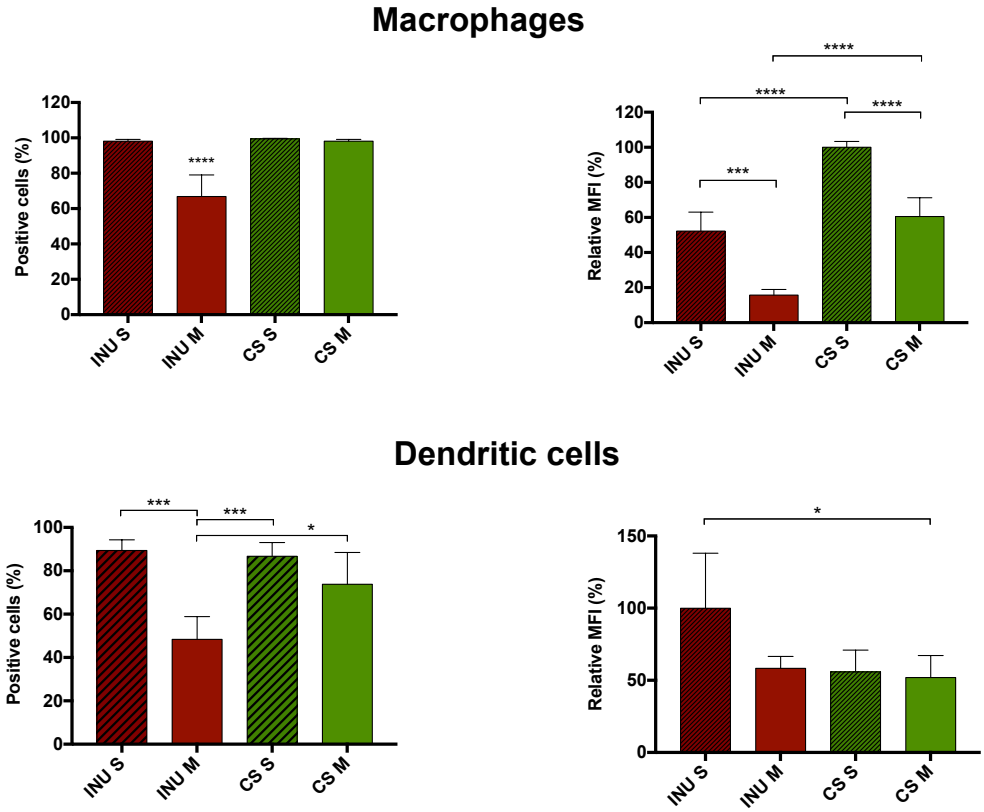

Figure 7. Interaction of the different labelled nanosystems with macrophages and dendritic cells. The interaction of the different nanocapsules (NCs) with the immune cells in terms of percentage of positive cells and normalized mean fluorescence intensity was determined. Inulin (INU) and chitosan (CS) NCs of two different sizes, small (S < 100 nm) and medium (M > 100 nm) were analyzed. Statistical analyses were done using a one-way ANOVA followed by a Tukey test. Significance levels * $p < 0.05$, *** $p < 0.001$ and **** $p < 0.0001$.

Knowing the critical role of DCs in the generation of an adaptive immune response we investigated the type of response that NCs produced on them. Different activation markers were analyzed by flow cytometry after DCs incubation with the four different nanosystems. After 2 h incubation, both, S and M, CS NCs (Fig. 8A) showed a higher capacity of DC activation compared to INU NCs causing a greater increase in the expression of CD80 and CD83 activation markers. Previous studies already reported the activation of these two markers in DCs by different CS NPs [79,80]. In the case of INU NCs, only the small particles showed slight increase in the upregulation of CD83 (Fig. 8B), with a similar tendency for INU NCs M. The higher upregulation of activation markers caused by CS NCs as compared to INU NCs could be related to their higher toxicity (Fig. 6). The induction of a higher cellular dead could contribute to the release of inflammatory signals that would explain also a higher capacity of DCs activation [81].

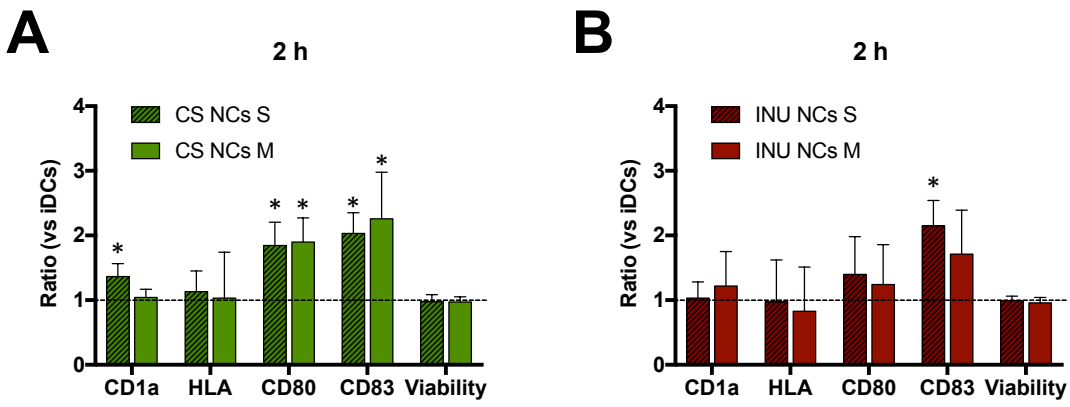

Figure 8. Dendritic cell (DC) activation by the different nanocapsules (NCs). Change in DCs phenotype induced by incubation with chitosan (CS) (A) and inulin (INU) (B) NCs. Small (S, <100 nm) and medium (M, >100 nm) size NCs were tested. Results are shown as the ratio between the iDCs incubated with NC *vs* iDCs incubated in culture media. *: ratio significantly higher than 1 ($p<0.05$; Student's T Test). n.d. Not determined.

To deeper analyze the kind of activation that the different nanosystems produce on DCs, we quantified the cytokines secreted to the culture media by DCs incubated with the different NCs for 24 h (Table 3). Again, CS NCs induced a higher cytokine secretion by DCs compared to INU NCs, a result that is in consonance with previous reports [80,82,83].

Table 1. Cytokine secretion by iDCs after incubation with different nanocapsules (NCs).

Cytokine*	CS NCs S	CS NCs M	INU NCs S	INU NCs M
IFN-γ	+	+	-	-
IL-10	+	++	-	-
IL-12p70	-	-	-	-
IL-5	+++	+++	-	-
IL-8	+	+	+	+
TNF-α	-	-	-	-
TNF-β	+++	+++	+	+

* Data is expressed as the ratio between cytokine secreted by iDCs after treatment with NCs and cytokine secreted by iDCs incubated in media alone. Symbols: -: ratio ≤ 1; +: ratio 1-2; ++: ratio 2-3; +++: ratio > 3.

The *in vitro* data suggest a clear difference between the CS and INU NCs in terms of DCs activation. Compared with INU NCs, CS NCs caused a higher upregulation of different activation markers and stimulated higher levels of cytokines that can be explain, at least partially, due to its higher toxicity. However, this does not necessarily mean that INU NCs cannot have and adjuvant effect *in vivo*. In fact, Advax® does not show DC activation *in vitro* but it does *in vivo* modulating the DC function and enhancing the antigen presentation to T and B cells [52,84]. Notably, delta-INU has shown to be safe in pregnant and very young animals [85,86], a feature that may be attributed to its non-inflammatory mode of action.

Regarding the particle size, although differences were found in terms of interaction, with S NCs rendering more positive cells than M size, these differences did not translated into higher up-regulation of biomarkers and production of cytokines. Probably the activation is not linear dependent with the number of particles that can enter the cells (DiD + cells), rather after reaching a threshold of NCs-cell interaction the DCs would get activated.

3.3. Biodistribution of inulin and chitosan NCs in zebrafish and their access to macrophages

In this work, the MΦ-labeled zebrafish model was adopted to monitor NPs-immune cells interaction *in vivo*. An advantage of this model relies on the fact that zebrafish MΦs have similar morphology and functions than their mammalians counterparts [87]. The results in Fig. 9 illustrate the different biodistribution of NCs with different particle size and polymeric shell. When injected intramuscularly (Fig. 9), the higher dissemination of S NCs, independently of the composition, led to their spreading all along the myomere and clearly limited by myosepta, a dense membrane of collagen

fibrils (Fig. 9, yellow dotted area). In addition, both NCs S were still found in the muscle at 24 h, both inside MΦs, as bright spots, and outside them, as more diffuse fluorescence. On the contrary, CS and INU NCs M hardly spread from the injection point at 2 - 4 hours post injection (Fig. 9, red dashed circles) and, at 24 h, only residual fluorescence was observed at the site of injection. It could be hypothesized that this clearance is mediated by MΦs, since the remaining fluorescence of NCs at 24 h was localized in spots inside the MΦs.

With regard to the influence of the NCs composition, CS NCs exhibited a high capacity to recruit MΦs at the injection site (Fig. 9, indicated as "MΦ", with green fluorescence from the MΦs and also yellow fluorescence due to the co-localization of MΦs and NCs, in red). On the contrary, INU NCs showed a lower capacity to attract MΦs. This different behavior could be attributed to the positive charge of CS NCs and the reported immune activation properties of CS [83,88,89]. Nevertheless, one should be cautious when considering the immunoactivation properties of CS, as they could be simply related to the purity and endotoxin content on the CS sources. In fact, when working with ultrapure CS, with no endotoxin content, CS NCs did not show an important activation of MΦs *in vitro* (see chapter 1). Irrespective of the lack of inherent immunoactivation properties of CS found in our lab, it is to be recognized its capacity to enhance the immune response to associated antigens [14,90].

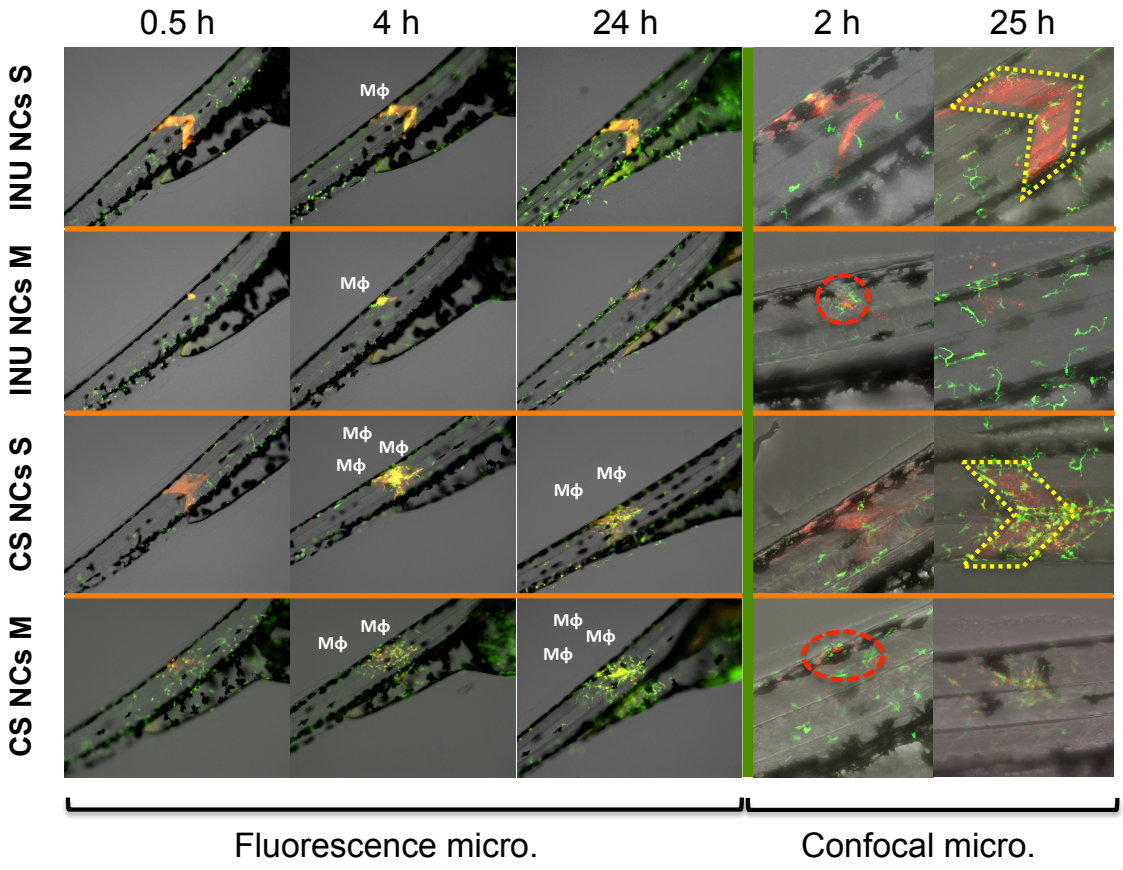

Figure 9. Nanocapsules (NCs) biodistribution in zebrafish after intramuscular injection. Representative scheme of the administration routes and relevant anatomical regions in the biodistribution studies of zebrafish embryos. Chitosan (CS) and inulin (INU) nanocapsules (NCs) of two different particle sizes (S <100 nm and M >100 nm) were administered intramuscularly in 48 hpf zebrafish embryos. Images were taken at 0.5, 4 and 24 h with a fluorescence zoom microscope and at 2 and 25 h with a confocal microscope (B). Red channel: NCs, green channel: macrophages, red dashed circles: low dissemination from the injection site; yellow dotted area: dissemination along the myomere; MΦ: macrophages recruitment. Zebrafish embryo drawing adapted from Lizzy Griffiths http://zebrafishart.blogspot.com/.

3.4. Lymphatic drainage of inulin and chitosan NCs in mice

As discussed above, recent data supports the hypothesis that free drainage of nanosystems to the LNs can improve the efficacy of vaccines [38]. These nanostructures, usually with particles sizes less than 100 nm, have shown to favor cross-presentation when interacting with the resident DCs in the LNs, triggering an important cellular response [42,91]. Besides, the direct interaction with B-cells can also improve the humoral branch of the immune response [92]. Having in mind the NCs developed in this work, our aim was to make a systematic study of the influence of the particle size (70 nm vs. 170-250 nm) and the polymeric shell of NCs (INU vs. CS) in their drainage to the LNs and accumulation in different subsets of immune cells.

DiD-labeled nanosystems were injected in the footpad of mice and the arrival of the structures to the popliteal lymph node (PLN) was evaluated using two different techniques, flow cytometry (Fig. 10A) and 2-photon microscopy (2PM) (Fig. 10B).

The results in Fig. 10 indicate that 12 h after the injection of the NCs in the footpad of the mice the four nanosystems were capable of reaching the PLN, independently of their size and charge. However, using both, flow cytometry and the 2PM studies, it was observed that INU NCs S reached the PLN in a higher extent than the rest of the prototypes. The small size of INU NCs S (70 nm) might explain the difference in their drainage with respect to the medium size ones (INU NCs M, 250 nm). On the other hand, their rapid lymphatic drainage with respect to that of S CS NC could be related to the positive charge of the latest ones. Finally, the behavior of CS NCs, was similar probably because the differences in size, in this case, were not very pronounced. Overall, we could conclude that both, small size together with negative charge (as compared to positive) where determinant factors of the improved lymphatic drainage of S INU NCs.

If we analyze the biodistribution inside the LN, the accumulation of the NCs mainly occurred in the medullar region, probably associated with the presence of different population of highly phagocytic cells such as medullary macrophages (MM) and different subtypes of LN resident DCs. The images of the excised PLNs also showed this distribution (Fig. 10C): DiD-labeled NCs appear in white, the follicles can be discerned by the presence of subcapsular sinus macrophages (SSM) (red dots) covering these areas. In the green channel, cells of myeloid origin expressing CX3CR1 receptor were visualized. These results are in accordance with previous experiments by other groups [93], showing the accumulation of nanosystems in the medulla of the LNs.

Comparably with what we found, other authors suggested the drainage to LNs of particles in the range of 10 – 200 nm [94–96], and preferably bellow 100 nm [42,91]. Within this range, some authors have pointed out that the optimum size might be between 20 - 50 nm. This was the case of 40 nm polyglutamic acid NPs, which were found to migrate more rapidly to the LNs and captured more efficiently by resident DCs compared with 100 and 200 nm NPs [97]. Similarly, 20 - 40 nm polystyrene nanoparticles were found to drain more rapidly than larger NPs in the nanometric range [74,93]. Overall, these previous works would be in agreement with the results found for INU NCs. Nevertheless, it should be highlighted that the threshold for the adequate particle diffusion will be ultimately influenced by their composition.

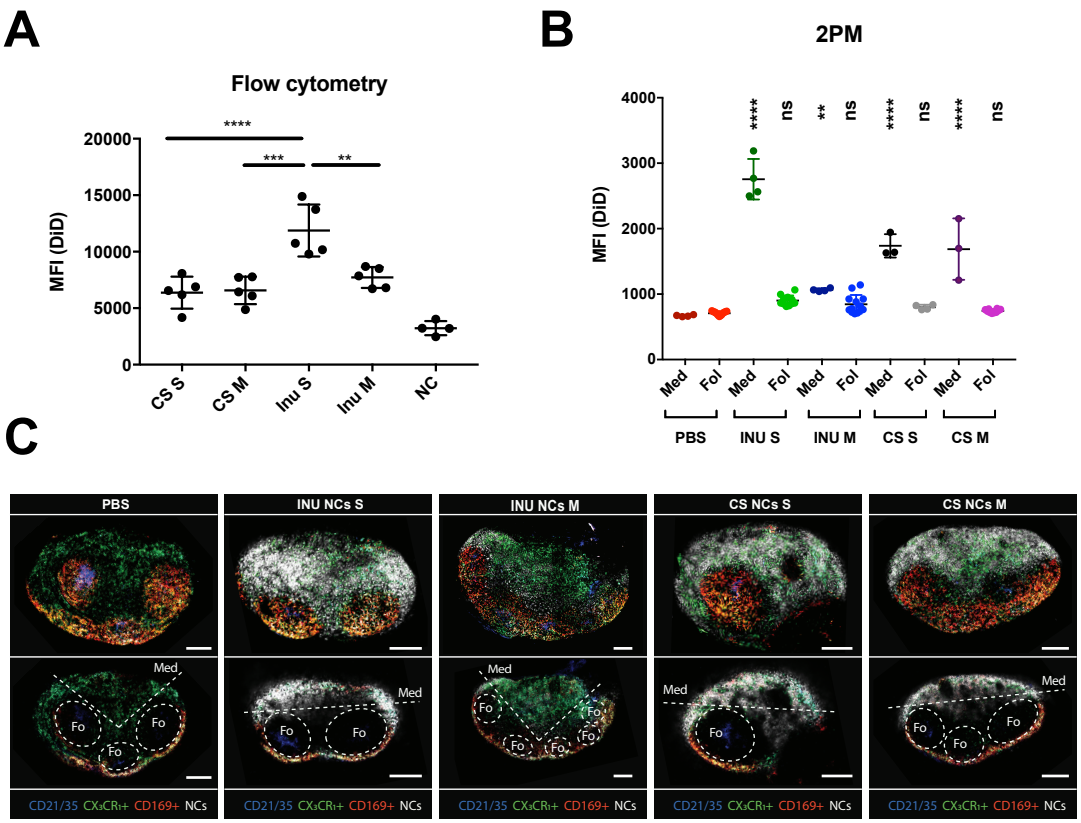

Figure 10: Accumulation of the different nanosystems in the popliteal lymph nodes (PLNs). Chitosan (CS) and inulin (INU) nanocapsules (NCs) of two different sizes (S, <100 nm and M, >100 nm) and labeled with DiD were injected in the footpad of $CX_3CR_1^{+/gfp}$ and C57BL/6JRj mice (5 animals per group). After 12 hours the PLNs from C57BL/6JRj were digested and the mean fluorescence intensity (MFI) evaluated (A). PLNs from $CX_3CR_1^{+/gfp}$ mice were evaluated using 2-photon microscopy. With this technique the MFI of each nanosytem in the medullar and the follicular region was quantified (B). In C, a representative image of the PLNs. The upper row shows a maximum intensity projection of the whole z-stack of the lymph node, while the lower row shows a slice with the different regions highlighted. Subcapsular sinus macrophages (CD169+) are shown in red, nanocapsules (NCs) in white, in blue the follicular dendritic cells (CD21/35+) and in green cells of myeloid origin expressing CX_3CR_1 receptor. One-way ANOVA, Brown-Forsythe test. The differences were considered significant for * $p < 0.05$, ** $p < 0.01$ and *** $p < 0.001$ and **** $p < 0.0001$.

In summary, INU NCs compared with similar size CS NCs, presented lower interaction with MΦs and DCs but considerably less toxicity. CS NCs activated DCs in a higher extent compared with INU NCs, although this activation was accompanied of a higher toxicity. However, inulin-based adjuvants have shown to operate by a non-inflammatory mechanism, explaining its low reactogenicity. In zebrafish, INU NCs with a size lower than 100 nm were rapidly disseminated. Besides, CS was found to positively influence the recruitment of MΦs, a result that could also be in relation with their higher toxicity.

Finally, the lymphatic drainage after subcutaneous administration showed that INU NCs S accumulated in a higher extent in the LNs compared with the rest of prototypes. Due to its non-inflammatory mechanism of adjuvancy, proved safety, good

capacity to disseminate and accumulation in the lymph nodes, we believe that INU NCs S should be further explored as new nanovaccines with lympho-targeting properties.

As a general conclusion, the work developed in this thesis showed the potential of polymeric NCs for their use as nanovaccines. We have expanded the technological possibilities to produce on-demand NCs with controllable particle size and with a shell made of one or multiple polymer layers. Then, we have studied how small changes in the nanometric region and different polymeric shells can drastically influence in their interaction with the immune cells, biodistribution, lymphatic targeting and release of the associated antigens. We believe that this knowledge will contribute to design the future nanovaccines in a more rational manner.

References

[1] I. Toth, M. Skwarczynski, The immune system likes nanotechnology, Nanomedicine. 9 (2014) 2607–2609. doi:10.2217/nnm.14.199.
[2] J.V. Gonzalez-Aramundiz, A.S. Cordeiro, N. Csaba, M. de la Fuente, M.J. Alonso, Nanovaccines : nanocarriers for antigen delivery, Biol. Aujourdhui. 206 (2012) 249–261. doi:10.1051/jbio/2012027.
[3] Y. Liu, Y. Xu, Y. Tian, C. Chen, C. Wang, X. Jiang, Functional Nanomaterials Can Optimize the Efficacy of Vaccines, Small. 10 (2014) 4505–4520. doi:10.1002/smll.201401707.
[4] H. Yue, G. Ma, Polymeric micro / nanoparticles : Particle design and potential vaccine delivery applications, Vaccine. 33 (2015) 5927–5936. doi:10.1016/j.vaccine.2015.07.100.
[5] M.-L. De Temmerman, J. Rejman, J. Demeester, D.J. Irvine, B. Gander, S.C. De Smedt, Particulate vaccines: on the quest for optimal delivery and immune response., Drug Discov. Today. 16 (2011) 569–82. doi:10.1016/j.drudis.2011.04.006.
[6] A.C. Rice-ficht, A.M. Arenas-gamboa, M.M. Kahl-mcdonagh, T.A. Ficht, Polymeric particles in vaccine delivery, Curr. Opin. Microbiol. 13 (2010) 106–112. doi:10.1016/j.mib.2009.12.001.
[7] S. Vicente, B. Diaz-Freitas, M. Peleteiro, A. Sanchez, D.W. Pascual, A. Gonzalez-Fernandez, et al., A Polymer/Oil Based Nanovaccine as a Single-Dose Immunization Approach, PLoS One. 8 (2013) e62500. doi:10.1371/journal.pone.0062500.
[8] M. Tobio, S.P. Schwendeman, Y. Guo, J. McIver, R. Langer, M.J. Alonso, Improved immunogenicity of a core-coated tetanus toxoid delivery system, Vaccine. 18 (1999) 618–622. doi:10.1016/S0264-410X(99)00313-8.
[9] C. Prego, D. Torres, M.J. Alonso, Chitosan nanocapsules: a new carrier for nasal peptide delivery, J. Drug Deliv. Sci. Technol. 16 (2006) 331–337. doi:10.1016/S1773-2247(06)50061-9.
[10] C. Prego, D. Torres, M.J. Alonso, Chitosan Nanocapsules as Carriers for Oral Peptide Delivery: Effect of Chitosan Molecular Weight and Type of Salt on the In Vitro Behaviour and In Vivo Effectiveness, J. Nanosci. Nanotechnol. 6 (2006) 2921–2928. doi:10.1166/jnn.2006.429.
[11] Z. Niu, E. Tedesco, F. Benetti, A. Mabondzo, I.M. Montagner, I. Marigo, et al., Rational design of polyarginine nanocapsules intended to help peptides overcoming intestinal barriers, J. Control. Release. 263 (2017) 4–17. doi:10.1016/j.jconrel.2017.02.024.
[12] M. V. Lozano, G. Lollo, M. Alonso-Nocelo, J. Brea, A. Vidal, D. Torres, et al., Polyarginine nanocapsules: A new platform for intracellular drug delivery, J. Nanoparticle Res. 15 (2013). doi:10.1007/s11051-013-1515-7.
[13] J.V. González-Aramundiz, E. Presas, I. Dalmau-Mena, S. Martínez-Pulgarín, C. Alonso, J.M. Escribano, et al., Rational design of protamine nanocapsules as antigen delivery carriers, J. Control. Release. 245 (2017) 62–69. doi:10.1016/j.jconrel.2016.11.012.
[14] S. Vicente, M. Peleteiro, J.V. González-Aramundiz, B. Díaz-Freitas, S. Martínez-Pulgarín, J.I. Neissa, et al., Highly versatile immunostimulating nanocapsules for specific immune potentiation., Nanomedicine (London). 9 (2014) 2273–2289. doi:10.2217/nnm.14.10.
[15] C. Prego, D. Torres, M.J. Alonso, Chitosan nanocapsules: a new carrier for nasal peptide delivery, J. Drug Deliv. Sci. Technol. 16 (2006) 331–337. doi:10.1016/S1773-2247(06)50061-9.
[16] S. Vicente, M. Peleteiro, B. Díaz-Freitas, A. Sanchez, Á. González-Fernández, M.J. Alonso, Co-delivery of viral proteins and a TLR7 agonist from polysaccharide nanocapsules: A needle-free vaccination strategy, J. Control. Release. 172 (2013) 773–781. doi:10.1016/j.jconrel.2013.09.012.
[17] H. Mobley, C. Alteri, Development of a Vaccine against Escherichia coli Urinary Tract Infections, Pathogens. 5 (2015) 1. doi:10.3390/pathogens5010001.
[18] L.A. Mike, S.N. Smith, C.A. Sumner, K.A. Eaton, H.L.T. Mobley, Siderophore vaccine conjugates protect against uropathogenic Escherichia coli urinary tract infection, Proc. Natl. Acad. Sci. 113 (2016) 13468–13473. doi:10.1073/pnas.1606324113.
[19] B. Slütter, P.C. Soema, Z. Ding, R. Verheul, W. Hennink, W. Jiskoot, Conjugation of ovalbumin to trimethyl chitosan improves immunogenicity of the antigen, J. Control. Release. 143 (2010) 207–214. doi:10.1016/j.jconrel.2010.01.007.
[20] S. Hirsjärvi, S. Dufort, G. Bastiat, P. Saulnier, C. Passirani, J.L. Coll, et al., Surface modification of lipid nanocapsules with polysaccharides: From physicochemical characteristics to in vivo aspects, Acta Biomater. 9 (2013) 6686–6693. doi:10.1016/j.actbio.2013.01.038.
[21] H.X. Wang, Z.Q. Zuo, J.Z. Du, Y.C. Wang, R. Sun, Z.T. Cao, et al., Surface charge critically affects tumor penetration and therapeutic efficacy of cancer nanomedicines, Nano Today. 11 (2016) 133–144.

doi:10.1016/j.nantod.2016.04.008.
[22] S. Sharma, T.K.S. Mukkur, H.A.E. Benson, Y. Chen, Enhanced Immune Response Against Pertussis Toxoid by IgA-Loaded Chitosan–Dextran Sulfate Nanoparticles, J. Pharm. Sci. 101 (2012) 233–244. doi:10.1002/jps.22763.
[23] S. Sharma, H. a E. Benson, T.K.S. Mukkur, P. Rigby, Y. Chen, Preliminary studies on the development of IgA-loaded chitosan-dextran sulphate nanoparticles as a potential nasal delivery system for protein antigens., J. Microencapsul. 30 (2013) 283–94. doi:10.3109/02652048.2012.726279.
[24] D.P. Gnanadhas, M. Ben Thomas, M. Elango, A.M. Raichur, D. Chakravortty, Chitosan-dextran sulphate nanocapsule drug delivery system as an effective therapeutic against intraphagosomal pathogen Salmonella, J. Antimicrob. Chemother. 68 (2013) 2576–2586. doi:10.1093/jac/dkt252.
[25] T. Delair, Colloidal polyelectrolyte complexes of chitosan and dextran sulfate towards versatile nanocarriers of bioactive molecules., Eur. J. Pharm. Biopharm. 78 (2011) 10–8. doi:10.1016/j.ejpb.2010.12.001.
[26] P. Zaman, J. Wang, A. Blau, W. Wang, T. Li, D.S. Kohane, et al., Incorporation of heparin-binding proteins into preformed dextran sulfate-chitosan nanoparticles, Int. J. Nanomedicine. 11 (2016) 6149–6159. doi:10.2147/IJN.S119174.
[27] W. Chaiyasan, S.P. Srinivas, W. Tiyaboonchai, Mucoadhesive Chitosan–Dextran Sulfate Nanoparticles for Sustained Drug Delivery to the Ocular Surface, J. Ocul. Pharmacol. Ther. 29 (2013) 200–207. doi:10.1089/jop.2012.0193.
[28] S. Hirsjärvi, Y. Qiao, A. Royere, J. Bibette, J. Benoit, Layer-by-layer surface modification of lipid nanocapsules, Eur. J. Pharm. Biopharm. 76 (2010) 200–207. doi:10.1016/j.ejpb.2010.07.010.
[29] J. Crecente-Campo, S. Lorenzo-Abalde, A. Mora, J. Marzoa, N. Csaba, J. Blanco, et al., Bilayer polymer nanocapsules: a formulation approach for a thermostable and adjuvanted E. coli antigen vaccine, J. Control. Release. Submitted (2018).
[30] D. Chen, D. Kristensen, Opportunities and challenges of developing thermostable vaccines, Expert Rev. Vaccines. 8 (2009) 547–557. doi:10.1586/erv.09.20.
[31] W. Abdelwahed, G. Degobert, S. Stainmesse, H. Fessi, Freeze-drying of nanoparticles: Formulation, process and storage considerations, Adv. Drug Deliv. Rev. 58 (2006) 1688–1713. doi:10.1016/j.addr.2006.09.017.
[32] M.M. Tobío, J. Nolley, Y. Guo, J. McIver, M.J. Alonso, A Novel System Based on a Poloxamer/PLGA Blend as a Tetanus Toxoid Delivery Vehicle, Pharm. Res. 16 (1999) 682–688. doi:10.1023/a:1018820507379.
[33] A. Vila, A. Sánchez, C. Évora, I. Soriano, O. McCallion, M.J. Alonso, PLA-PEG particles as nasal protein carriers: The influence of the particle size, Int. J. Pharm. 292 (2005) 43–52. doi:10.1016/j.ijpharm.2004.09.002.
[34] A. Vila, A. Sánchez, K. Janes, I. Behrens, T. Kissel, J.L. V Jato, et al., Low molecular weight chitosan nanoparticles as new carriers for nasal vaccine delivery in mice, Eur. J. Pharm. Biopharm. 57 (2004) 123–131. doi:10.1016/j.ejpb.2003.09.006.
[35] C. Prego, P. Paolicelli, B. Díaz, S. Vicente, A. Sánchez, Á. González-Fernández, et al., Chitosan-based nanoparticles for improving immunization against hepatitis B infection, Vaccine. 28 (2010) 2607–2614. doi:10.1016/j.vaccine.2010.01.011.
[36] T.G. Dacoba, A. Olivera, D. Torres, J. Crecente-Campo, M.J. Alonso, Modulating the immune system through nanotechnology., Semin. Immunol. 34 (2017) 78–102. doi:10.1016/j.smim.2017.09.007.
[37] Y. Liu, B. Workalemahu, X. Jiang, The Effects of Physicochemical Properties of Nanomaterials on Their Cellular Uptake In Vitro and In Vivo, Small. 13 (2017) 1–13. doi:10.1002/smll.201701815.
[38] H. Jiang, Q. Wang, X. Sun, Lymph node targeting strategies to improve vaccination efficacy, J. Control. Release. 267 (2017) 47–56. doi:10.1016/j.jconrel.2017.08.009.
[39] U. Bilati, E. Allémann, E. Doelker, Development of a nanoprecipitation method intended for the entrapment of hydrophilic drugs into nanoparticles, Eur. J. Pharm. Sci. 24 (2005) 67–75. doi:10.1016/j.ejps.2004.09.011.
[40] D. Moinard-Chécot, Y. Chevalier, S. Briançon, L. Beney, H. Fessi, Mechanism of nanocapsules formation by the emulsion-diffusion process., J. Colloid Interface Sci. 317 (2008) 458–68. doi:10.1016/j.jcis.2007.09.081.
[41] J.W. Hickey, J.L. Santos, J.M. Williford, H.Q. Mao, Control of polymeric nanoparticle size to improve therapeutic delivery, J. Control. Release. 219 (2015) 535–547. doi:10.1016/j.jconrel.2015.10.006.
[42] K.T. Gause, A.K. Wheatley, J. Cui, Y. Yan, S.J. Kent, F. Caruso, Immunological Principles Guiding

the Rational Design of Particles for Vaccine Delivery, ACS Nano. 11 (2017) 54–68. doi:10.1021/acsnano.6b07343.
[43] D.J. Irvine, M.A. Swartz, G.L. Szeto, Engineering synthetic vaccines using cues from natural immunity, Nat. Mater. 12 (2013) 978–990. doi:10.1038/nmat3775.
[44] D. Quintanar-Guerrero, E. Allémann, H. Fessi, E. Doelker, Preparation techniques and mechanism of formation of biodegradable nanoparticles from preformed polymers, Drug Dev. Ind. Pharm. 24 (1998) 1113–1128. doi:10.3109/03639049809108571.
[45] S. Galindo-rodriguez, E. Alle, H. Fessi, E. Doelker, Physicochemical Parameters Associated with Nanoparticle Formation in the Salting-out , Nanoprecipitation Methods, Pharm. Res. 21 (2004) 1428–1439. doi:10.1023/B:PHAM.0000036917.75634.be.
[46] F. Ganachaud, J.L. Katz, Nanoparticles and nanocapsules created using the ouzo effect: Spontaneous emulsification as an alternative to ultrasonic and high-shear devices, ChemPhysChem. 6 (2005) 209–216. doi:10.1002/cphc.200400527.
[47] M. Beck-Broichsitter, E. Rytting, T. Lebhardt, X. Wang, T. Kissel, Preparation of nanoparticles by solvent displacement for drug delivery: A shift in the " ouzo region" upon drug loading, Eur. J. Pharm. Sci. 41 (2010) 244–253. doi:10.1016/j.ejps.2010.06.007.
[48] W.S. Saad, R.K. Prud'Homme, Principles of nanoparticle formation by flash nanoprecipitation, Nano Today. 11 (2016) 212–227. doi:10.1016/j.nantod.2016.04.006.
[49] M.A. Mensink, H.W. Frijlink, K. Van Der Voort Maarschalk, W.L.J. Hinrichs, Inulin, a flexible oligosaccharide. II: Review of its pharmaceutical applications, Carbohydr. Polym. 134 (2015) 418–428. doi:10.1016/j.carbpol.2015.08.022.
[50] D.G. Silva, P.D. Cooper, N. Petrovsky, Inulin-derived adjuvants efficiently promote both Th1 and Th2 immune responses, Immunol. Cell Biol. 82 (2004) 611–616. doi:10.1111/j.1440-1711.2004.01290.x.
[51] N. Petrovsky, P.D. Cooper, Advax™, a novel microcrystalline polysaccharide particle engineered from delta inulin, provides robust adjuvant potency together with tolerability and safety, Vaccine. 33 (2015) 5920–5926. doi:10.1016/j.vaccine.2015.09.030.
[52] L. Li, Y. Honda-Okubo, C. Li, D. Sajkov, N. Petrovsky, Delta inulin adjuvant enhances plasmablast generation, expression of activation-induced cytidine deaminase and B-cell affinity maturation in human subjects receiving seasonal influenza vaccine, PLoS One. 10 (2015) 1–18. doi:10.1371/journal.pone.0132003.
[53] M. Hayashi, T. Aoshi, Y. Haseda, K. Kobiyama, E. Wijaya, N. Nakatsu, et al., Advax, a delta inulin microparticle, potentiates in-built adjuvant property of co-administered vaccines, EBioMedicine. 15 (2017) 127–136. doi:10.1016/j.ebiom.2016.11.015.
[54] C. Losa, L. Marchal-Heussler, F. Orallo, J.L. Vila Jato, M.J. Alonso, Design of new formulations for topical ocular administration: polymeric nanocapsules containing metipranolol., Pharm. Res. 10 (1993) 80–7. doi:10.1023/A:1018977130559.
[55] F.A. Oyarzun-Ampuero, G.R. Rivera-Rodríguez, M.J. Alonso, D. Torres, G.R. Rivera-Rodriguez, M.J. Alonso, et al., Hyaluronan nanocapsules as a new vehicle for intracellular drug delivery, Eur. J. Pharm. Sci. 49 (2013) 483–490. doi:10.1016/j.ejps.2013.05.008.
[56] G. Lollo, P. Hervella, P. Calvo, P. Aviles, M.J. Guillen, M. Garcia-Fuentes, et al., Enhanced in vivo therapeutic efficacy of plitidepsin-loaded nanocapsules decorated with a new poly-aminoacid-PEG derivative, Int. J. Pharm. 483 (2015) 212–219. doi:10.1016/j.ijpharm.2015.02.028.
[57] L.N. Thwala, A. Beloqui, N.S. Csaba, D. González-Touceda, S. Tovar, C. Dieguez, et al., The interaction of protamine nanocapsules with the intestinal epithelium: A mechanistic approach, J. Control. Release. 243 (2016) 109–120. doi:10.1016/j.jconrel.2016.10.002.
[58] G. Lollo, A. Gonzalez-Paredes, M. Garcia-Fuentes, P. Calvo, D. Torres, M.J. Alonso, Polyarginine Nanocapsules as a Potential Oral Peptide Delivery Carrier, J. Pharm. Sci. 106 (2017) 611–618. doi:10.1016/j.xphs.2016.09.029.
[59] C. V. Stevens, A. Meriggi, K. Booten, Chemical modification of inulin, a valuable renewable resource, and its industrial applications, Biomacromolecules. 2 (2001) 1–16. doi:10.1021/bm005642t.
[60] C. V. Stevens, A. Meriggi, M. Peristeropoulou, P.P. Christov, K. Booten, B. Levecke, et al., Polymeric surfactants based on inulin, a polysaccharide extracted from chicory. 1. Synthesis and interfacial properties, Biomacromolecules. 2 (2001) 1256–1259. doi:10.1021/bm015570l.
[61] G. Van den Mooter, I. Weuts, T. De Ridder, N. Blaton, Evaluation of Inutec SP1 as a new carrier in the formulation of solid dispersions for poorly soluble drugs, Int. J. Pharm. 316 (2006) 1–6. doi:10.1016/j.ijpharm.2006.02.025.
[62] P. Srinarong, S. Hämäläinen, M.R. Visser, W.L.J. Hinrichs, J. Ketolainen, H.W. Frijlink, Surface-

Active Derivative of Inulin (Inutec® SP1) Is a Superior Carrier for Solid Dispersions with a High Drug Load, J. Pharm. Sci. 100 (2011) 2333–2342. doi:10.1002/jps.22471.
[63] P.R. Mishra, L. Al Shaal, R.H. Müller, C.M. Keck, Production and characterization of Hesperetin nanosuspensions for dermal delivery, Int. J. Pharm. 371 (2009) 182–189. doi:10.1016/j.ijpharm.2008.12.030.
[64] P. Muley, S. Kumar, F. El Kourati, S.S. Kesharwani, H. Tummala, Hydrophobically modified inulin as an amphiphilic carbohydrate polymer for micellar delivery of paclitaxel for intravenous route, Int. J. Pharm. 500 (2016) 32–41. doi:10.1016/j.ijpharm.2016.01.005.
[65] T.F. Tadros, A. Vandamme, K. Booten, B. Levecke, C. V. Stevens, Stabilisation of emulsions using hydrophobically modified inulin (polyfructose), Colloids Surfaces A Physicochem. Eng. Asp. 250 (2004) 133–140. doi:10.1016/j.colsurfa.2004.03.041.
[66] A. Gamvrellis, D. Leong, J.C. Hanley, S.D. Xiang, P. Mottram, M. Plebanski, Vaccines that facilitate antigen entry into dendritic cells, Immunol. Cell Biol. 82 (2004) 506–516. doi:10.1111/j.0818-9641.2004.01271.x.
[67] N. Doshi, S. Mitragotri, Macrophages recognize size and shape of their targets, PLoS One. 5 (2010) 1–6. doi:10.1371/journal.pone.0010051.
[68] T. Fifis, A. Gamvrellis, B. Crimeen-Irwin, G.A. Pietersz, J. Li, P.L. Mottram, et al., Size-Dependent Immunogenicity: Therapeutic and Protective Properties of Nano-Vaccines against Tumors, J. Immunol. 173 (2004) 3148–3154. doi:10.4049/jimmunol.173.5.3148.
[69] C. He, Y. Hu, L. Yin, C. Tang, C. Yin, Effects of particle size and surface charge on cellular uptake and biodistribution of polymeric nanoparticles, Biomaterials. 31 (2010) 3657–3666. doi:10.1016/j.biomaterials.2010.01.065.
[70] J.S. Choi, J. Cao, M. Naeem, J. Noh, N. Hasan, H.K. Choi, et al., Size-controlled biodegradable nanoparticles: Preparation and size-dependent cellular uptake and tumor cell growth inhibition, Colloids Surfaces B Biointerfaces. 122 (2014) 545–551. doi:10.1016/j.colsurfb.2014.07.030.
[71] S. Hirsjärvi, S. Dufort, J. Gravier, I. Texier, Q. Yan, J. Bibette, et al., Influence of size, surface coating and fine chemical composition on the in vitro reactivity and in vivo biodistribution of lipid nanocapsules versus lipid nanoemulsions in cancer models, Nanomedicine Nanotechnology, Biol. Med. 9 (2013) 375–387. doi:10.1016/j.nano.2012.08.005.
[72] S. Kim, W.K. Oh, Y.S. Jeong, J.Y. Hong, B.R. Cho, J.S. Hahn, et al., Cytotoxicity of, and innate immune response to, size-controlled polypyrrole nanoparticles in mammalian cells, Biomaterials. 32 (2011) 2342–2350. doi:10.1016/j.biomaterials.2010.11.080.
[73] J. Huang, L. Bu, J. Xie, K. Chen, Z. Cheng, X. Li, et al., Effects of nanoparticle size on cellular uptake and liver MRI with polyvinylpyrrolidone-coated iron oxide nanoparticles, ACS Nano. (2010). doi:10.1021/nn101643u.
[74] T. Fifis, A. Gamvrellis, B. Crimeen-Irwin, G.A. Pietersz, J. Li, P.L. Mottram, et al., Size-dependent immunogenicity: therapeutic and protective properties of nano-vaccines against tumors, J. Immunol. 173 (2004) 3148–3154. doi:10.4049/jimmunol.173.5.3148.
[75] C. Foged, B. Brodin, S. Frokjaer, A. Sundblad, Particle size and surface charge affect particle uptake by human dendritic cells in an in vitro model, Int. J. Pharm. 298 (2005) 315–322. doi:10.1016/j.ijpharm.2005.03.035.
[76] L. Thiele, B. Rothen-Rutishauser, S. Jilek, H. Wunderli-Allenspach, H.P. Merkle, E. Walter, Evaluation of particle uptake in human blood monocyte-derived cells in vitro. Does phagocytosis activity of dendritic cells measure up with macrophages?, J. Control. Release. 76 (2001) 59–71.
[77] C.A. Fromen, T.B. Rahhal, G.R. Robbins, M.P. Kai, T.W. Shen, J.C. Luft, et al., Nanoparticle surface charge impacts distribution, uptake and lymph node trafficking by pulmonary antigen-presenting cells, Nanomedicine Nanotechnology, Biol. Med. 12 (2016) 677–687. doi:10.1016/j.nano.2015.11.002.
[78] L.J. Cruz, P.J. Tacken, R. Fokkink, C.G. Figdor, The influence of PEG chain length and targeting moiety on antibody-mediated delivery of nanoparticle vaccines to human dendritic cells, Biomaterials. 32 (2011) 6791–6803. doi:10.1016/j.biomaterials.2011.04.082.
[79] C. Villiers, M. Chevallet, H. Diemer, R. Couderc, H. Freitas, A. Van Dorsselaer, et al., From Secretome Analysis to Immunology, Mol. Cell. Proteomics. 8 (2009) 1252–1264. doi:10.1074/mcp.M800589-MCP200.
[80] B. Koppolu, D.A. Zaharoff, The effect of antigen encapsulation in chitosan particles on uptake, activation and presentation by antigen presenting cells, Biomaterials. 34 (2013) 2359–2369. doi:10.1016/j.biomaterials.2012.11.066.

[81] K.L. Rock, H. Kono, The Inflammatory Response to Cell Death, Annu. Rev. Pathol. Mech. Dis. 3 (2008) 99–126. doi:10.1146/annurev.pathmechdis.3.121806.151456.
[82] L. Jia, X. Gao, Y. Wang, N. Yao, X. Zhang, Structural, phenotypic and functional maturation of bone marrow dendritic cells (BMDCs) induced by Chitosan (CTS), Biologicals. 42 (2014) 334–338. doi:10.1016/j.biologicals.2014.07.004.
[83] M. Oliveira, S. Santos, M. Oliveira, A. Torres, M. Barbosa, Chitosan drives anti-inflammatory macrophage polarisation and pro-inflammatory dendritic cell stimulation, Eur. Cells Mater. 24 (2012) 136–153. doi:10.22203/eCM.v024a10.
[84] J. Tomar, H.P. Patil, G. Bracho, W.F. Tonnis, H.W. Frijlink, N. Petrovsky, et al., Advax augments B and T cell responses upon influenza vaccination via the respiratory tract and enables complete protection of mice against lethal influenza virus challenge, J. Control. Release. 288 (2018) 199–211. doi:10.1016/j.jconrel.2018.09.006.
[85] Y. Honda-Okubo, A. Kolpe, L. Li, N. Petrovsky, A single immunization with inactivated H1N1 influenza vaccine formulated with delta inulin adjuvant (Advax^{TM}) overcomes pregnancy-associated immune suppression and enhances passive neonatal protection, Vaccine. 32 (2014) 4651–4659. doi:10.1016/j.vaccine.2014.06.057.
[86] Y. Honda-Okubo, C.H. Ong, N. Petrovsky, Advax delta inulin adjuvant overcomes immune immaturity in neonatal mice thereby allowing single-dose influenza vaccine protection, Vaccine. 33 (2015) 4892–4900. doi:10.1016/j.vaccine.2015.07.051.
[87] N.D. Meeker, N.S. Trede, Immunology and zebrafish: Spawning new models of human disease, Dev. Comp. Immunol. 32 (2008) 745–757. doi:10.1016/j.dci.2007.11.011.
[88] S. Ravindranathan, B.P. Koppolu, S.G. Smith, D.A. Zaharoff, Effect of chitosan properties on immunoreactivity, Mar. Drugs. 14 (2016). doi:10.3390/md14050091.
[89] C.L. Bueter, C.K. Lee, J.P. Wang, G.R. Ostroff, C.A. Specht, S.M. Levitz, Spectrum and Mechanisms of Inflammasome Activation by Chitosan, J. Immunol. 192 (2014) 5943–5951. doi:10.4049/jimmunol.1301695.
[90] C. Nikapitiya, S.H.S. Dananjaya, B.C.J. De Silva, G.-J. Heo, C. Oh, M. De Zoysa, et al., Chitosan nanoparticles: A positive immune response modulator as display in zebrafish larvae against Aeromonas hydrophila infection, Fish Shellfish Immunol. 76 (2018) 240–246. doi:10.1016/j.fsi.2018.03.010.
[91] D.J. Irvine, M.C. Hanson, K. Rakhra, T. Tokatlian, Synthetic Nanoparticles for Vaccines and Immunotherapy, Chem. Rev. 115 (2015) 11109–11146. doi:10.1021/acs.chemrev.5b00109.
[92] S.N. Mueller, S. Tian, J.M. DeSimone, Rapid and Persistent Delivery of Antigen by Lymph Node Targeting PRINT Nanoparticle Vaccine Carrier To Promote Humoral Immunity, Mol. Pharm. 12 (2015) 1356–1365. doi:10.1021/mp500589c.
[93] V. Manolova, A. Flace, M. Bauer, K. Schwarz, P. Saudan, M.F. Bachmann, Nanoparticles target distinct dendritic cell populations according to their size., Eur. J. Immunol. 38 (2008) 1404–13. doi:10.1002/eji.200737984.
[94] M.F. Bachmann, G.T. Jennings, Vaccine delivery: a matter of size, geometry, kinetics and molecular patterns, Nat. Rev. Immunol. 10 (2010) 787–796. doi:10.1038/nri2868.
[95] M. Pitorre, G. Bastiat, E.M. dit Chatel, J.-P. Benoit, Passive and specific targeting of lymph nodes: the influence of the administration route, Eur. J. Nanomedicine. 7 (2015) 121–128. doi:10.1515/ejnm-2015-0003.
[96] R. Abellán-pose, N. Csaba, M.J. Alonso, Lymphatic Targeting of Nanosystems for Anticancer Drug Therapy, (2016) 1194–1209.
[97] F. Shima, T. Uto, T. Akagi, M. Baba, M. Akashi, Size effect of amphiphilic poly(γ-glutamic acid) nanoparticles on cellular uptake and maturation of dendritic cells in vivo., Acta Biomater. 9 (2013) 8894–901. doi:10.1016/j.actbio.2013.06.010.

Conclusions

The main objectives of this thesis were, first to develop new methods to prepare tuneable polymeric NCs regarding their particle size, polymeric shell and surface composition; and second, to study the influence of these parameters in the interaction of the NCs with immune cells, their dissemination, lymphatic drainage and their capacity to protect and release antigens to generate an adequate immune response. The data obtained from the experimental work done along this thesis allow us to conclude:

1. Specifically designed nanocapsules consisting of an oily core and a shell made of a bilayer of chitosan and dextran sulfate were found to efficiently associate the IutA antigen. Moreover, the bilayer nanosystem was able to protect the antigen and control its release leading to high IgG levels in immunized mice. Finally, the development of a freeze-drying process guaranteed the thermostability of the nanovaccine for at least 3 months at room temperature.

2. The modification of the solvent displacement technique allowed us to produce nanocapsules with one or multiple polymer layers and with a tunable size ranging from 50 nm to 500 nm. Besides, the production of nanocapsules could be miniaturized and adapted to a HTS procedure and scaled-up using a batch mode or a continuous process using microfluidics.

3. The use of hydrophobized inulin enabled the development of new nanocapsules with controllable particle size and charge. Their *in vitro* and *in vivo* toxicity was significantly lower compared with chitosan nanocapsules of similar size. The interaction with macrophages and dendritic cells was size-dependent, with a higher interaction of the smaller particles, but the influence of the polymeric shell was only evident in macrophages.

4. Both, particle size and surface composition were found to determine the biodistribution of the nanocapsules in zebrafish. Small size nanocapsules (< 100 nm) disseminated in a higher extent in zebrafish after intramuscular and intravenous injection compared with their counterparts of larger size (170 - 250 nm). Chitosan nanocapsules evoked a more remarkable recruitment of macrophages. Macrophage-labeled zebrafish is an interesting model to understand the interactions between nanosystems and immune cells in a dynamic and living environment.

5. Inulin nanocapsules of small particle size (70 nm) accumulated more efficiently in the draining lymph node after subcutaneous injection in mice compared with larger inulin particles (250 nm) and with chitosan nanocapsules of similar size (70 and 170 nm). Inside the popliteal lymph node, all nanosystems were found in macrophages, dendritic cells, monocytes, neutrophils and NK cells but in different proportions depending on the size and the shell polymer of the nanocapsules. The two-photon microscopy enabled a precise visualization of the NCs biodistribution in the different regions of the lymph node, highlighting the potential of this technique to analyze the lymphatic targeting of the nanosystems.

Overall, this works highlights the technological possibilities of polymeric nanocapsules and the capital importance of the rational design of the nanosystems in order to have an adequate biodistribution, immune cell-interaction and antigen protection and release. Besides, it provides the bases for the design of new nanovaccines with enhanced humoral and cellular responses using particles with lympho-targeting properties.

List of abbreviations

2PM: two-photon microscopy

AE: association efficiency

Alg: alginate

ANOVA: analysis of variance

APC: antigen-presenting cell

BSA: bovine serum albumin

ChS: chondroitin sulfate

CM-β-glucan, CMβG: carboxymethyl beta glucan

CS: chitosan

CTAB: cetyl trimethylammonium bromide

DC: dendritic cell

DiD: DilC18(5) oil (1,1'-dioctadecyl-3,3,3',3'-tetramethylindodicarbocyannine perchlorate)

DLS: dynamic light scattering

DS: dextran sulfate

EMA: European medicines agency

FACS: fluorescence-activated cell sorting (flow cytometry)

FD: freeze-dried

FESEM: field emission scanning electron microscopy

Fig: figure

GRAS: generally recognized as safe

HA: sodium hyaluronate

hpf: hours post-fertilization

h: hours post-injection

HTS: high-throughput screening

iDC: immature dendritic cells

IDO: indoleamine 2,3-dioxygenase

INU: inulin

IutA: ferric aerobactin receptor from *Escherichia coli*

LbL: layer-by-layer

Lec: lecithin

LC_{50}: median lethal concentration

LD_{50}: median lethal dose

LN: lymph node

LOEC: lowest observed effect concentration

M: medium

MALT: mucosal-associated lymphoid tissues

mDC: mature dendritic cell

MFI: mean fluorescence intensity

MHC: major histocompatibility complex

MM: medullary macrophages

MPs: microparticles

Mw: molecular weight

Mϕ: macrophage

NC: nanocapsules

NE: nanoemulsion

NOEC: no observed effect concentration

NP: nanoparticle

NTA: nanoparticle tracking analysis

OVA: ovoalbumin

O/W: oil in wáter

P407: poloxamer 407

PACA: polyisobutylcyanoacrylate

PAMPs: pathogen-associated molecular patterns

PArg: polyarginine

PBMC: peripheral blood mononuclear cell

PBS: phosphate buffered saline

PDI: polydispersity index

PEG: polyethylene glicol

PGA: polyglutamic acid

PLA: poly-(D,L-lactide)

PLGA: poly(lactic-co-glycolic acid)

PLN: popliteal lymph node

rHBsAg: recombinant hepatitis B surface antigen

RT: room temperature

S: small

SC: subcutaneous

SD: standard deviation

SSM: subcapsular sinus macrophages

TEM: transmission electron microscopy

TLR: toll-like receptor

TPGS: d-α-tocopherol poly(ethylene glicol) 1000 succinate

UPEC: uropathogenic *Escherichia coli*

W/O: water in oil

w/v: weight/volume

w/w: weight/weight

Ethical considerations

Animal studies

Immunization studies (chapter 1) were done in Lugo (laboratory AE-LU-002; REGA: ES270280331701) by Dra. Azucena Mora Gutiérrez (group of Prof. Jorge Blanco Álvarez) following European (Directive 2010/63/EU on the protection of animals used for scientific purposes) and National (RD 53/2013) regulations for transport, housing and care of laboratory animals. The protocol used was approved by the ethical committee of the USC and Xunta de Galicia (ID 001/14).

Studies in zebrafish embryos (chapter 3) were done in Lugo (laboratory AE-LU-003; REGA: ES270280346401) by Dr. Jorge Guerra Varela (group of Prof. Laura Sánchez Piñón) following European and National regulations. The procedures were approved by the ethical committee of the USC and Xunta de Galicia (ID 009/14).

Human peripheral blood mononuclear cells (chapter 1 and 4) were obtained by anonymous donors. Studies were done by Dr. Rubén Varela Calviño and Dra. Mercedes Peleteiro, and approved by the ethical committee of the Xunta de Galicia (register code 2014/543).

Biodistribution towards the lymph nodes (chapter 4) were done in Bellinzona (Switzerland) by Dr. Santiago F. González, and approved by the cantonal veterinarian authorities under the protocol ID: TI28/17 and were executed in accordance with governing Swiss legislation for animal experimentation.